UNIVERSITY OF CATANIA

PHD THESIS

Green infrastructures as a climate change adaptation measure: community awareness and hydrological modeling of green roofs under different emission scenarios

---

Author:
Paola NANNI

Supervisor and co-tutor:
Prof. Antonino CANCELLIERE
Prof.ssa Rosaria E. MUSUMECI

Assessment and mitigation of urban and territorial risks XXXIV cycle
Department of Civil Engineering and Architecture

November, 2021

Declaration of Authorship

I, Paola NANNI, declare that this thesis titled, "Green infrastructures as a climate change adaptation measure: community awareness and hydrological modeling of green roofs under different emission scenarios" and the work presented in it are my own. I confirm that:

- This work was done wholly or mainly while in candidature for a research degree at this University.
- Where any part of this thesis has previously been submitted for a degree or any other qualification at this University or any other institution, this has been clearly stated.
- Where I have consulted the published work of others, this is always clearly attributed.
- Where I have quoted from the work of others, the source is always given. With the exception of such quotations, this thesis is entirely my own work.
- I have acknowledged all main sources of help.
- Where the thesis is based on work done by myself jointly with others, I have made clear exactly what was done by others and what I have contributed myself.

Signed:

Date:

UNIVERSITY OF CATANIA

Abstract

Department of Civil Engineering and Architecture

Doctor of Philosophy

Green infrastructures as a climate change adaptation measure: community awareness and hydrological modeling of green roofs under different emission scenarios

by Paola NANNI

Many recent studies indicate the climate change as a phenomenon that significantly alters the water cycle in different regions of the world, also implying new challenges in water management and drought risk assessment. In addition to this problem, the loss of natural soil and vegetation within the urban environment can significantly affect the hydrological cycle, increasing the risk of urban flooding.

To mitigate these changes in urban areas, engineered systems are developed, such as green roofs, to mimic and replace functions (evapotranspiration, infiltration, percolation) that have been altered due to the impact of human development. These adaptation systems are able to reestablish the natural processes of the water cycle and to operate the hydrological control of the runoff of rainwater with consequent attenuation of the peak flow, reduction of the flow volume and increase of the concentration time.

In order to investigate the hydrological response of a green roof, the University of Catania (Italy) has recently built a green roof of about 800 m^2 to study the benefits that this infrastructure can bring in a Mediterranean climate.

The objectives of this thesis are to provide detailed information on the performance of the green roof in the current and future Mediterranean climate and to identify a suitable modeling approach to describe the associated hydrological response.

After investigating the research context through a survey for the local population on the perception of climate change and the need for adaptation measures, we proceeded with a modeling approach

First, the data collected during a monitoring campaign of about two years at the experimental site of the green roof of the University of Catania (Italy) are presented together with the results obtained in quantifying the hydrological performance of the green roof.

To examine the hydrological response of the green roof, the Hydrus 1D model was implemented, which solves the Richards equation for the flow of water over the soil column. The model adequately reproduces the moisture trend in the soil both during rain events and during dry periods.

In order to study the impact that a green roof can have in the future

climate, therefore in the different climate change scenarios, it is of fundamental importance to ascertain the quality of the regional climate models (RCM), which are commonly used to evaluate the future impacts of climate change on hydrological events.

In this thesis, a statistical methodological framework was proposed to evaluate the quality of the EURO-CORDEX RCMs with regard to their ability to simulate the historical climate (temperature and precipitation, the basic variables that determine meteorological drought) in Mediterranean regions, subsequently a study was conducted in various meteorological stations in Sicily to ascertain the ability of RCMs to reproduce the climate even on a reduced time scale.

The final results, with the application of RCMs on the physically-based model of the green roof, show that green roofs can be a valid infrastructure for the reduction of volumes and rain peaks in the next future. With its capacity to retain volumes and reduce peaks, the green roof effectively manages to bring the outflow to a level similar to that of the historical scenario, removing, partially or completely, the negative effect of climate change.

Acknowledgements

First, I want to thank my advisor Antonino Cancelliere, for offering me countless opportunities for growing from both a scientific and a human perspective.

Thanks to Rosaria Musumeci, my co-advisor, and David Peres for supporting me throughout the course of my Ph.D. and to all the other professors, researchers and students of the Catania University that offered me interesting insights, encouraging me to develop my investigation in various directions.

Particularly, thanks to LIFE SimetoRES project with all its collaborators. Much of this study was possible thanks to this project and to all those who are part of it.

Thanks to Claudio Ivan Meier for his helpful advice and for giving me the chance to live an international experience despite the global pandemic.

A special thanks to Prof. Athanasios Loukas and Prof. Pierluigi Claps who kindly agreed to revise this dissertation contributing to its improvement.

I owe a lot to all of my colleagues, for their friendship and their patience in helping me dealing with the daily difficulties. Thanks for contributing immensely to my personal and professional growth.

Last but not the least, I would like to thank my husband, my parents and my friends for supporting me every day of my life.

Data providers are acknowledged: SIAS (Servizio Informativo Agrometeorologico Siciliano) of Sicilian Region, WCRP CORDEX (Coordinated Regional Climate Downscaling Experiment).

Contents

List of Figures

List of Tables

List of Symbols

t	Time	[s]
w	Soil water Content	[%]
n	Parameter in the soil water retention function	[−]
Ks	Saturated hydraulic conductivity	[m/s]
l	Mualem's pore connectivity exponent	[−]
ET	Evapotranspiration	[mm]
Ra	Extraterrestrial radiation	[$MJm^{-2}d^{-1}$]
T	Temperature	[C]
NSE	Nash-Sutcliffe index	[−]
$NNSE$	Nash-Sutcliffe normalized index	[−]
$q(h)$	discharge rate	[s]
RV	Retained volume	[%]
PFR	Peak flow reduction	[%]
PFL	Peak flow lag-time	[min]
E_{m}	Percentage error	[%]
I	Sorting parameter	[−]
I	Sorting parameter by classes	[−]
θ	Volumetric water content	[%]
θr	Residual soil water content	[%]
θs	Saturated soil water content	[%]
α	Parameter in the soil water retention function	[m^{-1}]
μ_{m}	Mean	[−]
σ_{m}	Standard deviation	[−]
ϵ_{m}	Error metrics	[%]

To you.

From heaven you guided
and protected me.

Chapter 1

Introduction

1.1 Background

Human's impact on planet Earth has increased rapidly after the industrial revolution, inducing several of environmental problems. Urbanization has been mostly uncontrolled in many parts of the world, implying an increase of impervious surfaces and a drastic decrease of green surfaces, causing urban runoff and heating issues.

Preserve natural landscapes, biodiversity and natural cycles is of fundamental importance. For this reason the necessity to find alternative solutions to the reduction of impacts of urbanization arose.

Climate change has shown its effects in an increasingly evident way and, certainly, the Mediterranean area has not been excluded from the impacts. The Mediterranean region, given its location in a transition zone between the arid climate of North Africa and the temperate and rainy climate of central Europe, is affected by interactions between mid-latitude and tropical processes.

Because of these features, even relatively minor modifications of the general circulation can lead to substantial changes in the Mediterranean climate. This makes the Mediterranean a potentially vulnerable region to climatic changes (Giorgi and Lionello, 2008).

One of the main risks this area faces is flood risk. Short but increasingly intense rains have been recorded in recent decades in many locations in the Mediterranean also following long periods of drought. The cities in the area are often plagued by sudden and intense floods and urban drainage systems are not always able to cope with the emergency.

In this scenario, mitigation and adaptation actions are essential to reduce the impacts of climate change.

In general, adaptation refers to adjustments in ecological, social, or economic systems in response to actual or expected climatic stimuli and their effects or impacts. It refers to changes in processes, practices, and structures to moderate potential damages or to benefit from opportunities associated with climate change. In simple terms, countries and communities need to develop adaptation solution and implement action to respond to the impacts of climate change that are already happening, as well as prepare for future impacts.

Adaptation solutions take many shapes and forms, depending on the unique context of a community, business, organization, country or region. There is no 'one-size-fits-all-solution'—adaptation can range from building flood defences, setting up early warning systems for cyclones and switching to drought-resistant crops, to redesigning communication systems, business operations and government policies. Many nations and communities are already taking steps to build resilient societies and economies, but considerably greater action and ambition will be needed to cost-effectively manage the risks, both now and in the future (*UNFCCC*).

The concept of Green Infrastructures is born by this necessity and it allows to contrast many aspects of the mentioned problems. Green infrastructures are strategically planned networks of natural and semi-natural areas with other environmental elements, designed and managed in such a way as to provide a broad spectrum of services ecosystems.

The green infrastructure network seamlessly penetrates the entire territory creating continuity, functionality and eliminating barriers and waste. Nature, no longer reduced to object of consumption and only for aesthetic use, it recovers and focuses on the role of supplier of vital resources and balancing of global stability and sustainability (Commissione Europea, 2013).

The U.S. Environmental Protection Agency (EPA, 2015) has also identified Green Infrastructures as contributors to improved human health and air quality, lower energy demand, reduced capital cost savings, increased carbon storage, additional wildlife habitat and recreational space,

and even higher land-values of up to 30%.

Focusing on green infrastructure in an urban context the main benefits found in different parts of the world are reduction of the urban heat island effect, improvement of biodiversity in urban areas, reduction of surface runoff, and a contribution for sustainable drainage.

For the flood risk in urban areas green infrastructures have shown in numerous studies their significant ecological importance in urban areas given their ability to quickly infiltrate rainwater, reduce the runoff in the catchment area, and decrease runoff peak flows that may otherwise result in high influent flows to water reclamation plants (WRPs) and affect operations or cause local flooding and combined sewer overflow.

Several types of green infrastructures do exist, each with pros and cons. One of the most important type is that of green roofs, i.e. building roofs, that in contrast to traditional ones, present a vegetated covering producing several water and energy benefits.

The starting point of this dissertation is the construction of an instrumented green roof laboratory at the Campus of University of Catania. It was possible to carry out analyses to test this infrastructure as a tool of adaptation to climate change, in a Mediterranean area such as Eastern Sicily (Italy) and in an urban area like the city of Catania. In particular, we focused on this type of green infrastructures and its positive impacts on the urban water cycle in a climate change scenario.

1.2 Motivation of this research

As already briefly mentioned, this research stems from the need to test green roofs as a possible solution for adaptation to climate change in a Mediterranean area such as that of Eastern Sicily. Adaptation choices will play an increasingly crucial role from now on and it is essential to understand which are the best infrastructures depending on the area and the climatic scenario.

This research is set within a constantly evolving scenario of this sector. In fact, since the 1960s, the number of researches and articles has grown exponentially.

Green roofs have a potential for providing an attractive green space in downtown areas where the green space on the ground is limited or simply non-existing. The design of green roofs varies between different localities and depends on the roof purpose. The green roofs are often established because of aesthetic reasons.

The green roofs were used for isolation purposes in Nordic countries centuries ago. In Germany, the green roof movement started in late 1970s bringing research on biodiversity, roof construction, technology and substrates contributing to the development of the modern green roofs and design guidelines. In Switzerland, Basel, the construction of green roofs on newly built or renovated buildings with flat roofs is enforced by legislation.

The performance of green roofs in urban environment towards achieving various benefits is a hot-topic with new discoveries every year. The more investigations are made on green roofs performance in urban environment the more research needs are identified.

Green roofs are typically divided into two main engineering categories: intensive and extensive. Intensive green roofs are established with deep soil layers; they can support larger plants and bushes and typically require maintenance in the form of weeding, fertilizing, and watering. Extensive vegetated roofs are established with thin soil layers. They are planted with smaller plants which in the final stage are expected to provide full coverage of the vegetated roof (Czemiel Berndtsson, 2010).

The graph (Figure 1.1) clearly shows the evolution of green roof research. If, at first, the greatest interest was turned to the structure and architecture of green roofs, from 2005 the research has diversified into various sectors and in energy efficiency and heat reduction, in the control of pollutants and urban wastewater management.

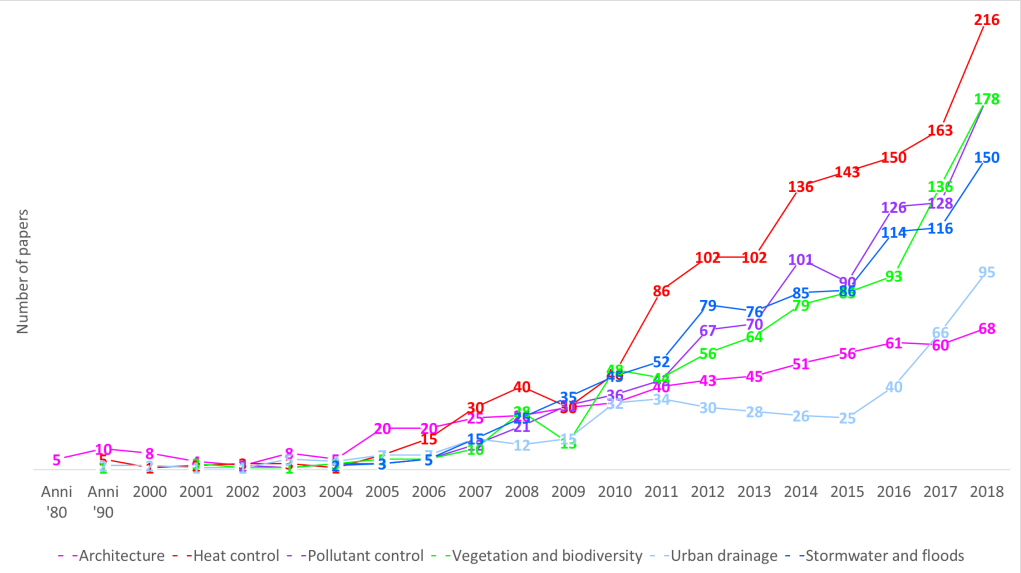

FIGURE 1.1 Evolution of green roof research, with numbers of papers in each field of research.

It is interesting, however, to correlate the study of the green roof as a rainwater retention tool with climate change and their evolutionary scenarios in the coming decades. From this perspective, literature is lacking. On the one hand this area of research is constantly growing, but on the other hand still few studies have focused on the study of these infrastructures in combination with future climate scenarios.

For this reason, this study does not stop only at evaluating the water retention capacity of the roof but uses some scenarios, global and regional circulation models (GCM-RCM models), to try to predict the response of the roof in the climate of the next future.

1.3 Aims and methods

1.3.1 Objectives

The general objective of this research is to define tools and methodologies to ascertain the efficiency of Green Infrastructures as a tool for adapting to climate change with specific reference to urban areas in the

Mediterranean, and, subsequently, the definition of a model on single-infrastructure-scale, an extensive green roof, for the analysis of the impacts of climate change on the hydrological-hydraulic response.

The goal to reach is evaluate the efficiency of green roofs in the current and future climate to mitigate the risk of urban flooding, in order to understand the role of green infrastructures as adaptation method to climate change. To do this, it was necessary to go through some phases with specific objectives.

First of all, to be familiar with the context in which this analysis was taking place, it was necessary to understand the role of flood risk in the daily life of the area, not only with meteorological data, but also involving the population. The goal was to understand the perception of flood risk and climate change that currently concerns this area of the Mediterranean with the aim of analysing how much residents feel the need for adaptation measures.

Once the first specific goal has been achieved, another goal was certainly to create a physically-based model of a single infrastructure in order to analyze the hydrological-hydraulic response of the green roof. To do this it was necessary to carry out both an experiment phase and a modeling phase.

Wanting to advance the research not only in the current state but also in a future scenario characterized by climate change, it was necessary to analyze the GCM-RCM circulation models. Therefore, two statistical analyses were carried out with the aim of ascertain the quality of the models and the goodness in the reproduction of rainfall and temperatures at different time scales. The final goal, before implementing the climate scenarios on the model, was to make sure that we could use the global and regional circulation models to obtain valid results. Assembling the results achieved with the different steps of the study, it was possible to achieve the general objective of this research.

1.3.2 Methodological approach

The methodological approach for the study presented in this dissertation did not follow a unitary path, as briefly mentioned in the previous paragraph, but consists of different phases all aimed at achieving the general goal. The general context concerns the climate change, which, in recent decades, is bringing numerous changes in the natural hydrological cycle. The cities of the Mediterranean area are increasingly affected by sudden and very intense storms. In this regard, the need to choose adaptation measures to ensure that the impacts are attenuated and therefore the dangers decrease is born.

It is necessary to take into account that it is difficult to have completely reliable predictions in a constantly evolving climate scenario and for this reason we rely on various circulation models which, however, must be tested according to the area of interest. In view of this, in order to study green roof as a solution for adaptation to climate change, it was interesting to understand how much the population feels the need for it. We investigated the perception of urban flood risk and climate change to understand how well the resident population is actually prepared to face the problem. So, as a background to all this research, a part was dedicated to the investigation of the perception of risk of urban floods in the eastern area of Sicily (Italy).

This part of the study aims at understanding, with reference to the Simeto River Valley (SRV) area in Sicily: what is the current level of worry of the population about the climate change; the level of individuals' risk preparedness (short-term preparedness); people's willingness to invest as individuals and as a community in climate change adaptation infrastructures for sustainable urban drainage.

We analysed the results of a 10-question survey on climate change and risk perception, in 11 municipalities of the Simeto River Valley (SRV) carried out within the activities of the LIFE project SimetoRES. This part of the research was fundamental to contextualize the subsequent analyses, once it was ascertained that in a Mediterranean area, such as that of eastern Sicily, there is a need for new adaptation measures.

Later the modeling part was carried out. This part of the study is divided into two types:

- Experimental: with the Green Roof on Building 15 of the University Campus;
- Modeling: starting from experimental data and climatic data for the creation of a model on a single infrastructure scale.

The experimental part involves the green roof (extensive type) of Catania University. In 2017, Catania University (UNICT) started planning the realization of a new building at "La Cittadella" campus (building 15), designed in order to allow the implementation of a green roof on the above terrace.

In June 2018, a sponsoring contract was signed between UNICT and Global Water Partnership (GWP), with a funding for the green roof realization and the monitoring instrumentation installation related to the project Non-Conventional Water Resources, financed by The Coca Cola Foundation and coordinated by GWP. In September 2018 the green roof was completed and in March 2019 the instruments were installed, and testing started. The monitoring system is composed by a meteorological station, a "master station" and a "slave station". The single components of the monitoring system are rain gauge, combined anemometer, thermo-hygrometer, pyranometer and TDRs probes.

The final configuration includes the Master station, in the South-West area of the Green Roof, the Slave station, located in the opposite direction, in the North-East area, and the Meteorological station, located at East of the Green Roof (for more details see paragraph 4.3.2).

The modeling activities takes place with HYDRUS-1D software. HYDRUS computer code, which numerically solves the Richards equation for variably-saturated water flow and advection dispersion type equations for heat and solute transport. The flow equation incorporates a sink term to account for water uptake by plant roots. The flow equation may also consider dual-porosity type flow in which one fraction of the water content is mobile and another fraction immobile, or dual-permeability type flow involving two mobile regions, one representing the matrix and one the macropores.

In order to test the effectiveness of the green roof also in the future, the model will have to run onto the evolutionary climate scenarios of the coming decades. However, to do this, it is necessary to make an assessment on the models that reproduce the climatic conditions in the Mediterranean area. For this reason, we conducted a research on global climate models combined with regional climate models (GCM-RCM) of the CORDEX project.

The CORDEX Regional Challenges provide a focus for downscaling research and a basis for making use of CMIP6 global climate model (GCM) output to produce downscaled projected changes in regional climates and assess sources of uncertainties in the projections, all of which can potentially be distilled into climate change information for vulnerability, impacts and adaptation studies (Gutowski Jr. et al., 2016).

This part of the study was split into two different analyses for the ultimate goal of this research. The first study analyses climate models to evaluate their reliability in the reproduction of rains, temperatures and periods of drought in the regions of Calabria and Sicily. The second study, with reference to 14 rain gauge stations in Sicily (Italy), evaluates historical simulations of precipitation data from 11 RCMs, in order to understand how they compare to fine-resolution observations.

In particular, we investigate the ability to reproduce rainfall event characteristics, as well as annual maxima precipitation at different durations. The proposed analysis highlights the differences between the different models, and, by ranking the RCMs, supports the selection of the most suitable climate model for assessing the impacts in the considered locations in terms of extreme event analysis.

Finally, with the results achieved, it was possible to conduct the final analysis of the research. To get the most reliable models possible, the RCM models have been corrected with the quantile-quantile mapping method. Subsequently, analyzes from the application of the RCM models on the green roof model were conducted.

First, a comparison was made between the output volumes and the rainfall peaks of the rain events belonging to the historical data and between those belonging to the scenarios data. Once it was ascertained that climate change negatively affects rain events, we proceeded with the

evaluation of the role of the green roof in these scenarios and finally, it was possible to obtain an evaluation of the efficiency of the green roof. For a clearer outline of the methodology and of the steps followed in this research, look at the flow chart in Figure 1.2.

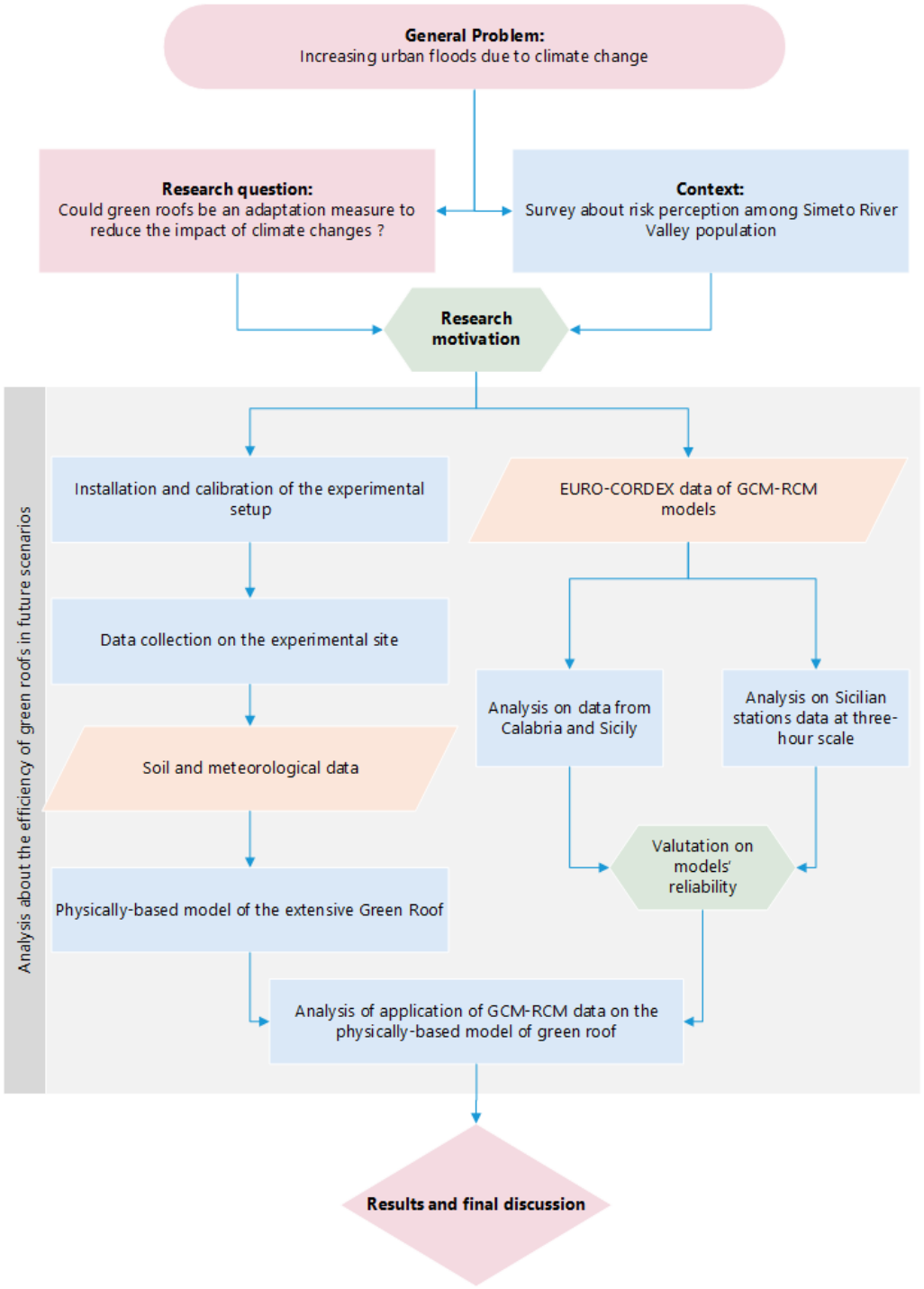

FIGURE 1.2 Outline of the methodology.

1.4 Outline of this thesis

This work is articulated in eight chapters, this introduction included as the first chapter.

The second chapter presents the state of the art. It was essential to know the different studies developed on green infrastructures, in particular on green roofs. Other studies on climate change, and how they affect urban floods, are also important for the background of this project. The evolution of research in the sector, the basic studies on green roofs, their history and their development, and in particular the studies on the hydrological response for stormwater retention, are exposted.

The third chapter deals with climate change and flood risk focusing on the results of a 10-question survey on climate change and risk perception, in 11 municipalities of the Simeto River Valley (SRV) carried out within the activities of the LIFE project SimetoRES.

The fourth chapter propose the methodology for the analysis on the green roof and in particular the part linked to the experimental site. The structure of the green roof and the chosen and installed vegetation is described in detail in this chapter. Then follows the complete description of the monitoring system and the data collection system, used for the collection of soil data and meteorological data.

In the fifth chapter the physically-based model is discussed. Before moving on to purely computational modeling, some laboratory tests were carried out to identify the hydraulic parameters of the soil. After the laboratory tests an heuristic calibration was carried out in order to best reproduce the hydrological-hydraulic response of the green roof. Finally, the efficiency of the green roof on the rainfall events from May 2019 to April 2021 was analyzed.

The sixth chapter relates to the part of the study on the GCM-RCM models. This chapter is divided into two parts, but both are aimed at ascertaining the reliability of the use of these models in research in the Mediterranean area.

The results of this study are presented in the seventh chapter. After presenting the correction with the quantile-quantile mapping method,

the chapter proceeds by presenting the results obtained first by comparing the historical events and showing the peak and volume reduction capacity of the green roof and then going to evaluate how much the peaks and volumes are affected by climate change. Once it is ascertained that climate change actually has a negative impact, the analyzes with the implementation of the green roof in order to evaluate its efficiency are presented .

The last chapter presents the conclusions. The results obtained from this study are discussed and a summary of all the work is presented. Some ideas for the future continuation of the research are also proposed.

1.5 Limits of the work

This study has some limits due both to the experimental setup and to the data used in the analyzes. The experimental site of the University of Catania certainly represents a reference point for the study of green roofs in the Mediterranean area. However, due to the very recent construction of this infrastructure, not all the necessary equipment has been installed.

Outflow measurement probes are still missing, which would allow for more accurate outflow data. In this analysis, the modeling was developed thanks to the TDR sensors and the calibration of hydrological-hydraulic parameters of the soil. Therefore the outflow rate of the traditional terrace and the green roof is only simulated by the software and is not measured with an instrument.

The data used to simulate the behavior of the green roof with climate change belongs to the EURO-CORDEX project. These data complement the GCMs with reduced data on a regional scale (RCM). However, in order to study short and intense rain events it was necessary to use a very short time scale (3 hours scale).

Globally, there is uncertainty about the reliability of small-time scale GCM-RCM data. There is some literature that does not believe that these data are reliable. However in this study, in order to use these data, a bias correction (widely approved in the literature) was carried out which takes the real data as a reference.

Chapter 2

State of art

2.1 Overview

This chapter shows the state of the art. First of all we investigated the studies on climate change, and how they affect urban floods, which are important for the background of this project. The numerous studies on natural hazard and on climate change perception were also examined. Then, to undertake this research project it was essential to know the different studies developed on green infrastructures, in particular on green roofs. The evolution of research in the sector of green infrastructures, the basic studies on green roofs, their history and their development, and in particular the studies on the hydrological response for stormwater retention, are detailed here.

2.2 Impacts of climate change on urban floods

Climate change (CC) is a major societal risk issue and there are increasing calls for urgent mitigation and adaptation actions (Spence, Poortinga, and Pidgeon, 2012). Over the last decade, many studies have highlighted the importance of adaptation by testing ecosystem-based approaches as a means of understanding and improving the integration of such approaches into climate change adaptation and mitigation strategies (Naumann, Gerardo, and Berry, 2011; Prutsch et al., 2014; Demski et al., 2017; Sussams, Sheate, and Eales, 2015).

A number of trends suggest that the problem of urban flooding is likely to increase (Hammond et al., 2015). The first of these is the growing

number of people that live in cities. The second trend arises from the climate change that lead to more extreme rainfall. Some studies have already shown statistically significant trends in extreme rainfall in the past century in Denmark (Arnbjerg-Nielsen, 2006), and in North America (Peterson et al., 2008).

The traditional approach to urbanization based exclusively on impervious paving of surfaces and stormwater management relying on grey infrastructures (sewers), is not sustainable and thus is no longer compatible with climate change adaptation strategies (Du et al., 2012; Palla et al., 2011; Haghighatafshar et al., 2020). The increasing urbanization leads to a greater share of impervious areas that result in increased flood risk and overloaded storm water pipe systems. For this reason, blue-green storm water and nature-based solutions have come to be seen as efficient measures against increasing flood risk in urban areas (Hammond et al., 2015; Haaland and Bosch, 2015; Berndtsson et al., 2019).

Flood risk may be defined as the product between the probability of flood hazard and the consequence of occurrence of flood event (Saidu and Lal, 2015) according to

$$Flood\,risk = probability\,of\,flood \times consequence\,of\,flood\,event \tag{2.1}$$

where consequence of occurrence of flood event is a function of hazard × vulnerability, the latter here including both exposure and susceptibility of harm. Several studies state that current understanding of flood risk focuses on two main factors: climate change and socioeconomic growth (Saidu and Lal, 2015; Berndtsson et al., 2019; Jongman, Ward, and Aerts, 2012).

The risk of flooding for city population has been generally increasing in the past decades, and not sufficiently contrasted in terms of retrofitting urban drainage systems to urban expansion, mainly because of the significant monetary investments needed, which are not sufficiently stimulated by citizens and local administrators due to low awareness of the issue (Petry, 2002; Meyer, Priest, and Kuhlicke, 2012).

In addition to mitigation and adaptation measures, other measures

contribute to solving the problem. Soft measures (i.e., non-infrastructural) oriented to increase risk awareness and preparedness of the population at all levels are of key importance, also given the comparatively low investments needed with respect to hard (i.e., infrastructural) urban flooding mitigation measures. In fact, education to flood risk awareness and preparedness has led to many benefits in several cases (Salvati et al., 2014). In this thesis the part concerning the risk awareness and perception is deepened in Chapter 3.

2.3 Natural Hazard Risk and Climate Change Perception

Early analyses of risk from natural hazards focused on the search for physical and tangible causes, while recently risk awareness has been gradually incorporated in several studies (Avvisati et al., 2019; Davis, Ricci, and Mitchell, 2005; Paton and Johnston, 2001; Ricci, Nave, and Barberi, 2013; Wachinger and Renn, 2010). Focus has been put, particularly, on the risk of floods and landslides (Salvati et al., 2014; Diakakis, Priskos, and Skordoulis, 2018; Gravina et al., 2017; Raaijmakers, Krywkow, and Veen, 2008; Shen, 2009).

The spectrum of risk perception in natural hazards includes three distinct elements: worry, awareness, and preparedness (Raaijmakers, Krywkow, and Veen, 2008; Lechowska, 2018; Bouman et al., 2020; Whitmarsh and Capstick, 2018; Linden and Linden, 2017). In particular, according to Raaijmakers et al. (2008), the following definitions can be given, which we use within this study: worry is the level of dread or concern associated with the given risk (climate change or urban flooding); awareness can be defined as knowledge or consciousness of the risk that an individual or a group of individuals is exposed to; preparedness is both the capability of coping with a flood throughout the inundation period, and post-flood recovery capability and strategies, and can be described in social, technical, economic and institutional dimensions.

Bubeck et al. (2012) suggest that the relationship between individual flood risk perceptions and mitigation behavior is hardly observed in

empirical studies. Other research has included the social perception of risk by using approaches that combine data on physical processes with individual interpretations of the risk (Bubeck, Botzen, and Aerts, 2012; Capstick et al., 2016; Morton et al., 2011; Johannesson et al., 2017).

At a national scale, investigators have estimated the individual and collective risk posed by landslides and floods to the population (Guzzetti, Stark, and Salvati, 2005), though the assessment of public perception of the risk posed by landslides and floods in Italy remains mostly unexplored. A number of studies have been focused on the use of specific surveys to investigate natural hazard risk perception.

For example, Avvisati et al. (2019) carried out a study of multi-risk perception in 12 municipalities and 2 territorial unions of Campania Region characterized by different risks: seismic, volcanic, hydrogeological (floods and landslides). The results showed that historical memory plays a crucial role in the perception of natural hazards.

On the other hand, looking at studies related to Europe, Diakakis, Priskos, and Skordoulis (2018) administered questionnaires to the population of the Attica Region in Greece, to obtain basic information on how individuals understand flood risk, risk mitigation and to what degree they take protection measures, investigating on which degree they trust relevant institutions and their awareness of flood warning and flood protection actions. Their results showed that respondents rank floods third in terms of importance behind earthquakes and forest fires among the more relevant risks in the region, despite the clear majority believed the risk is increasing, mostly due to anthropogenic factors. Responses illustrated low levels of trust in authorities and low levels of knowledge of protection actions and awareness regarding floods, as well as low levels of preparedness, in terms of undertaking private mitigation measures.

Other studies claim that the communication of information about natural hazard risks to the public is a difficult task for decision-makers. Feldman and Hart (2016) suggest that newer forms of technology present useful options for building disaster resilience and that age is the central factor in predicting the sources people use to receive risk information.

The literature concerning the perception of climate change has developed mainly in the last decade. Van Der Linden (2014) claims that climate

change compared with many other hazards is therefore relatively unique: not only because of its scope and breadth but also in the sense that it is not directly "situated" in our daily environment (Helgeson, Linden, and Chabay, 2012).

Nevertheless, an increasing amount of research has shown that people can (to some extent) accurately detect changes in their local climate and relate this perceptual experience to climate change (Akerlof et al., 2013). Moreover, the rising incidence rate of extreme weather events is now increasingly being associated with climate change (Coumou and Rahmstorf, 2012). In fact, a number of studies have indicated that personal experience with extreme weather events is a significant predictor of climate change risk perceptions (Akerlof et al., 2013; Brody et al., 2007; Krosnick et al., 2006; Spence et al., 2011).

The link between the various facets of risk perception (worry, awareness, and preparedness) is difficult to capture. In particular, as reviewed by Miceli, Sotgiu, and Settanni (2008), the literature reports either indifference or positive association between worry about risk and preparedness against it. Hence, further contributions to this aspect are important.

2.4 Green infrastructures for urban risk reduction

The progressive urbanization combined with climate change is causing through years consequences on the hydrological cycle. In particular, the increase of impervious surfaces is having a strong impact on this cycle, amplifying the risk of urban flooding (Li et al., 2019; Palla et al., 2011; Czemiel Berndtsson, 2010). Urban hydrological systems have been affected by this increasing imperviousness, as evidenced by increased surface runoff and peak flow, decreased rainwater infiltration and groundwater recharge, and deterioration of water quality (Bell et al., 2016; Chen et al., 2017; Du et al., 2012; Valtanen, Sillanpää, and Setälä, 2014; Yang et al., 2011). As mentioned before, the risk of urban flooding may be amplified due to the climate change combined with increasing occurrence

of heavy rainfall events and the insufficient capacity of drainage systems (Tao et al., 2014; Wu et al., 2012).

"Grey" infrastructures are conventional storage structures (reservoirs, detention ponds) and conveyances (pipes, canals) used to manage drinking, sewer, or storm water usually constructed of concrete or metal; also including streets, roads, bridges, and buildings that do no incorporate technologies intended to achieve environmental goals. Grey infrastructures focus on the reduction of the peak runoff discharge rate by removing water quickly from a site (Li et al., 2019), but rapid discharge of stormwater accelerates channel erosion and pollutant transport downstream (Bledsoe and Watson, 2001).

Therefore, several different strategies and technologies have been developed in some countries, such as the low impact development (LID) in the United States, the water sensitive urban design (WSUD) in Australia and the Sponge City in China, which providing a broader framework with a holistic urban water cycle for stormwater management issues (Huang et al., 2015).

There is no single, universally accepted definition of Green Infrastructure but with reference to the available literature, and according to several projects being undertaken by the European Commission, the following definition was agreed: "Green infrastructure is the network of natural and semi-natural areas, features and green spaces in rural and urban, and terrestrial, freshwater, coastal and marine areas, which together enhance ecosystem health and resilience, contribute to biodiversity conservation and benefit human populations through the maintenance and enhancement of ecosystem services. Green infrastructure can be strengthened through strategic and coordinated initiatives that focus on maintaining, restoring, improving and connecting existing areas and features as well as creating new areas and features." (Naumann, Gerardo, and Berry, 2011).

Among these strategies, the green infrastructure (GI), as an innovate stormwater management approach to mitigate urban hydrology and water quality issues, has been widely applied in many cities around the world (Ahiablame, Engel, and Chaubey, 2013; Liu et al., 2015; Wright et al., 2016). GI practices implement some on-site infrastructures that work

with nature to reduce the stormwater runoff and improve water quality from sources using landscape natural features (Ahiablame, Engel, and Chaubey, 2013; Dhakal and Chevalier, 2017; Liu, Chen, and Peng, 2014; Vogel et al., 2015).

Thus, GI practices can maintain the site's pre-development hydrological features or reduce the impacts of post-development on urban hydrology. The concept of Green Infrastructures is generated by this necessity and it allows to contrast many aspects of the mentioned problems, with the following main benefits: reduction of the urban heat island effect, improvement of biodiversity in urban areas, reduction of surface runoff, and a contribution for sustainable drainage (Sussams, Sheate, and Eales, 2015).

The U.S. Environmental Protection Agency (EPA) has also identified Green Infrastructures as contributors to improved human health and air quality, lower energy demand, reduced capital cost savings, increased carbon storage, additional wildlife habitat and recreational space, and even higher land-values of up to 30%.

Green infrastructure systems help protect and restore naturally functioning ecosystems by providing a framework for future development that fosters a diversity of ecological, social, and economic benefits. These include enriched habitat and biodiversity; maintenance of natural landscape processes; cleaner air and water; increased recreational opportunities; improved health; and better connection to nature and sense of place. Green space also increases property values and can decrease the costs of public infrastructure and services such as, flood control, water treatment systems and storm water management (Eckart, McPhee, and Bolisetti, 2017).

A universal set of typologies cannot be proposed but most studies have grouped GI into four high level categories: tree canopy, green open spaces, green roofs and vertical greenery systems (Bartesaghi Koc, Osmond, and Peters, 2017). This proposed classification doesn't include for example these other particular green infrastructures selected by Li et al. (Li et al., 2019) that are widely used for example bioretention or permeable pavement.

A report to the European Commission (Naumann, Gerardo, and

Berry, 2011) underlines the characteristics that a green infrastructure tends to emphasize, as:

- Critical mass. To be defined as such, the components of green infrastructure normally have some degree of scale, critical mass and/or connectivity. Thus, while an individual tree may be a component of green infrastructure, it is not normally recognized as such unless it forms part of a larger habitat, green area, corridor or network that serves a wider function.

- Benefits to people. Definitions of green infrastructure tend to stress the benefits and services that green spaces, semi-natural areas and features provide to people, i.e. their contribution to the delivery of ecosystem services;

- Multi-functionality. Green infrastructure is normally recognized as serving a variety of functions for both people and nature, and not just meeting single objectives such as nature conservation or public recreation.

- Substitutability with grey infrastructure. The term "infrastructure" implies that green infrastructure is a capital asset that requires investment and maintenance in order to deliver services to society. It has the potential to replace some of the functions that would otherwise be served by man-made or "grey infrastructure", such as flood defenses, water treatment and pollution control plant, and recreational infrastructure.

- Co-ordinated interventions. Green infrastructure is often defined by human interventions which aim to identify map, protect, restore, enhance or maintain it. In this sense green infrastructure may only be defined as such when it is included as part of a green infrastructure initiative or project.

2.5 Green roofs

2.5.1 Green roofs: history and development

A green roof is a rooftop vegetation that provides ecological value and habitat, reduces runoff, and enhances building performance. Commonly construction of green roofs involves four layers: drainage material, filter preventing the loss of soil particles, soil substrate and vegetation (Li and Yeung, 2014).

Green roofs are usually classified as either extensive or intensive depending on the thickness of the growing substrate layer. Extensive roofs are implemented more often since they are cheaper, lighter and require less maintenance compared to the intensive roofs. Extensive roofs have a substrate of 15 cm maximum, feature short rooting, drought resistant plants, instead intensive roofs have substrates of more than 15 cm and may feature deeper rooting plants (Carson et al., 2013).

Due to multiple benefits, green roofs are being implemented in many countries. More research is going on the implementation and performance of green roofs in different regions around the world. In recent decades, green roofs proved as the sustainable practices and have gained much popularity around the globe. Research on the green roofs shows numerous social, environmental and economical benefits. Significant evidence shows that green roofs can give multiple benefits, such as stormwater management, reduced urban heat island, increased urban plant, wildlife habitat and roof life, enhance the air and water quality and quality of life, decreased the energy consumptions costs of the building, decreased the noise pollution, procreates the recreational activities and increased the green areas and aesthetic value in urban environments. (Karteris et al., 2016; Theodosiou, 2009)

As the result of water quality enhancement, green roofs decrease the burden of the water treatment facilities in an area. Due to the above benefits many countries started to implement the green roofs in buildings. As the result of this more and more green roofs are established day by day around the globe (Shafique, Kim, and Rafiq, 2018).

Green roofs at the building rooftop are old techniques. At ancient times people constructed the green roofs on the rooftops as the rooftop

gardens for insulating qualities and to reduce the adverse effects of urbanization. One of the most famous ancient green roofs was the Hanging Gardens of Babylon constructed around 500 BC. Recently, many countries (Sweden, Finland, Iceland, Denmark, Norway, Greenland, Vinland and the Faeroe Islands) people tend to cover their rooftops with sod during the extreme climatic conditions. However, the present green roofs are the more efficient and effective due to the proper design and specifications used.

The modern green roofs started from Germany in the early 1960s when there were energy crises. Germans started constructing green roofs to reduce energy consumptions in the buildings. In modern green roofs, Germany is known as the world leader of green roofs, because green roofs on the large scale were being developed, designed and implemented (Zhang et al., 2015). In 1962, a German researcher, Reinhard Bornkamm, published his work on green roofs.

New development of roof gardens was initiated by BDLA at the Deubau trade fair in Essen in 1973. In the early 1980s, green roofs market expanded quickly, many green roofs were constructed in Germany and Forschungsgesellschaft Landschaftsentwicklung Landschaftsbau (FLL) published guidelines for constructing green roofs in the German language. In Germany, more than 10% of the buildings use green roofs practices for multiple benefits. Since most of the research and studies of green roofs were in Germany, Scandinavia, and Switzerland and also reported in their own languages other than English, therefore green roof information not readily available internationally. However, after the green roofs applications initiatives, green roofs become popular all around the globe. Nowadays, research and application of on green roofs at the building in Germany are very popular and green roof coverage is increasing by approximately 13.5 million m^2 every year.

Guidelines for green roofs were released by association of Standards and Testing Materials (ASTM) in 2005 and 2006, in which the construction of green roofs explained in detail. FLL published the latest guidelines for the planning, execution and upkeep the green roof sites. In 2009, USEPA report also released in which the construction and benefits of green roofs explained. More research of green roofs guidelines, implementing and

maintenance of green roofs was conducted in the USA and shared with other countries for implementing the green roofs. Nowadays, countries like USA, Canada, Singapore, Australia, Japan, China, Hong Kong and South Korea are making a strong initiative to apply the green roofs at the new as well as existing buildings to achieve the multiples benefits.

In Toronto Canada, building with the floor area of about 2000 m^2 mandate to apply the green roofs on 20–60% of the total roof area. In Japan, all the new construction should use the green roofs. Public buildings larger than 250 m^2 and private buildings larger than 1000 m^2 must green 20% of the rooftop or pay 2000 USD annually. In Portland, USA, 70% of the areas of all new buildings must use green roofs. In Portland, there were approximately 2 acres green roofs in 2005 and also more green roofs committed to build to achieve the multiple sustainable benefits. In China and Hong Kong, governments are encouraged to apply the green roofs as the green practices. In South Korea, the government is encouraging the public, private sector and stakeholders to apply the green roofs to make cities safe, sustainable and resilient to climate change (Shafique, Kim, and Rafiq, 2018).

Recently, more research on the green roofs include the country climate and building characteristics for the more efficient performances at different locations. Nowadays, the more research focuses on new, low cost or new innovative design of green roofs that can give multiple benefits practically on a large scale. With these successful implementations of green roofs in the USA and European countries, green roof research gaining more consideration to the rest of the world.

2.5.2 Green roofs: Stormwater retention

Green roofs are one of the best stormwater management practices in urban areas because the vegetation and substrate layers have abilities to store a large amount of water (Liu, Chen, and Peng, 2014; Stovin, Vesuviano, and Kasmin, 2012). As a result of this, the chances of flash flooding decrease in urban area thanks to their contribute to hydrological and hydraulic invariance. Vegetation and plant increases the evapotranspiration and growing medium absorbs a large amount of rainwater, this causes

the reduction in peak flow and runoff. The runoff reduction depends on the many factors which include the type of vegetation, thickness of growing medium, type of drainage material, rainfall intensity and slope of the green roof. The most important part is the substrate of green roof and it should have high moisture holding capacity to store more rainwater.

Maiolo et al. (2017) to assess the sustainability of the life cycle of a green roof materials and permeable pavement chose to identify a significant synthetic index. The synthetic index has been used to compare the environmental performance of the green roof and permeable pavement. The scores used are correlated to several layers of the LID (permeable pavement and green roof) and each is attributed a weight that summarizes its ability to contribute to hydrological and hydraulic invariance.

Razzaghmanesh and Beecham (2014) studied various indigenous Australian ground covers and grass species. From the result authors identified that Carpobrotus Rossii tolerated hot and dry conditions of South Australia with 100% survival rate and maximum growth. Mickovski et al. (Mickovski et al., 2013) compared the 3 different kinds of vegetations (sedum, long and short grass) to check the performance for surface runoff at different rainfall events. From the results, it is proved that the sedum produced the greater surface runoff volume than other vegetations.

Many authors studied the green roofs hydrological performance in different regions all around the world. Figure 2.1 shows the performance (percentage of water retention) of the green roofs in different countries with ranges from 55% to 78%.

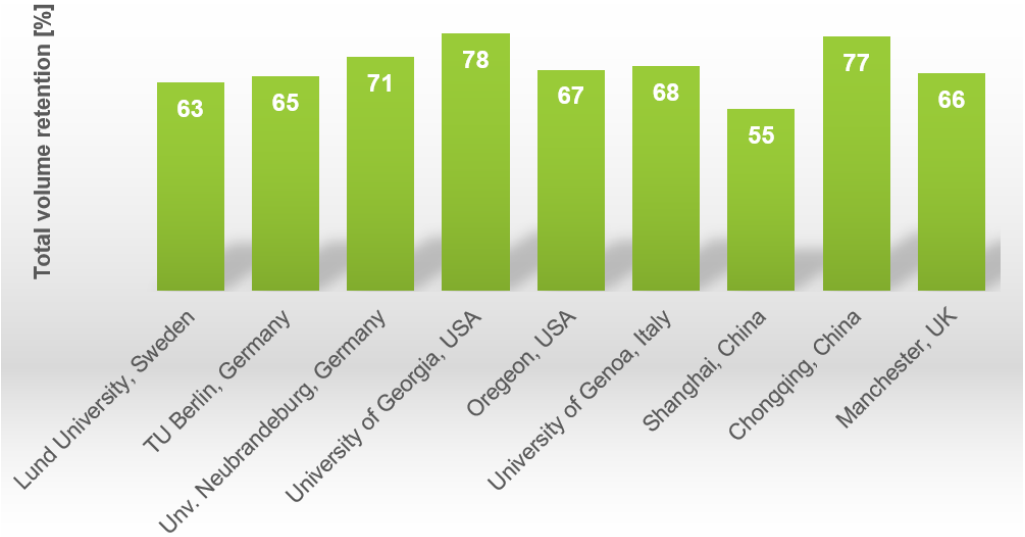

FIGURE 2.1 Performance of green roofs in different countries (Shafique, Kim, and Rafiq, 2018).

Berndtsson, Emilsson, and Bengtsson (2006) studied 3 cm thick sedum-moss roofs for the runoff analysis by using the real and artificial storms events. Results indicated that the green can reduce the runoff and it can be used to control runoff in urban areas. Vegetation of green roof plays an important role in the water retention because every plant has its own water holding and transpiration capacity. studied different plant species to check their relationship with runoff retention. Drainage layer and a green roof slope also affect the water retention from the green roofs.

Carter et al. (2017) indicated that the green roof runoff retention is more than as compared to the existing roof runoff retention. Moreover, peak outflows also reduce by using the green roof. Zhang et al. (2015) examined the stormwater retention capacity by using the green roof in Chongqing, China. Examining 19 rainfall events, the results indicated that the green roof retained the runoff on an average rate of 77.2%. This indicated that the green roofs are a suitable solution for stormwater management in urban areas.

A similar result was found when Speak et al. (2013) conducted the experiment an aged intensive green roof in Manchester, UK. They analyzed the 69 rainfall events; results indicated that the green roofs retained the

runoff 65.7%. Liu, Chen, and Peng (2014) checked the performance of green roof to control a large amount of rainfall runoff in Deakin University, Australia. From the geographic information system (GIS) analysis, the results manifested that the green roofs are very helpful in mitigating of urban flash floods. For the better performance of green roofs in runoff reduction, there is a need to consider all above factors while designing the green roof.

Stormwater retention in Mediterranean climate

In the Mediterranean area, rural abandonment and the rapid urbanisation after the 1950's have led to complex environmental problems, especially the unrestrained urban growth caused excessive pressure on the existing infrastructure, which affects buildings, public transportation, road networks, water quality, waste collection and public health. Green roofs are emerging building technologies that can help communities mitigate some of the above mentioned problems in this area. In Thessaloniki, Greece's second largest city, Karteris et al. (2016) studied the benefits of green roof using GIS to extrapolate the results from the building to the city scale and evaluate carbon sequestration potential, rainwater retention and energy conservation. In regard to rainwater retention, implementation of green roofs in Thessaloniki is estimated to contribute in rainwater retention by almost 45%, allowing more than half of the rainwater precipitation to be reserved at the 50% of the city blocks.

At the experimental site of the University of Calabria Piro et al. (2018) the retained volume, ranging between 15% and 100%, and the peak flow reduction, ranging from 25% to 100%, denote that the weather conditions prior a rainfall event and the hydrological features of the rainfall events itself significantly affect the hydraulic response of a green roof. However the performance of the green roof as a device for storm water control in the Mediterranean area appears good with a mean retained volume value of 57.5% really close to that obtained by Palla, Gnecco, and Lanza (2010).

Palla et al. (2011) studied detailed information about green roof performance in the Mediterranean climate (retained volume, peak flow reduction, runoff delay) to identify a suitable modelling approach for describing the associated hydrologic response. They collected data during

a 13-month monitoring campaign and a seasonal monitoring campaign (September–December 2008) at the green roof experimental site of the University of Genova (Italy). In order to examine the green roof hydrologic response they implemented the SWMS 2D model, that solves the Richards' equation for two-dimensional saturated-unsaturated water flow.

2.5.3 Green roofs: Other benefits

In addition to rainwater retention to reduce peak flow and runoff, green roofs have many other benefits for society and the environment. These include improving water quality, thermal benefits to improve the environment and reduce energy costs, air cleaning for easy comfort in urban areas, noise reduction and other ecological and social benefits. (Shafique, Kim, and Rafiq, 2018)

Green roof substrate and vegetation layers play an important role in runoff reduction and to absorb the different pollutant from the rainwater. Substrate absorbed the pollutants and heavy metals from the rainwater and enhances the water quality. Berndtsson et al. examined the extensive green roof to check the water quality. From the results, it is proved that the ammonia nitrogen percentage in runoff from the green roof is less as compared percentage in rainwater (Berndtsson, Emilsson, and Bengtsson, 2006). The proportions of heavy metals and nitrogen from the green roof runoff depend on the substrate type, the fertilizer used and the age of the green roof (Czemiel Berndtsson, 2010)

Reduction of surface temperature and thermal comfort are also the two important functions of the green roof in urban areas. Green roof vegetation and substrate absorbs fewer solar radiations than the other types of roofs, hence also saving the money use for cooling. A study from the Japan revealed that green roofs can reduce the surface temperature from 30 °C to 60 °C (Yan, 2011). Green roofs are suitable to decrease the surface temperature at cold as well as hot regions. Sun et al. (Sun et al., 2013) studied green roofs at two different locations; at the Tsinghua University in China and at Princeton University in the U.S to analyze the surface temperature variation. However, the results revealed that the

green roofs reduced the surface temperature and heat losses at both sites. To save energy from green roofs depend on many factors, such as the depth and composition of the substrate, the climatic conditions, plant type, type of irrigation, type of green roof and design insulation (Getter et al., 2011).

Green roof has ability to capture the harmful fine dust particles from the air that could help to comfort for human in highly developed urban areas. In urban areas, the air usually contained the fine dust particles that make the urban environment bad and discomfort. Green roofs help to pacify the air pollution by two different ways. First, the plants capture the small air pollutants through stomata (Yang, Yu, and Gong, 2008). Secondly, the green roofs lower the surface temperature which helps in fossils burning to meet energy requirements.

Green roofs also enhance the aesthetic of an area as well as the wildlife (Niu et al., 2010) and provide the relief from the concrete construction by introducing the green space in urban areas. Various studies indicated that the green roofs provide the pleasant effect to the urban inhabitants by reducing the air and noise pollution (Cook-Patton and Bauerle, 2012; Besir and Cuce, 2018; Zhang et al., 2015).

Chapter 3

Climate change and urban floods: an analysis of the perception in the Simeto River Valley

3.1 Overview

In order to study green roof as a solution for adaptation to climate change, it is interesting to understand how much the population feels the need for it. For this reason it is important to investigate the perception of urban flood risk and to understand how well the resident population is actually prepared to face the problem. This chapter deals with climate change and flood risk, but focusing on Eastern Sicily, an area with a typically Mediterranean climate.

Here the results of a 10-question survey on climate change and risk perception, in 11 municipalities of the Simeto River Valley (SRV) carried out within the activities of the LIFE project SimetoRES, are presented. This part of the study aims at understanding, with reference to the Simeto River Valley (SRV) area in Sicily, Italy: what is the current level of worry of the population about the climate change; the level of individuals' risk preparedness (short-term preparedness); people's willingness to invest as individuals and as a community in climate change adaptation infrastructures for sustainable urban drainage.

3.2 Flood events in Eastern Sicily

The urban areas of the Simeto River Valley (SRV), the largest river valley in Sicily (Italy), have been repeatedly hit by intense rainfall events in the last decades that lead to urban flooding, causing several damages and, in some instances, threats to population. The Eastern Sicily has been repeatedly hit in recent years by intense pluvial flooding events, caused by heavy rain in combination with an overwhelmed drainage system. These events proved that it is important to develop strategies with different time horizons and priorities for management alternatives to mitigate pluvial flooding risk.

The city of Paternò, which has about 50,000 residents, has experienced several times pluvial flooding episodes that affected the entire city. For instance, in the fall of 2009 and subsequently, in November 2011, March 2013, and August 2015, this city has been hit by intense rainfall and the city drainage system proved insufficient, with the consequence of flooding of the roadways and damages to public and private buildings. More recently, in October 2018, a flood caused a dangerous situation near the riverbed of the Simeto River, where some houses that fall along the banks had already been invaded by water and mud. The greatest damages recorded were those caused by the overflow of the Simeto River. The waters of the river invaded the Catania-Siracusa Highway, which was temporarily closed. Another event occurred in October 2019, when Paternò and the surrounding cities were hit by a heavy storm. The situation appeared critical and the peripheral roads were invaded by water and mud, a person was trapped in an underpass. Another person was rescued in extremis by a truck driver after his car was left at the mercy of the river of mud with no possibility of movement.

These episodes are just a few of the many signs that reveal the need for a better understanding of the potential risks for people's lives during intense rainfall and consequent flooding. Figure 3.1 shows some images of floods of recent years in the cities of Paternò and Catania.

FIGURE 3.1 Images of the floods of recent years: (a) street of Paternò during the flood of August 2015, (b) square of Paternò during the flood of March 2013, (c) Via Etnea of Catania during the flood of October 2018, (d) Piazza Università of Catania during the flood of October 2018.

3.3 Worry about climate change and urban flooding risk in the Simeto River Valley

There has been lengthy debate in the scholarly community about whether individuals can "experience" climate change on a first-hand basis (Akerlof et al., 2013). Some studies claim that global climate change is effectively invisible to laypeople, as climate change, by scientific definition, relies on statistical data compiled over long periods of time (Moser and Dilling, 2004; Weber, 2016). Ethnographic and survey results, however, have suggested that some members of the public believe that they have experienced climate change through seasonal changes, or living through extreme weather events (Akerlof et al., 2013; Ballew et al., 2019; Osaka and Bellamy, 2020).

The Simeto River basin (Figure 3.2) is located on the Southwest of Mount Etna, the largest active volcano in Europe, and is therefore characterized by quite unique natural features (Raciti and Saija, 2018). The basin extends in the territories of the provinces of Catania, Enna, and Messina, with a surface that measures approximately 4030 km2. The SRV is an area located along the central stretch of the Simeto River, which is the main river in Sicily, a few kilometers west of the Catania Metropolitan Area. Approximately 150,000 people live in the SRV area, distributed in 10 medium-small towns: the largest community is the city of Paternò with 50,000 residents, while the smallest is Ragalna with around 4,000 (ISTAT, 2018).

In the last two decades, part of this community has been involved in participatory actions for the sustainable development of the area. In particular, thanks to the cooperation between local groups of citizens, organized in an association named Participatory Presidium of the Simeto River Agreement (PSRA) (Saija et al., 2017), local administration bodies and the University of Ca-tania, in 2015 the municipalities of Paternò, Ragalna, S.M. di Licodia, Motta Sant'Anastasia, Belpasso, Biancavilla, Adrano, Centuripe, Troina, and Regalbuto, for a total of about 100,000 inhabitants, the PSRA and the University of Catania have signed the Simeto River Agreement (SRA), a river contract aiming at encouraging local development through participatory approaches (Figure 3.3).

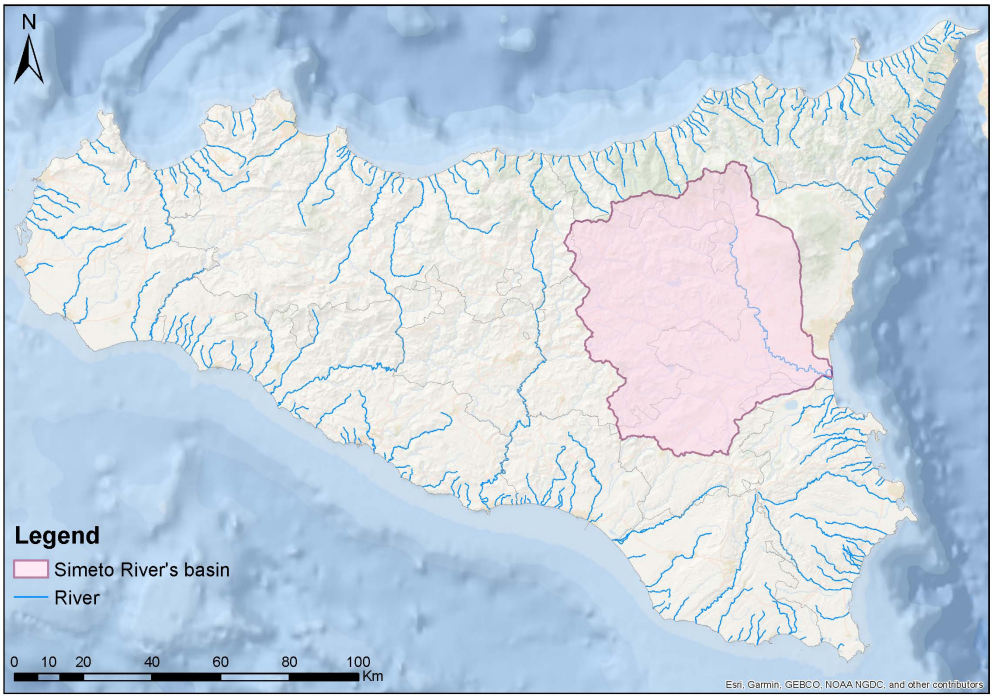

FIGURE 3.2 Location of the Simeto River basin on the east of Sicily (Italy).

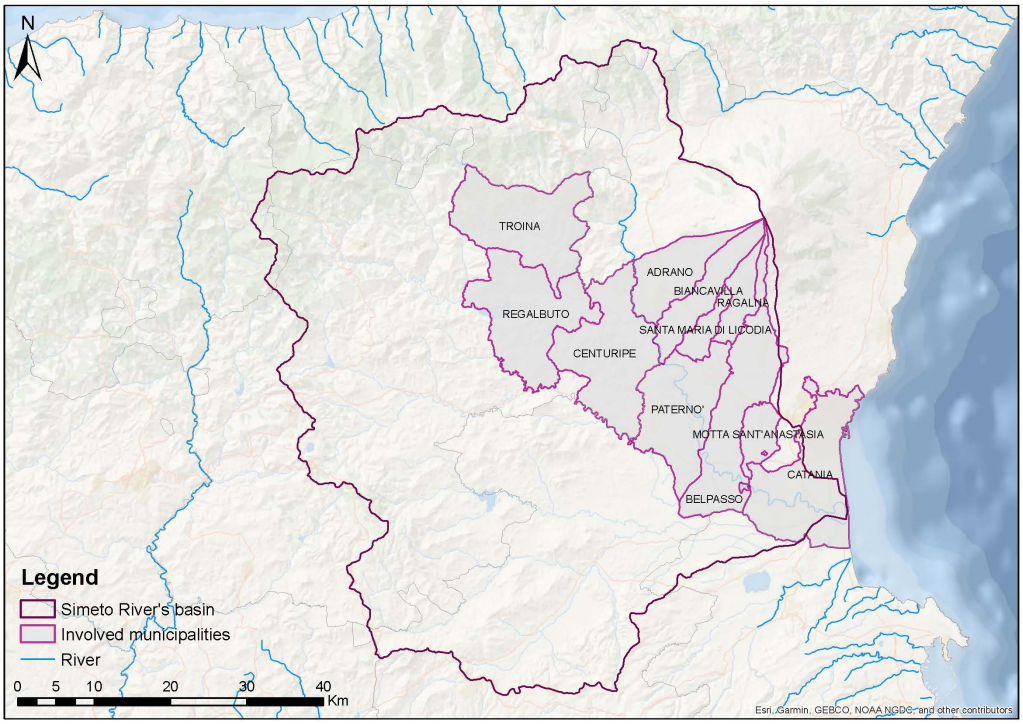

FIGURE 3.3 Location of the municipalities involved in the Simeto River Agreement, plus the city of Catania.

This part of the study aims at understanding, with reference to the Simeto River Valley (SRV):

- what is the current level of worry of the population about the climate change issue and to which extent they link urban flooding to climate change;
- the level of individuals' risk preparedness (short-term preparedness), specifically with reference to the way a person behaves during urban flooding events;
- long-term preparedness, specifically, people's willingness to invest as individuals and as a community in climate change adaptation infrastructures for sustainable urban drainage.

We also want to explore some of the links between the three listed aspects and in particular, the link between the level or worry about climate change and the short-term and long-term preparedness to urban flooding issues potentially exacerbated by climate change. To investigate these issues, a survey has been administered to the population, as part of the activities of EU LIFE project SimetoRES (www.lifesimetores.it, accessed on 15 February 2021).

In order to involve all age categories of the local population, the survey has been conceived to be simple and short. Given the characteristics of the population, the survey constituted also a "hook" for involving the citizens in more intensive and active initiatives. The survey was open for about three months and 1143 responses were received, which constitutes a large dataset in comparison to many other studies. The survey, consistent with the aims of the study, was articulated in three respective sections exploring each of the above-mentioned aspects.

The collected data can be considered representative of the perception of climate change effects on flood risk within urban contexts typical of Southern Italy. In this geographical area, urbanization has developed quite often with low attention to storm water management and urban planning in general; also, the seniors may have a quite low degree of education, given the predominantly agricultural vocation of the past economy in the area. Given these characteristics of the area, existing literature

on the subject, and relative to other sites in the globe, may not be enough representative.

3.4 Study design and sample

The design of the survey considered some other works, both Italian and foreign, which have a similar structure. For example, the municipality of Ferrara (Italy) in 2010 conducted a study based on nine multiple-choice questions to better understand knowledge, sensitivity and interest in climate change through the population (Westerhoff et al., 2010). The Joint Disaster Management Risk Assessment and Preparedness in the Danube Macro-region project (SEERISK, 2013) conducted a study to evaluate climate change perception, submitting to citizens multiple-choice questions, as in our case, about the involvement by the media on the treatment of the topic, the perception of climate change compared to past decades (especially for the adult population) and the actual derived risks, including extreme precipitation events and floods.

A study of Yale University estimates U.S. climate change beliefs, risk perceptions and policy preferences at State and local scale using the Yale Climate Opinion Maps based on 2018 data. This survey, with its about 20 questions with Likert scale (Likert, 1932), tried to investigate the opinions of the community regarding climate change and the risks deriving from it. In 2017, the European Commission published the special Eurobarometer 459, with the result of a large-scale survey proposed in some European countries. The key topic was, again, the perception of climate change, but with a focus to the responsibilities of national governments (European Commission, 2017).

The survey here in question, consisted of 10 questions, some of them structured with answers requiring a numerical value, following the Likert scale (Likert, 1932). The questions were formulated independently against each other and their number were reduced to the minimum in order to keep it less tedious for respondents, in order to reach a high number of participants. As already mentioned, the survey is divided in three sections.

In detail, the first part of the survey recalled recent episodes of severe flooding occurred in the Simeto Valley in the autumn of 2018. We asked if such events were related to climate change, or if they could be considered frequent events during the fall season or else if they were isolated phenomena. Subsequently, we asked how often they heard about climate change and through which channels.

The central part of the questionnaire started by analysing the day-life experience of citizens, by asking if they pass or live close to places frequently flooded during extreme rain events. Then we asked, using a Likert scale, how worried they feel about weather alerts, to understand how much confidence the citizen have in the Civil Protection and local authorities, which are responsible for issuing such alerts. Finally, we investigated their individual preparedness, i.e., their tendency to behave correctly during an urban flooding, asking them what they would do in three distinct possible scenarios: they are at work or at school, they have to go through an underpass or they have to pass a bridge.

The last part of the questionnaire concerned the community's willingness to adapt to climate change, as a further measure of long-term preparedness. First, we asked about the best practices for adapting to climate change according to citizens, to investigate whether they really knew the meaning of this type of practice. Finally, we investigated how much they would be willing to spend to implement measures for climate change adaptation. In this sense, they were asked whether they were willing to accept a municipal expense for the purpose, and whether they were willing to invest on new adaptation works on their private properties. This last part has been automatically submitted only to adults (over 19 years old), as for the children these questions are of difficult understanding or not relevant. The survey had anonymous answers, but prior to the 10 illustrated questions, the participants had to fill some general information on their age, gender, main occupation, education level and city of residence in order to socio-geographically characterize the answers.

It should be pointed out that this survey has been carried out in a local context where various community involvement actions are already active. As mentioned above, recently part of this community has been involved in participatory actions for the sustainable development of the

area, therefore some citizens are already somehow sensible to some of the topics of the survey. In a context like this, the questionnaire aims to serve not only as a statistical and investigative tool, but also represents a training opportunity for citizens, bringing their attention to its topics, as well as the possibility of encouraging and strengthening community involvement within the SRA.

The survey was published and distributed mainly electronically on the web-platform EU Survey (https://ec.europa.eu/eusurvey, accessed on 15 May 2021), for a period of about three months and was advertised through the social channels of the LIFE SimetoRES Project, Simeto River Agreement, and the University of Catania social channels (Facebook, Twitter, institutional websites). Such distribution was supported by the active work of volunteers from the Participatory Presidium of the Simeto river agreement, the umbrella of volunteer organizations deeply involved in several aspects of the project. Instant messaging (mainly WhatsApp) was also effectively used, sharing the link to the questionnaire in chatting groups of local community associations, school (parents and classes), professional orders, and others. A paper hardcopy version of the survey was also distributed during some public events in order to involve even those that may have been reached by social media only marginally. The answers were 1143 in total, 1078 collected electronically, and 65 hardcopies formats, distributed by individuals' characteristics as illustrated in Figure 3.4.

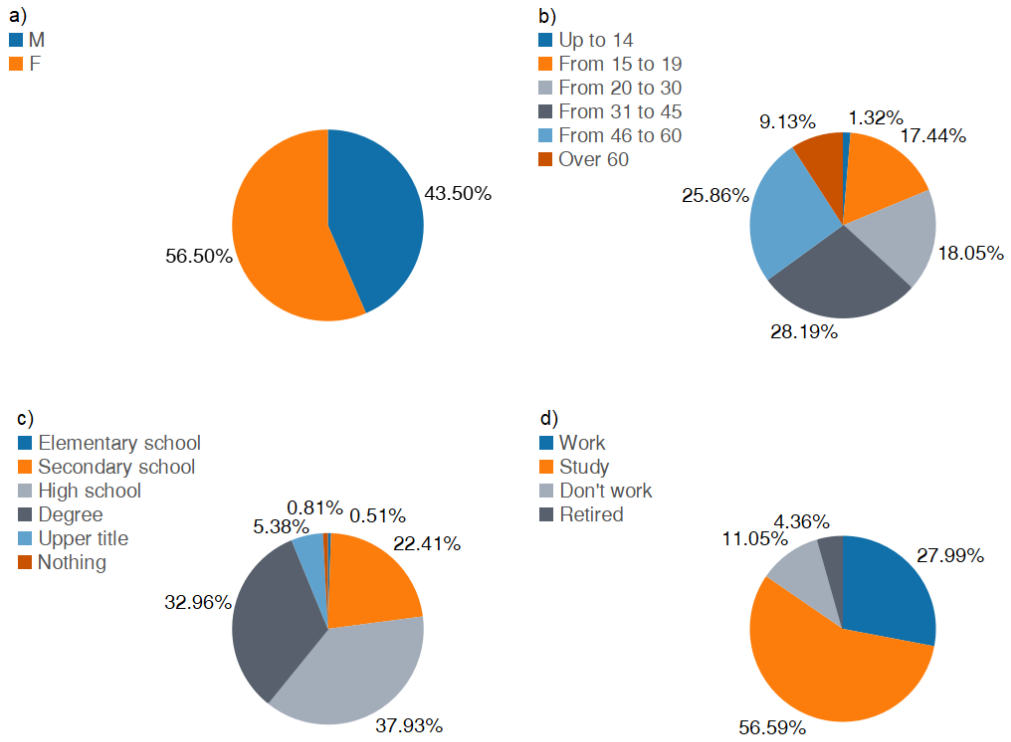

FIGURE 3.4 Social characterization of the participants to the survey in terms of (a) gender, (b) age, (c) education, (d) work.

3.5 Results of the survey

3.5.1 Worry about climate change

In the case of the Simeto River Valley around 84% of interviewees responded that the extreme rainfall events that hit Sicily in 2018 were mainly due to climate change. Only 8.7% of respondents believe that these phenomena have occurred as they are extreme events due to natural climate of the area. As a matter of fact, the study area has experienced even more severe events in the past, therefore the link with climate change is highly uncertain, so this question contributes in measuring the level of worry by the population.

It is interesting to note that the likely correct interpretation (Heavy rainfall events occur quite often in autumn, so there are quite normal in this season) is more frequent within the age group of over-60s, as the

20% of them answered so, while in the other age groups the percentage remains less than 10%. Also, rather a considerable percent-age of school-age students (30,77%) are not able to decide whether such events are due to natural climate variability or to changed conditions, i.e. they are not able to identify a possible cause for this type of events (Figure 3.5).

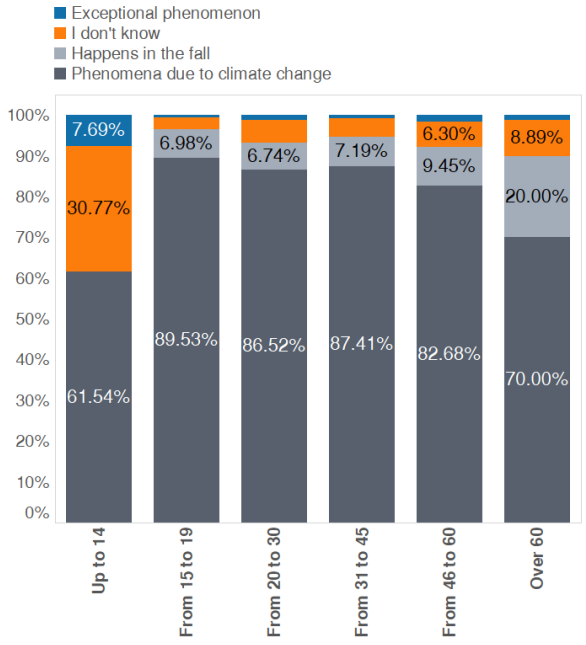

FIGURE 3.5 Results for the question: 'During the autumn of 2018, Sicily was hit by heavy rains in both the eastern and western parts, what do you think these phenomena are due?' Answers classified according to different age groups.

Regarding the exposure to information on climate change, over 44% of participants answered that they hear about climate change "at least once a week" and almost 30% even "once a day" 3.6. This indicates that the population is quite interested and worried about climate change as it is discussed in usual conversations, within all age groups. Table 3.1 shows the different information sources through which the inhabitants declared to "hear about" climate change. For this question, multiple answers were allowed. The table shows that the most frequent source of information on climate change are newspapers, radio and television (77.89%), followed by social media and the internet in general (66.53%).

TABLE 3.1 Sources from which population responded to hear about climate change. Respondents could select more than one answer (percentages do not sum up to 100% as multiple answers where accepted

Source	Percentage of answers
Talking with friends and family	44.12%
Social network / Internet	66.53%
Newspapers, Radio, TV	77.89%
At school / work	33.87%
During events / conferences	23.83%
Never heard of it	0.01%

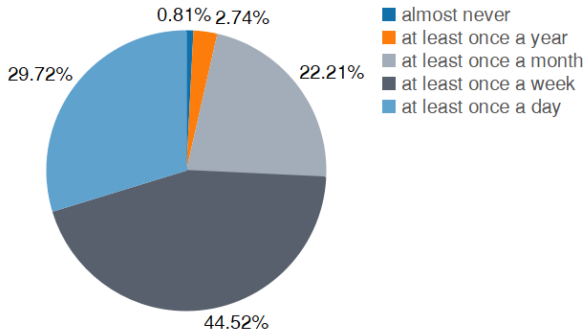

FIGURE 3.6 Responses to question 'In the last years, how often have you heard about climate change?'

3.5.2 Direct experience of urban flooding and risk preparedness

More than 62% of the respondents answered that they cross areas prone to flooding during heavy rainfall events. This could be related to the fact that the problem is diffused within a large area. Figure 3.7 shows the answers divided into the different municipalities. The chart shows that the municipalities where the higher number of respondents declared to cross floodable areas are Catania, Biancavilla and Adrano. Instead, the less interested by floods are Centuripe, Troina and Regalbuto, cities which are located at the top of mountain areas. However, even in these municipalities, more than 50% of participants stated that they cross dangerous areas during intense storms: this could is related to the

fact that these cities have many commuters that move out of their town for work/school on a daily basis, for example, it is possible that many citizens need to go to Catania for work, study or other needs, which is the closest city with services.

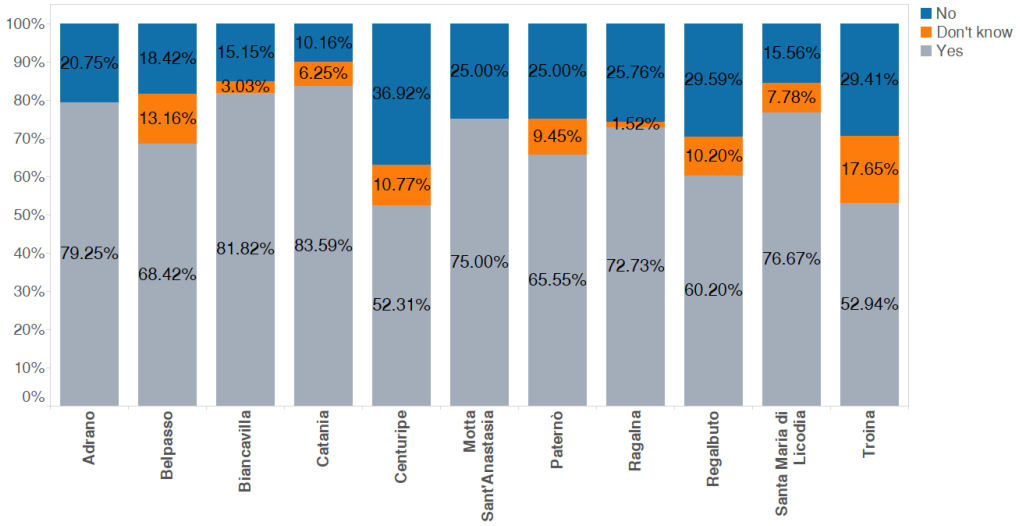

FIGURE 3.7 Responses to question 'Do you cross areas that are likely to be flooded during a rain event?' The size of the indicator represents the quantity of responses coming from individual municipalities, while the color indicates the type of response.

After this question, participants were asked to indicate their degree of concern during weather alerts. Table 5 shows that most of respondents (around 45%) have a "medium" level of concern and only 32% have a high or very high level of concern (the sum of 23% and 9%). This happens probably because of the relatively large spatial and temporal uncertainty of the weather alerts in the region, which remains significant to a degree that may induce a partial distrust about them – a phenomenon also known as cry-wolf syndrome (Breznitz, 1984). In fact, in recent years, there have been several cases in which weather warnings have been issued without any rain occurring, other times there have been very intense rain events without there being any weather warnings: these situations contribute to confuse citizens, who lose confidence in the weather alert service.

Regarding risk preparedness, the charts in Figure 3.8 show the answers on the behaviour during potentially dangerous scenarios in three

TABLE 3.2 Level of concern during a weather alert

Level of concern	Percentage of answers
very low level of concern	5.17%
low level of concern	16.53%
medium level of concern	45.84%
high level of concern	23.23%
very high level of concern	9.23%

different cases. In the first question, we asked how the citizens would behave in case of storm if they were indoors at school, work or gym. The chart shows that almost 74% know the right behaviour to take; in the second question, we asked what behaviour they would have if they were in the situation to decide to cross an underpass, even in this case almost 74% of the interlocutors answered correctly; instead, the third question asked about their choice in case of crossing of a bridge during an exceptional rain event. In this case only about 48% of participants gave the answer corresponding to the correct behaviour. As it can be seen from the graph, 20% of people would not actually know how to behave and about 33% of participant would have a risky behaviour. It is also interesting to investigate the answers according to the different age groups. We note that young people are actually the least aware about what to do in the case of an extreme rain event. Only 15% of children (up to 14) and 35% of teenagers (from 15 to 19) answered correctly.

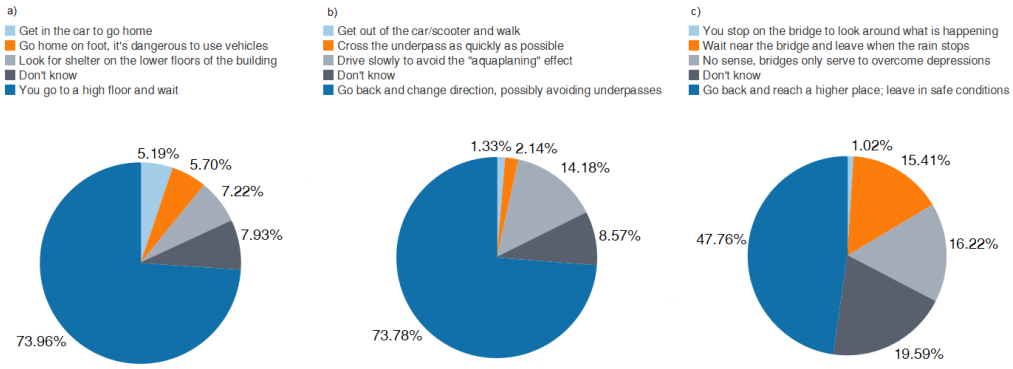

FIGURE 3.8 a) Answers to the question: "What do you do if there is a storm and you are at work / school / gym?" b) Answers to the question: "What do you do if there is a storm and you are in your car/scooter and you have to pass an underpass?" c) Answers to the question: "What do you do if there is a storm and you are in your car/scooter and you have to pass a bridge?"

Moreover, we asked if they feel personally responsible of flood prevention, and how much they think other public bodies are responsible for protection from the induced risk. The citizen had the possibility to assign a score based on the degree of assigned responsibility in the case of flood event for the different bodies indicated. Using a Likert scale the responsibilities were divided into low, medium or high. The result shows that only 35.5% of citizens consider themselves to have responsibility in flood prevention, while almost 30% believe they have a very low responsibility. It also shows that there is a high tendency to attribute most of the responsibility to public bodies, in particular to the Central Government (Figure 3.9).

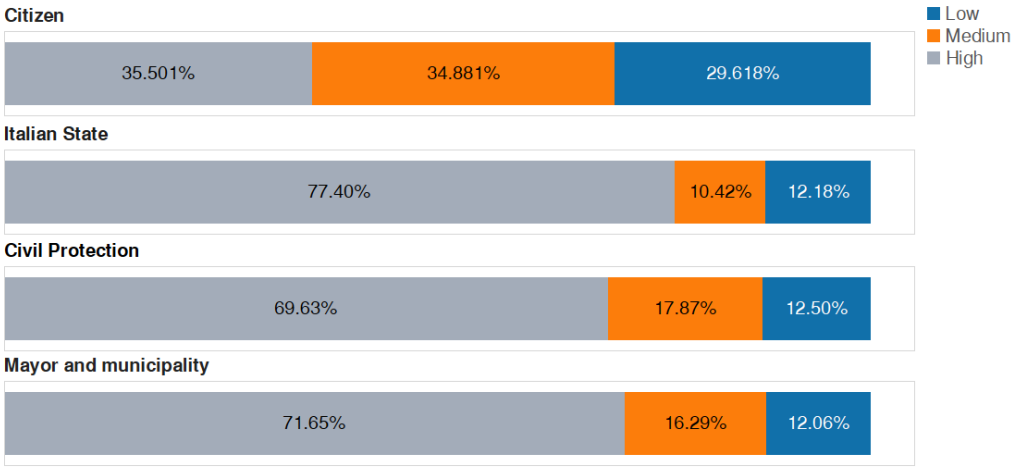

FIGURE 3.9 Answer to the question concerning the attribution of responsibility for the prevention of flood risk

3.5.3 Willingness to adaptation

The first question of this section asked to the participants to identify the best practices for adapting to climate change, in order to investigate whether respondents know the meaning of adaptation and how it differs from the concept of mitigation. Knowledge of this difference is fundamental to the population to be a catalyst for the implementation of adaptation actions, as these are of different nature than the mitigation actions. In fact, the former do not focus on a reduction of green-house gas emissions, while the latter are mainly oriented to that scope, thus requiring totally different strategies.

The outcomes of the survey show that citizens are mostly confused about this point (Table 3.3). Almost 44% of the interviewees answered that waste sorting is an adaptation measure and over 58% indicated renewable energy production, while both should be mainly considered mitigation measures. Then, more direct questions on the willingness for adaptation was asked. In particular, participants were first asked if they would be favourable to an increase of investments on sustainable drainage infrastructures by their municipality. The answers have been represented in Figure 3.10, as a function of the age group. Overall, almost 80% of the answers indicated willingness to accept an increase in public costs if well justified; however, mainly adult groups (i.e., over 30 years

TABLE 3.3 Responses to question 'Which of these are good practices for adaptation?'

Good practices for adaptation	Percentage of answers
Waste sorting	43.61%
Improve the quality of weather alerts	17.78%
Sewer maintenance	51.75%
Avoid wasting water	19.81%
Build infrastructures for flood protection	60.07%
Use of energy from renewable sources	58.23%

old) seemed more favourable to this type of initiative. Then, the question was oriented to a more individual statement: citizens were asked whether while re-structuring their own properties, they would be willing to increase their expenses to put in place sustainable drainage practices, such as increasing the surrounding pervious surfaces (Figure 3.11). Over 82% of young adults in the age between 31 and 45 years have responded to be willing to do that, while people aged less than 30 years seem to be the less willing to make such an investment.

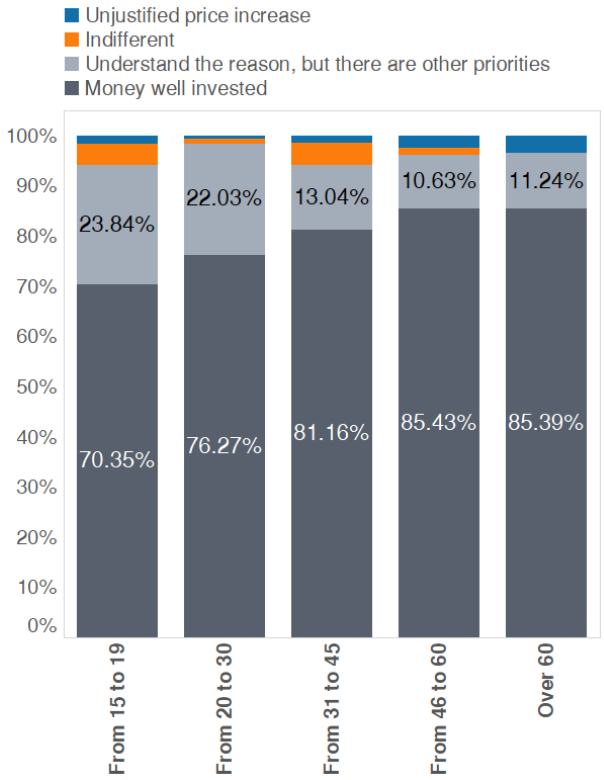

FIGURE 3.10 Answer to the question: "Your municipality is investing funds for the construction of a new parking and decides to spend 10% more for make it with previous materials that allow stormwater retention and therefore reduce urban flooding. What do you think about that?"

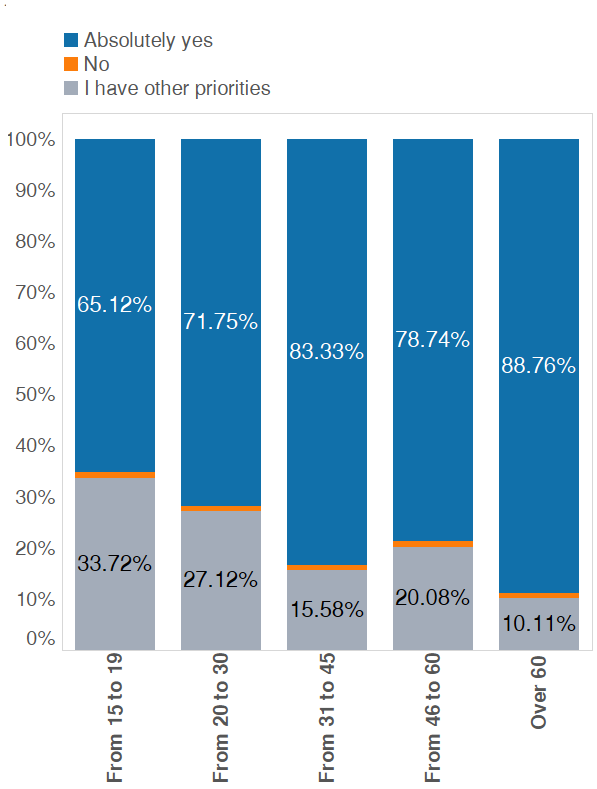

FIGURE 3.11 Answer to question: "In building or renovating your home would you be willing to spend more to introduce more green areas and less asphalted surfaces to better adapt to climate change?"

3.6 Conclusions about the perception of climate change and urban flooding risk in the Simeto River Valley

The results of a survey exploring worry about climate change and its possible relation with the behaviour during urban floods and the willingness to invest in adaptation actions have been presented, relatively to the Simeto River Valley area in Sicily. The data collection that was made is quite relevant respect to other studies, as here more than 1000 persons were interviewed, while it is difficult to find regional studies with more than a few hundreds of participants involved.

The simplicity of the survey was a crucial factor for collecting such a high number of answers, but, on the other hand, has not undermined the

possibility to arrive at important conclusions about the issues explored. The overall picture deriving from the present analysis highlights how there is a high concern for the possible impacts of climate change, specifically in connection to urban flooding. The climate change issue entered in almost every-day conversations by the population. However, this high level of concern does not correspond to a comparable level of knowledge of the correct behaviour during climate-related extreme events – specifically urban flooding – and the willingness to invest on adaptation measures. In fact, the population tends to attribute increasingly intense events to climate change but does not know the correct behaviour to take during the emergencies, does not correctly attribute the responsibility for flood-caused damage and does not trust authorities that are in charge of human safety.

The cross-analysis that we carried out, shows that there is no gain for these two resilience factors associated to a higher degree of concern about climate change. Overall, the outcomes of the survey suggest that the information that is conveyed by the media and taught in schools is mainly oriented to increase the worry about climate change and that this is not significantly useful for an increase in the resilience of the populations, i.e., specifically a higher risk awareness during urban flooding events and of the importance of investment in sustainable drainage practices. Hence, greater efforts should be spent through media and education to build a greater risk preparedness rather than prevalently a greater worry about climate change.

Chapter 4

Proposed methodology for the analysis on the experimental site

4.1 Overview

This chapter proposes the methodology of the research project and in particular the part linked to the experimental site. Since 2017, the University of Catania has been working for the construction of a green roof on a new building in the Campus. The structure of the green roof and the chosen and installed vegetation is then described in detail. Then follows the complete description of the monitoring system and the data collection system, used for the collection of soil data and meteorological data.

4.2 Proposed methodology for the analysis on the green roof

The main goal of this research is to define tools and methodologies to ascertain the efficiency of Green Infrastructures as a tool for adapting to climate change with specific reference to urban areas in the Mediterranean, and, subsequently, the definition of a model on single-infrastructure-scale (green roof) for the analysis of the impacts of climate change on the hydrological-hydraulic response.

The methodology concerning the study of the green roof is divided into two types:

- Experimental: with the green roof on Building 15 of the University Campus;
- Modeling: starting from experimental data and climatic data for the creation of a model on a single infrastructure scale.

In particular, the intent is to evaluate the effective efficiency of a green infrastructure, like the green roof, through the application of future rainfall scenarios. In this way, the response of the future green roof can be investigated by comparing it with the present efficiency.

To do this, the first step involves the experimental green roof with an active monitoring system to collect meteorological and soil humidity and temperature data. Secondly, we realized a physically-based model of the green roof calibrating the parameters so that they faithfully reproduce the hydrological-hydraulic response of the green roof during storms. At this point we were able to evaluate the efficiency of the infrastructure over a period of about two years: from May 2019 to April 2021.

To investigate the response of the green roof in possible scenarios we selected eleven GCM-RCM models (for the thirty-years 2021-2050 and 2041-2070 in RCP 4.5 and 8.5) to be applied to the physically-based model. At the conclusion of the study we were able to compare the current efficiency of the green roof with the efficiency derived from future scenarios.

In the following paragraph (4.3) the experimental site of the green roof is described in detail, instead in the next chapter the modeling part will be described.

4.3 The green roof of the Catania University Campus

In 2017, Catania University (UNICT) started planning the realization of a new building at "La Cittadella" Campus (Building 15), designed in order to allow the implementation of a green roof on the above terrace. In June 2018, a sponsoring contract was signed between UNICT and Global Water Partnership (GWP), with a funding for the green roof

realization and the monitoring instrumentation installation related to the project Non-Conventional Water Resources, financed by The Coca Cola Foundation and coordinated by GWP. In September 2018 the green roof was completed and in March 2019 the instruments were installed, and testing started.

Building 15 is a building with a total surface of approx. 800 m^2, which hosts three classrooms for the Engineering Departments of Catania University. The structure of the building is with a steel frame, with square pillars and trusses. The roof is a terrace in mixed concrete-steel, with a total surface of approx. 820 m^2. The whole building has been designed to withstand the excess loads deriving from a green roof installed on the terrace.

Given the experimental nature of the intervention, the whole terrace surface has been divided into four hydraulically separated sectors, in order to monitor the hydrological response of the green roof. One sector of approx. 50 m^2 has been covered with normal pavement, in order to simulate the hydrological response of a traditional impervious roof. Furthermore, a full climatological station as well as a second rain gauge is installed, in order to monitor the hydrometeorological variables.

The green roof is of the extensive type, with small vegetation species and limited soil depth (about 15 cm). An emergency drip irrigation system has also been installed to guarantee the survival of the vegetation during dry periods. The system is automatic, with a rain-check device to avoid irrigation during or after rainfall.

4.3.1 Layers and vegetation

The green roof is constituted by the following layers shown in Figure 4.1.

- Bitumen primer: the bitumen primer penetrates the porosity of the concrete surfaces and favors the adhesion of the above layers to the concrete surface. The primer has been applied by a roller.
- Vapor barrier: since the green roof has a thermo-isolating layer, a vapor barrier is necessary to avoid condensation, which would

limit the thermal insulation and cause damages to the layers. The vapor barrier has been created by means of a bitumen membrane of 3 mm, reinforced with glass fiber.

- Thermal isolating layer: the thermal isolating layer is necessary in order to increase the energy efficiency of the building, to absorb the movements of the structure due to thermal stress, as well as to avoid the formation of condensation. This has been created by rigid panels of 3 cm depth, with impermeable glass wool treated with resin, covered with a layer of bitumen reinforced with glass fiber and polypropylene film, that can be installed by heat.

- Impermeable layer and anti-root system: this layer avoids the deep drainage of the water to the underlying layers. It has been created by means of bitumen membranes, able to withstand chemical aggression by humic acids and fertilizers. This layer is characterized by high stress resistance, and therefore can be applied in total adherence with the underlying layers. This enables to quickly locate any water leakages. The resulting layer has a greater resistance to punching. This layer is made up by a first bitumen layer reinforced with polyester, and a further elastoplastomeric bitumen membrane reinforced with polyester geotextile with added anti root product.

- Drainage layer: the drainage layer is an important component of a green roof, since it must carry out two contrasting tasks: drain the excess water and retain part of the water to keep the soil moist. This layer has been made through a special membrane, covered with geotextile in polypropylene.

- Vegetal substrate: this is the soil were the vegetation will be placed. The soil is made of ¾ of ballast, and ¼ of vegetable humus enriched with clay and fibers. The total weight if about 1100 kg/m^3 for a 10 cm layer. The layering of the vegetative substrate started on September 4th 2018 and it was completed on September 11th 2018. The Green Roof was finally completed with the plants and the irrigation system on September 28th 2018.

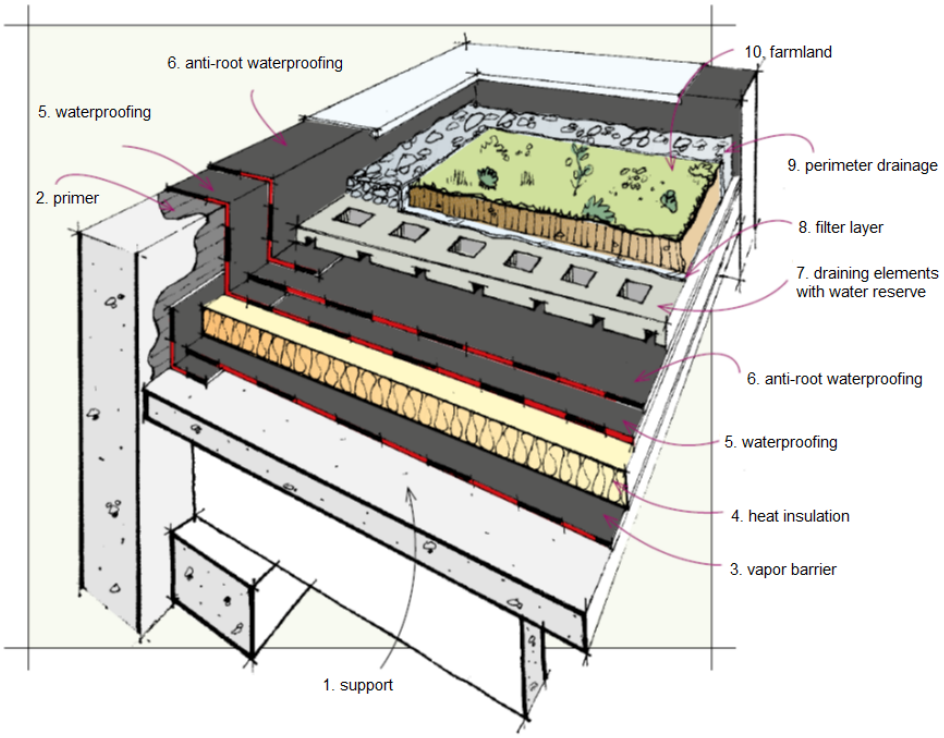

FIGURE 4.1 Layers of the Green Roof.

The combination of high temperatures, wind exposure and intense sunlight provide challenging conditions for plant growth on a green roof. Plant selection required careful consideration of site, micro-climate, substrate and maintenance factors, linked to the desired aesthetic, functional and management outcomes for the project. The vegetation has been chosen in order to protect the underlying soil. The plant species chosen for the green roof are:

- Muehlenbeckia Complexa (Figure 4.2): a very decorative climber, hardy in nature but requiring a good amount of sunshine to make it bloom. A well-drained, sandy soil is best for its growth, and it can be increased by cuttings of hardy shoots taken early in summer (Pink, 2004). It is native to New Zealand.

- Glandularia tenera (Spreng.) Cabrera (Figure 4.3): this plant is a member of the Verbena family (Verbenaceae). Other common names are Rock Verbena and Latin American Mock Vervain. It does

not withstand foot traffic. The uses of this plant can be ornamental, ground cover, erosion control on moist ground.

- Phyla nodiflora (L.) Greene (Figure 4.4): Phyla nodiflora is a common and a widespread species with no known threats. It is native to the whole of Africa, temperate and tropical Asia, Australasia, Europe and tropical America. In India, it occurs in almost all states at lower elevations. It is interesting to note how this type of plant has attracted numerous insects, in particular bees.

- Myoporum parvifolium (Figure 4.5): also known as Creeping Boobialla (Purple leaf form), it is extremely hardy weed-suppressing ground cover for embankments, verges, streetscapes and high traffic areas. Acts as a living mulch and weed suppressor. It is bird and butterfly attracting and it requires well-drained soils. This plant is indigenous to the botanical regions of South Australia.

FIGURE 4.2 Muehlenbeckia Complexa.

FIGURE 4.3 Glandularia tenera (Spreng.) Cabrera.

FIGURE 4.4 Phyla nodiflora (L.) Greene.

FIGURE 4.5 Myoporum parvifolium.

For the hydrological-hydraulic performance, these plant species were chosen for their characteristics of semi-succulent plants. This means that they are plants capable of withstanding the harshest climatic conditions, especially in summer, but at the same time they need water and have roots capable of absorbing enough. To prevent plant species from suffering during the driest periods, a programmed irrigation system was installed.

4.3.2 Monitoring system

The monitoring system is composed by a meteorological station, a "master station" and a "slave station". The single components of the monitoring system are:

- Rain gauge: the green roof is monitored by two different rain gauges. The instruments measure liquid rain fall amount and intensity. The device is composed of a rain collector cone and a

double-chamber tipping bucket connected to a magnet. This magnet operates one reed switch, which generates impulses that can be counted by external meters. It is with a siphon placed on the cone's nozzle; during heavy rain it regulates the flow into the bascule permitting all the water to fall inside the tipping bucket. The rain gauge measures a minimum value of 0.2 mm in a time step of 5 minutes. This solution gives its best results where the main need is the measurement of the total amount of rain over long periods.

- Combined anemometer: this sensor includes, in a single apparatus, the transducers for measuring wind speed and direction. Its use simplifies the installation and the plant design compared to the systems with separate units plus giving some other advantages being smaller, lighter and cheaper. The measurement system is made up of a sensor, the rotors DNA124 and DNA127 and the cable of DWA type.

- Thermohygrometer: this is the instrument for measuring temperature and relative humidity while a thermometer only measures the air temperature. LSI LASTEM supplies a precise and reliable set of probes, suitable for a continuous measurement in severe outdoor environment, in presence of deep thermal and hygrometric ranges and high solar energy. The thermohygrometer has supported a considerable improvement: a fan ensures a continuous air change around the sensor in order to eliminate temperature fault caused by radiant heat.

- Pyranometer: the pyranometer is the instrument to measure the solar irradiance (direct and diffuse) which reaches the terrestrial surface. With this instrument it is possible to measure not only the global radiation but also the reflected sun radiation (albedometer) and the diffuse radiation by means of the occultation band. The pyranometer measures radiation values within 300 and 3000 nm, with a visibility of 2π steradians. The element used to for the measurement is a thermopile whose external surface has been darkened with matt black paint bearing a reflecting power < than 2% (e>0.98) in the spectral area of the sensor.

- TDRs probes: the soil moisture of the green roof is monitored by three sensors based on TDR technology (Time Domain Reflectometry). This particular type of sensor ensures good accuracy even in very wet soils, and without special calibration for mineral soils. Using its rods, the sensor can be inserted in the material for 11 cm. It measures not only soil moisture (0-100% range) but also temperature. The TDR technique measures the velocity of propagation of a high-frequency signal down waveguides in the soil. The velocity is related to the dielectric constant of the soil, which is then related to the water content. The possibility of measurement errors increases with short waveguides (0,1 m) The quality of the measurements is also influenced by the length and characteristics of the coaxial cables, which need to be combined with the waveguides. The data is recorded by a data logger contained in each station.

The final configuration (Figure 4.6) includes the Master station in the South-West area of the Green Roof (Figure 4.7). It is connected to three TDR sensors, a rain gauge and two level sensors. The Slave station is located in the opposite direction, in the North-East area, it is connected to four TDR sensors and a level sensor. The Meteorological station is located at East of the Green Roof and all the remaining weather sensors plus a TDR sensor and a level sensor are connected to it (Figure 4.8). The Figures 4.9 and 4.10 shows the master station with 3 connected TDR sensors and the meteorological station.

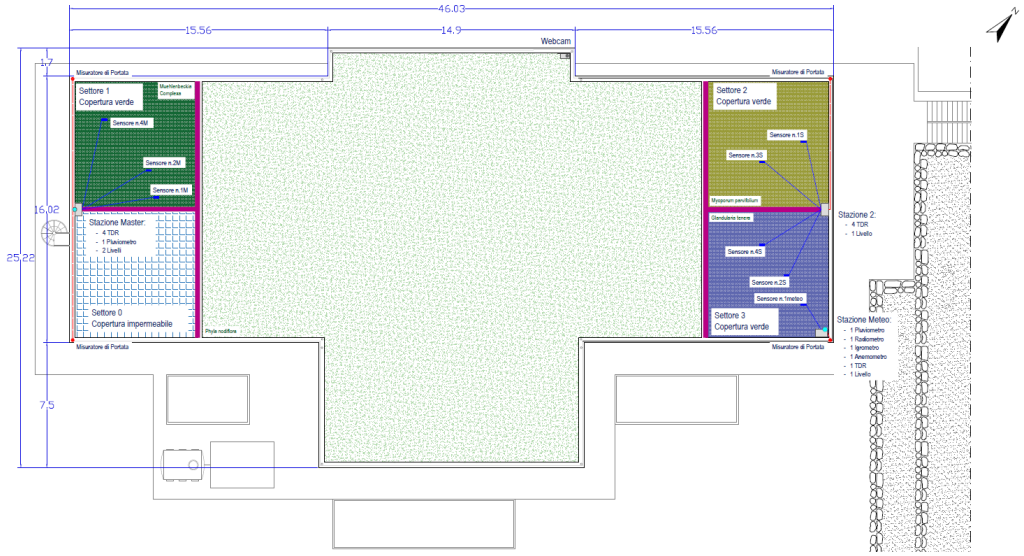

FIGURE 4.6 Planimetry of the final configuration.

FIGURE 4.7 Master station in the final configuration.

FIGURE 4.8 Slave and Meteo station in the final configuration.

FIGURE 4.9 Master station with 3 TDR sensors.

FIGURE 4.10 Meteorological station.

The data collection system is relatively simple. The Slave station and the Meteorological station are connected in series and transmit the recorded data to the Master station via serial link. The Master station is connected to the building 15 network, which can transmit the data to the university network. Through the university network the data is collected in a database accessible through the department computers.

Chapter 5

Hydrological modeling of the green roof

5.1 Overview

In this chapter the physically-based model is discussed. The realization of a physically based model was done with HYDRUS-1D software. However, before moving on to purely computational modeling, some laboratory tests were carried out to identify the hydraulic parameters of the soil. After the laboratory tests an heuristic calibration was carried out in order to best reproduce the hydrological-hydraulic response of the green roof. Finally, the efficiency of the green roof on the rainfall events from May 2019 to April 2021 was analyzed.

5.2 Green roof model building

The modeling activities takes place with HYDRUS-1D software. HYDRUS computer code numerically solves the Richards equation for variably-saturated water flow and advection dispersion type equations for heat and solute transport. The flow equation incorporates a sink term to account for water uptake by plant roots. The Figure 5.1 shows a graphic representation of the physical model and the conceptual model relating to water routing through an extensive green roof.

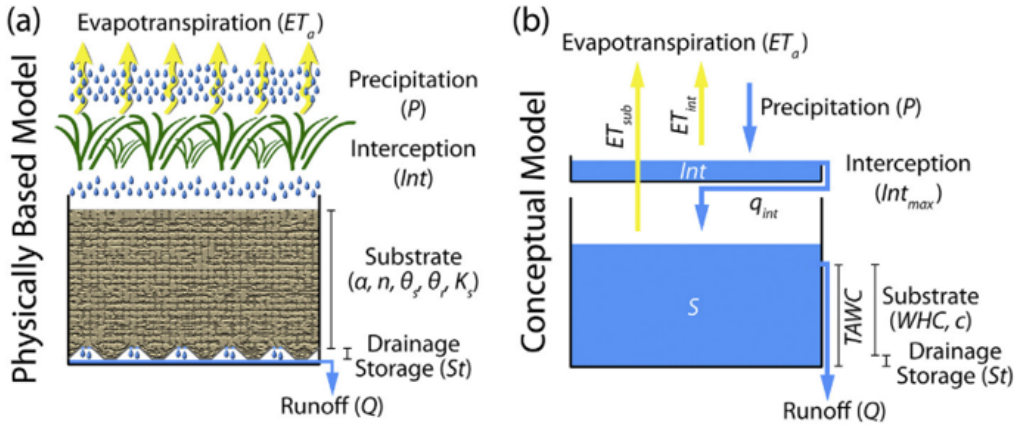

FIGURE 5.1 Graphic representation of: a) the physical model b) the conceptual model relating to water routing through an extensive green roof. (Kargas et al., 2017)

One-dimensional uniform (equilibrium) water movement in a partially saturated rigid porous medium is described by a modified form of the Richards equation using the assumptions that the air phase plays an insignificant role in the liquid flow process and that water flow due to thermal gradients can be neglected:

$$\frac{\delta\theta}{\delta t} = \frac{\delta}{\delta x}\left[K\left(\frac{\delta h}{\delta x} + \cos\alpha\right)\right] - S \tag{5.1}$$

where h is the water pressure head [L], θ is the volumetric water content $[L^3L^{-3}]$, t is time $[T]$, x is the spatial coordinate $[L]$ (positive upward), S is the sink term $[L^3L^{-3}T^{-1}]$, α is the angle between the flow direction and the vertical axis and K is the unsaturated hydraulic conductivity function $[LT^{-1}]$ given by:

$$K(h,x) = K_s(x)K_r(h,x) \tag{5.2}$$

where Kr is the relative hydraulic conductivity $[-]$ and Ks the saturated hydraulic conductivity $[LT^{-1}]$.

In addition to the simulation parameters, like geometry, time or print information, HYDRUS requires some basic input data to correctly simulate the behavior of the green roof. The Soil Hydraulic Parameters for the hydraulic property model can be selected from the Soil Catalogue or insert from actual measurements.

The parameters are:

- θr: residual water content;
- θs: saturated water content;
- α: the hydraulic shape parameter;
- n: the hydraulic parameter;
- Ks: the saturated hydraulic conductivity;
- l: Mualem's pore connectivity exponent.

The software requires information about the spatial discretization, initial conditions, spatial root distribution, scaling factors, and material distributions with depth. Other important data for the correct development of the model are precipitation and temperature data. These data are extracted from the meteorological station on the green roof.

In particular, for the calculation of the evapotranspiration the Hargreaves formula is used (Hargreaves and Samani, 1985), where ET is the evapotranspiration, $Tmax$ is the maximum monthly temperature, $Tmin$ is the minimum monthly temperature, T is the average temperature, Ra is the extraterrestrial radiation (calculated by the software).

$$ET = 0,0023Ra(T + 17,8)\sqrt{Tmax - Tmin} \tag{5.3}$$

The necessary input data are:

- Soil Hydraulic Parameters;
- Soil Profile;
- Precipitation;
- Meteorological Boundary Conditions.

5.3 Laboratory experiments for the definition of soil parameters

To start to research of the hydraulic parameters of the soil, some laboratory experiments were conducted. Laboratory experiments were carried out at the KORE University of Enna in order to obtain the grading curve. The experiments involved carrying out simultaneously the sieving and sedimentation experiments and the test for the calculation of the specific gravity of the soil, for a total of two days of experiments (8 October and 19 October 2020).

A sample of about two kilograms of soil from the green roof was taken and sent to the Kore University to be dried in a laboratory oven at 110 °C for 24 hours. Once the dry sample was obtained, the rough portion was divided from the fine portion by washing in a 75 micron diameter sieve. The rough and fine parts, once separated, were put back in the oven at 110 °C for a second drying. 40 grams of fine portion were used for the sedimentation test after being immersed in 125 ml of hexametaphosphate solution (flocculant). During the sedimentation test numerous readings with the density meter up to 48 hours were taken. The sieving test was carried out with the rough portion of soil, in a pile of 9 sieves left to vibrate for about 15 minutes. The following tables (5.1 and 5.2) show the results of the sedimentation and sieving test.

Once the results were obtained, it was possible to plot the grading curve of the soil of the green roof and obtain the percentages of sand, silt and clay (Figure 5.2).

TABLE 5.1 Result of sedimentation test

Time (min)	Diameter (mm)	Aerometer reading (-)	Passing part substance (%)	Passing part Pd (%)
0.5	0.0669	18.0	62.01	16.97
1	0.0476	17.5	59.93	16.40
2	0.0342	16.0	53.67	14.69
4	0.0244	15.0	49.50	13.55
8	0.0175	13.5	43.25	11.83
15	0.0129	12.5	39.08	10.69
30	0.0093	11.0	32.83	8.98
60	0.0066	10.5	30.74	8.41
120	0.0047	9.0	24.49	6.70
240	0.0034	7.5	18.24	4.99
960	0.0017	6.0	11.99	3.28
1440	0.0014	5.0	7.82	2.14

TABLE 5.2 Result of sieve test

Sieve (-)	Diameter (mm)	Weight in Sieve Td (g)	STd (g)	Retained part (%)	Passing part Pd (%)
3″	75	0	0	0	100
1,5″	37.5	0	0	0	100
3/4″	19	14.7	14.7	2.96	97.04
3/8″	9.5	36.53	51.23	10.31	89.69
4	4.75	15.82	67.05	13.49	86.51
10	2	26.59	93.64	18.84	81.16
20	0.85	40.84	134.48	27.06	72.94
40	0.425	57.23	191.71	38.57	61.43
60	0.25	52.97	244.68	49.23	50.77
140	0.106	104.47	349.15	70.25	29.75
200	0.075	11.82	360.97	72.63	27.37

TABLE 5.3 Hydraulic parameters of the soil

Hydraulic parameters	Result
θr [mm^3 mm^{-3}]	0,0398
θs [mm^3 mm^{-3}]	0,3866
α [mm^{-3}]	0,00421
n	1,9047
Ks [mm min^{-1}]	0,967778
l	0,5

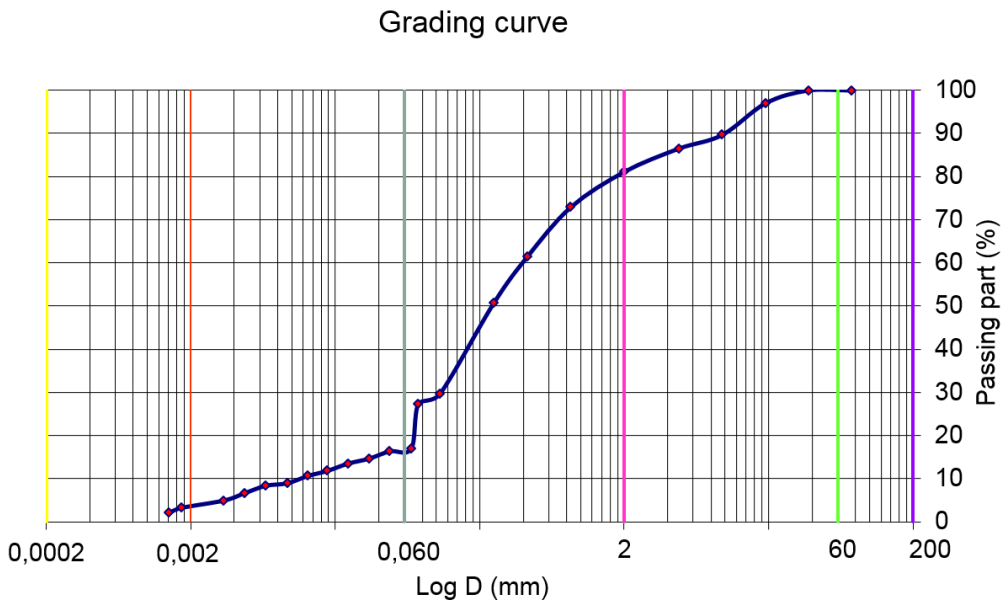

FIGURE 5.2 Grading curve obtained after the laboratory tests.

These laboratory tests were fundamental to obtain the hydraulic parameters of the soil as it was possible to apply the Rosetta method and the pedotransfer functions (Schaap, 2002) with the results shown in the Table 5.3. Once the parameters were experimentally obtained, it was possible to perform an additional optimization.

5.4 Model calibration

The model calibration phase was divided into two parts. A part of hydrological modeling of the rain events collected in the database (by calibrating the hydraulic parameters of the soil) and a part of modeling of the dry periods (by calibrating the evapotranspiration parameters). At the end of the calibration, a validation of the results was carried out to set the parameters and finish the realization of the physically based model. For the realization of the model an heuristic approach for calibration was followed, this means that, for each hydraulic parameter of the soil, a range of variation has been selected and consequently all possible combinations of parameters have been tested. After doing this, the performance of the model was evaluated by selecting the best one through the Nash-Sutcliffe normalized index. Finally the result was validated considering the best combination of parameters.

5.4.1 Hydrological modeling of rainfall events

For the hydrological modeling, 28 rain events were collected in about two years (from May 2019 to April 2021). The selected events reported at least 8 mm of total rain. Thanks to the roof monitoring system, the following parameters were measured for each event: start and end date, duration, intensity, inter-arrival and total rainfall. The Table 5.4 shows the events with their characteristics.

For the calibration phase 3 events were selected from the database and a heuristic calibration was made. The hydraulic parameters of the soil were varied within a range, with a specific step, and all possible combinations of parameters were tested.

The selected events are:

- 23 March 2020;
- 17 November 2020;
- 14 April 2021;

The ranges for each parameter are:

TABLE 5.4 Database of rainfall events from May 2019 to April 2021

Date start (-)	Date end (-)	Duration (-)	Max Intensity (h)	Inter-arrival (mm/min)	Cumulated rainfall (mm)
15.05.2019 17:35	16.05.2019 15:40	21.7	4.8	0.0	51
04.09.2019 10:55	04.09.2019 12:10	0.9	1.8	2660.5	9.2
07.10.2019 15:20	08.10.2019 02:25	11.2	0.8	806.5	12.6
09.10.2019 19:50	10.10.2019 05:55	9.4	1.2	51.0	10.2
25.10.2019 00:50	26.10.2019 04:45	27.8	9.6	382.3	52
03.11.2019 08:15	04.11.2019 01:10	16.3	7.2	211.9	16.4
06.11.2019 14:50	07.11.2019 05:55	14.6	2.4	76.8	11.8
11.11.2019 08:55	12.11.2019 23:55	37.0	2	67.3	55.6
19.11.2019 12:30	19.11.2019 17:45	4.6	2.4	162.9	19
24.11.2019 01:35	24.11.2019 17:25	14.9	8.4	119.5	36.8
21.01.2020 01:50	21.01.2020 07:30	5.0	1.8	1381.8	18.2
23.03.2020 09:20	26.03.2020 03:45	65.9	8.6	1555.8	178.2
15.07.2020 14:35	15.07.2020 17:30	2.3	4.2	2676.8	13
13.09.2020 09:40	14.09.2020 10:30	24.5	3.4	1457.0	31.8
16.09.2020 19:25	16.09.2020 23:00	2.8	1.4	60.5	14.8
21.09.2020 15:05	21.09.2020 18:45	2.3	3.4	115.8	28
23.09.2020 15:35	23.09.2020 17:50	1.8	3	46.9	17.6
17.11.2020 04:25	18.11.2020 18:05	37.4	2.2	1321.9	34.4
28.11.2020 14:40	29.11.2020 15:50	24.3	5.8	114.6	83.6
03.12.2020 07:05	03.12.2020 18:05	8.8	2	96.5	14.8
06.12.2020 09:20	06.12.2020 10:50	1.3	2.6	66.8	14.6
08.12.2020 18:55	09.12.2020 16:10	21.1	1.2	77.4	8.8
19.12.2020 20:55	21.12.2020 20:00	46.9	3.2	291.8	65
15.01.2021 08:30	16.01.2021 09:40	24.9	0.6	613.5	11.2
13.02.2021 15:10	14.02.2021 04:40	13.4	1.2	690.9	20.8
20.03.2021 08:50	23.03.2021 12:45	75.4	1.2	895.3	60.2
14.04.2021 20:45	16.04.2021 03:20	29.1	3.2	565.5	41.4
23.04.2021 17:35	23.04.2021 23:00	3.3	1	188.3	9.4

- θr (residual water content): from 0.04 to 0.08 with 0.01 step;
- θs (saturated water content): from 0.4 to 0.6 with 0.01 step;
- α (the hydraulic shape parameter): from 0.001 to 0.005 with 0.001 step;
- n (the hydraulic parameter): from 1 to 2 with 0.1 step;
- Ks (the saturated hydraulic conductivity): from 0.4 to 1.5 with 0.01 step;

The goodness of the calibration was evaluated through the Nash-Sutcliffe normalized index (formula 5.5 NNSE). The Nash–Sutcliffe efficiency is calculated as one minus the ratio of the error variance of the modeled time-series divided by the variance of the observed time-series (Nash and Sutcliffe, 1970). In the situation of a perfect model with an estimation error variance equal to zero, the resulting Nash–Sutcliffe Efficiency equals 1 (NSE = 1). Conversely, a model that produces an estimation error variance equal to the variance of the observed time series results in a Nash–Sutcliffe Efficiency of 0.0 (NSE = 0). In this application we used a Normalized Nash–Sutcliffe Efficiency (NNSE) that conveniently re-scale the NSE and allows easier interpretation. Results of NNSE between 0.5 and 1 are considered acceptable values for model evaluation.

$$NSE = 1 - \frac{\sum_{t=1}^{T} \left(Q_m^t - Q_o^t\right)^2}{\sum_{t=1}^{T} \left(Q_o^t - \bar{Q}_o\right)^2} \tag{5.4}$$

$$NNSE = \frac{1}{2 - NSE} \tag{5.5}$$

The following figures show the calibration results (Figure 5.3, 5.4 and 5.5). In each figure, the values measured by the green roof monitoring system are shown in the blue line, while the values reproduced by the model are the red line.

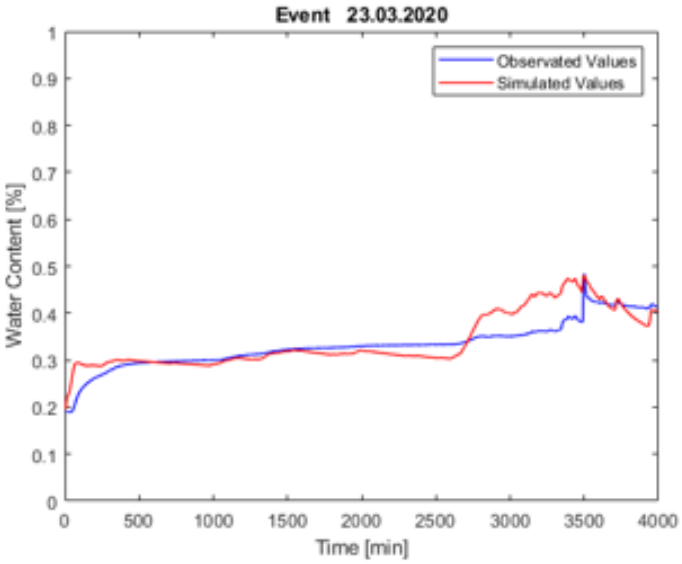

FIGURE 5.3 Calibration for the event of 23.03.2020

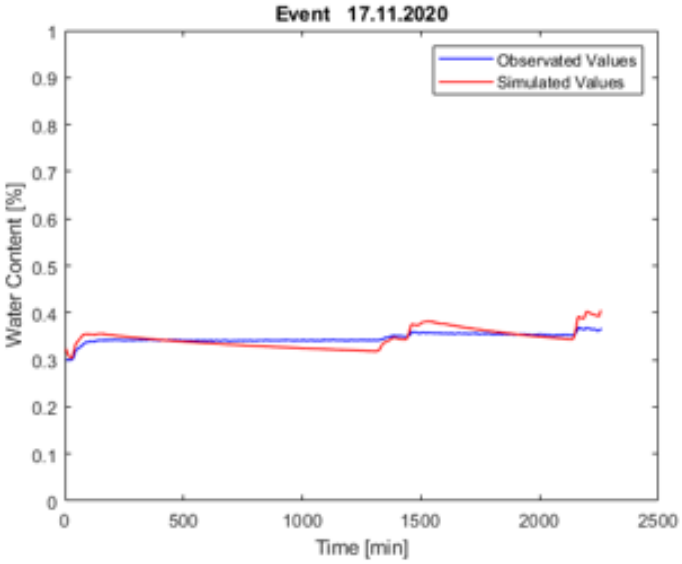

FIGURE 5.4 Calibration for the event of 17.11.2020

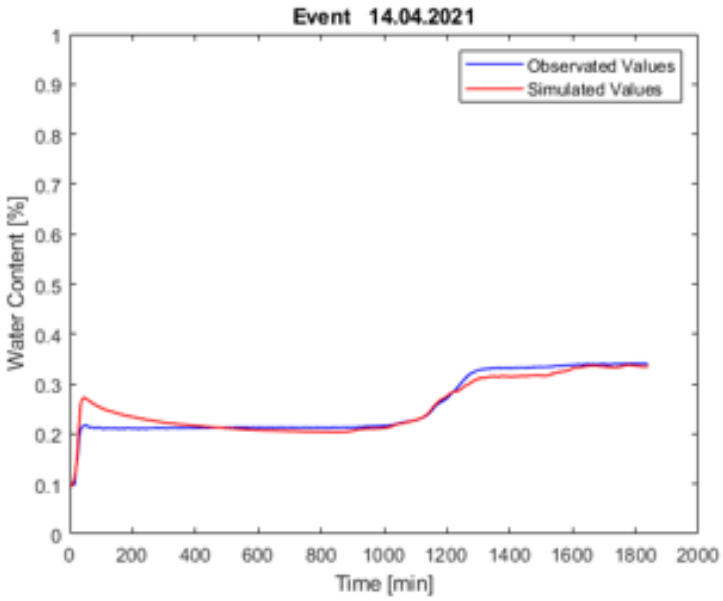

FIGURE 5.5 Calibration for the event of 14.04.2021

The table shows a summary of the calibrated parameters with the results for the three events analyzed. In addition to the best parameters for the individual events, the parameters that best fit all three events were sought (combined result).

TABLE 5.5 Parameters and NNSE after calibration

Hydraulic parameter	Range	Result Event 1	Result Event 2	Result Event 3	Combined Result
θr	0,06 - 0,08	0.08	0.08	0.08	0.08
θs	0,40 - 0,60	0.48	0.48	0.48	0.48
α	0,001 - 0,005	0.001	0.001	0.001	0.001
n	1 - 2	1.6	1.46	1.5	1.49
Ks	0,4 - 0.99	0.71	0.81	0.98	0.88
l	0.5	0.5	0.5	0.5	0.5
NNSE		0.6625	0.5724	0.936	0.5199

Validation of the results was carried out on three other rain events. The selected events are:

- 21 January 2020;

- 21 September 2020;
- 20 March 2021;

For each event, the parameters obtained from the combined result were tested and the normalized efficiency of Nash-Sutcliffe was calculated. The figures 5.6, 5.7 and 5.8 show the trends of the values in the validation events and the Table 5.6 summarizes the results.

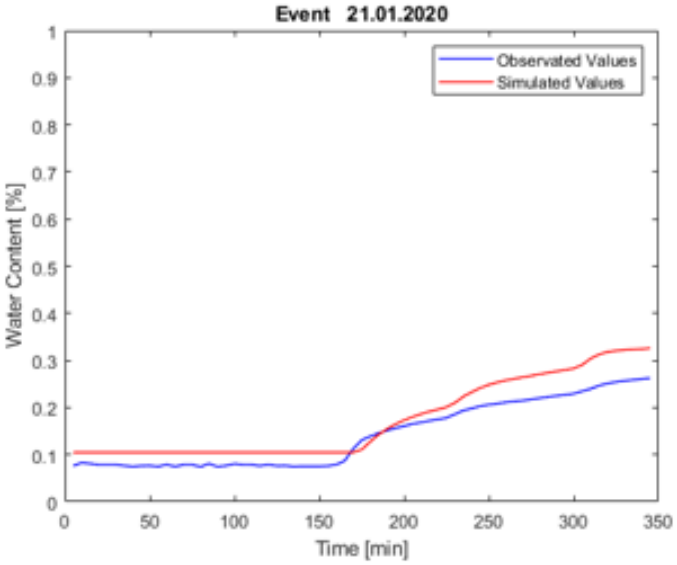

FIGURE 5.6 Validation for the event of 21.01.2020

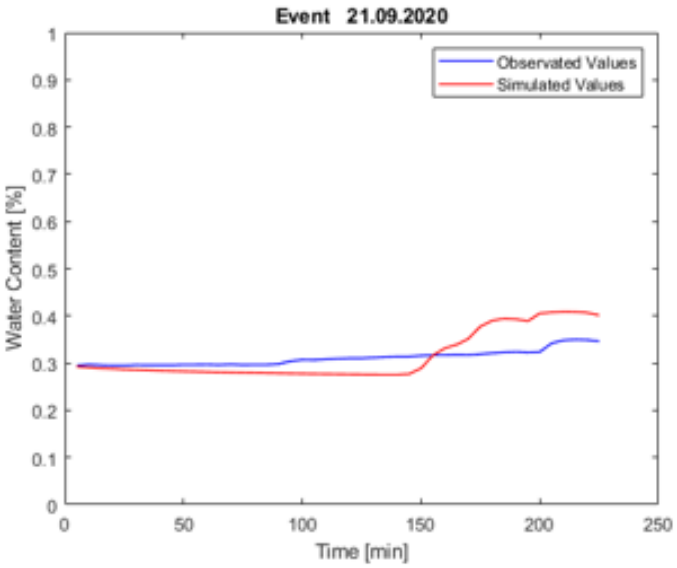

FIGURE 5.7 Validation for the event of 21.09.2020

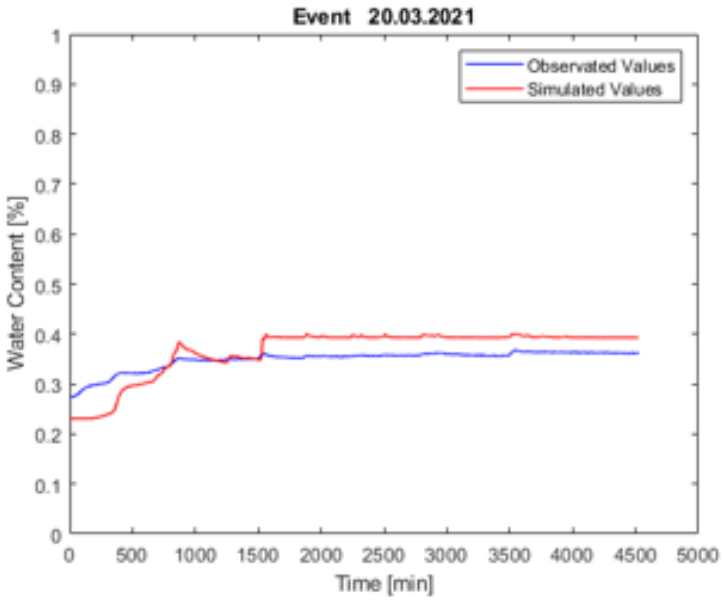

FIGURE 5.8 Validation for the event of 20.03.2021

TABLE 5.6 NNSE after validation

Hydraulic parameter	Range	Result Event 1	Result Event 2	Result Event 3
θr	0,06 - 0,08	0.08	0.08	0.08
θs	0,40 - 0,60	0.48	0.48	0.48
α	0,001 - 0,005	0.001	0.001	0.001
n	1 - 2	1.49	1.49	1.49
Ks	0,4 - 0.99	0.88	0.88	0.88
l	0.5	0.5	0.5	0.5
NNSE		0.5949	0.5740	0.5141

5.4.2 Modeling of depletion curves

To obtain a model of the green roof as faithful as possible to reality, it was also necessary to calibrate the dry periods. The dry periods are no longer influenced by the hydraulic parameters of the soil, but they are influenced by the parameters that regulate evapotranspiration and by the boundary conditions of the soil column.

As boundary condition at the top of the soil column the atmospheric BC with surface layer was chosen. This because this condition permits water to build up on the surface within the limit of 30 mm in this case. The height of the surface water layer increases due to precipitation and reduces because of infiltration and evaporation.

As a boundary condition at the bottom of the column "Water Flow Deep Drainage BC" was inserted. Deep Drainage from the soil profile is a vertical drainage, q(h), across the lower boundary of the soil profile and it is sometimes approximated by a flux which depends on the position of the groundwater level (Hopmans and Stricker, 1989).

If available, such a relationship can be implemented in the form of a variable flux boundary condition; the code in that case internally sets the variable KodBot equal to -7. This boundary condition will be implemented in HYDRUS if the logical variable qGWLF in the input file SELECTOR.IN is set equal to .true. The discharge rate q(n) assigned to bottom node n is determined by the program as q(n)=q(h), where h is the local value of the pressure head, and q(h) is given by the 5.6 equation.

$$q(h) = -A_{qh} \exp\left(B_{qh}|h - GWL0L|\right) \tag{5.6}$$

where Aqh and Bqh are empirical parameters which must be specified in input file, together with GWL0L which represents the reference position of the groundwater level (in this case set to zero). The parameters to be calibrated for the depletion curves are the crop data and the deep drainage data. The tables 5.7 and 5.8 show a summary.

TABLE 5.7 Crop data parameters

Crop Data	
Crop height [mm]	200
Root depth [mm]	150
LAI	0.1 – 3.5
Interception	1 – 1.5

TABLE 5.8 Deep drainage parameters

Deep drainage boundary condition	
Aqh parameter [mm/min]	-0.15 – -0.80
Bqh parameter [1/mm]	-0.0015 – -0.0021
Reference Ground water level [mm]	0

Also in this case it was possible to carry out the calibration on three periods. Periods of about a week that were not affected by the automatic irrigation of the green roof were chosen. The dates selected were from 6 to 12 May 2020, from 1 to 5 June 2020 and from 6 to 12 April 2021. The figures 5.9, 5.10 and 5.11 show the trend of the calibration, and the Table 5.9 summarize the results.

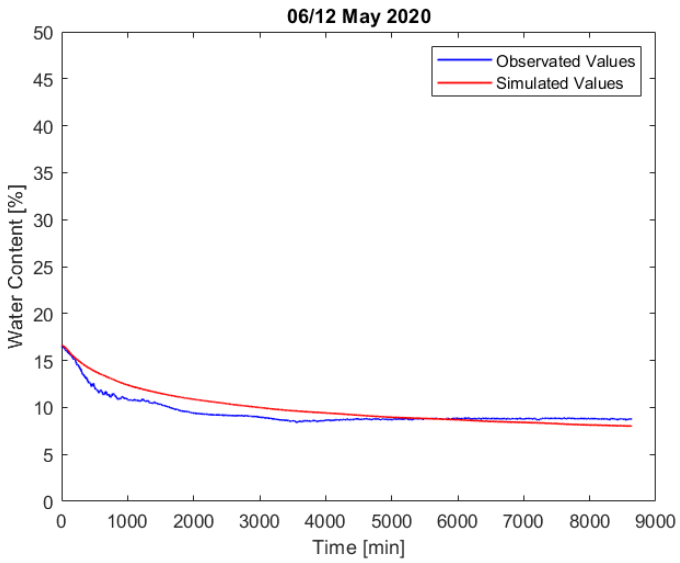

FIGURE 5.9 Calibration for the period 6-12 May 2020

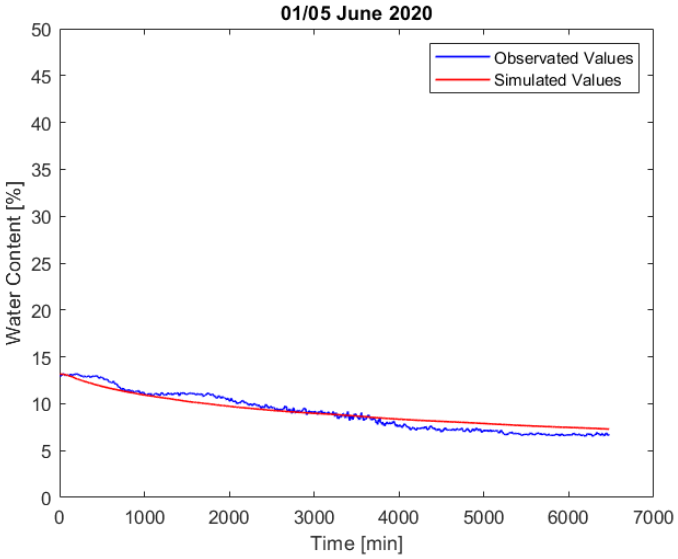

FIGURE 5.10 Calibration for the period 1-5 June 2020

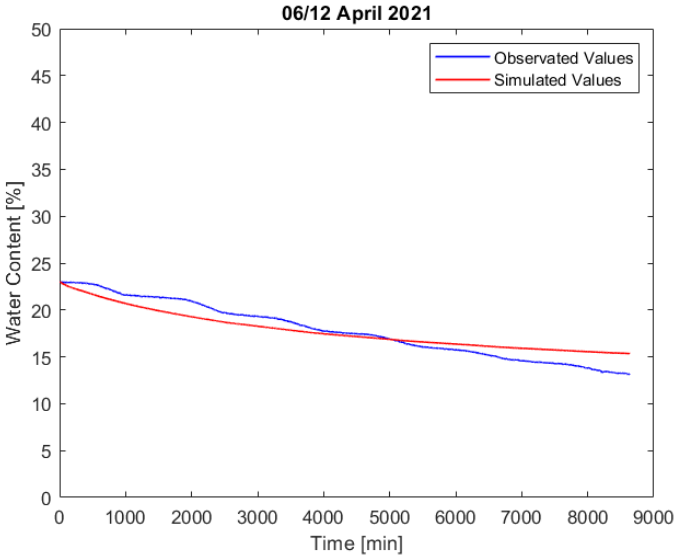

FIGURE 5.11 Calibration for the period 6-12 April 2021

5.5 Green roof modeling results

Once the model calibration was completed, it was possible to analyze the 28 rain events recorded in the database from May 2019 to April 2020.

TABLE 5.9 Results of the calibration for depletion curves

Results	
Crop height [mm]	200
Root depth [mm]	150
LAI	2.51
Interception	1.2
Aqh parameter [mm/min]	-0.75
Bqh parameter [1/mm]	-0.0016
Reference Ground water level [mm]	0

For each event, the volume of water retained by the roof (Retained volume RV), the reduction of the rainfall peak (PFR) and the delay in the peak (Peak flow lag-time PFL) were calculated, with the formulas 5.7, 5.8 and 5.9.

$$RV(\%) = \frac{\mathrm{RV_{IR}} - \mathrm{RV_{GR}}}{\mathrm{RV_{IR}}} \times 100 \tag{5.7}$$

$$PFR(\%) = \frac{\mathrm{PF_{IR}} - \mathrm{PF_{GR}}}{\mathrm{PF_{IR}}} \times 100 \tag{5.8}$$

$$PFL(\mathrm{min}) = t_{P_{GR}} - t_P \tag{5.9}$$

The Table 5.10 shows the results for the recorded rain events.

The results are quite varied: the retention of the volume of water is between about 10% and 99%; the reduction of the rain peak is between 11% and 100%, while the delay of the peak varies between 0 minutes and over 1000 minutes. On average, the volume retention is around 67.5%, while the mean peak reduction is over 89%. As for the mean delay of the peak is about 295 minutes.

TABLE 5.10 Hydrological performance indicators for the green roof at event scale. RV-retained volume, PFR—peak flow reduction, PFL—peak flow lag-time

N°	Date start	RV [%]	PFR [%]	PFL [min]
1	15.05.2019	82.919	93.74	490.00
2	04.09.2019	99.999	100.00	55.00
3	07.10.2019	17.118	91.16	175.00
4	09.10.2019	48.702	93.98	585.00
5	25.10.2019	28.583	95.99	75.00
6	03.11.2019	90.262	99.33	50.00
7	06.11.2019	77.147	99.28	550.00
8	11.11.2019	19.982	81.78	110.00
9	19.11.2019	96.196	98.33	265.00
10	24.11.2019	32.083	93.17	35.00
11	21.01.2020	99.997	99.999	135
12	23.03.2020	10.503	11.116	0
13	15.07.2020	96.523	99.29	165
14	13.09.2020	99.739	99.558	125
15	16.09.2020	97.594	98.072	20
16	21.09.2020	99.7	98.848	25
17	23.09.2020	96.183	96.468	25
18	17.11.2020	55.238	93.115	55
19	28.11.2020	9.603	23.285	0
20	03.12.2020	79.138	97.764	145
21	06.12.2020	99.849	99.714	70
22	08.12.2020	72.446	98.61	900
23	19.12.2020	26.762	66.253	20
24	15.01.2021	55.578	96.727	170
25	13.02.2021	83.27	94.413	355
26	20.03.2021	23.307	89.648	1795
27	14.04.2021	93.342	98.811	1780
28	23.04.2021	99.819	99.897	90

Chapter 6

Evaluation of EURO-CORDEX (Coordinated Regional Climate Downscaling Experiment for the Euro-Mediterranean area)

6.1 Overview

To test the effectiveness of green roofs as a tool for reducing rain peaks and volumes, it is necessary to have reliable climate models. For this reason, an in-depth analysis was carried out on some CORDEX data (COordinated Regional Downscaling EXperiment). This chapter deals with two analysis to reach the ultimate goal of this research. The first study analyses climate models to evaluate their reliability in the reproduction of rains, temperatures and periods of drought in the regions of Calabria and Sicily (Italy).

The second study, with reference to 14 rain gauge stations in Sicily (Italy), evaluates historical simulations of precipitation data from 11 RCMs, in order to understand how they compare to fine-resolution observations. In particular, we investigate the ability to reproduce rainfall event characteristics, as well as annual maxima precipitation at different durations. The proposed analysis highlights the differences between the different models, and, by ranking the RCMs, supports the selection of the most suitable climate model for assessing the impacts in the considered locations in terms of extreme event analysis. This analysis on the

GCM-RCM circulation models was fundamental to advance the research not only in the current state but also in a future scenario.

6.2 Evaluation of GCM-RCM models historical simulations by high-quality observational datasets in southern Italy

6.2.1 Overview on Global Circulation and Regional Climate Models and their use for future predictions

The COordinated Regional Downscaling EXperiment (CORDEX) is a diagnostic model intercomparison project (MIP) in CMIP6. CORDEX builds on a foundation of previous downscaling intercomparison projects to provide a common framework for downscaling activities around the world. The CORDEX regional challenges provide a focus for downscaling research and a basis for making use of CMIP6 global climate model (GCM) output to produce downscaled projected changes in regional climates and assess sources of uncertainties in the projections, all of which can potentially be distilled into climate change information for vulnerability, impacts and adaptation studies (Gutowski Jr. et al., 2016).

A growing number of scientific studies claims that climate change due to global warming will significantly alter the water cycle, with an increase of the intensity and frequency of extreme hydro-climatic events in several areas around the globe (Arnell et al., 2001; Ipcc and Report, 2018). These include the Mediterranean region, which is recognized as one of the major hot spots of climate change due to future projections of temperature increase and annual precipitation decrease (Giorgi and Lionello, 2008; Christensen et al., 2013), which determines a potential increase of drought frequency and severity.

Global Circulation and Regional Climate Models (GCMs and RCMs) can play a crucial role in understanding the potential spatio-temporal evolution of climate change in the future, thus improving current monitoring and planning tools (Mendicino and Versace, 2007; Hart and

Halden, 2019) and supporting decision-makers to choose and implement the best solutions to minimize the impact of climate change on human systems and the environment at the regional scale.

While GCMs' simulations describe climate evolution at large scale, by using coarse resolution information, RCMs simulations, derived through climate-downscaling techniques, aim at representing regional and local scale weather conditions with grid resolutions lower than 50 km down to about 10 km (Kotlarski et al., 2014; Peres, Caruso, and Cancelliere, 2017).

Several studies, focused on the use of climate models to simulate future climate scenarios for hydrological analyses, have shown that changes in temperature and precipitation vary in space depending on the future climate scenario, type, and resolution of the models, as well as on spatial heterogeneity of climatic features.

This is particularly evident in the Mediterranean region where, for instance, precipitation is partially controlled by orography, shows strong seasonality and large interannual fluctuations, and is characterized by the occurrence of particularly intense extreme events, such as prolonged droughts and high-intensity storms leading to floods (Bonaccorso et al., 2015; Bonaccorso, Cancelliere, and Rossi, 2015; Senatore, Furnari, and Mendicino, 2020).

Recently, there is a growing interest in the implementation of RCMs derived by dynamical downscaling of GCM outputs for climate change impact studies at small spatial scales. These are high-resolution models able to provide a more realistic representation of important surface heterogeneities (such as topography, coastlines, and land surface characteristics) and mesoscale atmospheric processes.

The Coordinated Regional Climate Downscaling Experiment (CORDEX) initiative is the first international program providing a common framework to simulate both historical and future climate at the regional level, under different Representative Concentration Pathways (RCPs) (Vuuren et al., 2011), and over different domains which cover all the land areas.

In the present analysis, we refer to the CORDEX domain centred on the Euro-Mediterranean area, known as EURO-CORDEX (www.euro-cordex.net). In particular, EURO-CORDEX provides simulations for a

historic reference period (baseline) and future projections up to 2100, with a 12.5 km grid resolution, available for four RCPs defined at the international level within CMIP5.

The reliability of individual RCMs in representing climate effects on the hydrological cycle depends on the quality of historical simulations and must be evaluated before using their output for impact assessment. Assessing RCMs performance is essential to either select single models for further applications (Senatore et al., 2011; Peres, Caruso, and Cancelliere, 2017; Smiatek and Kunstmann, 2019) to predict future impacts of climate change on hydrological processes (Christensen et al., 2008).

This study presents an enhanced analysis over a different Mediterranean area with complex topography, namely Sicily and Calabria regions (Southern Italy). In particular, after investigating the ability of the EURO-CORDEX models to simulate the annual and seasonal temperature and precipitation regime, we analysed the skill in reproducing drought event characteristics identified through the run method (Yevjevich, 1969).

Within the drought analysis, we also investigated the return period of drought events of fixed duration at both the annual and seasonal scales. In this case, given the limited number of droughts in a thirty-year long time series, an analytical framework was applied that allow computing return period based on reasonable assumptions on the probabilistic structure of annual and seasonal precipitation (Bonaccorso et al., 2003; Cancelliere and Salas, 2004).

Furthermore, we analysed model skills at a sub-regional level. To this aim, we proposed the use of Principal Component Analysis (PCA) for delimitation of climatically homogeneous areas. The ability of climate models to reproduce observed precipitation, temperature and drought features was analysed both per single characteristic as well as per multiple characteristics (e.g. precipitation and temperature together), by introducing a specific ranking criterion.

Nineteen coupled GCM and RCM simulations within the EURO-CORDEX framework were evaluated against a high-density and

high-quality monitoring station-based reference dataset. Monthly temperature and precipitation records were retrieved by two monitoring networks, operated by the former Regional Hydrographic Services, whose density is significantly higher than observational datasets available at the European scale, allowing for a more accurate evaluation of the models.

6.2.2 Study area and datasets

The analyses were focused on Calabria and Sicily regions in Southern Italy, which respectively have an extension of 15.080 km^2 and 25.460 km^2, for a total area of 40.540 km^2 (Figure 6.1).

Climate is of Mediterranean type with hot and dry summers and moderately cold winters with peak monthly precipitation occurring mostly in late autumn and winter. About 75% of the total precipitation in the study area occurs from October to March, because of cyclonic storms. These climate features make the area particularly prone to droughts, with the most recent severe episode occurred in 2017.

Climate features are also highly variable in space due to a rather complex orography. In particular, the mountain chains close to the coast enhance intense orographic precipitation and lead to relatively cold temperatures at the highest altitudes.

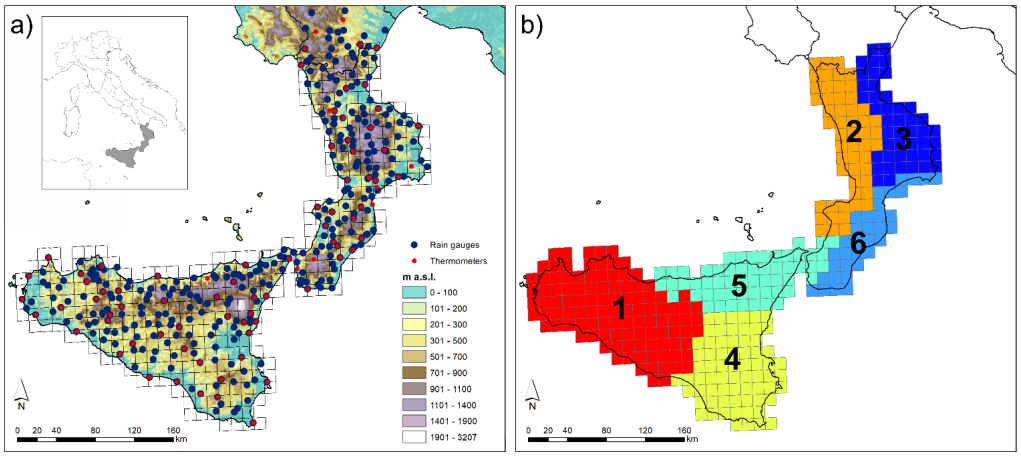

FIGURE 6.1 The study area. Calabria and Sicily regions in Southern Italy

Within the EURO-CORDEX control period (1951-2005), the comparison with observations was performed in the period from 1971 to 2000.

These three decades had the greatest availability of historical series of precipitation and temperature recorded by both the regional monitoring networks of Calabria and Sicily, managed by the Multirisk Operational Centre of Calabria region (ArpaCal) and the Water Observatory of Sicily region (WOS), respectively.

Specifically, 84 thermometers (43 in Sicily and 41 in Calabria Calabria and near the regional borders) and 335 rain gauges (173 in Sicily and 162 in Calabria and near the regional borders) were used (Figure 6.1).

The corresponding data were retrieved by the WOS (www.osservatorioacque.it) and the ArpaCal (www.cfdcalabria.it) websites. Observations were enough widespread to represent the quite heterogeneous features of the study area. The temperature stations were located between 2 and 1295 m a.s.l., with annual average values ranging from 9.2 °C to 20.6 °C (mean value = 16.2±2.4 °C), while the rain gauge elevations varied from 1 to 1369 m a.s.l., with annual accumulated values ranging from 373 mm to 1736 mm (mean value = 812±287 mm).

Monthly precipitation and monthly mean air temperature data from the EURO-CORDEX CMIP5 simulations (https://www.euro-cordex.net/) were retrieved from the nodes of the Earth System Grid Federation (ESGF, e.g. https://esgf.llnl.gov).

We analysed the data at the finest resolution, 0.11° (12.5 km), EUR-11 and considered the period 1971-2000 as a baseline. In particular, the combination of six GCMs (Table 6.1) and eight RCMs (Table 6.2) leading to 17 datasets were collected for the study.

TABLE 6.1 List of GCMs, together with the abbreviations used in this paper, included at least once in the EURO-CORDEX ensemble

Model name	Abbreviation	Institution
CNRM-CERFACS-CNRM-CM5	CM5	Centre National de Recherches Météorologique
ICHEC-EC-EARTH	ECE	Irish Centre for High-End Computing
IPSL-IPSL-CM5A-MR	IPS	Institut Pierre Simon Laplace
MOHC-HadGEM2-ES	Had	Met Office Hadley Centre
MPI-M-MPI-ESM-LR	MPI	Max-Planck-Institute für Meteorologie
NCC-NorESM1-M	Nor	Norwegian Earth System Model

TABLE 6.2 List of RCMs, together with the abbreviations used in this paper, included at least once in the EURO-CORDEX ensemble

Model name	Abbreviation	Institution
CNRM-ALADIN53	ALAD	Météo-France / Centre National de Recherches Météorologiques
RMIB-UGent-ALARO-0	ALAR	Royal Meteorological Institute of Belgium and Ghent University
CLMcom-CCLM4-8-17	CCLM	Climate Limited-area Modelling Community (CLM-Community)
DMI-HIRHAM5	HIRH	Danish Meteorological Institute
KNMI-RACMO22E	RACM	Royal Netherlands Meteorological Institute, De Bilt, The Netherlands
SMHI-RCA4	RCA4	Swedish Meteorological and Hydrological Institute, Rossby Centre
MPI-CSC-REMO2009	REMO	Helmholtz-Zentrum Geesthacht, Climate Service Center, Max Planck Institute for Meteorology
IPSL-INERIS-WRF331F	WRF3	Institut Pierre-Simon Laplace and French National Institute for Industrial Environment and Risks

Therefore, an overall ensemble of 19 combined models (CMs) was analysed. The ensemble mean of the 19 CMs was also evaluated. Even if the CMs have the same spatial resolution, each one is distributed on a specific grid (with slightly different origin and orientation of the axis).

Therefore, the various data sets were resampled on the grid of the ECE-HIRH CM, which is shown in Figure 6.1

6.2.3 Methodology to investigate the ability of the EURO-CORDEX models to simulate temperature, precipitation and drought

To allow the comparison between the spatially distributed RCMs data and site-specific observations, the latter were spatially interpolated using the CORDEX 0.11° grid as reference (Figure 6.1). In this way, month by month, each cell of the CORDEX grid could be associated with a single temperature or precipitation value derived from the observations network.

Specifically, concerning temperature, an Inverse Distance Weighting (IDW) interpolation was applied to the residuals of the values obtained using a regression model with the altitude.

For precipitation, whose measurement network is much denser, a simple IDW interpolation was performed. As shown in Figure 6.1, the CORDEX grid cells which are not covered by any rain gauge are relatively few (less than 30%) and, except one case, the distance of the closest rain gauge to every grid cell is always less than 10 km.

The precipitation patterns obtained by the interpolation procedure were analyzed adopting a methodology based on the Principal Component Analysis (PCA) to distinguish zones with rather independent climatic variability within the area under investigation. PCA is a well-known statistical tool used to transform an original set of intercorrelated variables into a reduced number of new linearly uncorrelated ones explaining most of the total variance.

The latter, derived as linear combinations of the original variables, are the principal components (PCs), while the coefficients of the linear combinations are the loadings, which in turn represent the weight of the original variables in the PCs. From a procedural standpoint, PCA consists of solving an eigenvalue-eigenvector problem applied to the covariance matrix.

The eigenvectors, properly normalized, are the loadings of the principal components, while the eigenvalues provide a measure of the total variance explained by each loading (Bordi and Sutera, 2001). Under this decomposition, the loadings represent the correlation between the associated PCs and observed time series. Mapping the loading patterns of each PC among those selected, based on the percentage of the total explained variance of the process, largely allow to identify independent climatic areas within the study region.

Moreover, it may be useful to apply a rotation operation to the eigenvectors, so that the corresponding loadings are more spatially localized. In other words, the rotation leads to loadings with a high correlation with a smaller set of spatial variables and a low correlation with the remaining variables. Clearly, each rotated pattern will not explain the same variance of the unrotated one, although the total variance explained remains unchanged.

In the present study, the first nine rotated PCs both at the annual and seasonal (DJF, MAM, JJA, SON) scales were investigated. Regardless of the considered period, the selected PCs always explain more than 78% of the total variance, with a maximum of 85% in the winter season (DJF).

The loading patterns of these rotated PCs were mapped for each considered period to identify climatically homogeneous regions. Homogeneous sub-regions were detected at the annual scale and in autumn and

winter seasons, whereas a confusing picture arose in spring and summer seasons.

Furthermore, since about 75% of the total annual rainfall of the case-study area occurs between autumn and winter (as a result of cyclonic storms), the climatically homogeneous sub-regions identified at the annual scale approximately overlap with those identified at seasons SON and DJF. Isolated grid cells showing a different PC correspondence with respect to the surrounding cells, were manually corrected to simplify the delimitation of the homogeneous sub-regions.

This approach led in dividing the whole area into six climatically homogenous zones, three for Sicily and three for Calabria (Figure 6.1), for which separate performance assessments were carried out.

Concerning Sicily region, the three identified sub-regions roughly coincide with the ones detected by Bonaccorso et al., 2003, who investigated the spatial variability of droughts in Sicily region based on SPI series computed on monthly precipitation observed in traditional rain gauges and on NCEP/NCAR reanalysis data from 1926 to 1996.

In particular, three distinct areas, namely North-Eastern (identified in the PCA as zone 5, Figure 6.1b), South-Central Eastern (zone 4), and Central-Western (zone 1), were identified. In Calabria, three main zones were also determined, namely North-Western (zone 2), North-Eastern (zone 3) and South-Eastern (zone 6). Interestingly, the South-Western tip of Calabria is identified as a part of a broader area (zone 5) extending over the North-Eastern Sicily.

The CMs were evaluated based on their performances in capturing specific properties, namely: the interannual and seasonal variability of precipitation, temperature and drought characteristics. Such properties were expressed based on some relevant statistics.

Let X_j and $X_{\tau j}$ be the variable under investigation (precipitation or mean temperature) at grid cell j at the annual and seasonal scale, respectively.

For precipitation and mean air temperature, the following statistics were derived for each CM and cell in the area of interest:

- Seasonal mean (eq. 6.1); where $x_{\nu\,\tau\,m}(j)$ is the value of the variable in season τ (τ=1, 2, 3, 4) and year ν (ν = 1, 2, ...N) produced by the

mth CM (m = 1, 2, ...) at grid cell j. Seasons are DJF, MAM, JJA, and SON.

- Seasonal standard deviation (eq. 6.2);
- Annual mean (eq. 6.3); where $x_{\nu\ m}(j)$ is the value of the variable in year ν (ν = 1, 2, ...N) produced by the mth CM at grid cell j.
- Annual standard deviation (eq. 6.4).

$$\mu_m\left(X_\tau(j)\right) = \frac{\sum_{v=1}^{N} x_{v,\tau,m}(j)}{N} \tag{6.1}$$

$$\sigma_m\left(X_\tau(j)\right) = \sqrt{\frac{\sum_{v=1}^{N}\left(x_{v,\tau,m}(j) - \mu_m\left(X_\tau(j)\right)\right)^2}{N-1}} \tag{6.2}$$

$$\mu_m\left(X(j)\right) = \frac{\sum_{v=1}^{N} x_{v,m}(j)}{N} \tag{6.3}$$

$$\sigma_m\left(X(j)\right) = \sqrt{\frac{\sum_{v=1}^{N}\left(x_{v,m}(j) - \mu_m\left(X_\tau(j)\right)\right)^2}{N-1}} \tag{6.4}$$

Drought events were identified on both annual and seasonal (DJF, MAM, JJA, SON) precipitation values simulated for the period 1971-2000, according to the theory of runs (Yevjevich, 1969).

In particular, drought events were selected as the periods during which consecutive annual or seasonal values of precipitation did not exceed a given threshold, here assumed equal to the long term means of annual and seasonal data (i.e. one threshold for each season).

Once drought events were identified, the corresponding drought characteristics in each cell were determined. In particular, the following statistics for drought characteristics are considered hereafter to assess the models' performance:

- Maximum drought duration Lmax: maximum length of periods with consecutive annual precipitation values below the threshold;
- Maximum drought accumulated deficit Dmax: maximum of the sums of the differences between the threshold and the precipitation values along with the drought duration;

- Maximum drought intensity Imax: maximum of the ratio between drought accumulated deficit and duration;
- Return period of drought events of fixed duration (at both annual and seasonal scales).

Concerning the return period of drought events, let E be a critical drought (e.g., a drought with duration L equal to a fixed value). Assuming independence between consecutive drought events, the return period of drought event E can be expressed as the equation 6.5 (Cancelliere and Salas, 2004; Cancelliere and Salas, 2010; Bonaccorso, Cancelliere, and Rossi, 2012):

$$T_E = \frac{E[L] + E\left[L_{\mathrm{n}}\right]}{P[E]} \tag{6.5}$$

where E[L] is the expected value of drought duration L and E[Ln] is the expected value of the non-drought duration Ln and P[E] is the probability of occurrence of a critical drought E, which can be determined once that the probability distribution function of the event E is known.

Models' skills in reproducing the interannual and seasonal variability of precipitation and mean air temperature variables were first assessed through:

- boxplots of the errors and percentage errors of the mean values in all the grid cells of the investigated areas, which allow analysing the spatial variability of the models' bias;
- Taylor diagrams (Taylor, 2001), which show three metrics at the same time, i.e.: coefficient of correlation, standard deviation, and centred root mean square error of the anomalies (i.e., the variables of interest minus the corresponding means). It is noteworthy that standard Taylor diagrams do not provide any information about first-order statistics (i.e., bias).

Later, to provide synthetic information about each CM starting from the various statistics computed for each property, a method based on Mascaro, Viola, and Deidda, 2018 was used.

Specifically, for each property (i.e. seasonal and interannual variability of precipitation and mean temperature and drought characteristics), a single dimensionless error metric that combines multiple statistics characterizing that property was estimated. The error metrics follows the equation 6.6:

$$\varepsilon_m = \sqrt{\sum_{k=1}^{S} \left(\frac{\sum_{j=1}^{P} E_{k,m}(j)}{\sum_{m=1}^{M} \sum_{j=1}^{P} E_{k,m}(j)} \right)^2} \tag{6.6}$$

where $E_{k,m}(j)$ represents an error metric between observed and simulated data of the statistics k (k = 1,..., S) at grid cell j (j=1, ... P, where P is the total number of grid cells), whose sum over the whole area was divided by the sum of the error metrics of all models, therefore resulting in a dimensionless indicator for each statistic k of any property.

Based on the values of the error metrics, a ranking of the models, describing the skills in reproducing each property, was obtained.

It should be specified that while, for the sake of brevity, the boxplots and the Taylor diagrams illustrated in the next section refer to the whole study area, the ranking of the models for the mean air temperature, precipitation and drought characteristics also refers to the six climatically homogenous zones identified through PCA. This analysis, indeed, can help to highlight whether some models are more suitable than others to simulate certain variables in a given zone.

6.2.4 Results of the analysis

Mean air temperature

The observed and modelled means of the annual mean air temperature values in each of the grid cells within the study area were calculated and compared. More specifically, for each cell j, the error corresponding to the m-th CM was computed as in formula 6.7.

$$E_{m,j} = \mu_m(T(j)) - \mu_0(T(j)) \tag{6.7}$$

where T(j) is the mean annual temperature at cell j, whereas μm and μ0 are the modelled and observed means respectively.

For each model, the distribution of the errors computed for all the grid cells of the study area based on equation 6.7, is represented in the form of box-plots in Figure 6.2a.

In particular, the central line represents the median value and the box is delimited by the first and the third quartile. The width of the box corresponds to the inter-quartile range (IQR), a well-known measure of dispersion. Values outside the whiskers, distant from the box at least 1.5 IQR, can be assumed as outliers.

The overall tendency of the models is to underestimate temperatures, as the medians are negative. Errors are predominantly comprised between the values -5 and -1 °C, thus implying that the models underestimate up to 5 °C.

The CMs that produce the most extreme negative errors are the ECE-RACM, ECE-RACMr12 and CM5-ALAD, with the latter showing the broader IQR (e.g. the highest spatial variability of the errors) and the greatest median error. All the CMs with RCA4 show the smallest IQR. The models with the smallest median error are MPI-REMO and MPI-REMOr2.

To extend the CM skill comparison to other statistics, the Taylor diagram for the annual mean air temperature values was developed (Figure 6.2b). For the sake of simplicity, standard deviations of the CMs are indicated as σ hereinafter.

The diagram allows visualizing if there are clusters of performances related to specific GCMs or RCMs among those considered. In the diagram, GCMs are indicated with different markers, while RCMs with different colors. The value corresponding to the observations is the dot on the x-axis, whose standard deviation is marked through a continuous circular arc. In addition to every single model, the ensemble mean model result is reported in the diagram.

Figure 6.2b shows that the simulated means are well correlated with the observations, with values larger than 0.8 for all the considered models. Furthermore, the diagram seems to reveal that, on equal GCMs, RCMs play a significant role in determining the performance of the combinations.

In general, for most of the models, the best performances are obtained

when the RCM RCA4 is used. The only exception is CM5, performing better in combination with CCLM. The worst models are CM5-ALAD and IPS-WRF.

Finally, the ranking analysis described before yields the results in Figure 6.3.

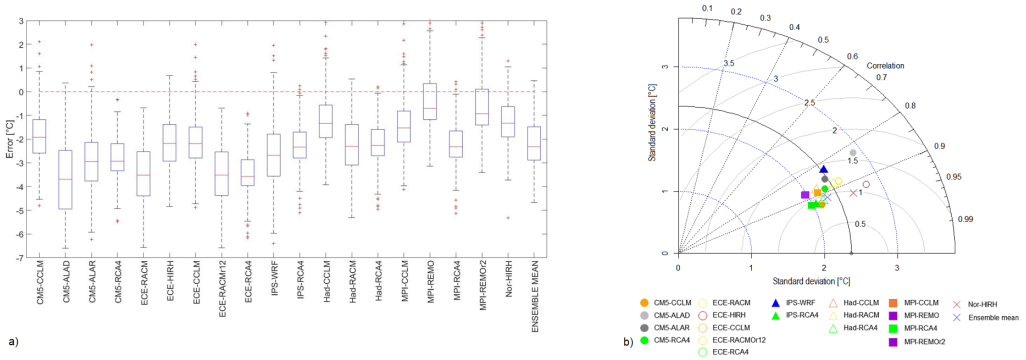

FIGURE 6.2 (a) Box plots representing the frequency distribution of RCM errors in mean annual temperature for the whole study area. (b) Taylor diagram comparing model performances in reproducing the inter-annual variability of mean temperature for the whole study area.

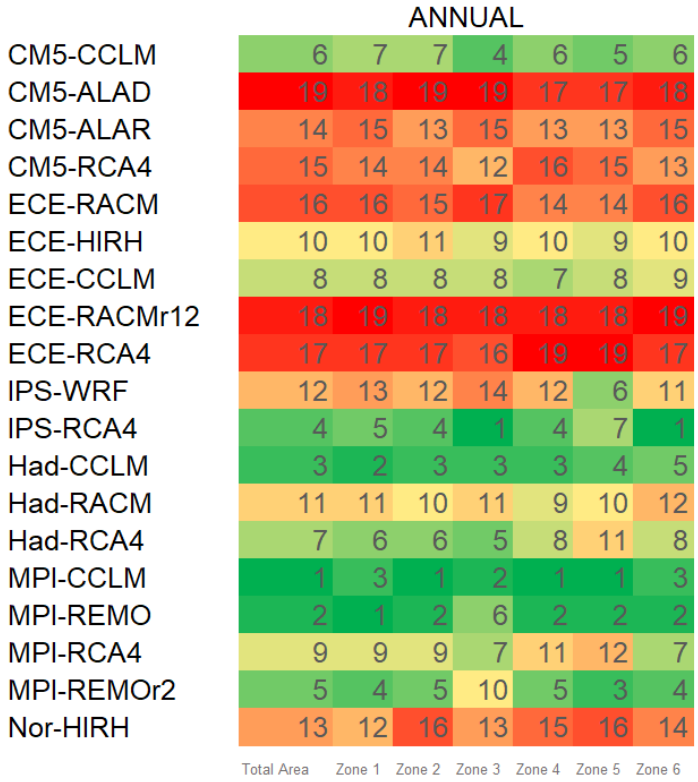

FIGURE 6.3 RCM ranking with respect to inter-annual variability of mean temperature, for the entire area and the climatically homogenous zones.

The lower the rank, the lower is the error metrics in equation 6.7 and the better is the model. For better readability, ranking values are indicated through a chromatic scale, ranging from dark green (first ranked model) to dark red (last ranked model).

The best performing models, in terms of ranking order for the whole study area, are MPI-CCLM, MPI-REMO, and Had-CCLM. ECE-RCA4 and CM5-CCLM are also good models as highlighted by the Taylor diagrams.

Figure 6.3 also shows rankings for each of the six homogeneous areas. As it can be observed, based on the range of colours in each row, MPI-CCLM and MPI-REMO provide the best performance for almost all the zones.

Indeed, some differences exist for Zones 3 and 6 (North and South-Eastern Calabria), whose best CM is IPS-RCA4. Overall, results show that the worst model is CM5-ALAD for entity and dispersion of errors, lower

correlations, higher RMSE, greater deviation from the standard deviation of the observed values, both for the whole study area and individual zones.

ECE-RACM, ECE-RACMr12, and ECE-RCA4 also show bad performance (the latter mainly because of its relatively strong bias).

For the sake of brevity, the box-plots related to the seasonal variability of mean air temperature are not shown since they provide similar results to the case of annual variability.

Figure 6.4 shows the Taylor diagrams obtained from the analysis of the individual seasons. CM5-ALAD and IPS-WRF (and, to a slightly lesser extent, CM5-ALAR) appear as the worst models regardless of the season, although in summer (JJA) the worst-performing models are MPI-REMO and MPI-REMOr2. Summer is also the season with the (slightly) lowest values of correlation coefficients.

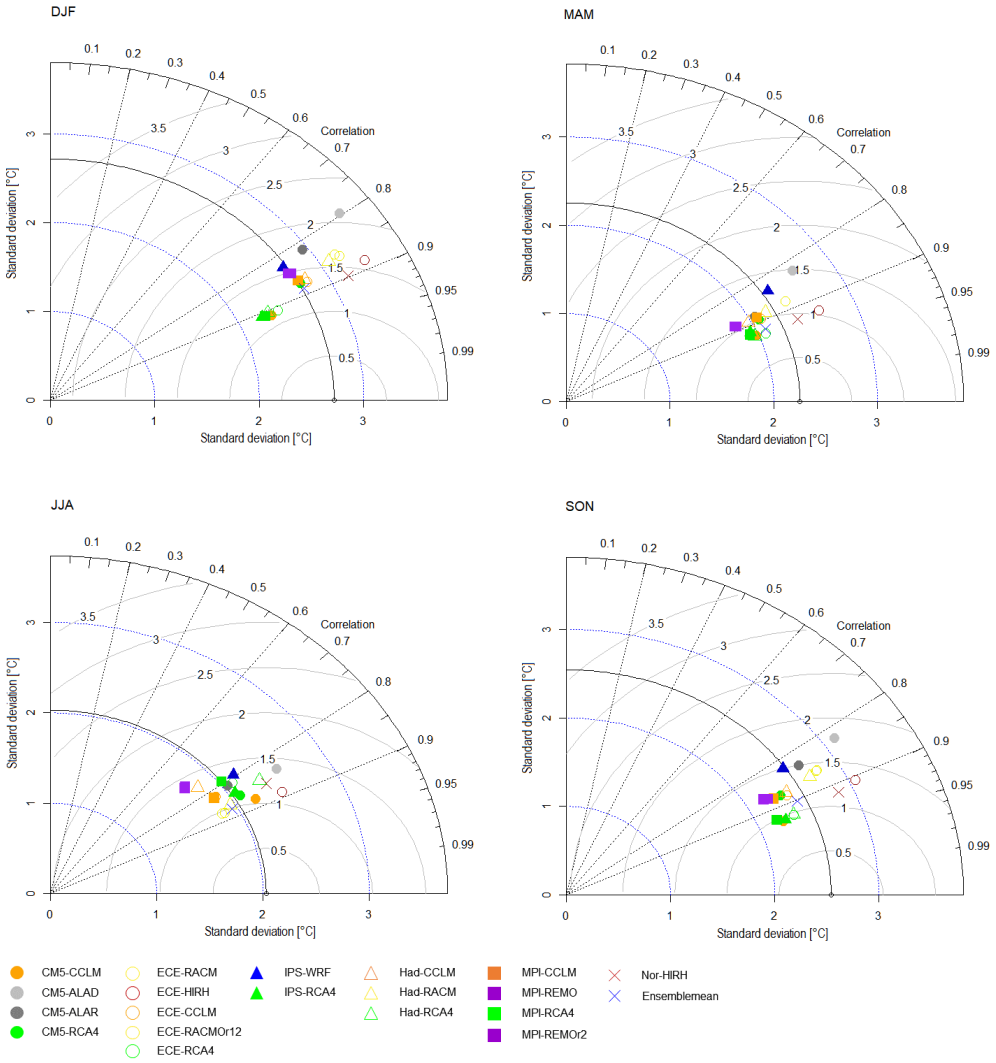

FIGURE 6.4 Taylor diagram comparing model performances in reproducing the seasonal variability of mean temperature for the whole study area.

Regarding the best models, in general, all the combinations with RCA4 and the CM5-CCLM work better, as for the interannual variability analysis. However, in summer better performances are obtained with ECE-RACM and ECE-RACMr12.

Figure 5 represents the rankings of the models for the individual seasons and all the study areas, namely the whole case study and the six zones.

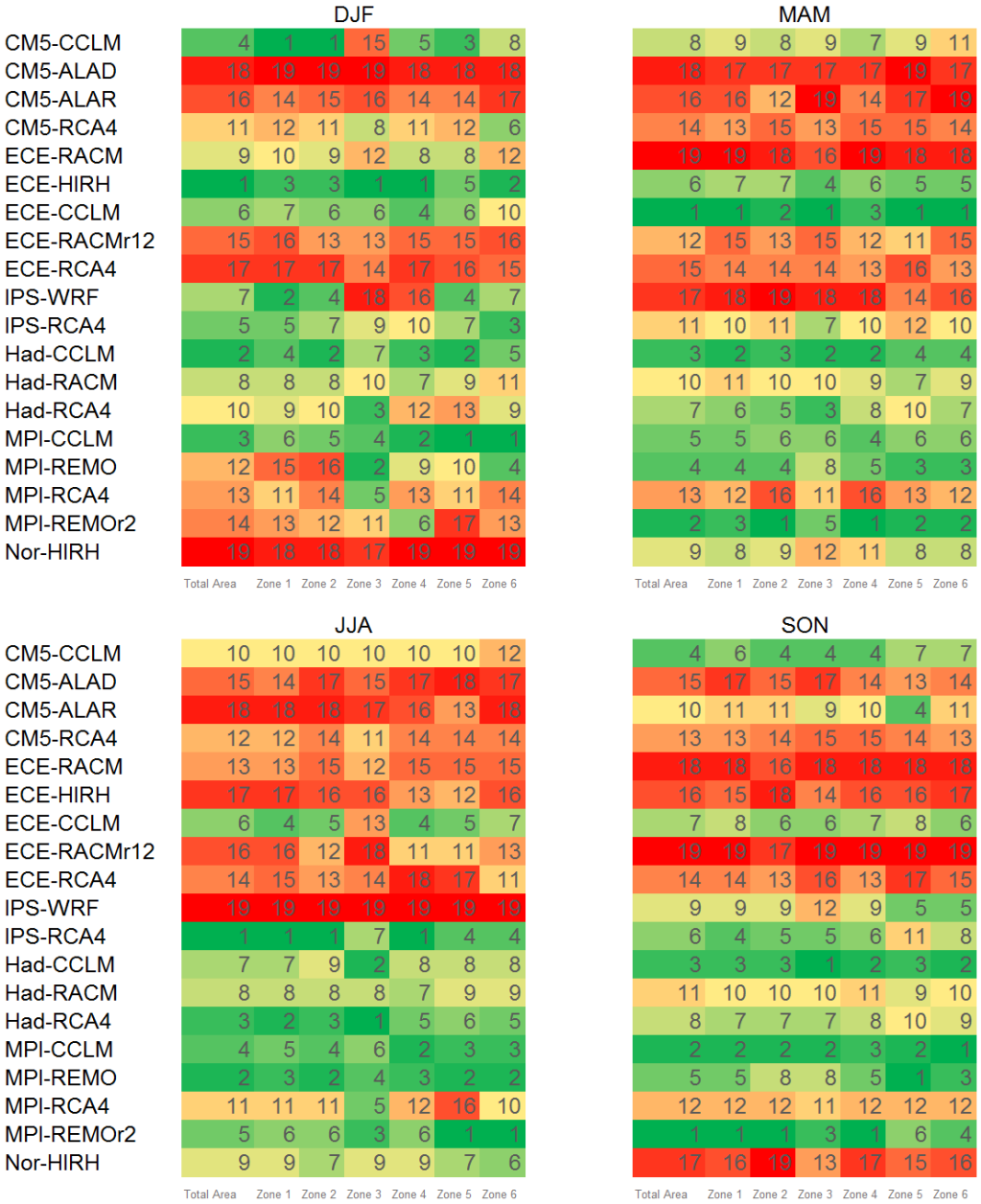

FIGURE 6.5 RCM ranking with respect to seasonal variability of mean temperature for the entire area and the climatically homogenous zones.

There is a certain correspondence on the least performing models between figures 6.4 and 6.5. Nonetheless, differently from the results in Figure 6.3, models' performances may change significantly from season to season and, in the same season, from zone to zone.

The best models for most of the zones are ECE-HIRH in winter (DJF), ECE-CCLM in spring (MAM), IPS-RCA4 in summer (JJA) and

MPI-REMOr2 in autumn (SON). It's worth highlighting that the latter provides the best performances also for Zones 2 and 4 in spring and Zones 5 and 6 in summer.

Conversely, ECE-HIRH, which is the best model in winter, works poorly in summer and autumn. The Zones 1 (Western Sicily) and 2 (Western Calabria) show a uniform behaviour in all seasons, with the only exception of spring, while Zones 5 (North-Eastern Sicily) and 6 (South-Eastern Calabria) show a uniform behaviour in all seasons but autumn. Besides, in summer and autumn, the best performing models for Zones 1, 2 and 4 (South-Eastern Sicily) are the same as for the whole study area. Zone 3 (North-Eastern Calabria) behaves like Zone 4 in winter and like Zones 1, 5 and 6 in spring.

Precipitation

Figure 6.6a shows box-plots for the percentage errors in mean annual precipitation, calculated following the equation 6.8, where P(j) is the total annual precipitation at the grid cell j.

$$E_{m,j} = \frac{\mu_m(P(j)) - \mu_0(P(j))}{\mu_0(P(j))} \cdot 100 \tag{6.8}$$

In comparison to temperature, the errors are much larger, as well as the differences between the various models. There is a general tendency for the models to underestimate the total annual precipitation, except for some models like IPS-WRF, which also shows the largest IQR.

The median value of the relative errors for some models is less than 20%; however, many models have a large dispersion with error values over 100%. The CM with the highest positive error is IPS-WRF, while the ones with the highest negative errors are the IPS-RCA4 and Nor-HIRH models.

The GCM-RCM combinations with the smallest IQR of errors are those using CCLM RCMs. The model with the smallest bias is Had-RACM.

The Taylor diagram in Figure 6.6b confirms that the best combinations are those with CCLM RCMs. In particular, the best one seems ECE-CCLM. However, when used in combination with CM5, the corresponding model provides poor performance.

The worst performing models are ECE-HIRH and Nor-HIRH. The diagram confirms that precipitation is modelled with less accuracy than temperature, as correlations are lower.

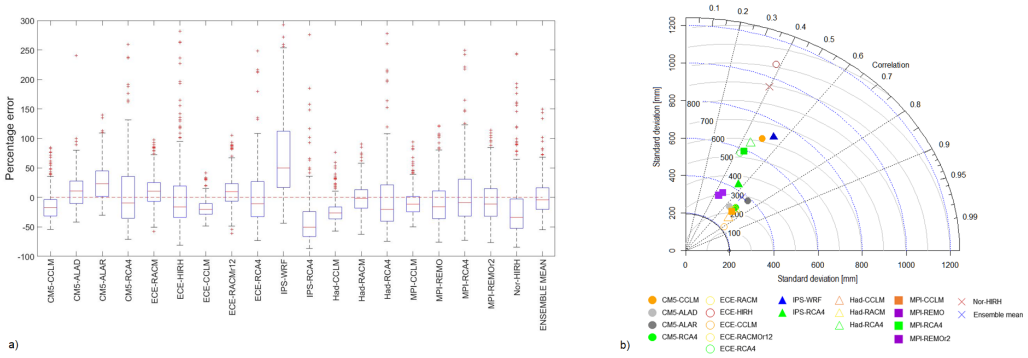

FIGURE 6.6 (a) As Figure 6.2a but for annual precipitation. (b) As Figure 6.2b but for annual precipitation.

The application of the ranking criteria (see Figure 6.7) suggests Had-RACM and ECE-CCLM as the best combinations for the entire area and most of the zones. Also, CM5-ALAD works well for the whole area and almost all the zones, except for Zone 4, where it ranks the 11th. IPS-WRF, IPS-RCA4, Nor-HIR, and CM5-RCA4 are the worst models.

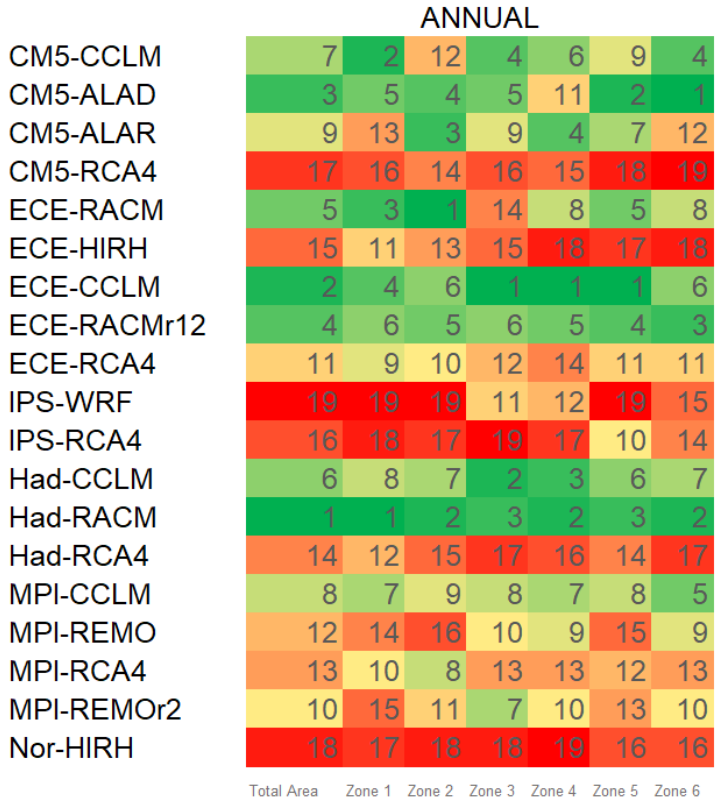

FIGURE 6.7 As Figure 6.3 but for annual precipitation.

The seasonal variability analysis carried out on precipitation shows (Figure 6.8) a lower error dispersion in the wet seasons (i.e., autumn and winter) with respect to summer.

In summer, several models show broader IQR, such as all the CM5 models and IPS-WRF, with the latter showing the largest median error. On the one hand, these outcomes depend on the poor performance of some models in reproducing the seasonal cycle, and on the other hand, are due to the fact that in the dry season where rainfall is normally low, large errors may result even though the departure from the observed mean is relatively small.

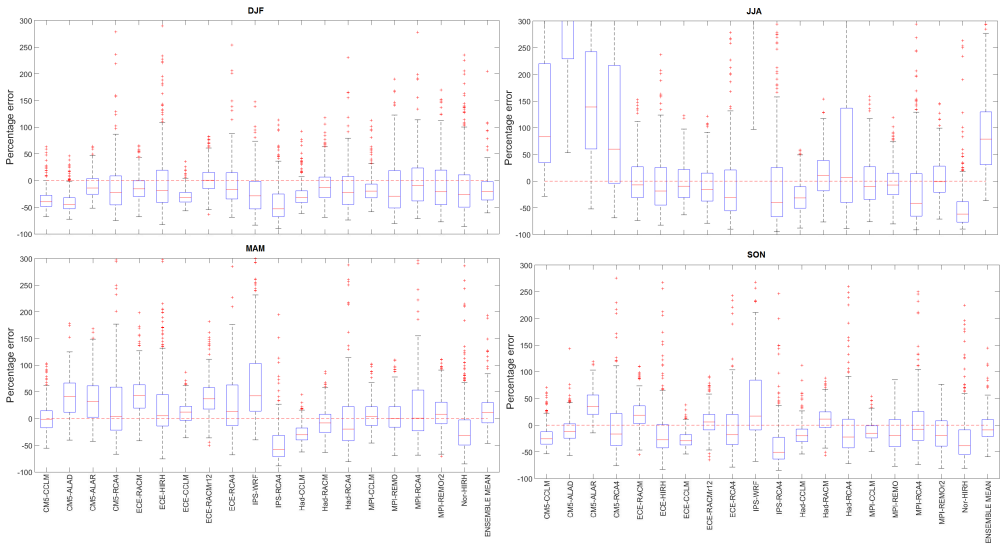

FIGURE 6.8 Box plots representing the frequency distribution of RCM percentage errors in seasonal precipitation for the whole study area.

The Taylor diagrams in Figure 6.9 highlight that NOR-HIRH and ECE-HIRH are the worst models for all the seasons but summer, where the IPS-WRF is the worst-performing.

These indications are confirmed by the ranking results in Figure 6.10.

Concerning the best models, the following CMs perform the best in their respective seasons: ECE-RACMr12 in winter (DJF), ECE-CCLM in spring (MAM), MPI-REMOr2 in summer (JJA), MPI-CCLM and Had-RACM in autumn (SON). It is worth highlighting that ECE-RACMr12 provides the best rank also for Zone 2 in autumn; ECE-CCLM is the best performing also for Zone 6 in summer; MPI-CCLM provides the best performances also for Zone 1 in winter and Zone 4 in spring and Had-RACM is the best model for Zone 2 in spring. For summer precipitation, MPI-REMOr2 is the best performing CM also for Zones 1, 2, 3 and 4. As for the ranking of seasonal mean temperature, once again there is no uniform behaviour of the models between the different seasons and zones.

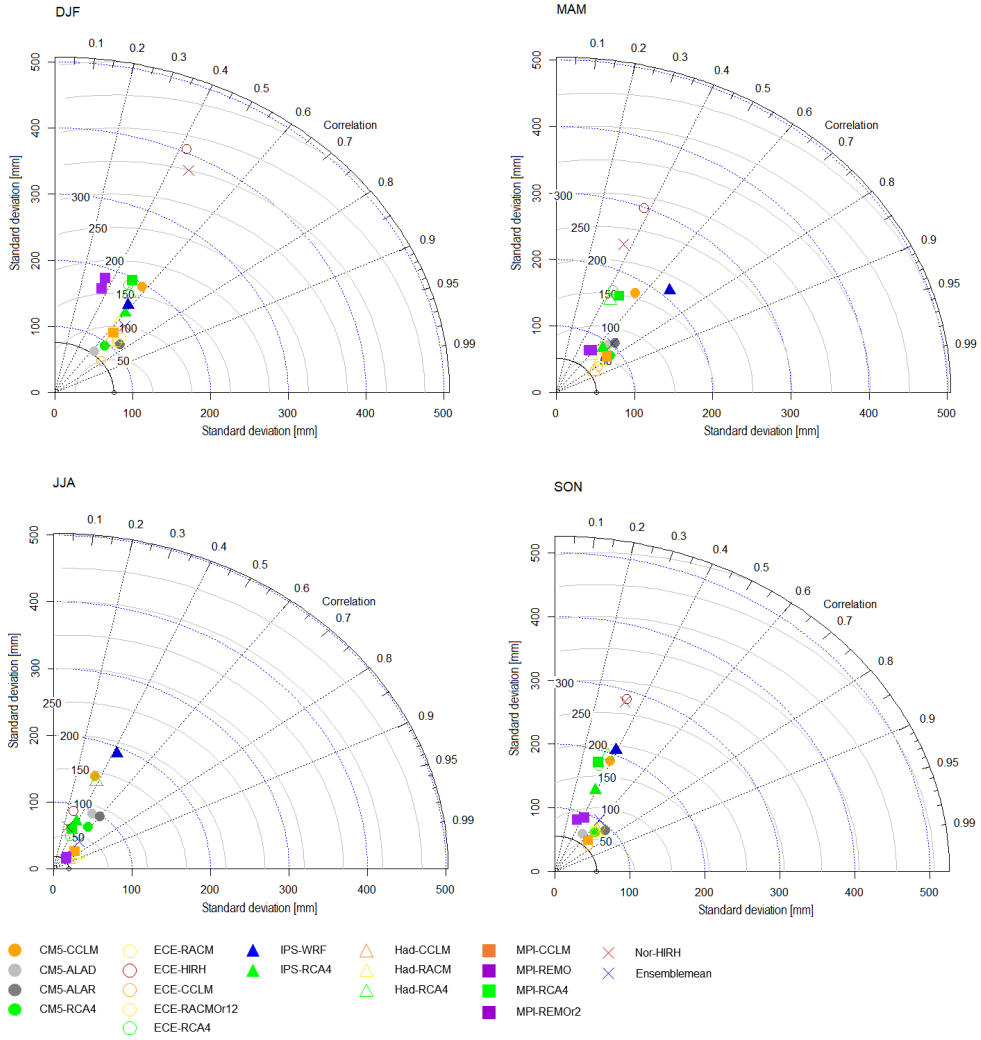

FIGURE 6.9 As Figure 6.4 but for seasonal precipitation.

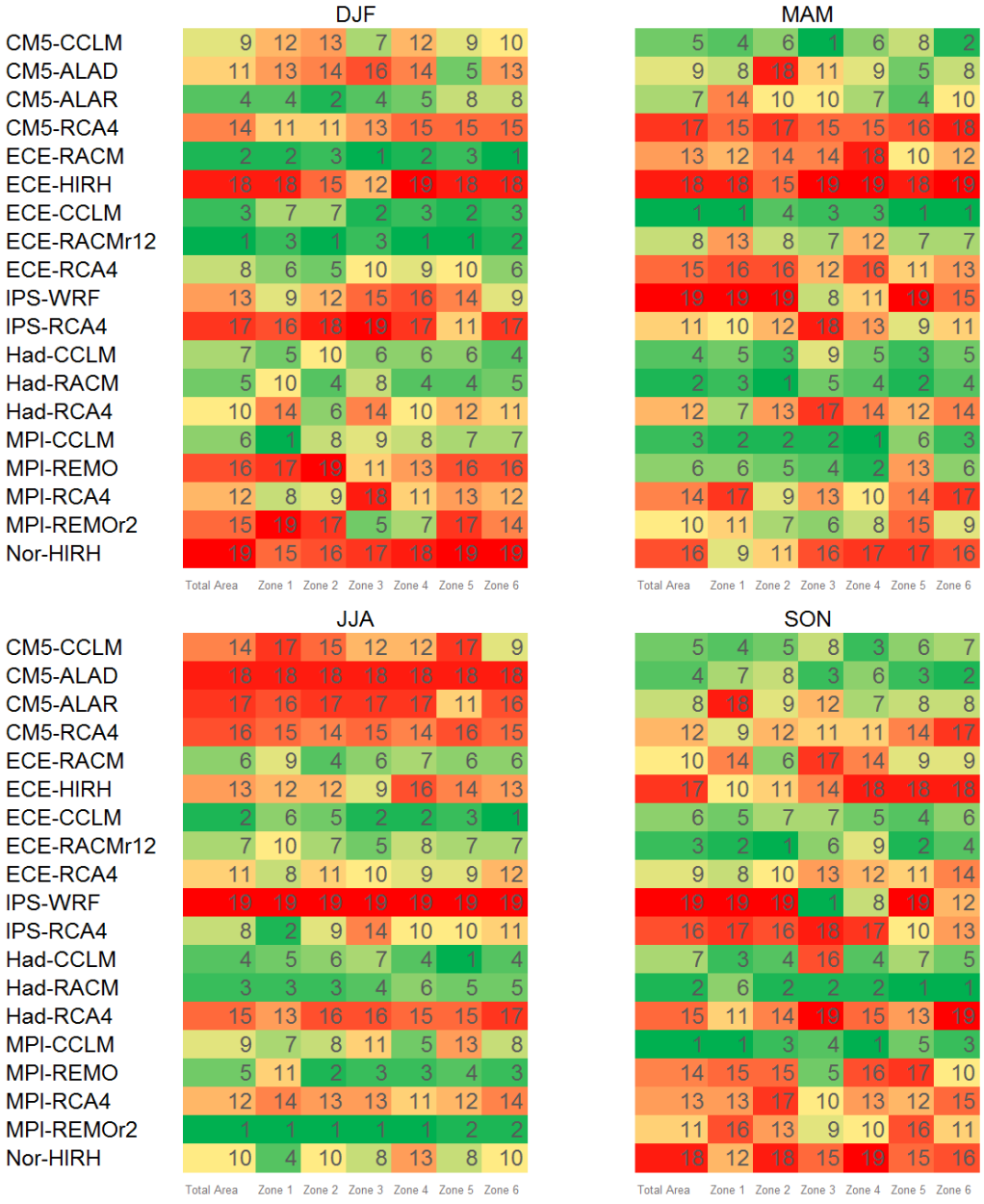

FIGURE 6.10 As Figure 6.5 but for seasonal precipitation.

Drought characteristics

The models' performance in reproducing historical drought characteristics both at the annual and the seasonal scale was also tested. In particular, the following drought characteristics derived from the theory

of runs were analysed: maximum duration (Lmax), maximum accumulated deficit (Dmax), and maximum intensity (Imax) and return period of drought duration.

With reference to the drought characteristics identified on annual precipitation, figures 6.11a, b and c represent the boxplots of the errors related to maximum drought duration, accumulated deficit, and intensity, respectively.

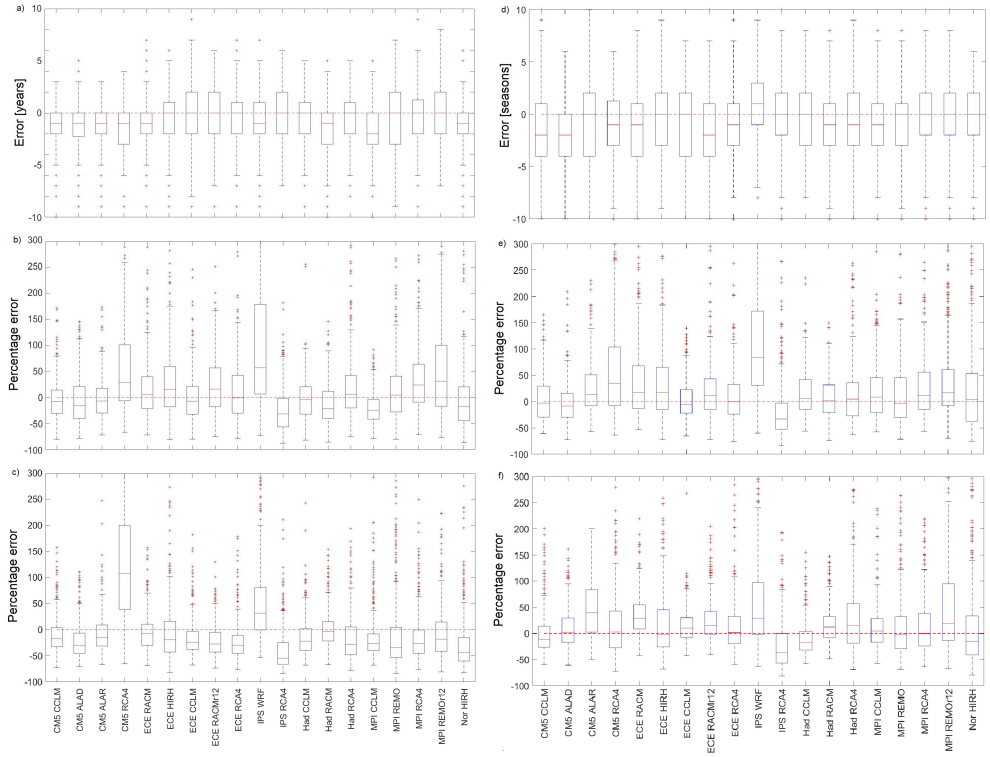

FIGURE 6.11 Box plots representing the frequency distribution of RCM percentage errors in (a) maximum drought duration (annual analysis), (b) maximum drought accumulated deficit (annual analysis), (c) maximum drought intensity (annual analysis), (d) maximum drought duration (seasonal analysis), (e) maximum drought accumulated deficit (seasonal analysis), and (f) maximum drought intensity (seasonal analysis).

In particular, for drought duration, the errors were computed through equation 6.7 by simply replacing T with Lmax, whereas for maximum drought accumulated deficit and intensity, the percentage errors were calculated through equation 6.8, by replacing P first with Dmax and then with Imax.

There is a slight tendency of some models to underestimate drought duration (Figure 6.11a). Overall, the errors span from -3 and +2 years.

The broadest IQR is associated with MPI-REMO, while some models, such as CM5-CCLM, CM5-ALAR, ECE-RACM and, Nor-HIRH seem equally reliable.

The boxplots obtained for Dmax (Figure 6.11b), show that the models may yield considerable errors, which can potentially be larger than those for annual precipitation, as the accumulated deficit, given by the sum of precipitation deficits on a time interval lasting several years, can be affected by multiple errors.

For some models, the IQRs are not larger than 50%. The most reliable model is Had-CCLM, but comparable performances are given by models CM5-CCLM, CM5-ALAR and ECE-CCLM, while the least dispersed is MPI-CCLM (for this model, however, the median error is larger than others). The least reliable is IPS-WRF, followed by CM5-RCA4 and MPI-REMOr2.

In general, as it can be seen from the box-plots, this feature is underestimated. Concerning Imax, the results indicate Had-RACM as the best model and CM5-RCA4 as the worst, followed by IPS-WRF (Figure 6.11c).

Errors for this feature are less scattered than for accumulated deficit, and there is a general tendency for Imax to be underestimated by models.

Figure 6.12 shows box-plots of the errors in the return period of drought events of duration L equal to 1, 3, 5 and 7 years, respectively.

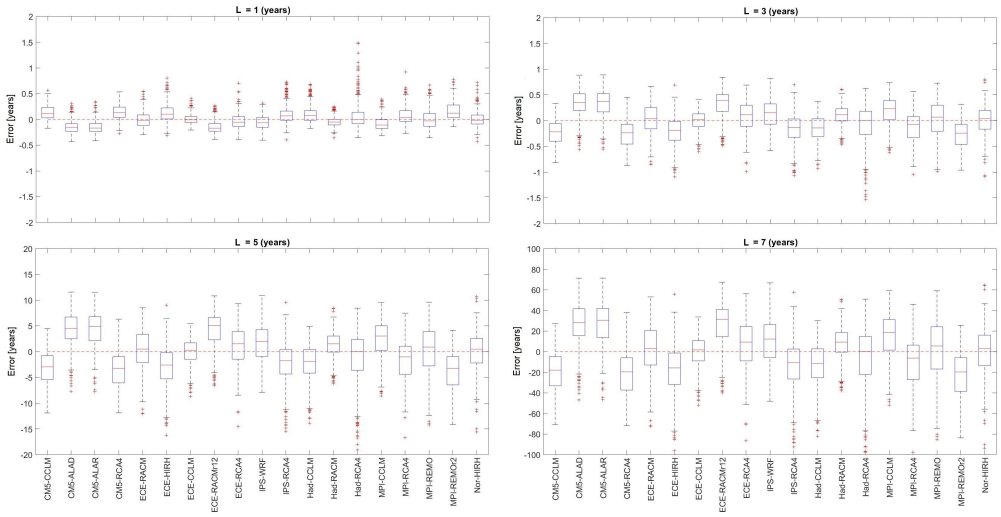

FIGURE 6.12 Box plots representing the frequency distribution of RCM errors in the return period of drought events of duration L equal to 1, 3, 5, and 7 years.

In particular, the error was calculated as in equation 6.9

$$E_{m,j} = \mu_m\left(T_y(j)\right) - \mu_0\left(T_y(j)\right)\varepsilon_j = \mu_{\mathrm{m}}(X(j)) - \mu_0(X(j)) \tag{6.9}$$

where Ty(j) is the return period of a drought event of fixed duration at the grid cell j.

As expected, on equal model, the error increases as the considered drought duration increases. However, regardless of the drought duration, there is no general tendency of the models towards overestimation or underestimation of the return periods. ECE-CCLM and Had-RACM are the models with the smallest IQR, with ECE-CCLM showing the lowest median error.

Overall, the performance of the models looks rather similar, with limited errors until L=3 years (± 0.5 years).

Finally, the models were also ranked according to their ability in reproducing both observed drought maximum intensities and return periods of drought events with duration L=3 years (Figure 6.14a).

Drought intensity was selected as it merges drought accumulated deficit and duration of each drought event.

Concerning the return period, it is worth pointing out that the choice of the considered drought duration only affects the magnitude of the errors, while the performance of each model with respect to the others does not change (see Figure 6.12).

As shown in Figure 6.14a, the best models for the whole study area are confirmed to be ECE-CCLM, Had-RACM, ECE-RACM, and Had-CCLM.

Interestingly, CM5-ALAR is the best model for Zone 3, but unsuitable for the remaining zones. The worst model for all the zones is CM5-RCA4, whereas poor performances are associated to ECE-RACMr12 for Zones 1 and 2, Had-RCA4 for Zone 3, MPI-REMOr2 for Zones 4 and 6 and IPS-WRF for Zone 5.

Figures 6.11d, e and f represent the boxplots of the errors related to maximum drought duration, accumulated deficit, and intensity identified on seasonal precipitation data.

Concerning drought duration (Figure 6.11d), several models (9 out of 19) show a median error equal to 0, while the other models tend to underestimate, with the only exception of IPS-WRF.

Overall, the errors span from -4 and +3 seasons. The broadest IQR is associated with CMC5-ALAR and ECE-CCLM, while some models, such as IPS-RCA4, MPI-RCA4, MPI-REMOr2 and, Nor-HIRH seem equally reliable.

As for Dmax (Figure 6.11e), some similarities can be observed concerning the annual time scale (Figure 6.11b) in terms of magnitude of percentage errors, although in the seasonal case most of the models tend to overestimate.

The most reliable models are CM5-ALAD, ECE-CCLM and Had-RACM. As for the annual scale, the least reliable is IPS-WRF, followed by CM5-RCA4 and Nor-HIRH.

Concerning Imax, also in the seasonal case Had-RACM is confirmed as the best model, while MPI-REMOr2 and IPS-WRF are the worst (Figure 6.11e).

Once again, errors for this feature are less scattered than for accumulated deficit. Only four models underestimate Imax while most of the models are close to a zero median percentage error.

Figure 6.13 shows box-plots of the errors in the return period of drought event of duration L equal to 2, 4, 6 and 8 seasons, respectively.

In particular, the error was calculated as in equation 6.9 by replacing Ty with Ts, namely the return period of a drought event of fixed duration identified on seasonal data. As for the annual case, the performance of the models looks rather similar, with limited errors (± 5 seasons) until L=4 seasons, with the exception of CM5-ALAD, CM5-ALAR, CM5-RCA4 and Had-RCA4.

Figure 6.14b illustrates the ranking of the models in reproducing the drought maximum intensities and return periods of drought events with duration L=4 seasons. With respect to the annual scale, there is a certain agreement in identifying the best performance models, that in this case are Had-RACM, Had-CCLM, and ECE-CCLM. In particular, Had-RACM performs well in every zone, while Had-CCLM is the best model for Zones 1, 2, 5 and 6. The least performing models are CM5-ALAD, CM5-ALAR, albeit it ranks second for Zone 5, CM5-RCA4 and Nor-HIRH.

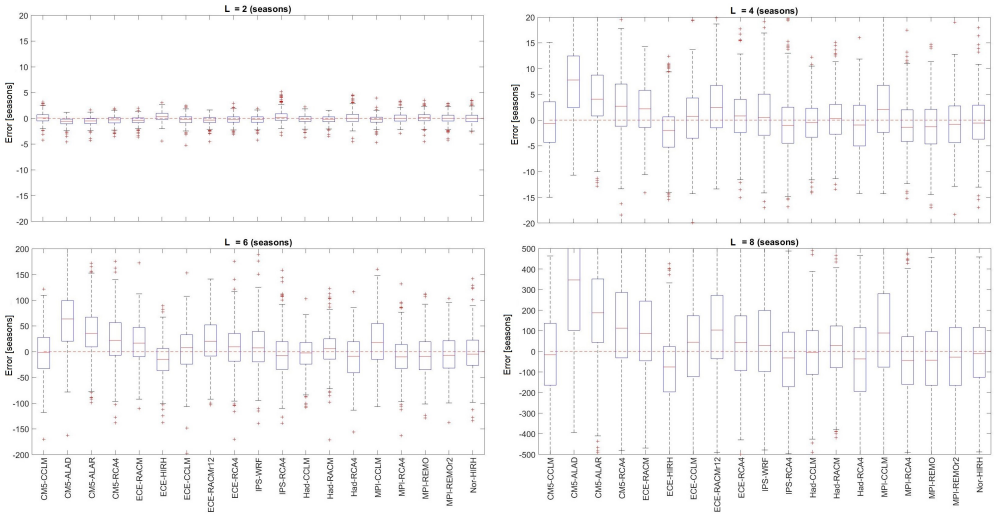

FIGURE 6.13 Box plots representing the frequency distribution of RCM percentage errors in the return period of drought events of duration L equal to 2, 4, 6, and 8 seasons.

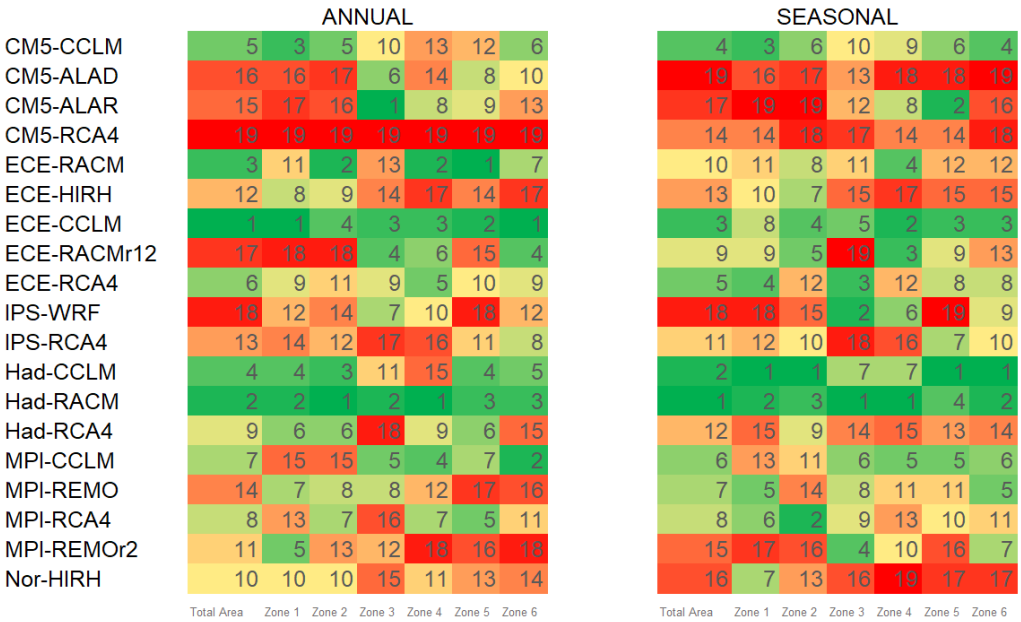

FIGURE 6.14 RCM ranking with respect to their ability to reproduce both observed drought maximum intensities and return periods of drought events with duration L=3 years (left) and L=4 seasons (right).

6.2.5 Discussion of the results

Figure 6.15 illustrates the best performing models according to the ranking approach for each of the considered variables over the whole area and the six homogeneous zones, respectively.

In particular, the three best performing models are reported for the mean temperature and precipitation interannual variability and drought intensity and return period of drought duration, while only the best CM for each season is indicated for seasonal variability.

		Whole area	Zone 1	Zone 2	Zone 3	Zone 4	Zone 5	Zone 6
T interannual variability		MPI-REMO	MPI-REMO	MPI-CCLM	IPS-RCA4	MPI-CCLM	MPI-CCLM	IPS-RCA4
		MPI-CCLM	Had-CCLM	MPI-REMO	MPI-CCLM	MPI-REMO	MPI-REMO	MPI-REMO
		Had-CCLM	MPI-CCLM	Had-CCLM	Had-CCLM	Had-CCLM	Had-CCLM	MPI-CCLM
T seasonal variability	DJF	ECE-HIRH	CM5-CCLM	CM5-CCLM	ECE-HIRH	ECE-HIRH	MPI-CCLM	MPI-CCLM
	MAM	ECE-CCLM	ECE-CCLM	MPI-REMOr2	ECE-CCLM	MPI-REMOr2	ECE-CCLM	ECE-CCLM
	JJA	IPS-RCA4	IPS-RCA4	IPS-RAC4	Had-RCA4	IPS-RCA4	MPI-REMOr2	MPI-REMOr2
	SON	MPI-REMOr2	MPI-REMOr2	MPI-REMOr2	Had-CCLM	MPI-REMOr2	MPI-REMOr-12	MPI-CCLM
P interannual variability		Had-RACM	Had-RACM	ECE-RACM	ECE-CCLM	ECE-CCLM	ECE-CCLM	CM5-ALAD
		ECE-CCLM	CM5-CCLM	Had-RACM	Had-CCLM	Had-RACM	CM5-ALAD	Had-RACM
		CM5-ALAD	CM5-ALAD	CM5-ALAR	Had-RACM	Had-CCLM	Had-RACM	ECE-RACMr12
P seasonal variability	DJF	ECE-RACMr12	MPI-CCLM	ECE-RACMr12	ECE-RACM	ECE-RACMr12	ECE-RACMr12	ECE-RACM
	MAM	ECE-CCLM	ECE-CCLM	Had-RACM	CM5-CCLM	MPI-CCLM	ECE-CCLM	ECE-CCLM
	JJA	MPI-REMOr2	MPI-REMOr2	MPI-REMOr2	MPI-REMOr2	MPI-REMOr2	Had-CCLM	ECE-CCLM
	SON	MPI-CCLM	MPI-CCLM	ECE-RACMr12	IPS-WRF	MPI-CCLM	Had-RACM	Had-RACM
I + T_y(L=3 years) (annual scale)		ECE-CCLM	ECE-CCLM	Had-RACM	CM5-ALAR	Had-RACM	ECE-RACM	ECE-CCLM
		Had-RACM	Had-RACM	ECE-RACM	Had-RACM	ECE-RACM	ECE-CCLM	MPI-CCLM
		ECE-RACM	CM5-CCLM	Had-CCLM	ECE-CCLM	ECE-CCLM	Had-RACM	Had-RACM
I+T_s(L=4 seasons) (seasonal scale)		Had-RACM	Had-CCLM	Had-CCLM	Had-RACM	Had-RACM	Had-CCLM	Had-CCLM
		Had-CCLM	Had-RACM	MPI-RCA4	IPS-WRF	ECE-CCLM	CM5-ALAR	Had-RACM
		ECE-CCLM	CM5-CCLM	Had-RACM	ECE-RCA4	ECE-RACMr12	ECE-CCLM	ECE-CCLM

FIGURE 6.15 Best-performing RCMs according to the ranking at the annual and seasonal scale.

It is worth underlining that the rankings are aimed to provide straightforward information about the relative accuracies of the models, e.g., for supporting the selection of a single or few models in a specific area, therefore, for the sake of simplicity, they provide reduced information based on cardinal numbering. However, the actual performance of each CM compared to the others can be highlighted by looking closer at the ϵm values, which reflect and summarize the results provided by the box-plots and the Taylor diagrams.

Two kinds of comparisons are carried out in this section: 1) on the same variable, across different time scales; 2) on the same time scale, across different variables. Further discussion is provided about relative impacts of different GCMs and RCMs and, finally, an overall ranking is attempted aimed at providing a global evaluation of the CMs performance.

Analyses across different time scales (interannual and seasonal)

Concerning temperature, the intercomparison between the interannual and seasonal variability is rather straightforward. All the simulations are characterized by a more or less pronounced underestimation (Figure 6.2a), together with a usually high correlation with observations (figures 6.2b and 6.4), i.e. both the observed interannual and seasonal variability are well reproduced.

This is somehow confirmed by the rankings, where the relative differences among the models' performances are not very marked.

Conversely, in the case of precipitation, the performances of the models change significantly with the time scale.

The most interesting case with this variable is CM5-ALAD that, considering the total area, ranked 3rd with the annual precipitation, but provided low performances in most of the seasons (9th in MAM, 11th in DJF and 18th in JJA). Though CM5-ALAD can reproduce relatively well the annual amount of rainfall, it is not as much able to simulate the seasonal variability, therefore the good performance at the annual time scale is due to the counterbalancing effects of the errors in different seasons.

This feature of CM5-ALAD is amplified in several of the six zones, e.g., zone 2 (where it is ranked 4th with the mean annual value, but 14th in DJF and 18th in MAM and JJA) or zone 6 (1st with the mean annual value, but 13th on DJF and 18th on JJA).

On the other hand, MPI-CCLM in the total area ranked 8th considering the annual precipitation but provided rather good results in single seasons (it is ranked 3rd on MAM and 1st on SON).

However, considering the total area and the annual precipitation, the values of the error metric ϵm leading to the rankings are not very different among the first 9 models, being the ϵm value of the model ranked 9th (i.e., CM5-ALAR) only 37% higher than the best.

The difference with respect to the best ϵm value is lower than 50% in DJF for the first 7 models, in MAM for the first 5 models, in JJA for the first 6 models and in SON for the first 7 models.

The models providing always (i.e., considering both the annual and the seasonal values) differences lower than 50% with respect to the best

ϵm value are Had-RACM, ECE-CCLM and Had-CCLM.

Figure 6.16 shows a comparison between the ranking of interannual variability of annual precipitation and the average position in the ranking of seasonal precipitation. It highlights possible deviations of the performances of the models at different time scales (the higher the deviation, the higher the distance from the bisector).

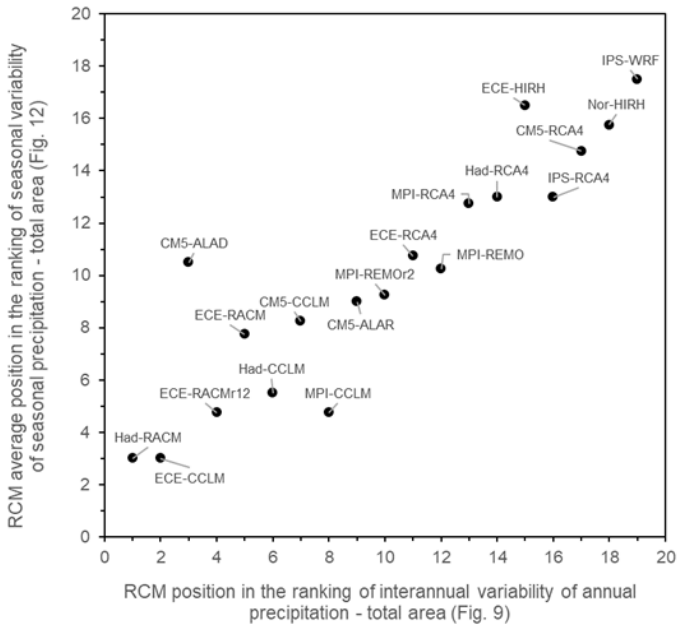

FIGURE 6.16 Comparison between the RCM position in the ranking of interannual variability of annual precipitation versus the average position in the ranking of seasonal variability of seasonal precipitation. Data concern the whole study area (Calabria and Sicily).

When considering the seasonal scale, the reduced performance of CM5-ALAD is evident, such as the better ranking of MPI-CCLM. In general, the best models, both at the interannual and the seasonal scale, are Had-RACM and ECE-CCLM, followed by the two versions of ECE-RACM and two other CCLM models (namely, MPI-CCLM and Had-CCLM, the latter being penalized by the relatively lower ranking in winter).

Focusing on drought analysis, box-plots highlight a relevant variability in the frequency distribution of the error for all the considered drought characteristics.

As for drought duration (figures 6.11a and d), the differences among the models appear more evident at the annual scale, while at the seasonal scale the models' behaviour looks rather similar.

A general agreement can be observed between the box-plots of drought accumulated deficit at the annual and the seasonal scale (figures 6.11b and e), where the IPS-WRF is confirmed as the worst model.

Concerning drought intensity (figures 6.11c and f), CM5-RC4 provides a very poor performance at the annual scale, but a light improvement can be observed at the seasonal scale.

As for the return periods (figures 6.12 and 6.13), the seasonal scale emphasizes the poor quality of CM5-ALAD, which is also confirmed at the annual scale, together with CM5-ALAR, ECE-RACMr12 and MPI-CCLM.

Finally, the rankings combining the performance of the models to simulate maximum drought intensity and return period of drought event of fixed duration (figures 6.14a and b) agree in considering Had-RACM and ECE-CCLM as the best models both at the annual and seasonal scale.

Analyses across different variables

In terms of interannual variability, it's worth observing that, while MPI models appear the most suitable for mean temperature regardless of the area of investigation, especially regarding those in combination with REMO and CCLM RCMs, this is not the case for precipitation, although both the boxplot and the Taylor diagram indicate some potential of the MPI-CCLM for precipitation (Figure 6.6).

The boxplots for both variables displayed a large spatial variability of the errors, suggesting the limited capacity of RCMs to properly capture spatial variations of both temperature and precipitation patterns.

Regarding precipitation, a similar result was obtained by Mascaro et al. (2018) for the Sardinia region. To find a possible explanation, we decided to investigate possible relationships between the amount of the errors and the cells' mean altitude.

In particular, correlation analyses between the elevation and the mean and the standard deviation of the mean annual air temperature

and precipitation errors were carried out. Nonetheless, results, here not shown for the sake of brevity, did not provide significant correlations.

Turning to seasonal variability, some similarities between mean temperature and precipitation arise in spring, with the ECE-CCLM model looking valuable for both variables.

ECE models also perform well in winter but in combination with different RCMs (i.e. HIRH for temperature and RACM for precipitation). In summer, MPI-REMOr2 model is the best option for precipitation but works well also for mean temperature, mainly for Zones 5 and 6. In autumn, MPI-REMOr2 is once again the best performing model but for mean temperature only.

Alternatively, MPI-CCLM looks valuable for both mean temperature and precipitation during this season, as also confirmed by the Taylor diagrams (figures 6.4 and 6.9). Finally, the best models for drought intensity broadly recall those identified for annual precipitation, specifically for ECE-CCLM and Had-RACM.

The skills of CMs in reproducing drought characteristics and variability of precipitation are significantly linked. Drought characteristics, derived through the application of theory of runs, are functions of the departure from the thresholds rather than of the modelled precipitation itself.

In other words, although a CM could significantly underestimate or overestimate annual and seasonal precipitation values (i.e. the data in the boxplots in figures 6.6a and 6.8 may look loosely grouped and the medians very far from 0), still it could provide good performance in terms of drought characteristics simulation if it can reproduce time variability.

It is interesting to observe that the distribution of the percentage error of drought intensity (figures 6.11c and f) is, in general, less scattered than that related to the accumulated deficit (figures 6.11b and e); therefore, one can conclude that a partial error compensation occurs when the modelled accumulated deficit is divided by the modelled duration.

Despite the differences in the percentage errors, however, there is a general agreement in the identification of the best and, mainly, the worst models, also confirmed by the ranking of the models in reproducing

drought intensity and return period of drought events with fixed duration (figures 6.14a and b) both at the annual and the seasonal time scale.

Impact of GCM and RCM choice and different realizations

Overall, no GCM prevails on the others because the RCMs deeply affect the final results. For example, concerning annual precipitation, the simulations relying on the Had GCM provide two high-ranked models (i.e., Had-CCLM and Had-RACM) and a low-ranked model (i.e., Had-RCA4).

In the case of precipitation, only one among the GCMs used more than once coherently provides always bad results (IPS).

Concerning the most used RCMs, CCLM seems able to improve performances always with temperature (figure 3) and in most cases with precipitation (Figure 6.7). Also, RACM usually provides high rankings with precipitation, while lower performances are found with temperature. The five occurrences of RCA4 very seldom provide high rankings with precipitation, as well as the two occurrences of HIRH.

It is of some interest to analyse the behaviour of different realizations of the same CM, which provide insight into the effects of the variability of a multi-member GCM ensemble (von Trentini et al., 2019).

In this study, two cases occur, i.e., ECE-RACM and MPI-REMO. Looking at all the box-plots and Taylor diagrams, the two versions of the models behave rather coherently. Nevertheless, because of the variability of the overall model ensemble, usually, they are not ranked in subsequent positions.

E.g., considering annual drought ranking and the total area, ECE-RACM is ranked 3rd and ECE-RACMr12 17th, while in the seasonal drought ranking MPI-REMO is ranked 7th and MPI-REMOr2 15th.

This result highlights that, at least to a certain extent, the variability induced by different driving ensemble members is of the same order of the variability given by other GCM-RCM combinations. On the other hand, given the similar performances of the different realizations pointed out by the box-plots and Taylor diagrams, it is confirmed that rather slight differences in models' performance can be found even for distances of 4-5 positions in the rankings.

Overall ranking

For a final evaluation of the models, an overall ranking criterion was applied. This ranking takes into consideration both the skills of the considered GCM-RCMs models to replicate annual precipitation and temperature variability, as well as drought characteristics.

As shown in Figure 6.17, the models with the best overall performances, both in the whole case study area and in the six climatically homogeneous zones are those in combination with CCLM RCMs, with the significant exception of Had-RACM, which is ranked 1st considering the total area and Zones 2 and 4 for the annul time scale. Generally, the worst models both at the annual and the seasonal scale are Nor-HIRH, IPS-WRF, and CM5-RCA4, although at the seasonal scale also CM5-ALAD and CM5-ALAR have poor performances.

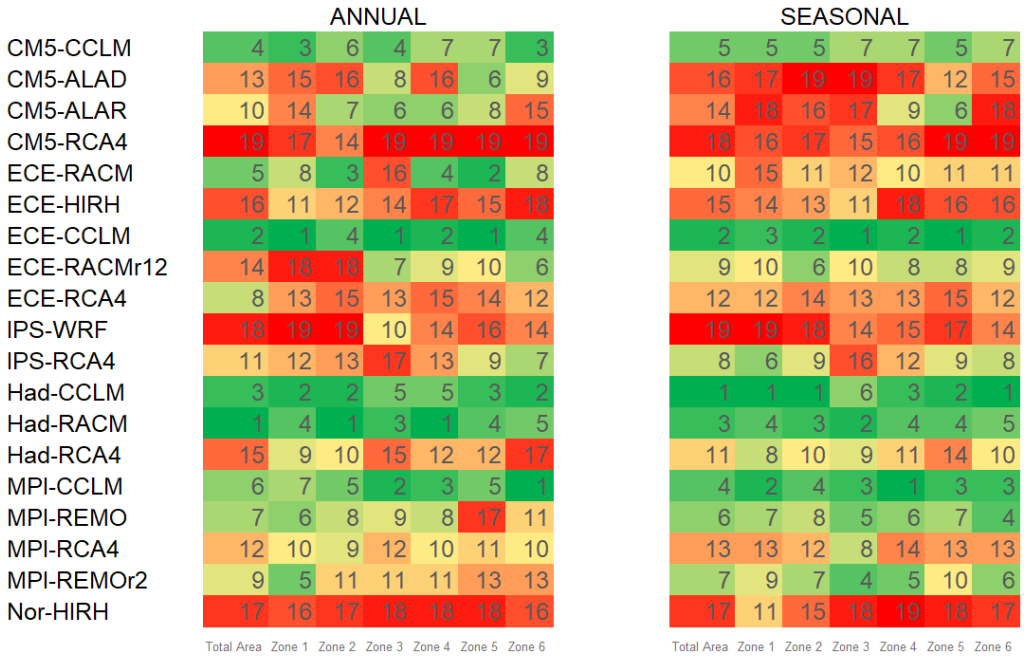

FIGURE 6.17 Overall ranking.

6.2.6 Main findings

In this study we compared the skill of nineteen EURO-CORDEX RCMs at 0.11° (12.5 km) grid spatial resolution in reproducing the annual and seasonal temperature and precipitation regime, as well as

several drought features, observed in the period 1971-2000 in a dense network of rain gauges in Sicily and Calabria regions (Southern Italy).

From our investigation study a few general and specific conclusions can be drawn. From a general point of view, the model combinations are able to simulate temperature better than precipitation, even though important biases do exist in both variables.

Models which are reliable in simulating precipitation may not be the same with respect to temperature. This is the case, for instance, of the ECE-RACM model which is in the top ranks for precipitation, while being in the lower ranks for temperature.

Models that perform best for precipitation do almost the same for drought features. Differences between the rankings of annual respect to seasonal characteristics do exist, but top-ranking models at the annual scale mostly perform well in the single season, both for precipitation and temperature. Looking more specifically to the models, the Had-RACM, ECE-CCLM, Had-CCLM and ECE-RACM are those that perform best for precipitation and drought, while the CM5-RCA4 and IPS-WRF are those that perform worst.

For temperature, models that perform best are MPI-CCLM, MPI-REMO and Had-CCLM, while the worst are CM5-ALAD, ECE-RCA4, ECE-RACM and CM-RCA4. Had-CCLM performs well for both precipitation and temperature, while the CM5-RCA4 performs bad for both. Slight changes in models' performance occur when moving from the whole study area to the single zones, mainly at the seasonal scale.

For instance, IPS-WRF is the best performing model for Zone 3 (North-Eastern Calabria) for seasonal precipitation at SON, in contrast to what happens in the other zones. Differing behaviour of Zone 3 is also observed for drought investigations for CM5-ALAR and IPS-WRF models, respectively.

Results of this study reveal insight on RCMs performances in small-scale regions, which are often targeted by impact studies and have so far received less attention, and provide some guidance to select the best models about the variable and the area under investigation.

This is a key issue before addressing projections changes in the evolution of extreme hydro-meteorological events, such as drought characteristics (frequency, duration, and magnitude).

6.3 Analysis of EURO-CORDEX sub-daily precipitation simulations for the study of the rainfall annual maxima and the estimation of future rainfall intensity-duration-frequency curves in Sicily (Italy)

6.3.1 Overview on the analysis

Climate change is a phenomenon that is claimed to be responsible for a significant alteration of the precipitation regime in different regions worldwide and for the induced potential changes on related hydrological hazards. In particular, some consensus has raised about the fact that climate changes can induce a shift to shorter but more intense rainfall events, causing an intensification of urban and flash flooding hazards. Regional climate models (RCMs) are a useful tool for predicting the potential future impacts of climate change on hydrological events.

The analysis of intense rainfall and the derivation of intensity-duration-frequency (IDF) curves is of key importance for taking into account of climate change for the design of infrastructures. As a preliminary step for reaching the final aim of deriving IDF future curves, the quality of regional climate models (RCMs) should be assessed, for instance by checking their ability to reproduce the main climatological regimes with respect to an historical period. To this end, several studies have focused on the analysis of annual or monthly data, while few studies do exist that analyze the sub-daily data that are made available by the regional climate projection initiatives.

In this study, with reference to 14 rain gauge stations in Sicily (Italy), we first evaluate historical simulations of precipitation data from 11 RCMs belonging to the Euro-CORDEX (Coordinated Regional Climate Downscaling Experiment for the Euro-Mediterranean area) with high temporal resolution (three-hourly), in order to understand how they compare to fine-resolution observations.

In particular, we investigate the ability to reproduce rainfall event

characteristics, as well as annual maxima precipitation at different durations. Annual maxima are analyzed at durations 3, 6, 12 and 24 hours. The proposed analysis highlights the differences between the different models, and, by ranking the RCMs, supports the selection of the most suitable climate model for assessing the impacts in the considered locations in terms of extreme event analysis.

Finally, we present the preliminary results relative to the determination of the IDF curves that can be expected in future periods and scenarios and how they compare to the climate in the control period (1975-2005).

6.3.2 Study area and datasets

This study aims to evaluate historical simulations of precipitation data from selected RCMs belonging to the Euro-CORDEX (Coordinated Regional Climate Downscaling Experiment for the Euro-Mediterranean area) with high temporal resolution (three-hourly), in order to understand how they compare to fine-resolution observations.

So, we investigate the ability to reproduce event characteristics as well as the rainfall maxima annual at different durations and we aim to highlight the differences between RCMs, supporting the selection of the most suitable climate model to assess the impacts in the locations considered, and to understand which trends of intense precipitation are expected in the future.

This study was carried out our study in Sicily (island of southern Italy) using:

- 14 stations selected in 3 climatic homogeneous areas obtained by PCA (Principal Component Analysis);
- 11 RCM to be tested on each station;
- Rainfall maxima annual data in the period 1975-2005.

As for the rainfall data used, as already mentioned, they belong to the thirty years 1975-2005 and are on a three-hour scale. For each RCM, all the data matrices of the EUR-11 area were downloaded and then the data of the cells corresponding to the 14 stations were extrapolated. The

observed data, used as a comparison measure for the RCMs, are the data of the annual maxima deriving from the historical archive. It should be noted that not all stations have the complete time series from 1975 to 2005.

The combinations of GCM-RCM models used in this analysis are the following:

- CM5-ALAD
- CM5-RACM22
- ECE-HIRH
- ECE-RACM22
- ECE-RCA4
- HAD-HIRH
- HAD-RACM22
- HAD-RCA4
- MPI-RCA4
- NOR-RCA4
- NOR-REMO15

In Sicily, 14 stations were selected, trying to choose stations that fell within the three different regions of PCA (see paragraph 6.2.3) and at the same time that had the most complete data series of observed annual maxima possible. The Figure 6.18 shows the selected stations and their geographical location. The Table 6.3 summarizes the membership of the different stations in the PCA areas.

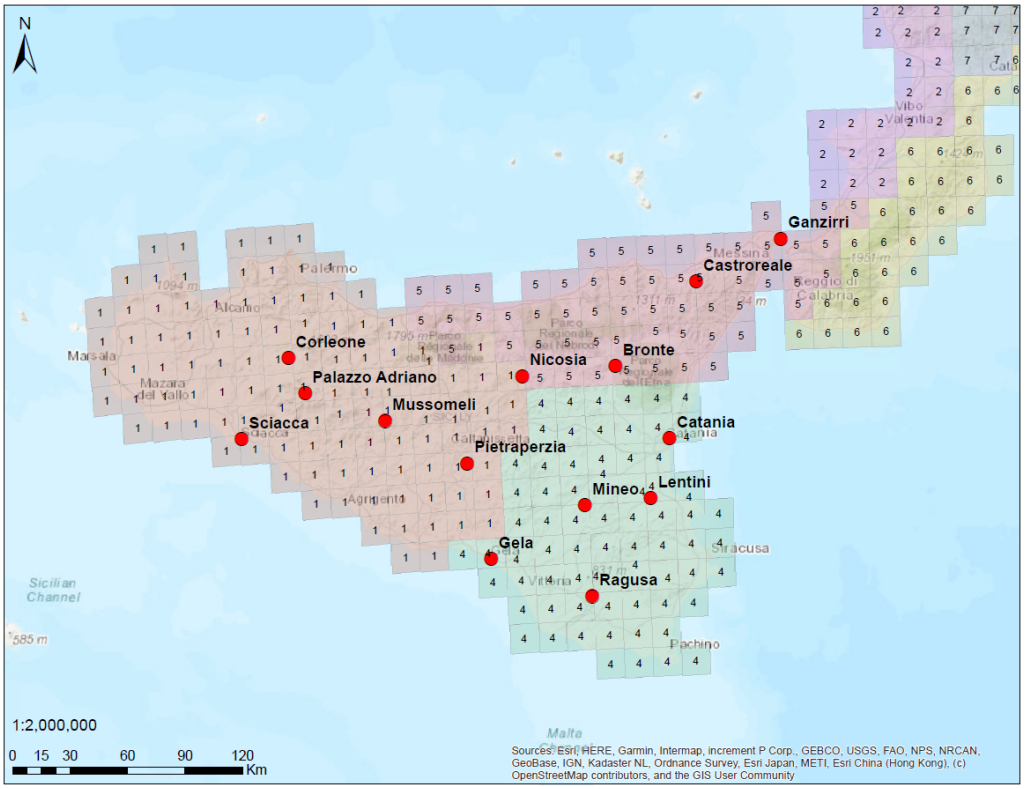

FIGURE 6.18 Cartography of the study area with the position of the 14 stations selected in the different PCA areas.

TABLE 6.3 List of selected stations and relative PCA area to which they belong.

Station	PCA zone
Bronte	5
Catania	4
Castroreale	5
Corleone	1
Ganzirri	5
Gela	4
Lentini	4
Mineo	4
Mussomeli	1
Nicosia	1
Palazzo Adriano	1
Pietraperzia	1
Ragusa	4
Sciacca	1

6.3.3 Methodology to evaluate the models and to obtain the IDF curves

The rainfall data used belong to the thirty years 1975-2005 at three-hour scale. For each RCM model all the data matrices of the EUR-11 area were downloaded and then the data of the cells corresponding to the 14 stations were extrapolated. The observed data, used as a comparison measure for the RCM models, are the data of the annual maxima deriving from the historical archive. It should be noted that not all stations have the complete time series from 1975 to 2005. The aim of this study is to evaluate the ability of each model in reproducing rainfall annual maxima at 3h – 6h – 12h – 24h. At first, to understand the goodness of each model we elaborated a ranking of the RCM models.

The ranking of the models was first prepared as an absolute ranking, where the models are classified from best to worst, and subsequently with a ranking by classes, where the are subdivided in quality classes. The absolute ranking of the models on the maxima at 3h, 6h, 12h and 24h

was made taking into consideration the 25th percentile (Prc_{25}) and the 75th percentile (Prc_{75}). The formula used to calculate the I value that is used to define the position of the RCM model in the ranking is the equation 6.10. The parameter I was used to sort in ascending order the RCM models.

$$I = |Prc_{25RCM} - Prc_{25OBS}| + |Prc_{75RCM} - Prc_{75OBS}| \tag{6.10}$$

The ranking by classes of the RCM models on the maxima at 3h, 6h, 12h and 24h was made taking into consideration the 25th percentile (Prc_{25}) and the 75th percentile (Prc_{75}).

The formula used to calculate the IP value used to define the position of the RCM model in the ranking is in the equation 6.11.

$$IP = (I - I_{min})/(I_{max} - I_{min}) \tag{6.11}$$

The results were then divided into 4 classes:

1. Class 1, IP $\leq$ 0.25
2. Class 2, 0.26 $\leq$ IP $\leq$ 0.5
3. Class 3, 0.51 $\leq$ IP $\leq$ 0.75
4. Class 4, IP $\geq$ 0.76

The ranking was calculated for each station and for each duration and finally the number of occurrences for each RCM in each class of the ranking was counted. After this first classification of the models, the invariant-scale method was applied to define the IDF curves.

For the scale-invariant method, the normalization and ascending ordering process of all the RCM datasets and the observed data is performed. A single series is obtained for each RCM and for the observed consisting of: 31 (years) x 4 (durations) = 124 (data).

The parameters of the GEV and Gumbel distributions have been calculated in this first step. Subsequently, a first comparison was made between the annual maxima recorded in each station with respect to the

maxima of the RCM models in the same station. The non-dimensional precipitation quantiles are calculated for the return time of 10 years, thus obtaining the dimensionless precipitation heights h_{T^*}. Subsequently, the mean values are regularized through an interpolated power curve with the equation 6.12.

$$m(t) = bt^k \tag{6.12}$$

Once parameters b and k have been obtained, by fitting the curve, the equation of the IDF curve can be determined with the equation 6.13

$$h(t) = h_T * bt^k \tag{6.13}$$

6.3.4 Results of the analysis

First of all, comparative boxplots are reported (Figure 6.19 between the maxima values simulated by the RCM models and the data actually recorded in the Catania station (see the other stations in the appendix). This preliminary comparison allowed us to evaluate the different trends of the models, understanding whether they were more or less realistic in the various stations (see appendix at section A.2 for all the graphs).

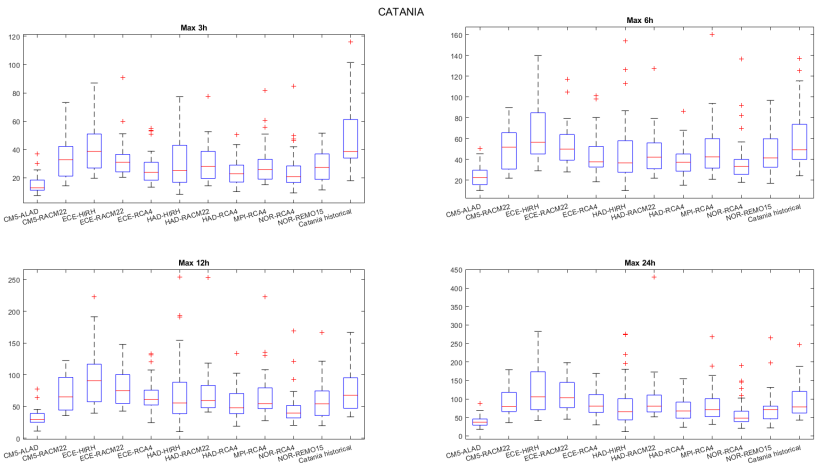

FIGURE 6.19 Comparative boxplot at 3 - 6 - 12 - 24 hours

As general results we can deduce that:

- In almost all cases the RCM models tend to underestimate the real data;
- The results of the maxima at 3h are less significant, since the RCM datum is already a three-hour datum;
- In the Castroreale and Ganzirri stations there is greater variability in the results of the RCMs;
- In the stations of Corleone, Mussomeli, Pietraperzia and Sciacca there is less variability in the RCM results;

As explained in the paragraph 6.3.3, the models were classified according to an absolute ranking. The Figure 6.20 shows the classification for each station, for each model, for each time scale (there is a ranking on each column).

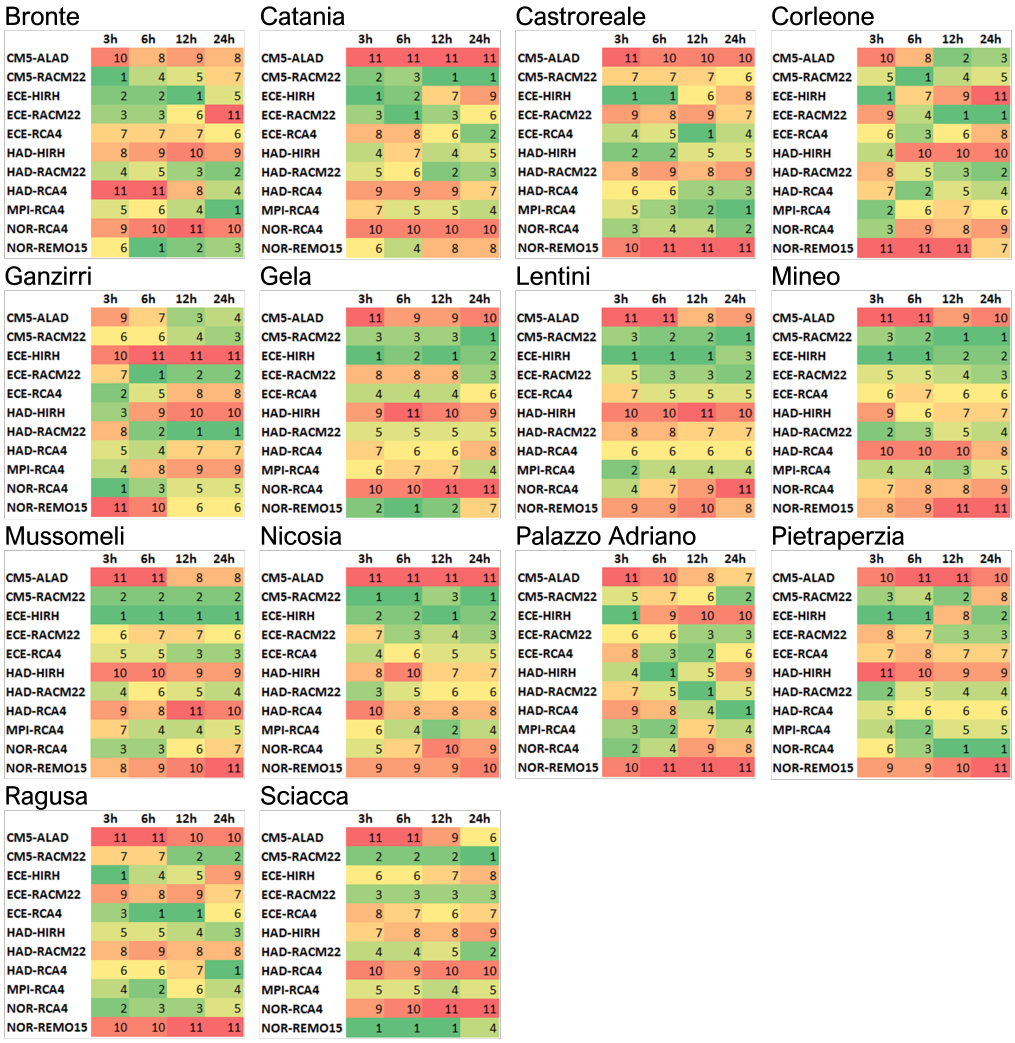

FIGURE 6.20 Absolute ranking

From this first ranking we can deduced that: the best models globally are CM5-RACM22, ECE-HIRH and MPI-RCA4; the worst models globally are CM5-ALAD, HAD-HIRH and NOR-REMO15; at 3h the best model is ECE-HIRH while the worst is CM5-ALAD; at 6h the best model is ECE-HIRH while the worst is CM5-ALAD; at 12h the best model is CM5-RACM22 while the worst is CM5-ALAD; at 24h the best model is CM5-RACM22 while the worst is NOR-REMO15.

Subsequently, the ranking by classes was proposed. The Figure 6.21 shows the ranking for each station, for each model, for each time scale (you can read a ranking on each column). In this case it is clear that: the

best models are CM5-RACM22, ECE-HIRH and MPI-RCA4; the worst models are CM5-ALAD, HAD-HIRH, NOR-RCA4 and NOR-REMO15.

Bronte

	3h	6h	12h	24h
CM5-ALAD	0.93	0.87	0.54	0.77
CM5-RACM22	0.00	0.09	0.27	0.68
ECE-HIRH	0.01	0.08	0.00	0.35
ECE-RACM22	0.23	0.09	0.30	1.00
ECE-RCA4	0.66	0.61	0.31	0.53
HAD-HIRH	0.75	0.89	0.76	0.90
HAD-RACM22	0.39	0.11	0.11	0.16
HAD-RCA4	1.00	1.00	0.43	0.33
MPI-RCA4	0.48	0.22	0.15	0.00
NOR-RCA4	0.80	0.94	1.00	0.99
NOR-REMO15	0.52	0.00	0.01	0.17

Catania

	3h	6h	12h	24h
CM5-ALAD	1.00	1.00	1.00	1.00
CM5-RACM22	0.30	0.12	0.00	0.00
ECE-HIRH	0.00	0.10	0.37	0.55
ECE-RACM22	0.36	0.00	0.12	0.32
ECE-RCA4	0.59	0.31	0.28	0.03
HAD-HIRH	0.38	0.31	0.16	0.32
HAD-RACM22	0.41	0.28	0.12	0.06
HAD-RCA4	0.66	0.51	0.40	0.36
MPI-RCA4	0.53	0.20	0.17	0.23
NOR-RCA4	0.68	0.65	0.74	0.70
NOR-REMO15	0.46	0.19	0.38	0.48

Castroreale

	3h	6h	12h	24h
CM5-ALAD	1.00	0.95	0.88	0.90
CM5-RACM22	0.55	0.47	0.29	0.34
ECE-HIRH	0.00	0.00	0.18	0.46
ECE-RACM22	0.73	0.63	0.48	0.41
ECE-RCA4	0.36	0.29	0.00	0.11
HAD-HIRH	0.06	0.16	0.11	0.24
HAD-RACM22	0.55	0.63	0.45	0.52
HAD-RCA4	0.51	0.41	0.06	0.06
MPI-RCA4	0.37	0.19	0.01	0.00
NOR-RCA4	0.30	0.22	0.07	0.06
NOR-REMO15	0.99	1.00	1.00	1.00

Corleone

	3h	6h	12h	24h
CM5-ALAD	0.68	0.52	0.18	0.15
CM5-RACM22	0.22	0.00	0.23	0.39
ECE-HIRH	0.00	0.51	0.78	1.00
ECE-RACM22	0.42	0.09	0.00	0.00
ECE-RCA4	0.27	0.05	0.55	0.72
HAD-HIRH	0.20	0.57	0.91	0.93
HAD-RACM22	0.37	0.11	0.19	0.09
HAD-RCA4	0.31	0.02	0.27	0.34
MPI-RCA4	0.09	0.27	0.57	0.63
NOR-RCA4	0.13	0.52	0.74	0.90
NOR-REMO15	1.00	1.00	1.00	0.69

Ganzirri

	3h	6h	12h	24h
CM5-ALAD	0.75	0.24	0.14	0.19
CM5-RACM22	0.16	0.21	0.24	0.18
ECE-HIRH	0.87	1.00	1.00	1.00
ECE-RACM22	0.36	0.00	0.06	0.02
ECE-RCA4	0.00	0.18	0.40	0.45
HAD-HIRH	0.01	0.40	0.59	0.63
HAD-RACM22	0.56	0.10	0.00	0.00
HAD-RCA4	0.09	0.15	0.38	0.40
MPI-RCA4	0.04	0.36	0.53	0.46
NOR-RCA4	0.00	0.12	0.29	0.35
NOR-REMO15	1.00	0.47	0.33	0.36

Gela

	3h	6h	12h	24h
CM5-ALAD	1.00	0.83	0.87	0.74
CM5-RACM22	0.24	0.21	0.34	0.00
ECE-HIRH	0.00	0.08	0.00	0.04
ECE-RACM22	0.83	0.79	0.76	0.24
ECE-RCA4	0.26	0.37	0.49	0.32
HAD-HIRH	0.95	1.00	0.90	0.65
HAD-RACM22	0.45	0.50	0.56	0.26
HAD-RCA4	0.71	0.69	0.63	0.41
MPI-RCA4	0.65	0.75	0.63	0.24
NOR-RCA4	1.00	0.99	1.00	1.00
NOR-REMO15	0.07	0.00	0.22	0.32

Lentini

	3h	6h	12h	24h
CM5-ALAD	1.00	1.00	0.96	0.86
CM5-RACM22	0.41	0.39	0.17	0.00
ECE-HIRH	0.00	0.00	0.00	0.15
ECE-RACM22	0.60	0.47	0.20	0.13
ECE-RCA4	0.61	0.70	0.63	0.52
HAD-HIRH	0.83	0.94	1.00	0.97
HAD-RACM22	0.70	0.77	0.71	0.66
HAD-RCA4	0.61	0.71	0.65	0.52
MPI-RCA4	0.41	0.52	0.27	0.45
NOR-RCA4	0.60	0.74	0.97	1.00
NOR-REMO15	0.70	0.88	0.97	0.81

Mineo

	3h	6h	12h	24h
CM5-ALAD	1.00	1.00	0.97	0.96
CM5-RACM22	0.37	0.27	0.00	0.00
ECE-HIRH	0.00	0.00	0.08	0.12
ECE-RACM22	0.59	0.49	0.48	0.37
ECE-RCA4	0.67	0.67	0.54	0.62
HAD-HIRH	0.79	0.66	0.73	0.70
HAD-RACM22	0.31	0.32	0.48	0.38
HAD-RCA4	0.89	0.91	0.98	0.77
MPI-RCA4	0.46	0.38	0.27	0.44
NOR-RCA4	0.70	0.76	0.89	0.87
NOR-REMO15	0.77	0.83	1.00	1.00

Mussomeli

	3h	6h	12h	24h
CM5-ALAD	1.00	1.00	0.70	0.57
CM5-RACM22	0.12	0.20	0.13	0.09
ECE-HIRH	0.00	0.00	0.00	0.00
ECE-RACM22	0.52	0.55	0.45	0.32
ECE-RCA4	0.46	0.39	0.18	0.20
HAD-HIRH	0.90	0.92	0.92	0.75
HAD-RACM22	0.34	0.41	0.39	0.24
HAD-RCA4	0.78	0.65	1.00	0.88
MPI-RCA4	0.53	0.36	0.24	0.28
NOR-RCA4	0.31	0.29	0.44	0.46
NOR-REMO15	0.55	0.71	0.98	1.00

Nicosia

	3h	6h	12h	24h
CM5-ALAD	1.00	1.00	1.00	1.00
CM5-RACM22	0.00	0.00	0.31	0.00
ECE-HIRH	0.12	0.09	0.00	0.03
ECE-RACM22	0.57	0.26	0.37	0.20
ECE-RCA4	0.34	0.49	0.55	0.36
HAD-HIRH	0.73	0.90	0.62	0.46
HAD-RACM22	0.25	0.37	0.56	0.39
HAD-RCA4	0.74	0.75	0.71	0.49
MPI-RCA4	0.49	0.27	0.28	0.25
NOR-RCA4	0.45	0.63	0.81	0.78
NOR-REMO15	0.74	0.81	0.76	0.78

Palazzo Adriano

	3h	6h	12h	24h
CM5-ALAD	1.00	0.78	0.36	0.32
CM5-RACM22	0.38	0.26	0.16	0.02
ECE-HIRH	0.00	0.36	0.50	0.60
ECE-RACM22	0.43	0.20	0.07	0.05
ECE-RCA4	0.60	0.07	0.02	0.21
HAD-HIRH	0.31	0.00	0.11	0.43
HAD-RACM22	0.51	0.14	0.00	0.13
HAD-RCA4	0.62	0.36	0.10	0.00
MPI-RCA4	0.27	0.06	0.25	0.06
NOR-RCA4	0.20	0.11	0.36	0.38
NOR-REMO15	0.99	1.00	1.00	1.00

Pietraperzia

	3h	6h	12h	24h
CM5-ALAD	0.91	1.00	1.00	0.73
CM5-RACM22	0.16	0.33	0.09	0.25
ECE-HIRH	0.00	0.00	0.35	0.05
ECE-RACM22	0.46	0.47	0.12	0.07
ECE-RCA4	0.39	0.52	0.29	0.19
HAD-HIRH	1.00	0.96	0.57	0.41
HAD-RACM22	0.06	0.40	0.22	0.08
HAD-RCA4	0.35	0.47	0.28	0.18
MPI-RCA4	0.18	0.22	0.23	0.16
NOR-RCA4	0.39	0.31	0.00	0.00
NOR-REMO15	0.58	0.77	0.96	1.00

Ragusa

	3h	6h	12h	24h
CM5-ALAD	1.00	1.00	0.76	0.65
CM5-RACM22	0.52	0.36	0.01	0.02
ECE-HIRH	0.00	0.22	0.13	0.63
ECE-RACM22	0.76	0.61	0.55	0.28
ECE-RCA4	0.21	0.00	0.00	0.20
HAD-HIRH	0.26	0.23	0.10	0.13
HAD-RACM22	0.67	0.65	0.54	0.39
HAD-RCA4	0.49	0.31	0.21	0.00
MPI-RCA4	0.22	0.01	0.17	0.13
NOR-RCA4	0.19	0.02	0.10	0.14
NOR-REMO15	0.76	1.00	1.00	1.00

Sciacca

	3h	6h	12h	24h
CM5-ALAD	1.00	1.00	0.87	0.35
CM5-RACM22	0.05	0.29	0.33	0.00
ECE-HIRH	0.47	0.68	0.75	0.68
ECE-RACM22	0.32	0.39	0.39	0.01
ECE-RCA4	0.67	0.75	0.70	0.56
HAD-HIRH	0.64	0.77	0.77	0.71
HAD-RACM22	0.35	0.47	0.46	0.01
HAD-RCA4	0.78	0.87	0.95	0.94
MPI-RCA4	0.38	0.49	0.39	0.32
NOR-RCA4	0.69	0.88	1.00	1.00
NOR-REMO15	0.00	0.00	0.00	0.24

Class 1	0 - 0.25
Class 2	0.26 - 0.5
Class 3	0.51 - 0.75
Class 4	0.76 - 1

FIGURE 6.21 Ranking by classes

To obtain the IDF curves, the Figure 6.22 shows a first comparison between the mean annual maxima recorded in the Catania station with those of the RCM models. Then the IDF curves (Figure 6.23) obtained with the scale-invariant method for the Catania station using with distributions: Gumbel, GEV and Log-norm. For all other IDF curves see the appendix at section A.3 and A.4.

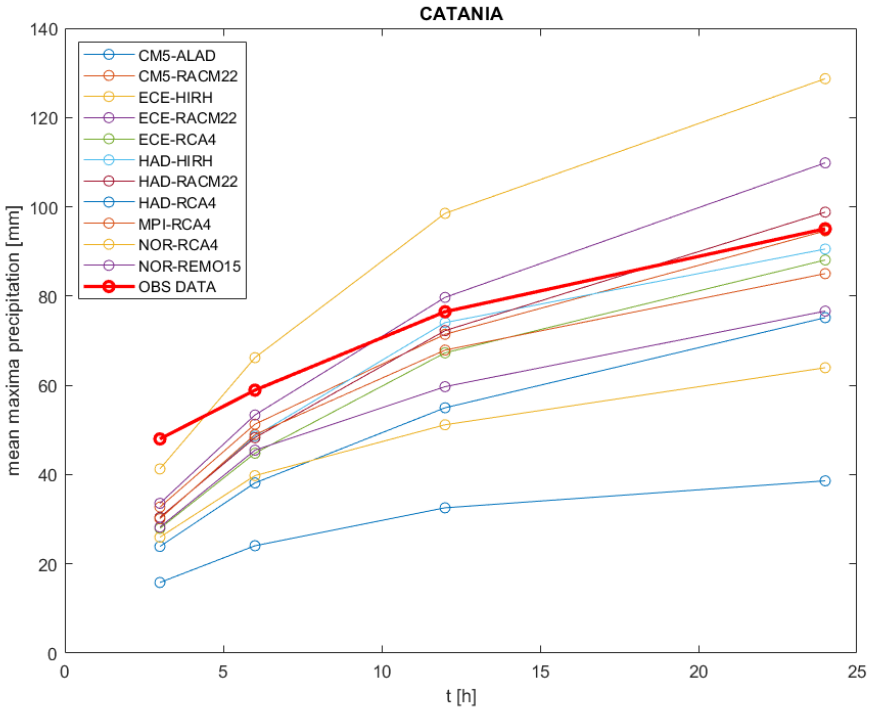

FIGURE 6.22 Comparison between the annual maxima recorded in the Catania station with those of the RCM models

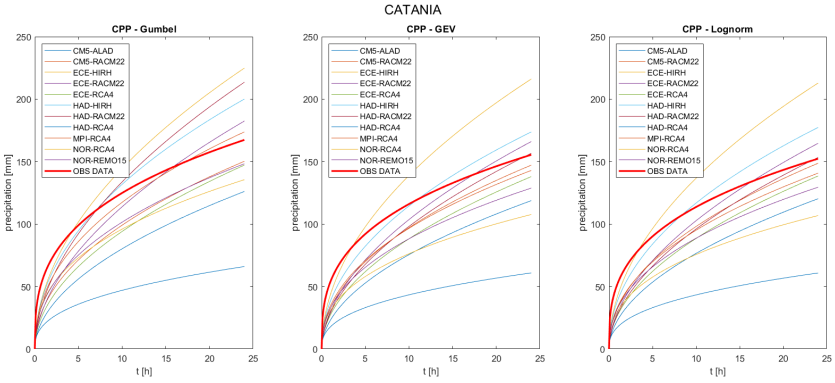

FIGURE 6.23 IDF curves for Catania station - TR = 10 years

6.3.5 Main findings

At the beginning of the analysis in the first results, in almost all cases, the RCM models tend to underestimate the real data and it is clear that

the results of the maximua at 3h are less significant, since the RCM datum is already a three-hour datum. In some stations like Castroreale and Ganzirri there is greater variability in the results of the RCMs, and in other stations like Corleone, Mussomeli, Pietraperzia and Sciacca there is less variability in the RCM results.

In the first ranking the result shows that the best models are CM5-RACM22, ECE-HIRH and MPI-RCA4, while the worst models globally are CM5-ALAD, HAD-HIRH and NOR-REMO15. At 3h the best model is ECE-HIRH and the worst is CM5-ALAD; at 6h the best model is ECE-HIRH and the worst is CM5-ALAD; at 12h the best model is CM5-RACM22 and the worst is CM5-ALAD; at 24h the best model is CM5-RACM22 and the worst is NOR-REMO15.

The ranking by classes shows that the best models are CM5-RACM22, ECE-HIRH and MPI-RCA4, instead the worst models are CM5-ALAD, HAD-HIRH, NOR-RCA4 and NOR-REMO15. By comparing the mean of the annual maximua, using the scale-invariant method, further differences between the models were highlighted. For the Catania station, for example, all models underestimate the mean at 3h. The ECE-HIRH and ECE-RACM22 models are closer to the mean at 6h, while the ECE-HIRH and HAD-RACM models are closer to the mean at 12h. MPI-RCA4 is the model that is more similar to the 24h mean. A similar trend is reflected in the IDF curves. In all distributions the maxima rainfall values at 3h are underestimated and no model is able to reflect the IDF curve of the observed data.

Chapter 7

Application of GCM-RCM on green roof model

7.1 Overview

The final results of this dissertation are presented in this chapter. After investigating the performance of the different RCM models (see chapter 6) it was possible to apply the climatic data on the model of the green roof made previously (see chapter 5). First of all, this chapter shows how the RCM models have been corrected with the quantile-quantile mapping method. Subsequently, some results obtained from the application of the RCM models on the green roof model are illustrated.

A comparison was made between the output volumes and the rainfall peaks of the rain events belonging to the historical data and between those belonging to the scenarios data. Once it was ascertained that climate change negatively affects rain events, we proceeded with the evaluation of the role of the green roof in these scenarios. Finally, an assessment of the efficiency of the green roof is presented.

7.2 Bias correction of GCM-RCM models

The sensitivity of regional hydrology to variable climate conditions makes climate-change projections essential for the assessment of future variations in the hydrologic cycle. A common method to estimate future climate change impacts on hydrology involves climate variables (e.g., temperature, water vapor and pre- cipitation) from global climate models

(GCMs) in combination with hydrological models. Progress in regional climate models (RCMs) has recently made the use of RCM simulations as a basis for hydrological studies more attractive. RCMs transfer the large-scale information from GCMs to scales (25–50 km), which are closer to the catchment scale (Teutschbein and Seibert, 2012).

However, also RCM simulations of temperature and precipitation must be handled with caution as they often show significant biases. The reasons for such biases include systematic model errors caused by imperfect conceptualization, discretization and spatial averaging within grid cells. This makes the use of RCM simulations as direct input data for hydrological impact studies more complicated (Christensen et al., 2008; Teutschbein and Seibert, 2010).

Bias correction methods are applied to help remedy the various problems with biased RCM output. Typical biases are the occurrence of too many wet days with low-intensity rain or incorrect estimation of extreme temperatures but also include general under or overestimation and incorrect seasonal variations of precipitation (Christensen et al., 2008; Terink et al., 2009; Teutschbein and Seibert, 2010).

Several bias correction methods have been developed to downscale climate variables from climate models. These methods range from simple scaling approaches to rather sophisticated methods employing probability mapping or weather genera- tors. They were originally designed to downscale GCM data, but can also be applied to adjust RCM simulated temperature and precipitation (Teutschbein and Seibert, 2012).

There are many methods of bias correction, but in this study the quantile-quantile mapping method is used. The idea of distribution mapping is to correct the distribution function of RCM simulated climate values to agree with the observed distribution function. This can be done by creating a transfer function to shift the occurrence distributions of precipitation and temperature.

The Gamma distribution with shape parameter α and scale parameter β is often assumed to be suitable for distributions of precipitation events. The shape parameter a controls the profile of the distribution: (1) $\alpha < 1$ indicates an exponentially shaped Gamma distribution which is asymptotic at both axes, (2) $\alpha = 1$ is a special case and characterizes

an exponential distribution and (3) $\alpha > 1$ shapes a skewed unimodal distribution curve. The scale parameter b determines the dispersion of the Gamma distribution. A smaller β leads to a more compressed distribution and, therefore, to lower probabilities of extreme events. A larger b, on the other hand, causes a stretched distribution, which implies higher probabilities of extreme events (equation 7.1).

$$f_\gamma(x \mid \alpha, \beta) = x^{\alpha-1} \frac{1}{\beta^\alpha \Gamma(\alpha)} e^{\frac{-x}{\beta}}; x > 0; \quad \alpha, \beta > 0 \tag{7.1}$$

For temperature time series, the Gaussian distribution with location parameter μ and scale parameter σ is usually assumed to fit best. The scale parameter σ determines the standard deviation, i.e., how much the range of the Gaussian distribution is stretched or com- pressed. A smaller value for σ results in a more compressed distribution with lower probabilities of extreme values. Contrary, a larger value for σ indicates a stretched shape with higher probabilities of extreme values. The location parameter μ directly controls the mean and, therefore, the location of the distribution (equation 7.2).

$$f_N\left(x \mid \mu, \sigma^2\right) = x^{\alpha-1} \frac{1}{\sigma\sqrt{2\pi}} e^{\frac{-(x-\mu)^2}{2\sigma^2}} \tag{7.2}$$

In this study, cumulative distribution functions (CDFs) were constructed for both the observed historical data (1975-2004) and the RCM scenario data (2021-2070). Then, the value of the RCM precipitation/temperature of day d within month m was searched on the empirical CDF of the RCM simulations together with its corresponding cumulative probability. A clear example is shown in the Figure 7.1.

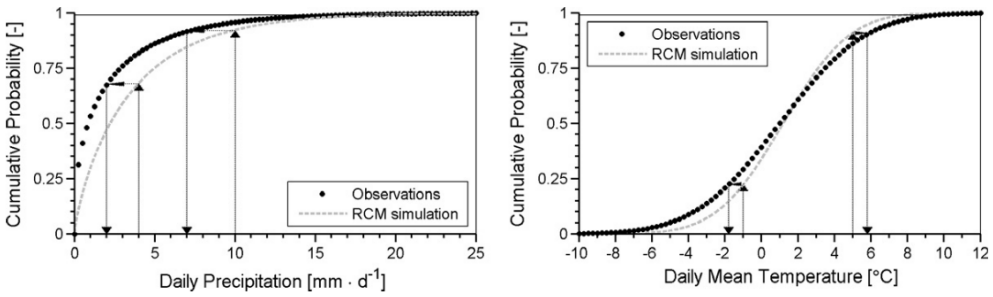

FIGURE 7.1 Exemplary procedure of the distribution mapping. Left: The Gamma distribution of RCM-simulated daily precipitation (dashed gray) was shifted towards the Gamma distribution of the observations (black circles). Right: The Gaussian distribution of RCM-simulated daily mean temperature (dashed gray) was shifted towards the Gaussian distribution of the observations (black circles). (Teutschbein and Seibert, 2012)

7.2.1 Application of quantile-quantile mapping method

The aim of the following analysis is to obtain the correct dataset to apply on the green roof model. The selected RCM models are the same of the paragraph 6.3.2:

- CM5-ALAD
- CM5-RACM22
- ECE-HIRH
- ECE-RACM22
- ECE-RCA4
- HAD-HIRH
- HAD-RACM22
- HAD-RCA4
- MPI-RCA4
- NOR-RCA4
- NOR-REMO15

First of all, it was necessary to choose the precipitation threshold. It means choosing the value below which rainfall is considered equal to 0. The percentage Π of zeros of the series is calculated as: Π = number of zeros / number tot of data (excluding NaN, present in the Sias dataset). In the logarithmic graph, the percentages Π are highlighted on the ordinate and the thresholds on the abscissa. The curve relating to the SIAS observed data is in red (Figure 7.2).

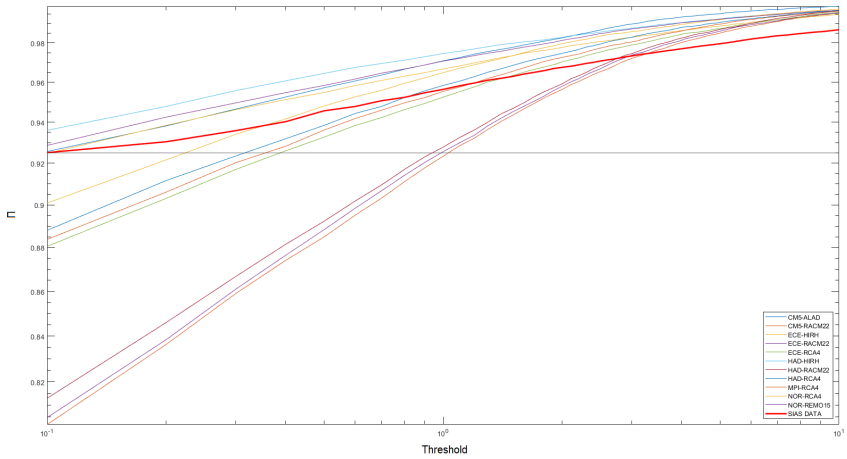

FIGURE 7.2 Choice of threshold

Taking the minimum value of Π of the SIAS data (Π0 = 0.925) we found the threshold values corresponding to the same percentage Π0 for the RCM data series (Table 7.1). The thresholds found were applied to the RCM datasets generating the correct datasets.

TABLE 7.1 List of RCM models with the corresponding threshold.

RCM	Threshold
CM5-ALAD	0.1
CM5-RACM22	1.03
ECE-HIRH	0.1
ECE-RACM22	0.98
ECE-RCA4	0.39
HAD-HIRH	0.1
HAD-RACM22	0.93
HAD-RCA4	0.31
MPI-RCA4	0.36
NOR-RCA4	0.22
NOR-REMO15	0.1

As said before, the idea of quantile-quantile mapping method is to correct the distribution of the RCM scenario through a function that makes the observed distribution agree with the distribution of the scenario in the reference period. For example, for RCM n.6 HAD-HIRH, the application of quantile mapping can be seen in the Figure 7.3.

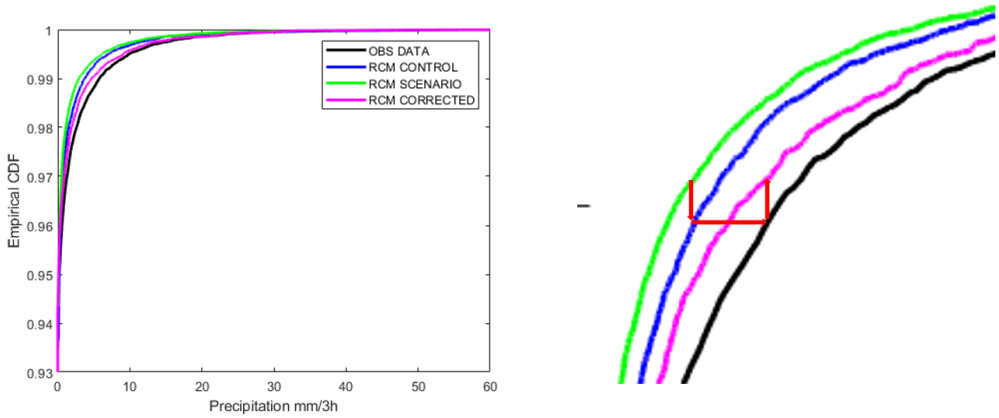

FIGURE 7.3 Example of application of quantile mapping for the model HAD-HIRH

The Figure 7.4 shows the ecdf graph of NOR-REMO15 RCM model after the bias correction for the scenatio RCP 4.5 in the years 2021-2050. In

this first case a seasonal window for bias correction was not considered. For the sake of brevity, only the graph of this model has been reported.

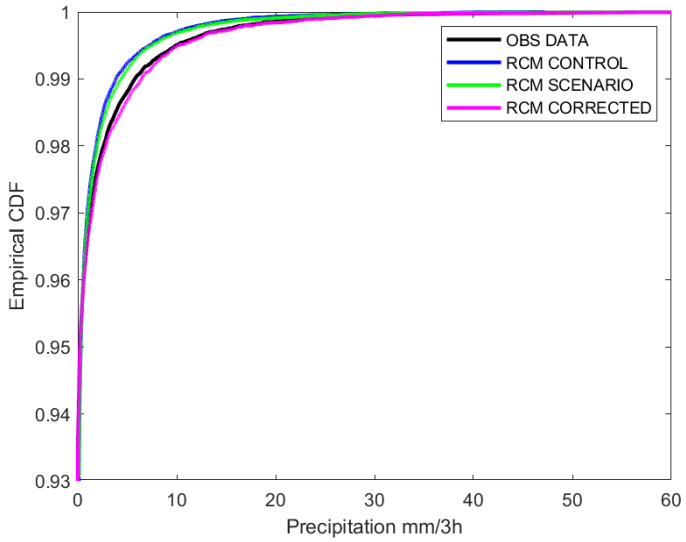

FIGURE 7.4 Application of bias correction for the model NOR-REMO15

The same bias correction procedure was done considering a seasonal window for the data correction. This means that the data have been grouped into 4 subgroups and corrected according to the relative season they belong to. At the end of the correction the data was reordered in chronological order, to obtain the corrected serie. In some cases the difference is imperceptible, in others it is possible to distinguish the two curves (cyan and magenta). This procedure was carried out for all rainfall and temperature data for all scenarios and years considered (RCP 4.5 2021-2050, RCP 4.5 201-2070, RCP 8.5 2021-2050 and RCP 8.5 2041-2070).

Again in the Figure 7.5 is shown the graph for the NOR-REMO15 model in the scenario RCP 4.5 2021-2050 with a comparison between annual and seasonal correction. The other comparison graphs, both for rainfall and temperature data and for the same scenario, are shown in the appendix.

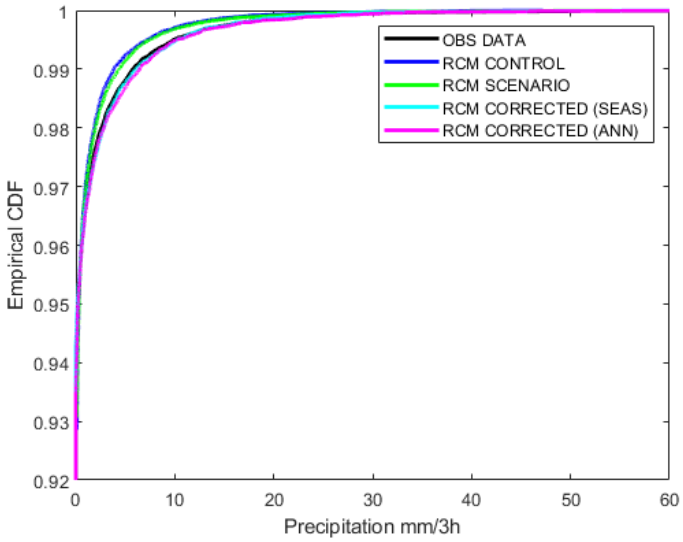

FIGURE 7.5 Application of bias correction for the model NOR-REMO15 with comparison between annual and seasonal window

7.3 Results of the application of RCM models on the green roof model

In urban water management, green roofs provide a sustainable solution for adapting to flood risk. Numerous studies have investigated the hydrological effectiveness of green roofs and the parameters that influence their functioning; many were conducted on a small scale, while only a few of these were performed on full-scale rooftop installations.

Several models have been developed and several physical parameters that can influence the storage capacity of the roof have been studied, but very few have studied how green roofs can respond to future climate scenarios. In this broader context, this final paragraph presents the results of the analysis conducted on the extensive green roof located at the University of Catania, in Sicily (Italy), in a region with a purely Mediterranean climate.

To achieve this goal, 11 climate models belonging to the Euro-CORDEX project were used, and each was analyzed in 4 different scenarios: RCP 4.5 in the thirty years 2021-2050 and in the thirty years 2041-2070, RCP 8.5 in the thirty years 2021-2050 and in the thirty years

2041-2070. The analysis was carried out using the rain and temperature data of the RCMs in input to the physically based model of the green roof, after making the bias correction. To evaluate, therefore, the efficiency of the green roof, the percentage of volume of rain water retained and the reduction of the rain peak, on a single event scale, were assessed.

7.3.1 RCM models used for the analyses

The rainfall and temperature data of the following RCM models were first corrected with the quantile-quantile mapping bias correction method, and were subsequently used in 2 different 30-year-olds:

- RCP 4.5 2021-2050;
- RCP 4.5 2041-2070;
- RCP 8.5 2021-2050;
- RCP 8.5 2041-2070.

The eleven RCM models used are listed in the Table 7.1. We have chosen to use all the RCM analysed at chapter 6.3 to evaluate the uncertainty related to the choice of models in the most exhaustive way possible.

7.3.2 Brief summary of the green roof model

This paragraph summarizes the physical parameters used for the physically based model of the green roof summarizing what is reported in the chapter 5.

1. The model (made with Hydrus 1D) simulates the behavior of the water flow within a 150 mm column of soil with presence of vegetation.
2. The simulation takes place continuously over the thirty years of data and 3 hour rainfall data are used.
3. Evapotranspiration is calculated using the Hargreaves formula and for this reason the temperature data (maximum and minimum)

are used on a monthly scale (as suggested by FAO-56). Then the maximum and minimum temperature values are selected for each month of the thirty years and inserted in the formula 5.3.

4. The Van Genuchten-Mualem model, (M. Th. van Genuchten, 1980), is used for the hydraulic properties of the soil and is not considered hysteresis.

5. The hydraulic parameters of the soil are those obtained from laboratory tests and perfected with the heuristic calibration and are the following:

   - θr = 0.04
   - θs = 0.48
   - α = 0.001 [1/mm]
   - n = 1.49
   - Ks = 52.8 [mm/h]
   - l = 0.5

6. The surface boundary condition provides atmospheric pressure with a surface layer, it allows water to accumulate on the surface. The height of the surface water layer increases due to precipitation and decreases due to infiltration and evaporation, the limit is 30 mm.

7. The bottom boundary condition provides for deep drainage, vertical drainage through the lower limit of the soil profile is approximated by a flow that depends on the position of the saturated zone level within the soil layer. The inflow / outflow velocity assigned to the lower limit condition is determined by the function g = - A esp (B | h - GWL0L |). The parameters have been calibrated and are Aqh = -0.75, Bqh = -0.0016 and GWL = 0.

8. The Feddes parameters for the root system in a first approximation were defined as similar to the grass.

9. The crop parameters were estimated as follows:

- Crop height = 200 [mm]
- Root depth = 150 [mm]
- LAI = 2.51
- Interception constant = 1.5 [mm]

7.3.3 Rain events compared with historical events

After carrying out the simulations of the various RCMs, the different rain events were extrapolated for each model over thirty years, then they could be analyzed.

Rain events were considered:

- With a minimum precipitation threshold of 0.2 mm;
- With a minimum height of 10 mm for the event;
- For each rain event, more than 24 dry hours post-event were evaluated to also take into account the release from the green roof (for the calculation of the outgoing volumes).

Taking into account that the objective is to evaluate whether the green roof can compensate for the impacts of climate change, it is necessary to ensure that any increase in flow associated with climate change in correspondence with a traditional pavement can be compensated for by the reduction in flow rate that is obtained thanks to the green roof. So two analyzes were carried out, one as a consequence of the other:

1. The volume V_{0H} and the peak P_{0H} (for each event) of the hydrogram in an outlet from a traditional roof (runoff coefficient 0.9) was calculated in correspondence with the historical scenario for each RCM (1975-2004) and this was compared with the volume V_{0F} and the peak P_{0F} (for each event) of the hydrogram leaving a traditional roof (runoff coefficient 0.9) in correspondence with the generic future scenario. So by ascertaining that $V_{0F} > V_{0H}$ and / or $P_{0F} > P_{0H}$, we can deduce that climate change can cause an increase in flooding problems (Figures from 7.6 to 7.13).

2. The volume V_{1F} and the peak P_{1F} (for each event) of the hydrogram leaving the green roof were then calculated in correspondence with the generic future scenario to ensure that $V_{1F} < V_{0H}$ and / or $P_{1F} < P_{0H}$, and to be able to state that the green roof actually manages to offset the impact of climate change (Figures from 7.14 to 7.21).

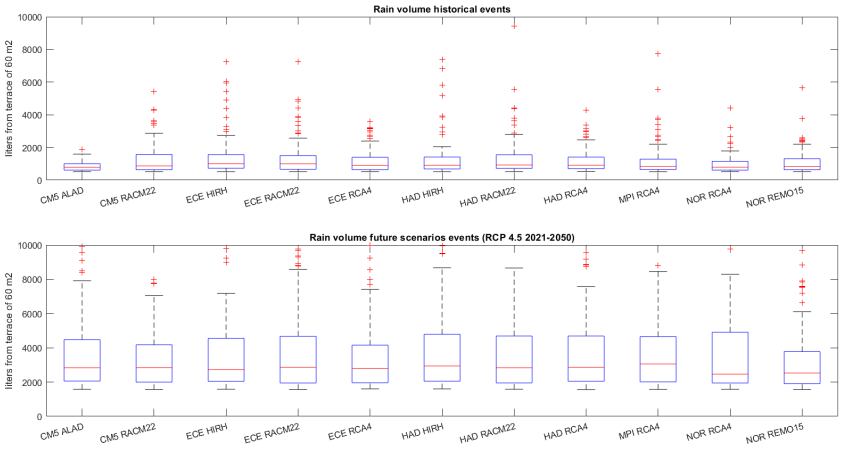

FIGURE 7.6 Comparison of outflow volume between historical and scenario data. RCP 4.5 period 2021-2050

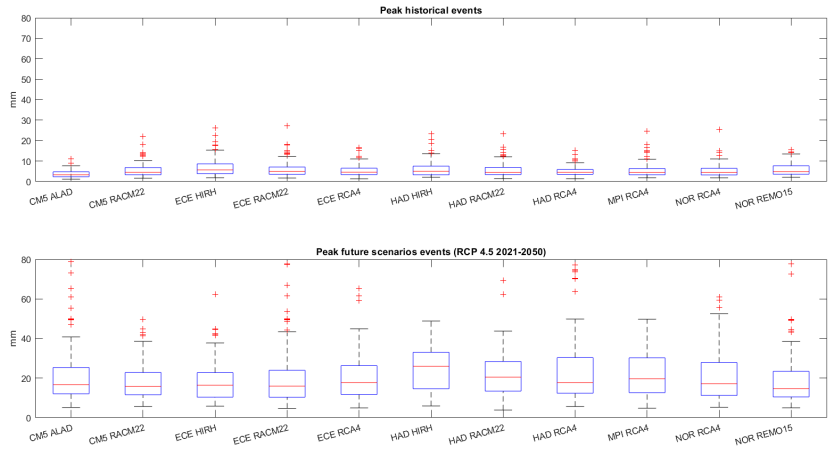

FIGURE 7.7 Comparison of peak between historical and scenario data. RCP 4.5 period 2021-2050

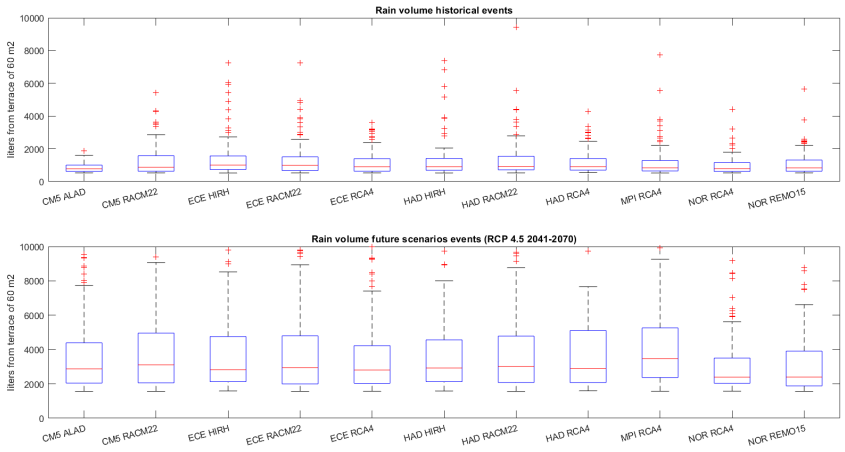

FIGURE 7.8 Comparison of outflow volume between historical and scenario data. RCP 4.5 period 2041-2070

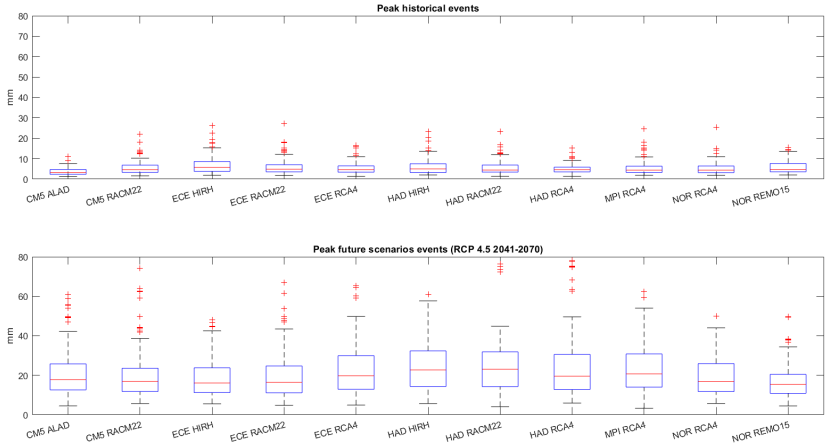

FIGURE 7.9 Comparison of peak between historical and scenario data. RCP 4.5 period 2041-2070

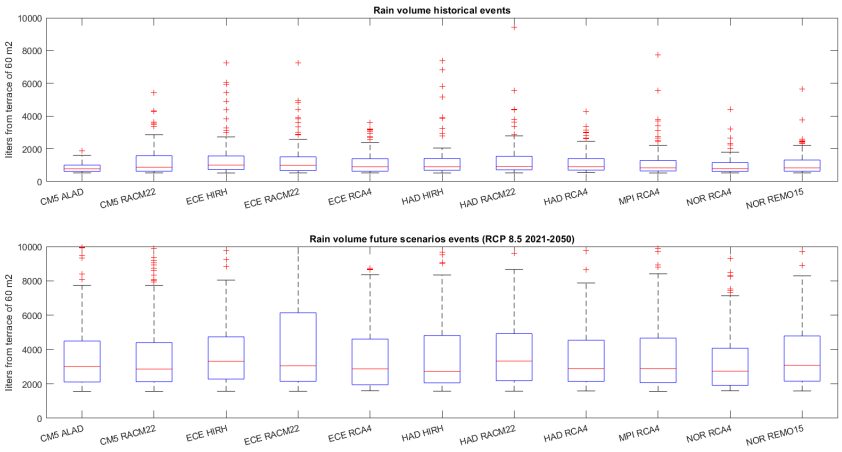

FIGURE 7.10 Comparison of outflow volume between historical and scenario data. RCP 8.5 period 2021-2050

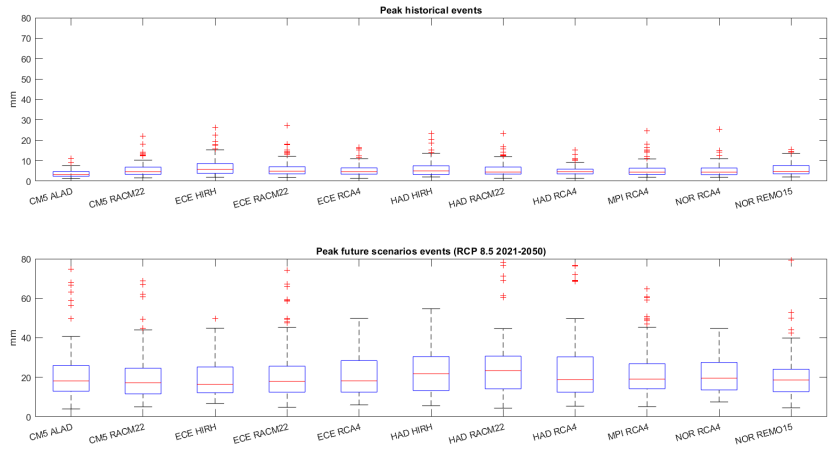

FIGURE 7.11 Comparison of peak between historical and scenario data. RCP 8.5 period 2021-2050

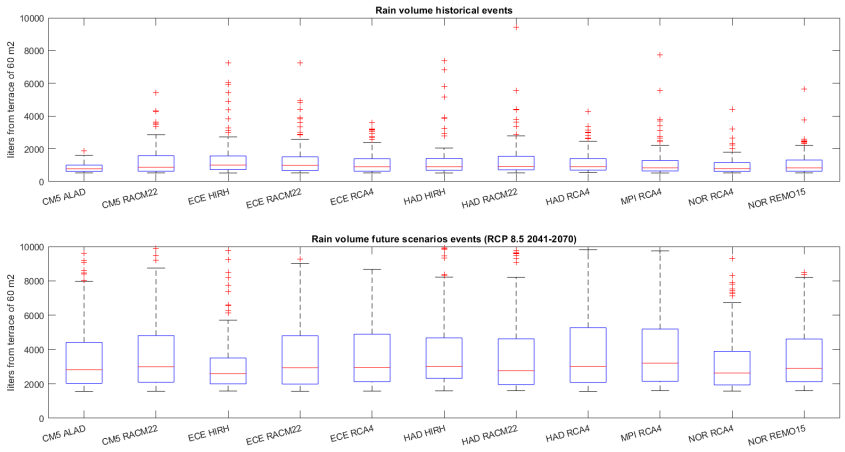

FIGURE 7.12 Comparison of outflow volume between historical and scenario data. RCP 8.5 period 2041-2070

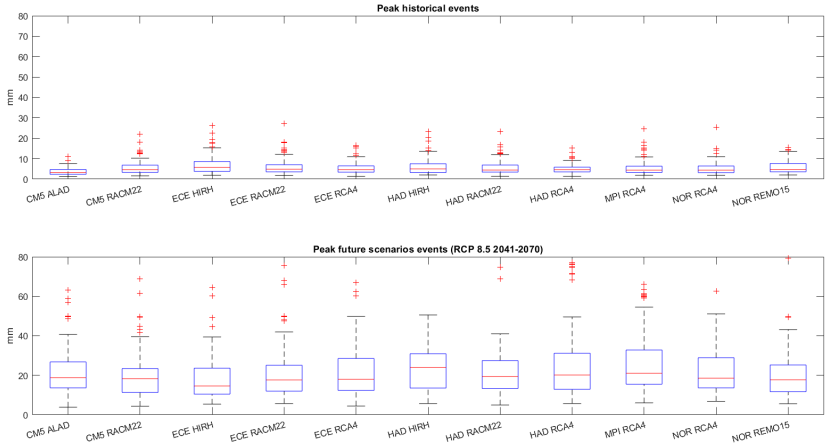

FIGURE 7.13 Comparison of peak between historical and scenario data. RCP 8.5 period 2041-2070

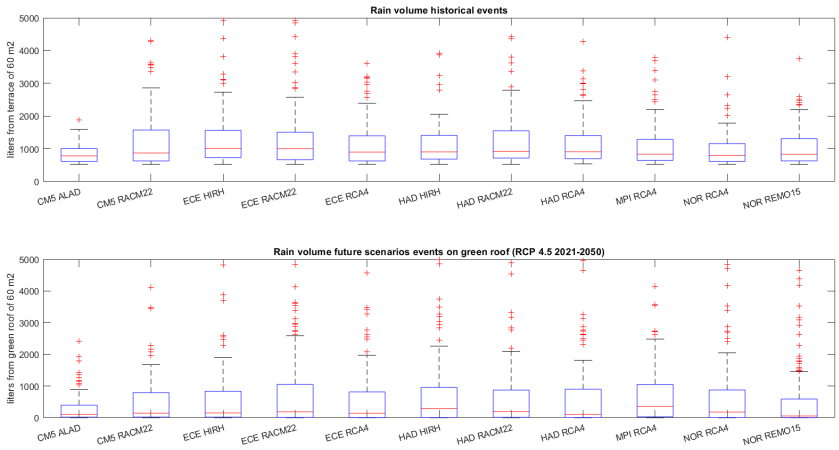

FIGURE 7.14 Comparison of outflow volume between historical and scenario data with green roof. RCP 4.5 period 2021-2050

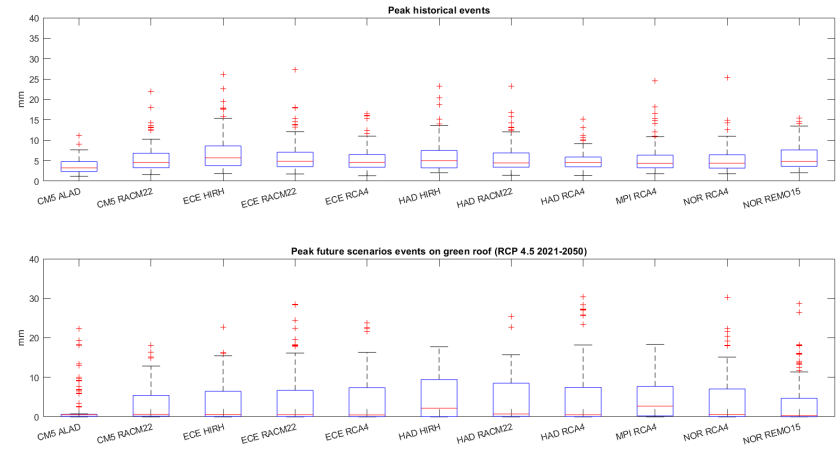

FIGURE 7.15 Comparison of peak between historical and scenario data with green roof. RCP 4.5 period 2021-2050

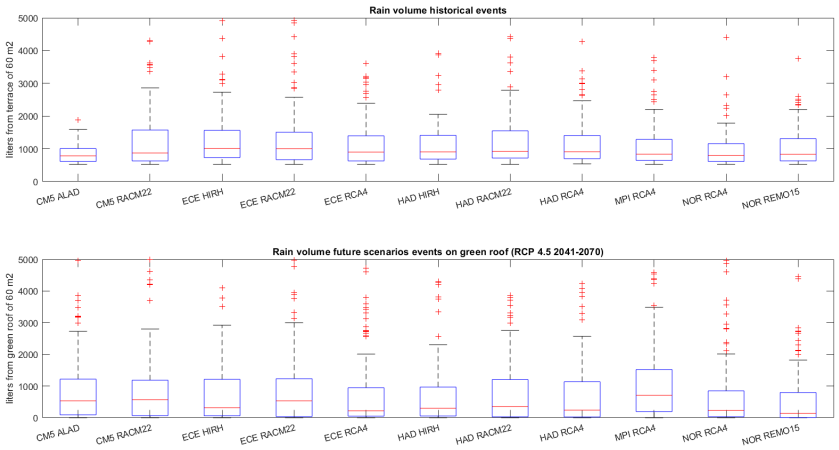

FIGURE 7.16 Comparison of outflow volume between historical and scenario data with green roof. RCP 4.5 period 2041-2070

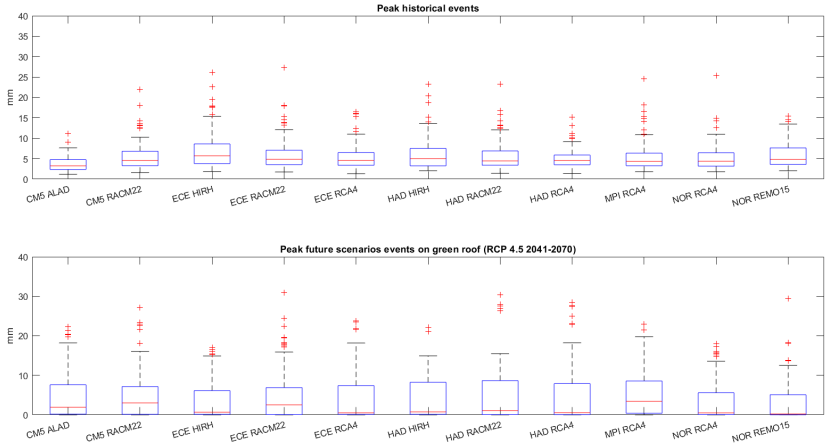

FIGURE 7.17 Comparison of peak between historical and scenario data with green roof. RCP 4.5 period 2041-2070

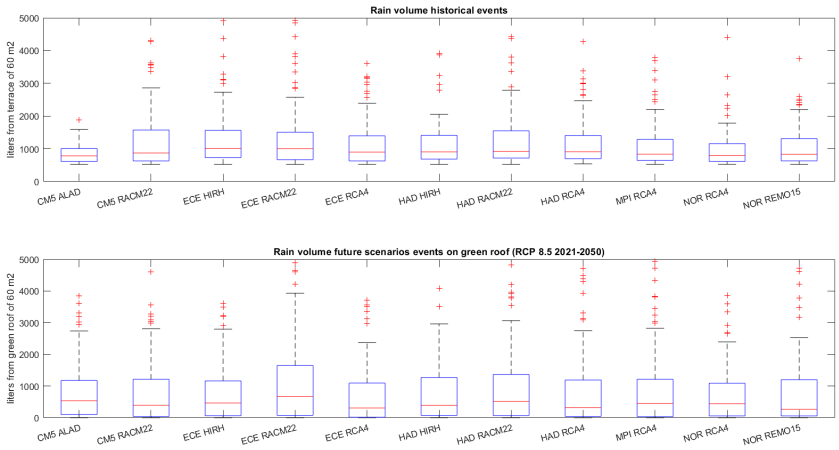

FIGURE 7.18 Comparison of outflow volume between historical and scenario data with green roof. RCP 8.5 period 2021-2050

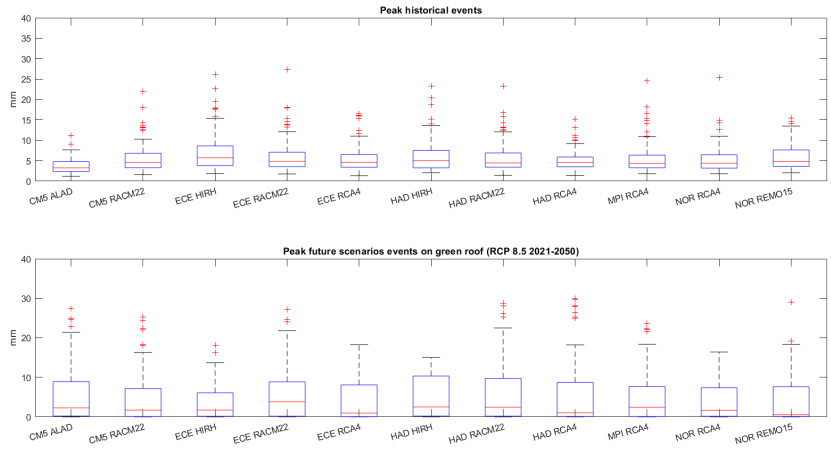

FIGURE 7.19 Comparison of peak between historical and scenario data with green roof. RCP 8.5 period 2021-2050

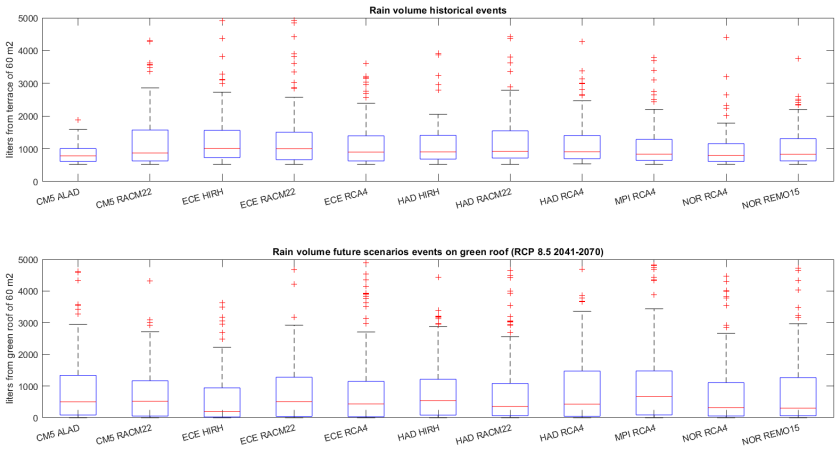

FIGURE 7.20 Comparison of outflow volume between historical and scenario data with green roof. RCP 8.5 period 2041-2070

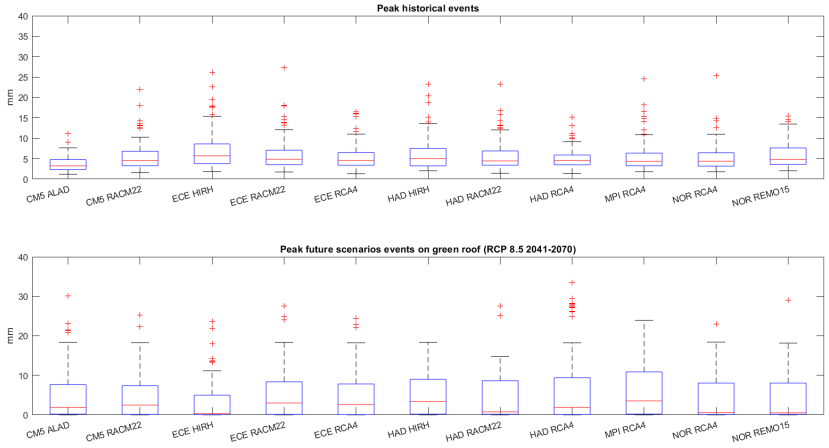

FIGURE 7.21 Comparison of peak between historical and scenario data with green roof. RCP 8.5 period 2041-2070

7.3.4 Evaluation on the maxima values of volume and peak

After making the comparisons based on all the rain events in the future and in the historical series, we proceeded with a further analysis based only on the maxima events. This comparison is made considering only the maxima of volumes and peaks for each year and not taking into

consideration all the values of volumes and peaks. (In this way for each thirty years there are 30 values). Specifically, the processing consists in:

1. Extrapolation of historical events;
2. Calculation of volumes and peaks for all historical events;
3. Extrapolation of the events from the considered scenario with the green roof action;
4. Calculation of volumes and peaks for all events found;
5. Extrapolation of the maximum volume / peak for each year in the history;
6. Extrapolation of the maximum volume / peak for each year in the scenario with the green roof;
7. Creation of the graphic comparison.

The graphs (from Figure 7.22 to 7.29) show how effectively the action of the green roof in future scenarios brings the maxima values to values comparable with historical data.

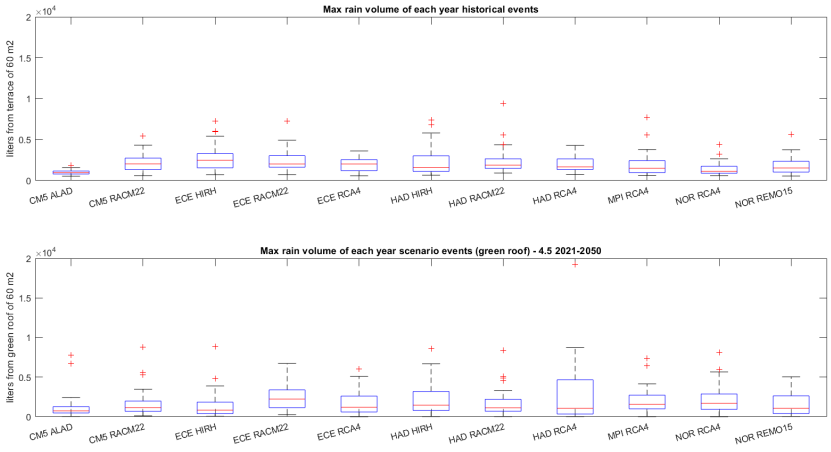

FIGURE 7.22 Comparison of outflow volume between historical and scenario data with green roof (Maxima values for each year). RCP 4.5 period 2021-2050

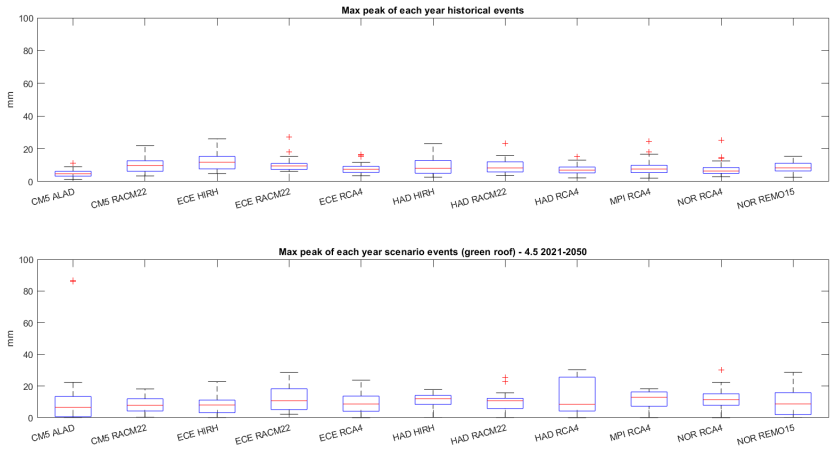

FIGURE 7.23 Comparison of peak between historical and scenario data with green roof (Maxima values for each year). RCP 4.5 period 2021-2050

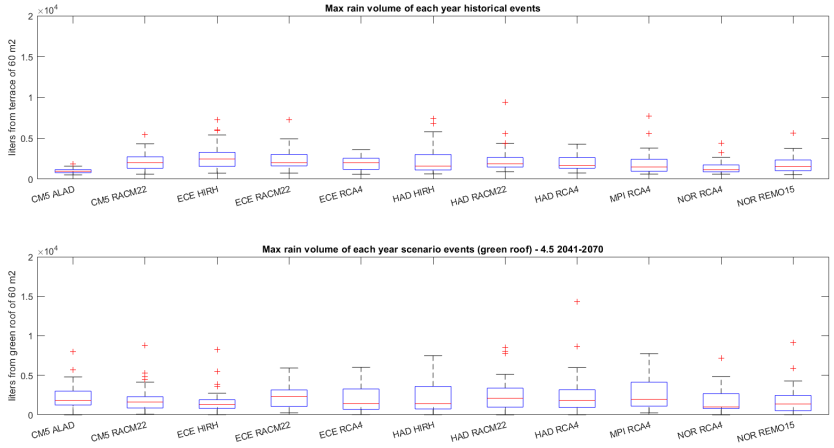

FIGURE 7.24 Comparison of outflow volume between historical and scenario data with green roof (Maxima values for each year). RCP 4.5 period 2041-2070

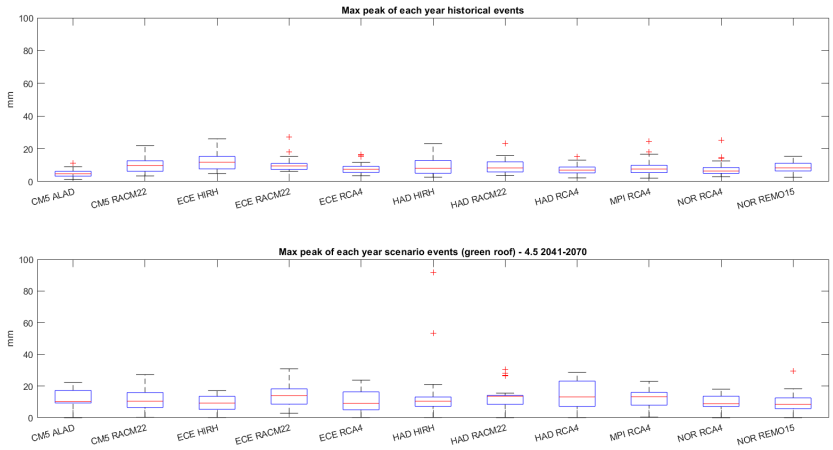

FIGURE 7.25 Comparison of peak between historical and scenario data with green roof (Maxima values for each year). RCP 4.5 period 2041-2070

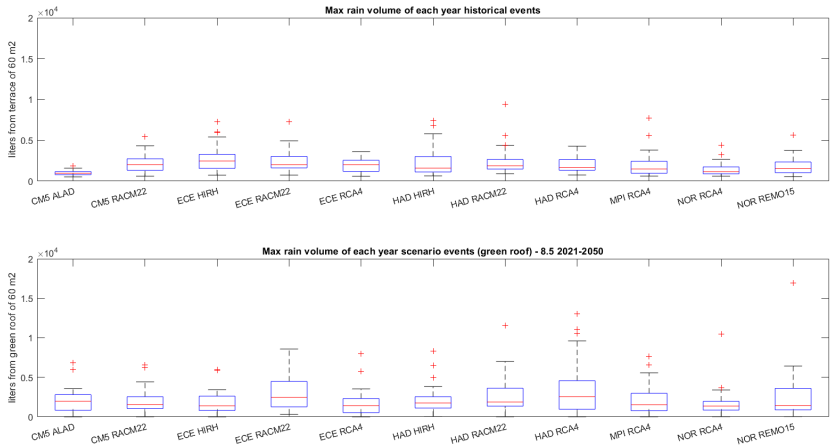

FIGURE 7.26 Comparison of outflow volume between historical and scenario data with green roof (Maxima values for each year). RCP 8.5 period 2021-2050

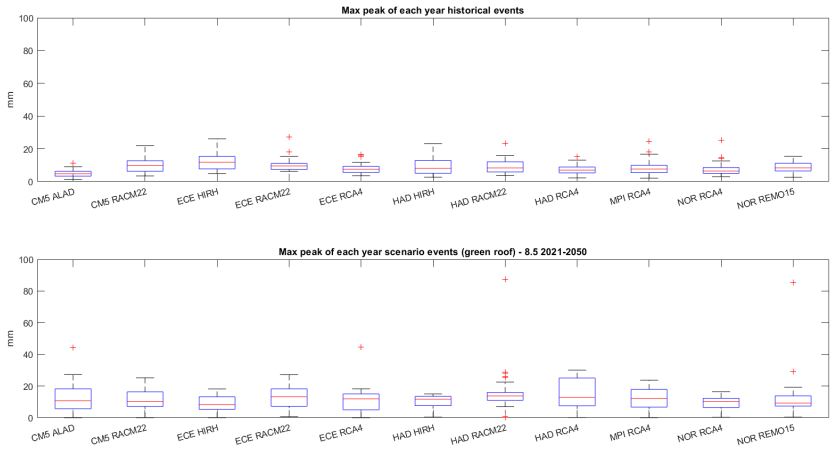

FIGURE 7.27 Comparison of peak between historical and scenario data with green roof (Maxima values for each year). RCP 8.5 period 2021-2050

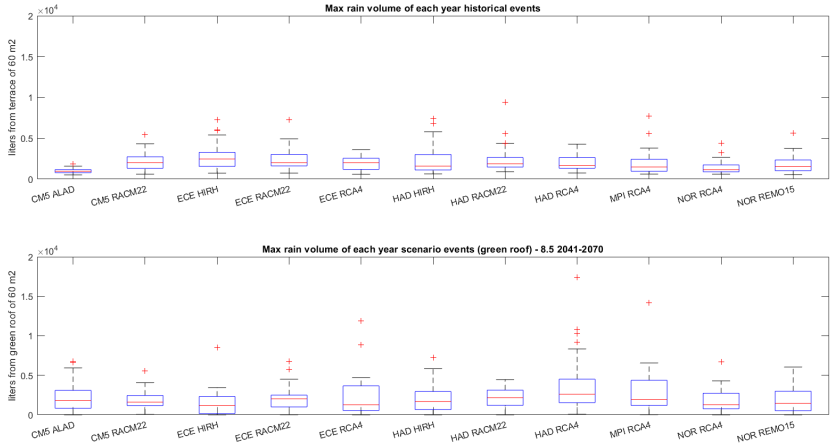

FIGURE 7.28 Comparison of outflow volume between historical and scenario data with green roof (Maxima values for each year). RCP 8.5 period 2041-2070

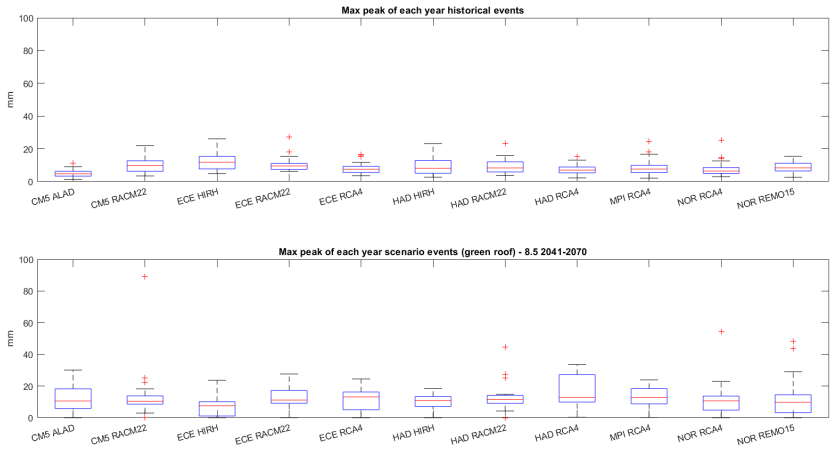

FIGURE 7.29 Comparison of peak between historical and scenario data with green roof (Maxima values for each year). RCP 8.5 period 2041-2070

7.3.5 Green roof efficiency

To evaluate the efficiency of the green roof, the following were considered in the first instance:

1. The retention volume with the formula 7.3 where R_F is the total volume exiting a classic paved terrace (runoff coefficient 0.9) and R_{GR} is the total volume exiting a portion of green roof as large as the paved terrace.

$$RetainedVolume = ((R_F - R_{GR})/R_F)100 \tag{7.3}$$

2. The peak's reduction with the formula 7.4 where PF_{IR} is the peak of the classic paved terrace (runoff coefficient 0.9) and PF_{GR} is the peak of the green roof portion as large as the terrace.

$$PeakReduction = ((PF_{IR} - PF_{GR})/PF_{IR})100 \tag{7.4}$$

The results are shown from Figure 7.30 to 7.37.

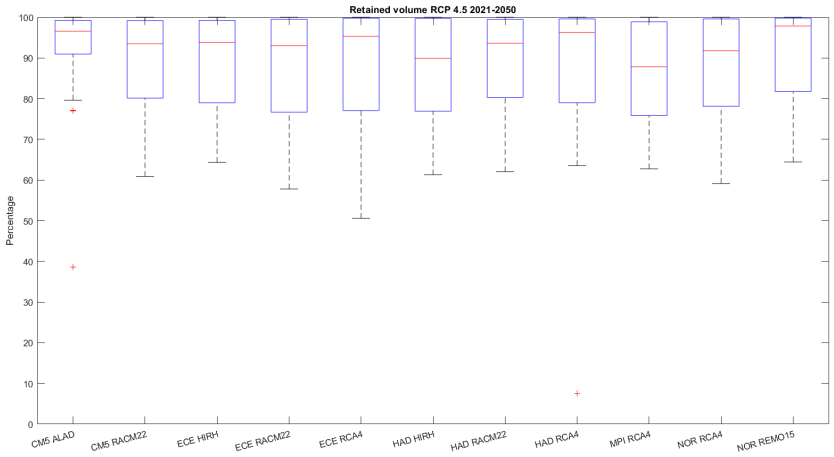

FIGURE 7.30 Percentage of retained volume. RCP 4.5 period 2021-2050

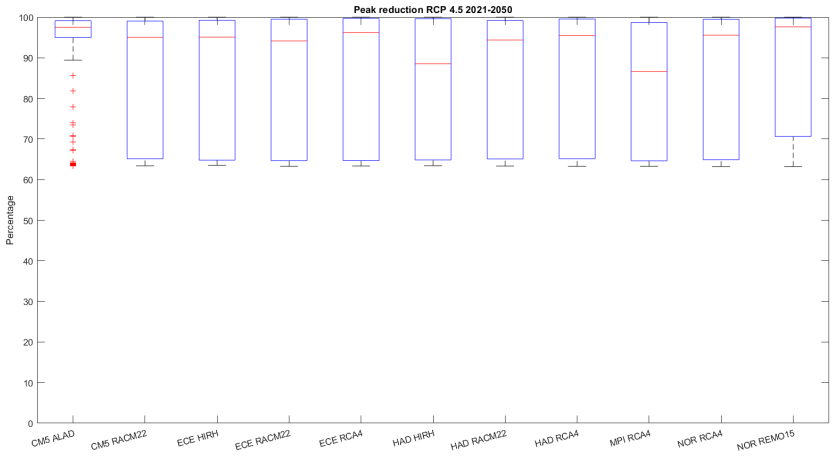

FIGURE 7.31 Percentage of peak reduction. RCP 4.5 period 2021-2050

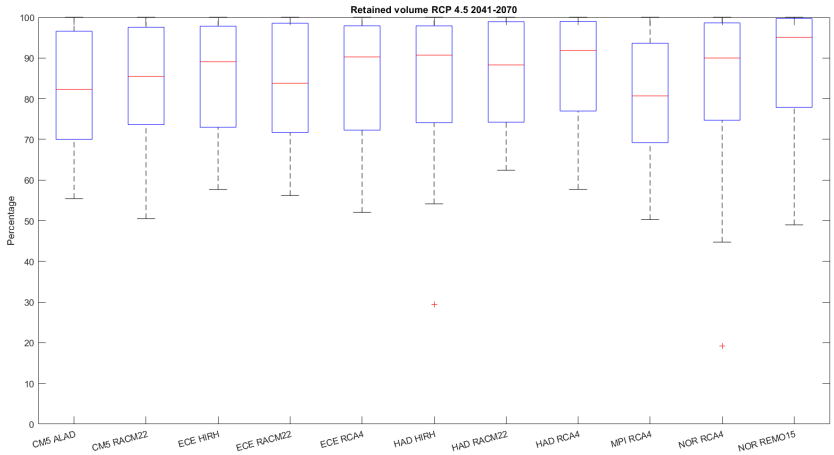

FIGURE 7.32 Percentage of retained volume. RCP 4.5 period 2041-2070

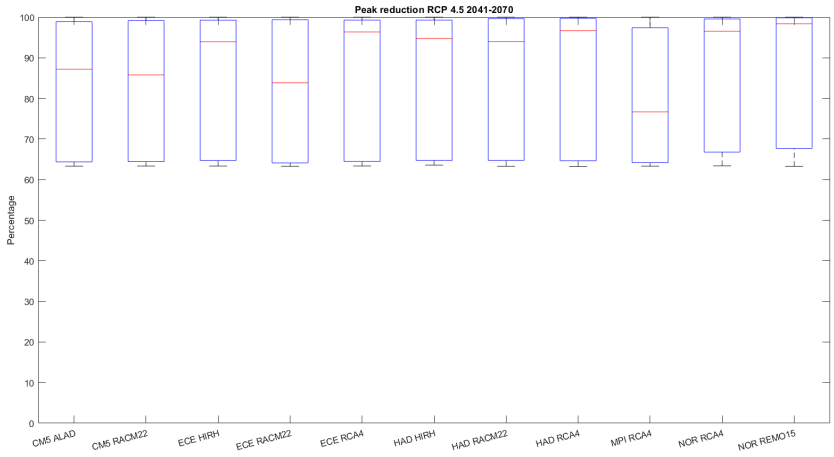

FIGURE 7.33 Percentage of peak reduction. RCP 4.5 period 2041-2070

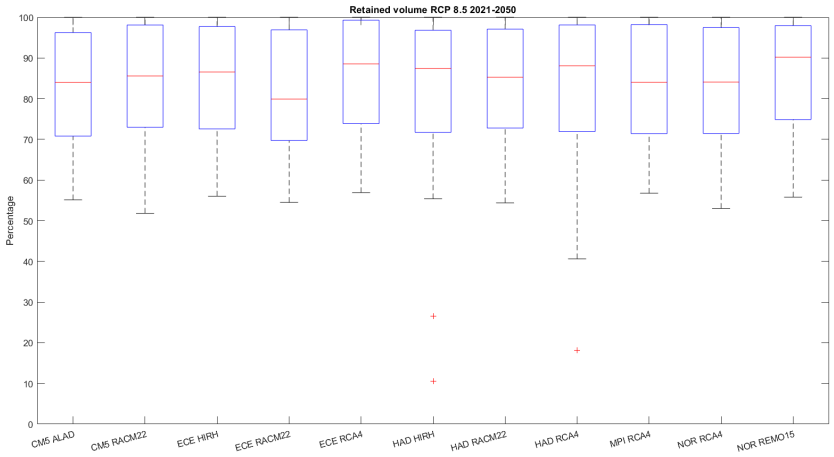

FIGURE 7.34 Percentage of retained volume. RCP 8.5 period 2021-2050

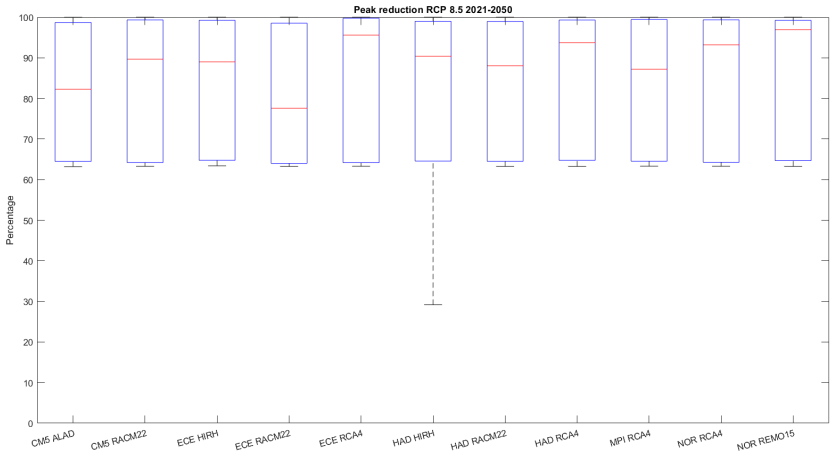

FIGURE 7.35 Percentage of peak reduction. RCP 8.5 period 2021-2050

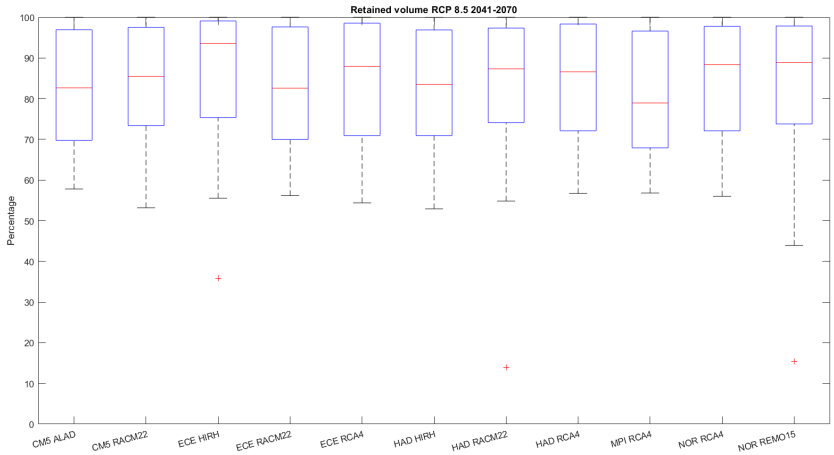

FIGURE 7.36 Percentage of retained volume. RCP 8.5 period 2041-2070

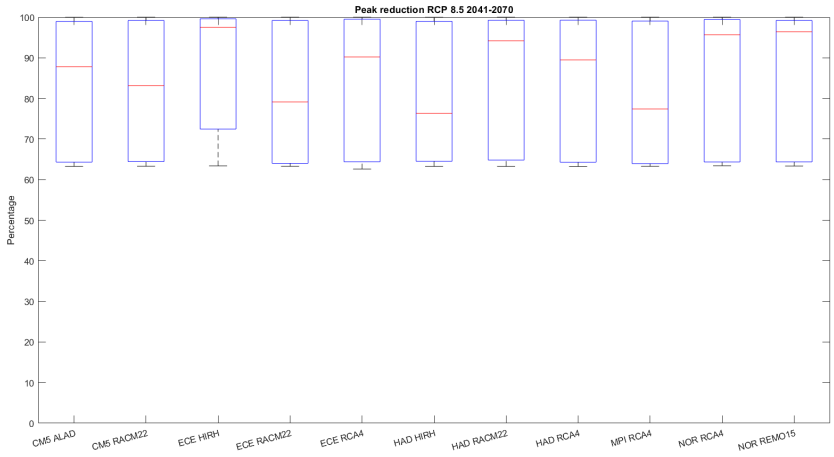

FIGURE 7.37 Percentage of peak reduction. RCP 8.5 period 2041-2070

7.3.6 Discussion of the results

The results refer to an extensive green roof model, taking into consideration a portion of the roof of 60 m^2 and a soil thickness of 15 cm. The experiment and the analyzes were conducted with data belonging to an area characterized by a typically Mediterranean climate. The data of the climatic scenarios used belong to the EURO-CORDEX project (GCM-RCM models) extracted for the Catania station, where the experimental site of the green roof is located.

The results shown in the previous paragraphs can be summarized as shown below. With paved roofs (traditional terraces) it is clear that climate change can actually lead to an increase in volumes and an increase in peaks. In our case, taking into account a terrace of about 60 m^2, the volumes will be increased from about 1000 liters to over 2000 liters outflow from the terraced roof. The same for the rain peaks which, for the historical series, have values below 10 mm and, on the other hand, for scenarios they exceed 20 mm on average. Evaluating the action of the green roof, the results show that the infrastructure actually restores the values of volumes and peaks around the values of the historical series.

As regards the RCP 4.5 scenario in the thirty years 2021-2050, the results highlight that volumes are reduced, with respect to the historical series, by approximately 70% on average. The peaks also have a reduction with values that are below 5 mm. In the RCP 4.5 scenario in the thirty-year period 2041-2070 volumes are reduced on average by approximately 50% respect to the historical series and the peaks, in some models are reported to values similar to the historical series, in other models they have a decrease. Also, with regard to the RCP 8.5 scenario in the thirty-year period 2021-2050, the volumes are on average reduced by approximately 45-50% compared to the historical series, while the peaks have values comparable with the peaks of the historical series. For the RCP 8.5 scenario in the thirty years 2041-2050 the volumes are on average reduced by approximately 45-50% compared to the historical series and the peaks have values comparable with the peaks of the historical series, if not lower.

Evaluating the results of the analysis on the maxima rainfall values in the different models, the results suggest that the action of the green roof in future scenarios actually brings the values to values comparable with historical data. In fact, in the RCP 4.5 scenario in the thirty years 2021-2050 the maximum volumes are restored by the green roof around the values of the historical series, while the peaks of the scenario are slightly higher than the peaks of the historical series. In the RCP 4.5 scenario in the thirty-year period 2041-2070, the values of the maximum volumes reflect those of the historical series on average, while the peaks are in some cases slightly higher, in others they are similar to the historical series. As

regards the RCP 8.5 scenario in the thirty years 2021-2050 and in the thirty years 2041-2050, both the volumes and the peaks are slightly higher than the historical series by about 25% on average.

Finally, the efficiency of the green roof in terms of retained volume and peak reduction was evaluated. The results show a positive effect of the green roof. In all considered scenarios retained volumes of at least 78% are reached with the effect of the green roof and, at the same time, the peaks are reduced by at least 75%. Evaluating the volume considered by the green roof in the RCP 4.5 scenario in the thirty years 2021-2050, the graphs show that it stands at around 90%, exceeding the threshold of 95% for some models such as CM5-ALAD, HAD-RCA4 and NOR-REMO15. Also the reduction of the peaks in many cases exceeds 95%, except for HAD-HIRH and MPI-RCA4 for which it is around 85%. In the RCP 4.5 scenario in the thirty-year period 2041-2070 the retained volume exceed 80% and for some models such as ECE-RCA4, HAD-HIRH, HAD-RCA4 and NOR-REMO15 it is around 90%. The peaks are also reduced with values higher than 80% and for some models even more than 90%. In the RCP 8.5 scenario in the thirty-year period 2021-2050, the estimated volume for each model is between 82 and 87% except for the ECE-RACM22 model for which the value is approximately 78%. As for the reduction of rain peaks, the values are between 80% and 90%. Finally, in the RCP 8.5 scenario in the thirty years 2041-2070, the volume considered for each model is between 82 and 87% except for the ECE-HIRH model for which the retention value exceeds 90% and for the MPI-RCA4 model for which the value is about 78%. In this case, the peaks are reduced in any case by at least 75%.

At the conclusion of these results it is possible to state that the green roof can be a valid infrastructure for the reduction of volumes and rain peaks in the near future. With its capacity to retain volumes and reduce peaks, the green roof effectively manages to bring the outflow to a level similar to that of the historical scenario, removing, partially or completely, the negative effect of climate change.

Chapter 8

Conclusions

The research work described in this dissertation investigates empirical evidences, systematic data, tools and methodologies to clarify the usefulness of green roofs as a choice to adaptation to climate change. The dissertation reports the efforts made in different directions, aimed at providing advances for the definition of a comprehensive framework on these specific green infrastructures for the reduction of flood risk in urban areas in a Mediterranean climate. This research could be innovative because it correlates the study of the green roof, as a rainwater retention tool, with climate change and their evolutionary scenarios in the coming decades. In addition to this, the study finds its motivation in a context where the population perceives climate change and feels the need for new adaptation infrastructures. So, this work is not just a modeling study, but also offers a general framework on the population of eastern Sicily to capture the current perception linked to the flood risk.

For the future climate scenarios, the RCM models are not only used, but are first ranked, studied on different time scales and then corrected in order to understand which perform better in the considered Mediterranean area. In this regard, each chapter individually covers a defined domain, as summarized below.

The first chapter introduces the research, its motivations, the structure, the objectives and the methodology followed. The aim of this research is to define tools and methodologies to ascertain the efficiency of green infrastructures as a tool for adapting to climate change with specific reference to urban areas in the Mediterranean, and, subsequently, the definition of a model on single-infrastructure-scale for the analysis of the impacts of climate change on the hydrological-hydraulic response.

At the beginning of this dissertation the state of the art is described. the starting point is to have an overall picture on the numerous existing studies developed on green infrastructures, in particular on green roofs. Other studies on climate change, the related problem of increasing flood risk and the natural hazards and risk perception are also important for the background. The literature presentation analyses in detail the evolution of research in the sector, the basic studies on green roofs, their history and their development, and in particular the studies on the hydrological response for stormwater retention. The state of the art shows how the topic is widely spread among researchers around the world. There are numerous experimental green roofs in universities or research centers. Numerous studies have been conducted on the hydrological performance of green roofs, however, at the moment, there is still no solid literature that evaluates this infrastructure as a valid choice for adaptation in future climate scenarios.

To obtain a more complete overview of the area affected by this work, the third chapter deals with climate change and flood risk, but focuses on eastern Sicily. The results of a survey on climate change and risk perception carried out as part of the activities of the LIFE SimetoRES project are presented. This research involved some municipalities of the Simeto River Valley, the largest river valley in Sicily (Italy), that have been repeatedly hit by intense rainfall events in the last decades causing urban flooding, several damages and, in some instances, threats to population.

This part of the study was essential to contextualize the research and to strengthen the motivations to undertake it. We wanted to investigate the current situation from the point of view of the population that has to face, now more and more often, the risk of flooding in their cities.

Subsequently the methodology of the experimental and modeling phase is exposed. To achieve this goal the part concerning the green roof model is divided into two parts: an experimental part with the green roof of the University Campus and a modeling part that, starting from experimental data and climatic data, try to generate a model at single infrastructure scale to test the green roof's response to climate change.

The same chapter later focuses on the experimental part of the project, that is, on the experimental green roof recently installed at the campus of

the University of Catania. The structure of the green roof and the chosen and installed vegetation is then described in detail, then follows the complete description of the monitoring system and the data collection system, used for the collection of soil data and meteorological data.

Chapter 5 presents the physically-based model. The HYDRUS-1D software was used for the realization of a physically based model, but before moving on to purely computational modeling, some laboratory tests were carried out to identify the hydraulic parameters of the soil. After obtaining the grading curve and having a first estimate of the hydraulic parameters of the soil an heuristic calibration was carried out in order to best reproduce the hydrological-hydraulic response of the green roof. Some rain events recorded during the two years of monitoring and some dry periods were used. In this way, a consistent model of the green roof was obtained.

The same chapter also shows the analysis on the efficiency of the green roof on the rainfall events from May 2019 to April 2021. We discovered that, on average, the volume retention is around 67.5%, while the mean peak reduction is over 89%. As for the mean delay of the peak is about 295 minutes.

The thesis continues by presenting two studies for the ultimate goal of this research. The first study analyzes climate models to evaluate their reliability in the reproduction of rains, temperatures and periods of drought in the regions of Calabria and Sicily. This analysis is of key importance to understand which climate models are actually realistic and therefore usable in a Mediterranean area.

The second study, with reference to 14 rain gauge stations in Sicily, evaluates historical simulations of precipitation data from 11 RCMs, in order to understand how they compare to fine-resolution observations. This analysis highlights the differences between the different models, and, by ranking the RCMs, supports the selection of the most suitable climate model for assessing the impacts in the considered locations in terms of extreme event analysis.

This chapter plays a crucial role as it evaluates the best performing models to simulate the present climate and subsequently the future climate. In order to understand if green roofs can be an infrastructure that

is actually suitable for the climate scenarios of the coming decades, it is important to know that reliable climate models are available.

The last part presents the results of this research. First of all, it shows the procedure for correcting climate models through the quantile-quantile mapping method. Subsequently, some results obtained from the application of the RCM models on the green roof model are illustrated. A comparison was made between the output volumes and the rainfall peaks of the rain events belonging to the historical data and between those belonging to the scenarios data. Once it was ascertained that climate change negatively affects rain events, we proceeded with the evaluation of the role of the green roof in these scenarios and then an assessment of the efficiency of the green roof is presented.

With paved roofs (traditional terraces) it is clear that climate change can actually lead to an increase in volumes and an increase in peaks. The outflow volumes will be increased and the same for the rain peaks which. Evaluating the action of the green roof, the results show that the infrastructure actually restores the values of volumes and peaks around the values of the historical series.

Evaluating the results of the analysis on the maxima rainfall values for the different models, the results suggest that the action of the green roof in future scenarios actually brings the values to values comparable with historical data reducing the effect of climate change.

Finally, the efficiency of the green roof in terms of retained volume and peak reduction was evaluated. The results show a positive effect of the green roof. In all considered scenarios retained volumes of at least 78% are reached with the effect of the green roof and, at the same time, the peaks are reduced by at least 75%.

In conclusion of this dissertation it is essential to underline that this study has some limits due both to the experimental setup and to the data used in the analyzes. Nowadays, the experimental site of the University of Catania certainly represents a reference point for the study of green roofs in the Mediterranean area, since it is one of the last green roofs built in the area. However, due to the very recent construction of this infrastructure, some equipment needed to complete the experimental setup is

still missing. New installations will allow an ever more precise and reliable data collection in order to be able to continue with new studies both in hydrology and in other scientific branches.

As already widely discussed, the data used to simulate the behavior of the green roof to climate change belong to the EURO-CORDEX project. These data complement the GCMs with Regional Reduced Data (RCM). To study short and intense rain events it was necessary to use a short time scale (3 hour scale) and this does not benefit the research, as there is currently uncertainty about the reliability of the small scale GCM-RCM data. Although the models have been classified, we preferred to use all those available to evaluate the uncertainty as exhaustively as possible.

In order to start developing a study in this direction, however, it was of fundamental importance to be able to use these data and we are confident that from now on it will be possible to have more and more precise data in order to be able to develop more reliable models.

This study can represent a starting point for new developments. It'll be possible to investigate the hydrological performance of different plant species suitable for a Mediterranean climate and, with the collection of data on new rain events, it'll be possible to further refine the study on the ability to reduce volumes and rain peaks. It would also be desirable to conduct new surveys in the area to understand if the population is well disposed towards these new infrastructures and especially if they found an effective benefit in flooding reduction.

Regarding the analysis of RCM models many directions could be taken. Certainly refining the statistical analysis it'll possible to carry out studies on different types of green roofs, varying thickness or type of soil. In this way it might be possible to define an optimal configuration of the green roof that can represent an adaptation infrastructure to climate change.

Appendix A

Appendix of figures

A.1 Survey in Simeto River Valley

The survey consists of a combination of 10 questions, including some multiple choice and others using the Likert scale (1932), preceded by 5 questions related to the characterization of the sample. The questions were formulated to be independent of each other and each of them is aimed at extrapolating precise information. The survey was administered in Italian language. Below we show the questions translated in English.

A.1.1 Sample characterization

Gender

- M
- F

How old are you?

- Up to 14 years
- Between 15 and 19 years old
- Between 20 and 30 years
- Between 31 and 45 years old
- Between 46 and 60 years old

- Over 60 years old

Education

- None
- Primary school diploma
- Middle School diploma
- High school diploma
- Graduation
- Higher qualification (Ph.D., Master, etc.)

What is your current occupation?

- Student
- Worker
- Unemployed
- Retired

Where do you live?

- Adrano
- Belpasso
- Biancavilla
- Catania
- Centuripe
- Motta Sant'Anastasia
- Paternò
- Ragalna
- Regalbuto

- Santa Maria di Licodia
- Troina
- Other

A.1.2 Perception of climate change

Question No. 1 During the autumn of 2018, Sicily was hit by heavy rains in both the eastern and western parts, what do you think these phenomena are due?

- Heavy rainfall events occur quite often in autumn, so there are quite normal in this season;
- These are phenomena due to climatic changes taking place on the planet;
- It was an isolated phenomenon;
- I do not know.

Question No. 2 In the last years, how often have you heard about climate change?

- At least once a day;
- At least once a week;
- At least once a month;
- At least once a year;
- Almost never;
- Never.

Question No. 3 Where did you hear about climate change? (More options can be selected)

- Talking to friends, family;
- Social networks/internet;

- Newspapers/magazines/TV/Radio;
- At school/university/work;
- During events/conferences;
- I don't remember hearing about it.

A.1.3 Perception of flood events, behaviour during weather alerts and related responsibilities

Question No. 4 Do you cross areas that are likely to be flooded during a rain event?

- Yes;
- No;
- I do not know.

Question No. 5 The news talks about a serious weather alert for tomorrow, how do you feel? Indicate your degree of worry (1 means "very little", 5 means "very much")

- 1;
- 2;
- 3;
- 4;
- 5.

Question No. 6 In the event of a flood what do you do if: a. you are at work/school/gym

- Make sure you get in the car to go home;
- You go to a mezzanine floor of a building, and wait for the return to normality before going out;

- Go home by feet as quickly as possible because it could be dangerous to use any means of transport;
- You take shelter on the lower floors of a building, and wait for the return to normality before going out;
- I do not know.

b. you are in your car/scooter and you have to pass an underpass?

- You go through the underpass as fast as possible to get into safety;
- You go back and change directions, possibly avoiding other underpasses;
- You cross slowly to avoid the danger of "aquaplaning";
- Get off the car/scooter and cross on foot;
- I do not know.

c. you are in your car/scooter and you have to pass a bridge?

- You stop on the bridge to check what's going on;
- Go back and reach a higher place; leave only after the situation has returned to normal;
- The question makes little sense, bridges only serve to overcome dips of the soil that have little relationship with water;
- Wait near the bridge and leave when it stops raining;
- I do not know.

Question No. 7 Indicates the degree of responsibility for the prevention of flood risk of the following figures where 1 means very little and very much 5. The citizens

- 1;
- 2;
- 3;

- 4;
- 5.

The Mayor and the Municipality

- 1;
- 2;
- 3;
- 4;
- 5.

Civil Protection and Firefighters

- 1;
- 2;
- 3;
- 4;
- 5.

The State

- 1;
- 2;
- 3;
- 4;
- 5.

A.1.4 Willingness to adapt to climate change

Question No. 8 What are good practices for adaptation? (Choose max 3 options)

- Waste sorting
- Improve the quality of weather warnings
- Sewer maintenance
- Avoid wasting water
- Build infrastructures that help to avoid flooding
- Production and use of energy from renewable sources

Question No. 9 Your municipality is investing funds for the construction of a new parking and decides to spend 10% more for make it with pervious materials that allow stormwater retention and therefore reduce urban flooding. What do you think about that?

- It's well-spent money, the Municipality has done a good thing;
- I understand the reason, but there are other priorities to invest in;
- It seems absurd to me; it is an unjustified increase of public expenditures;
- Indifferent.

Question No. 10 In building or renovating your home would you be willing to spend more to introduce more green areas and less asphalted surfaces to better adapt to climate change?

- Absolutely yes;
- Maybe, as I have other priorities;
- No.

A.2 Comparative boxplot

Below are reported comparative boxplots between the maximum values simulated by the RCM models and the data actually recorded in the others 13 stations in Sicily.

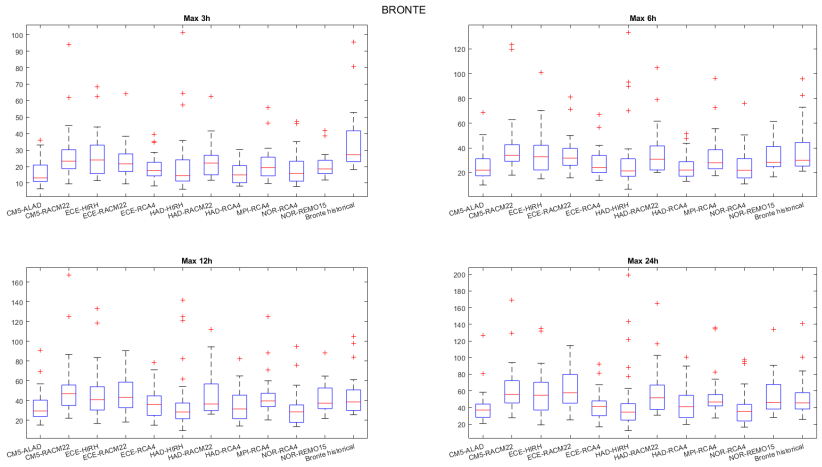

FIGURE A.1 Comparative boxplot at 3 - 6 - 12 - 24 hours for Bronte station

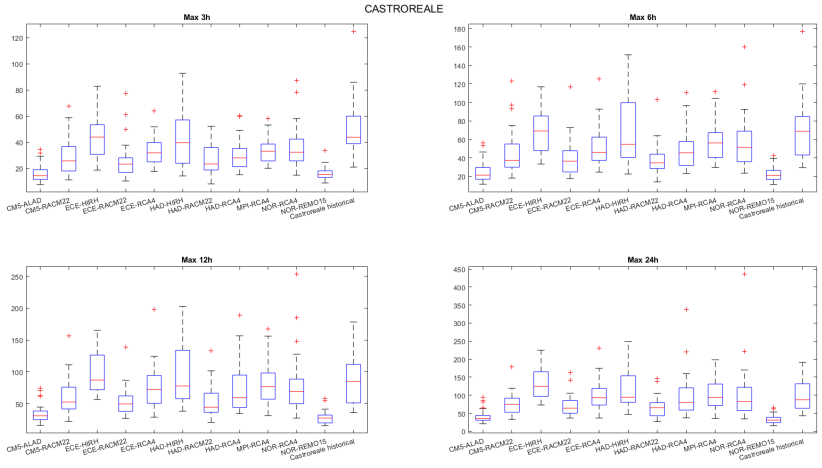

FIGURE A.2 Comparative boxplot at 3 - 6 - 12 - 24 hours for Castroreale station

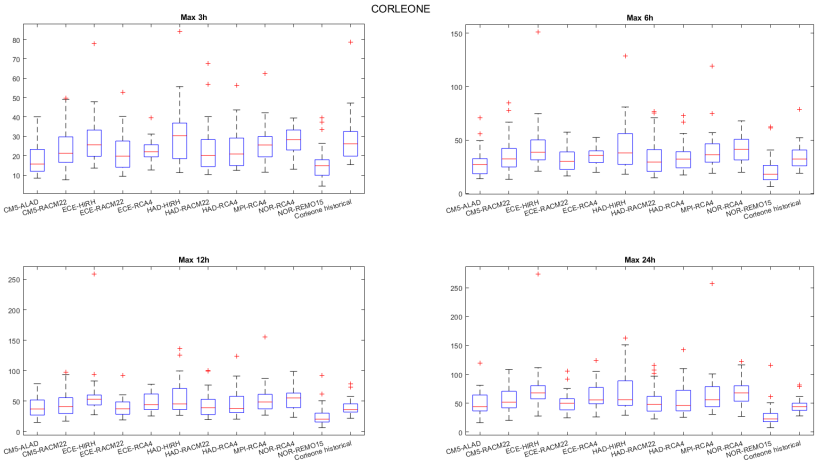

FIGURE A.3 Comparative boxplot at 3 - 6 - 12 - 24 hours for Corleone station

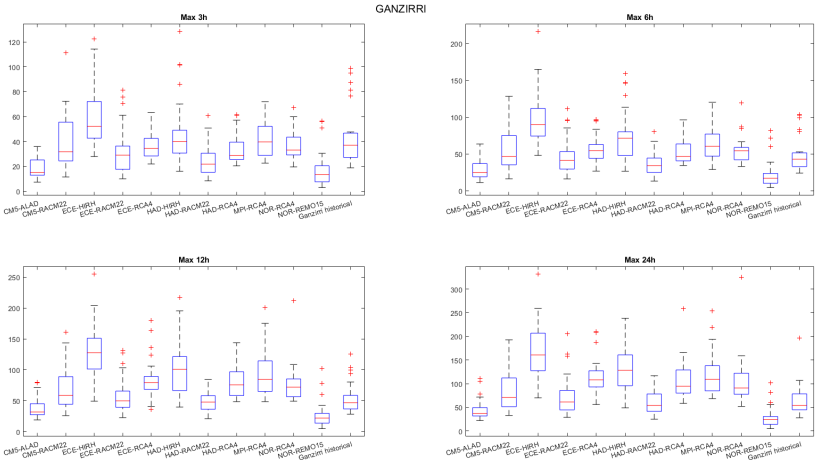

FIGURE A.4 Comparative boxplot at 3 - 6 - 12 - 24 hours for Ganzirri station

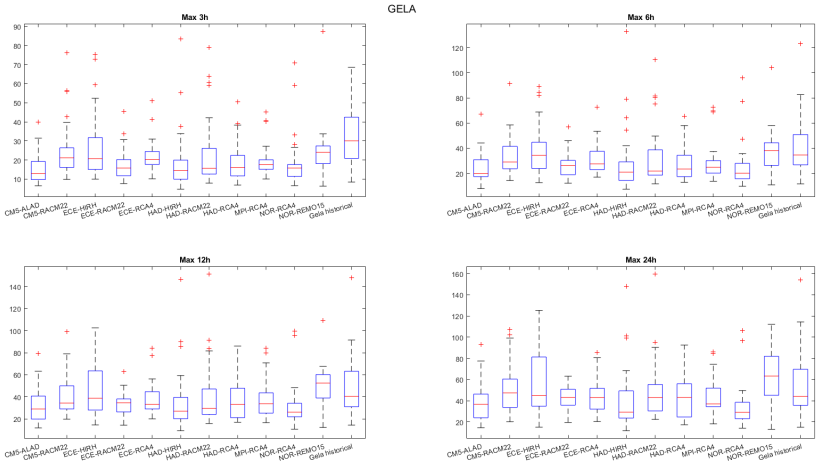

FIGURE A.5 Comparative boxplot at 3 - 6 - 12 - 24 hours for Gela station

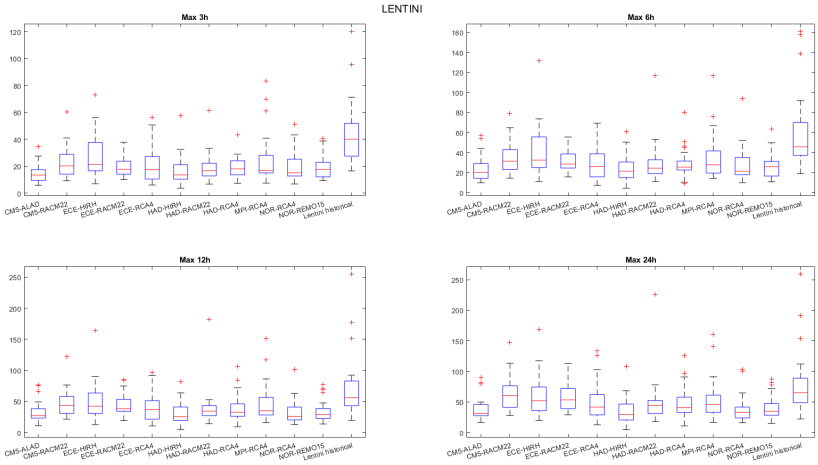

FIGURE A.6 Comparative boxplot at 3 - 6 - 12 - 24 hours for Lentini station

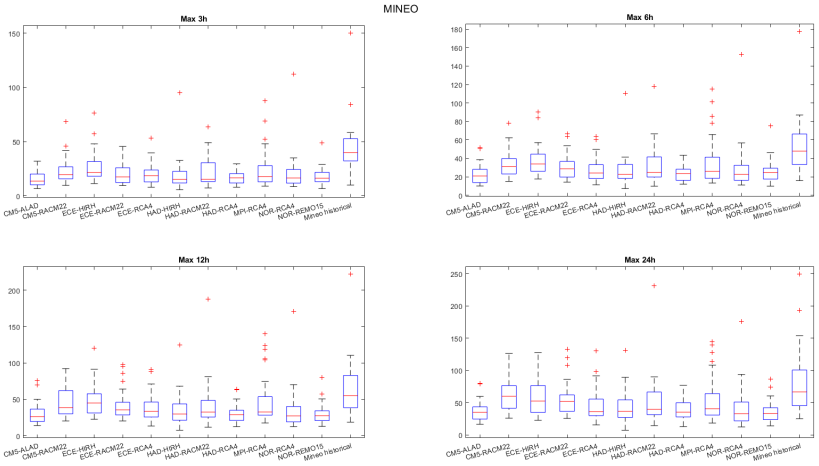

FIGURE A.7 Comparative boxplot at 3 - 6 - 12 - 24 hours for Mineo station

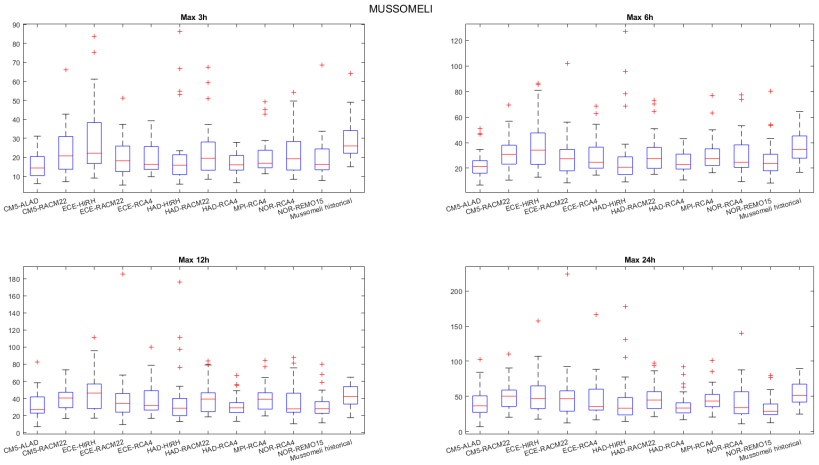

FIGURE A.8 Comparative boxplot at 3 - 6 - 12 - 24 hours for Mussomeli station

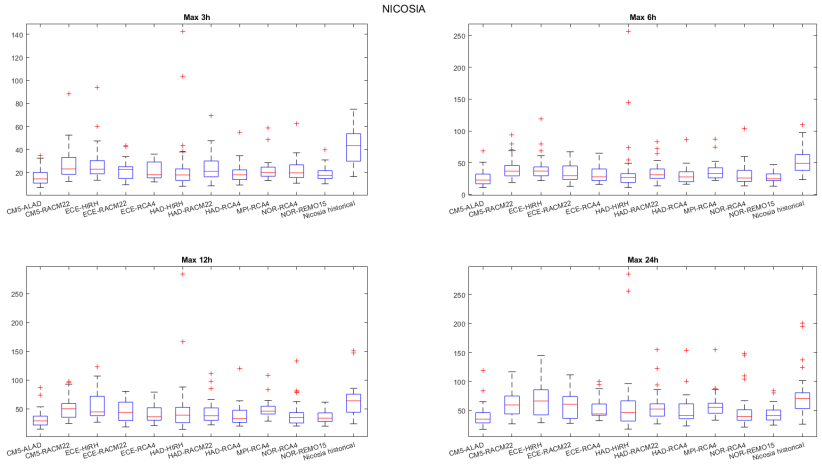

FIGURE A.9 Comparative boxplot at 3 - 6 - 12 - 24 hours for Nicosia station

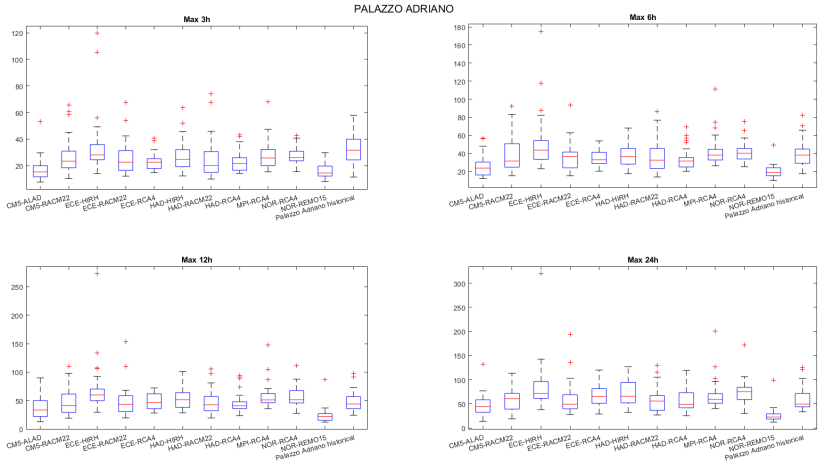

FIGURE A.10 Comparative boxplot at 3 - 6 - 12 - 24 hours for Palazzo Adriano station

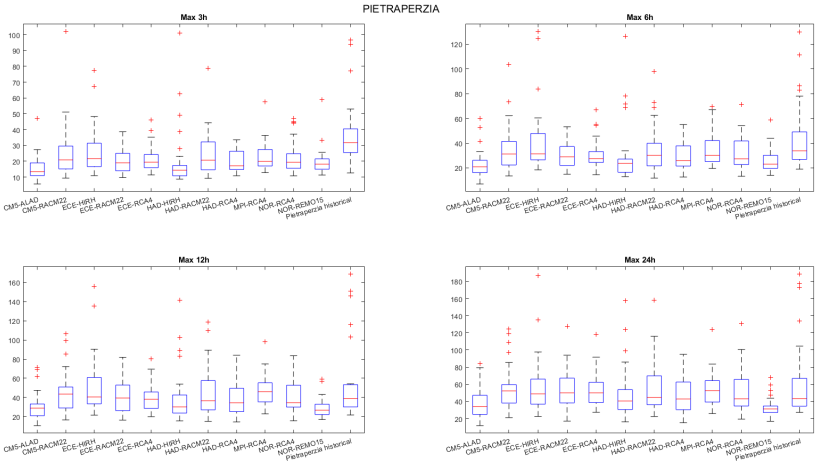

FIGURE A.11 Comparative boxplot at 3 - 6 - 12 - 24 hours for Pietraperzia station

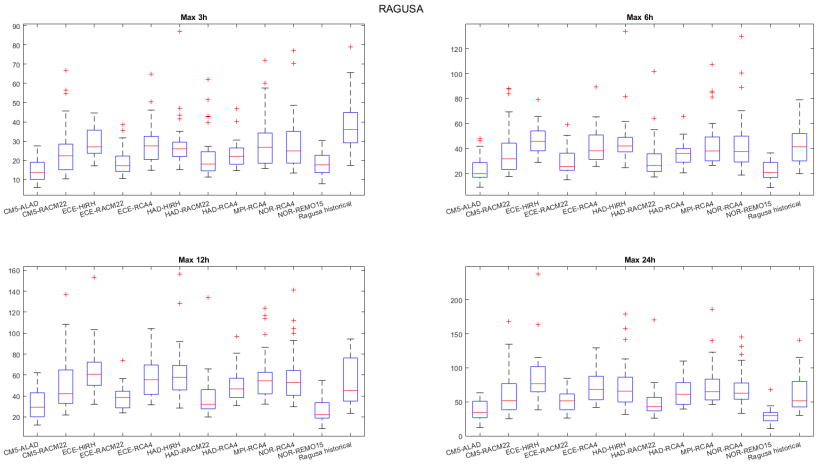

FIGURE A.12 Comparative boxplot at 3 - 6 - 12 - 24 hours for Ragusa station

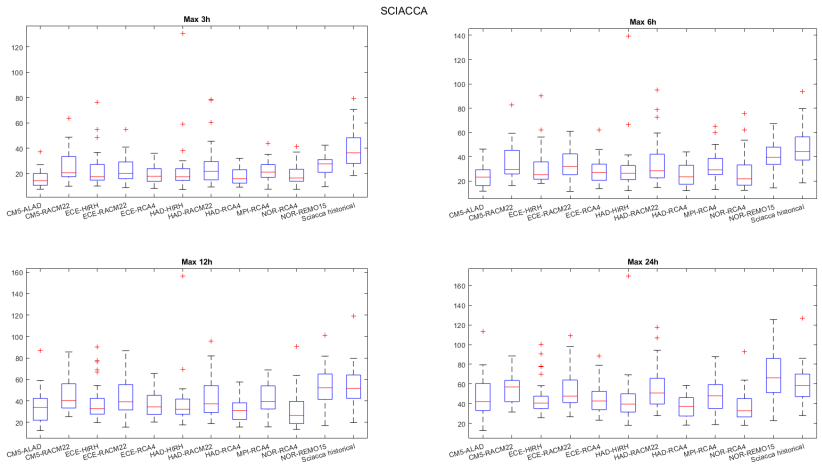

FIGURE A.13 Comparative boxplot at 3 - 6 - 12 - 24 hours for Sciacca station

A.3 Mean annual maxima

Below are reported comparative graphs between the mean annual maxima recorded in the 13 stations station, in addition to Catania station, with those of the RCM models.

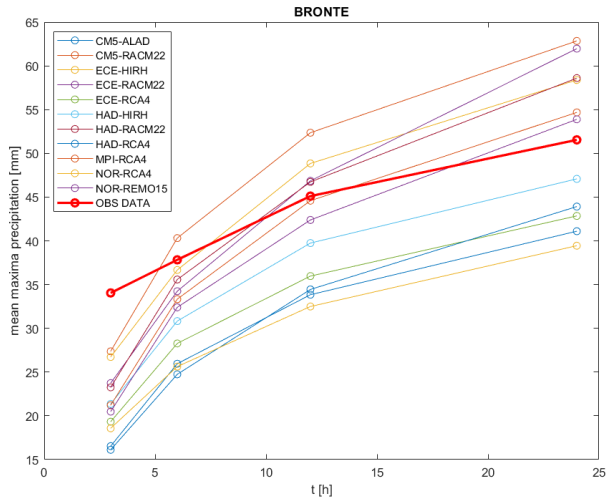

FIGURE A.14 Comparison between the annual maximums recorded in the Bronte station with those of the RCM models

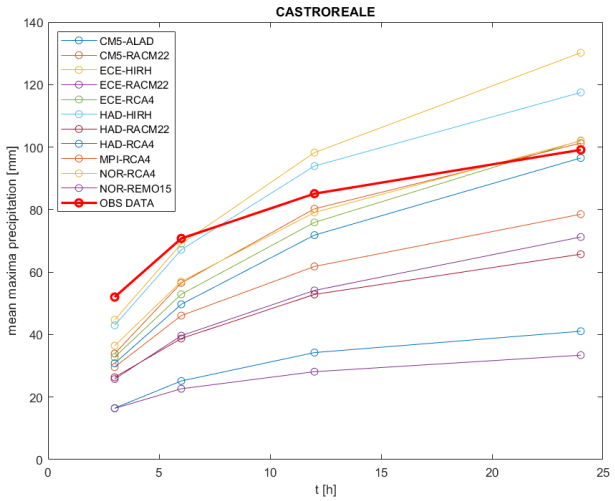

FIGURE A.15 Comparison between the annual maximums recorded in the Castroreale station with those of the RCM models

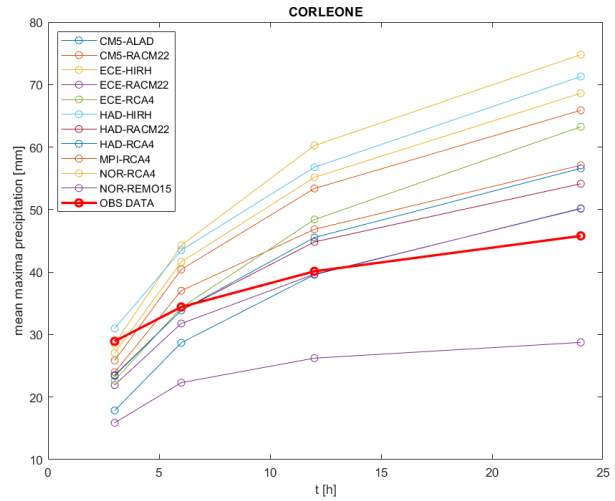

FIGURE A.16 Comparison between the annual maximums recorded in the Corleone station with those of the RCM models

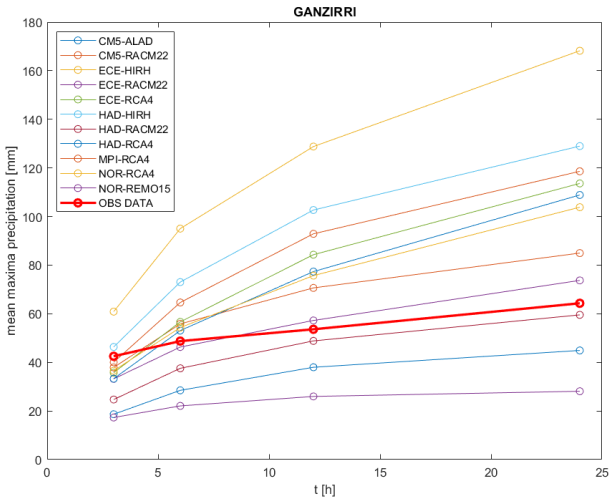

FIGURE A.17 Comparison between the annual maximums recorded in the Ganzirri station with those of the RCM models

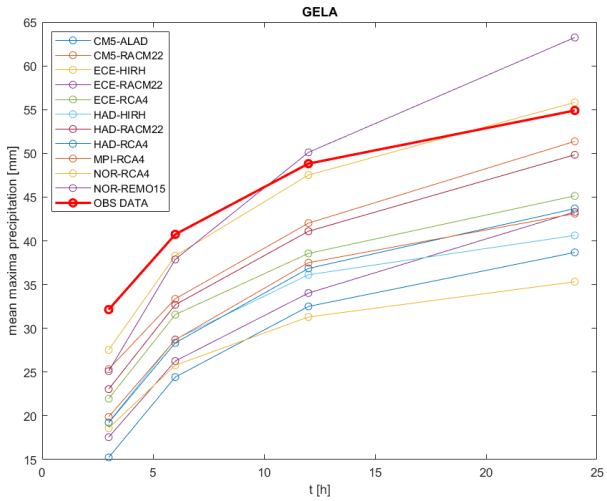

FIGURE A.18 Comparison between the annual maximums recorded in the Gela station with those of the RCM models

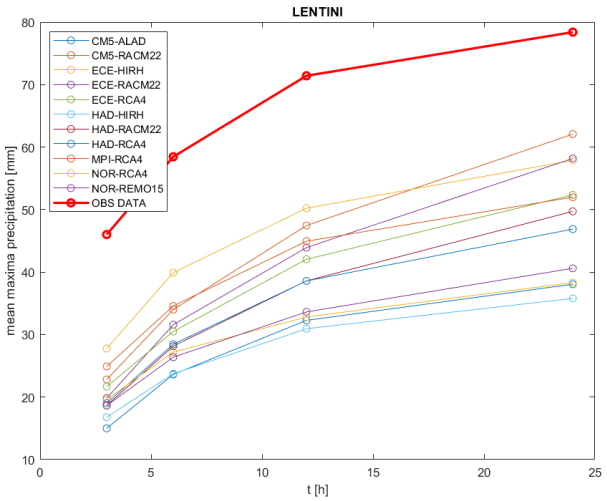

FIGURE A.19 Comparison between the annual maximums recorded in the Lentini station with those of the RCM models

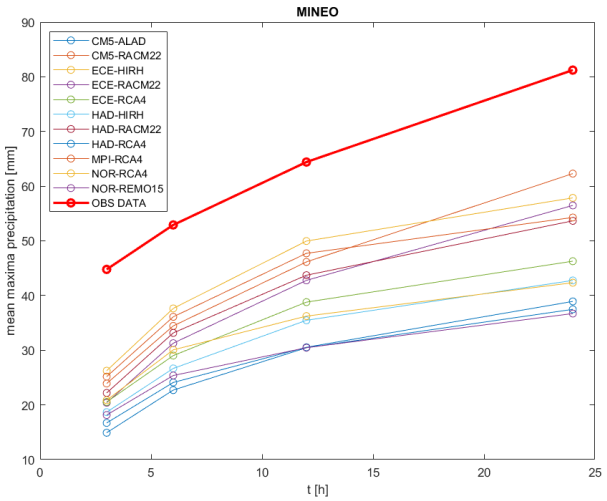

FIGURE A.20 Comparison between the annual maximums recorded in the Mineo station with those of the RCM models

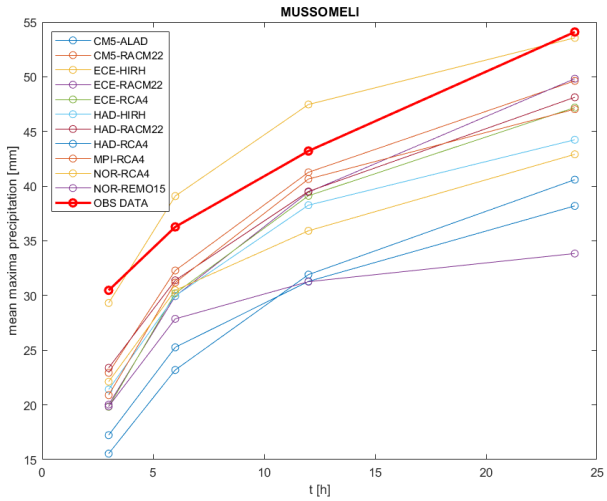

FIGURE A.21 Comparison between the annual maximums recorded in the Mussomeli station with those of the RCM models

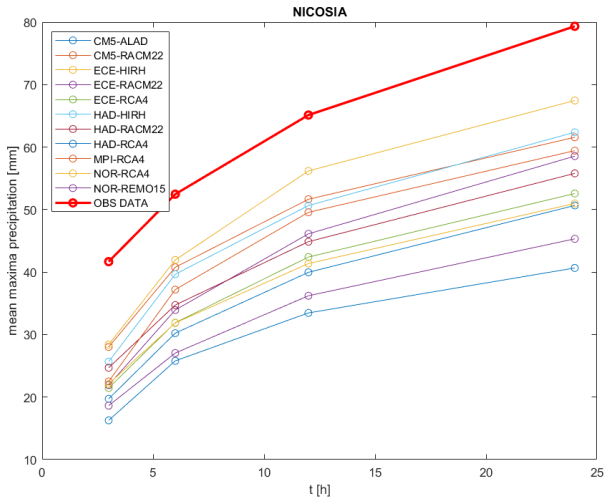

FIGURE A.22 Comparison between the annual maximums recorded in the Nicosia station with those of the RCM models

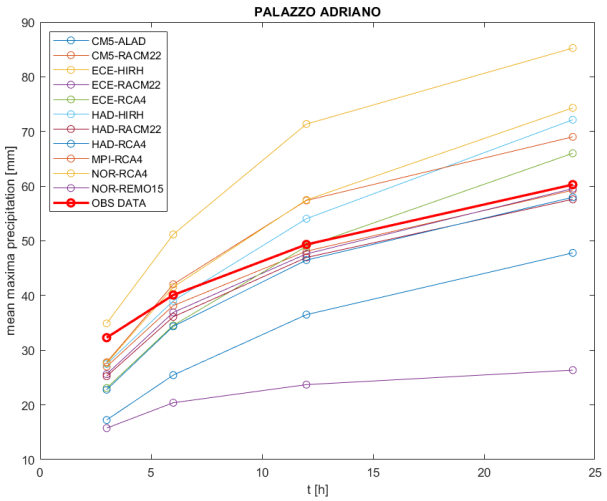

FIGURE A.23 Comparison between the annual maximums recorded in the Palazzo Adriano station with those of the RCM models

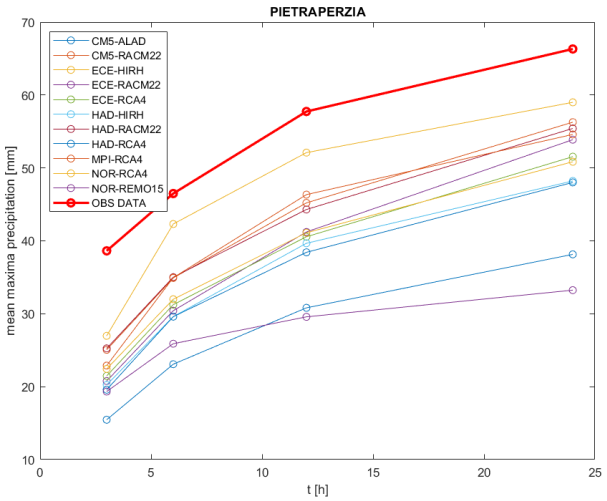

FIGURE A.24 Comparison between the annual maximums recorded in the Pietraperzia station with those of the RCM models

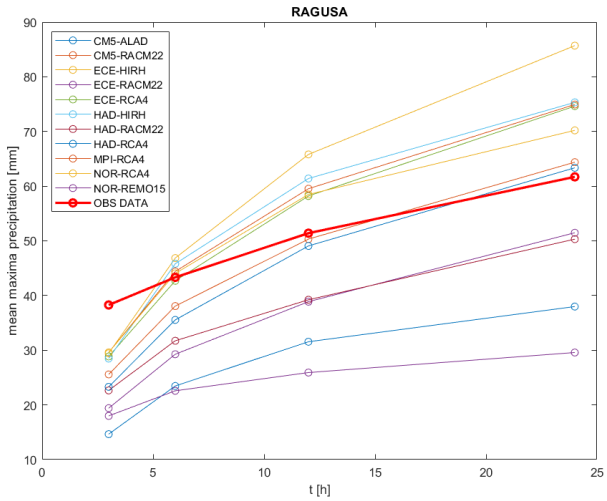

FIGURE A.25 Comparison between the annual maximums recorded in the Ragusa station with those of the RCM models

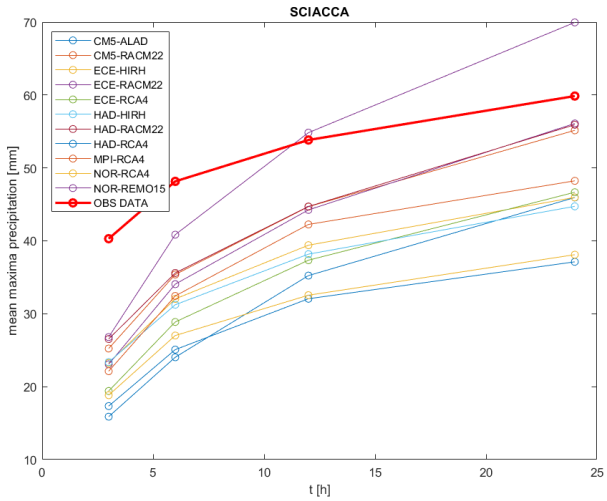

FIGURE A.26 Comparison between the annual maximums recorded in the Sciacca station with those of the RCM models

A.4 IDF curves

Below are reported graphs of the IDF curves obtained with the scale-invariant method obtained for the other stations using distributions: Gumbel, GEV and Log-norm.

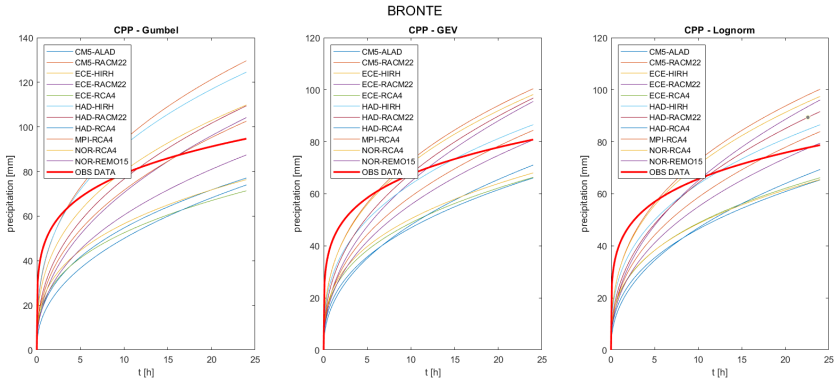

FIGURE A.27 IDF curves for Bronte station - TR = 10 years

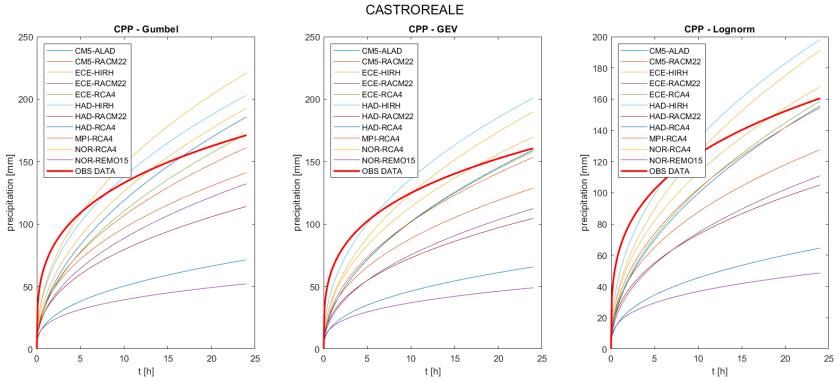

FIGURE A.28 IDF curves for Castroreale station - TR = 10 years

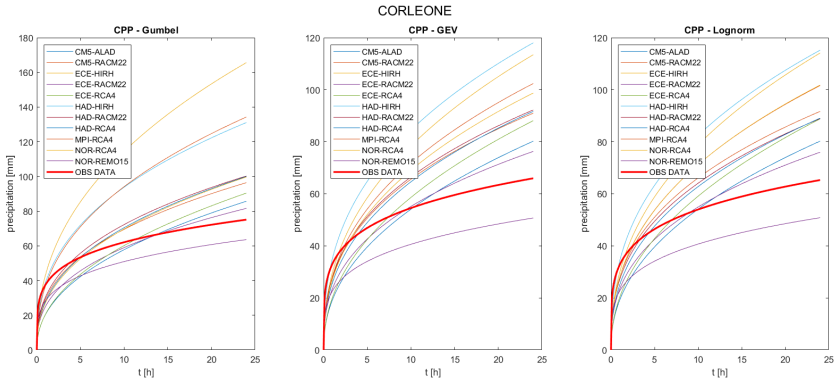

FIGURE A.29 IDF curves for Corleone station - TR = 10 years

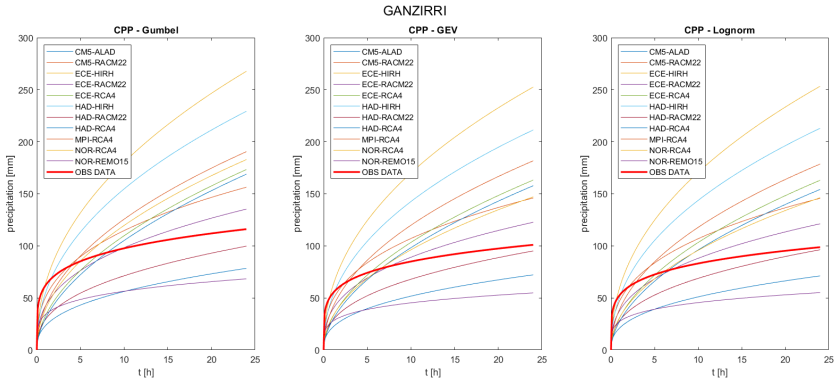

FIGURE A.30 IDF curves for Ganzirri station - TR = 10 years

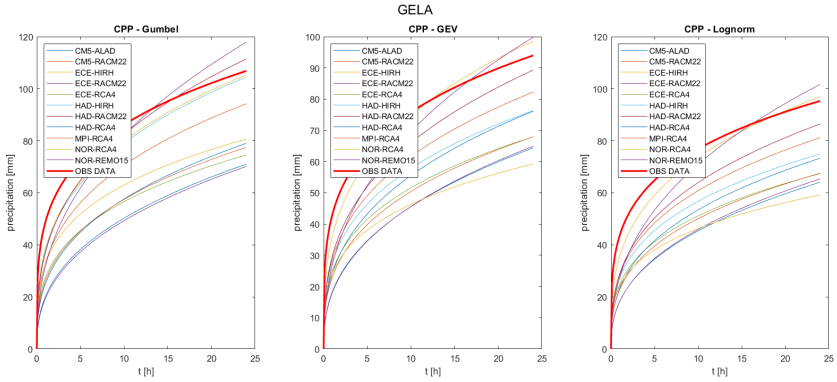

FIGURE A.31 IDF curves for Gela station - TR = 10 years

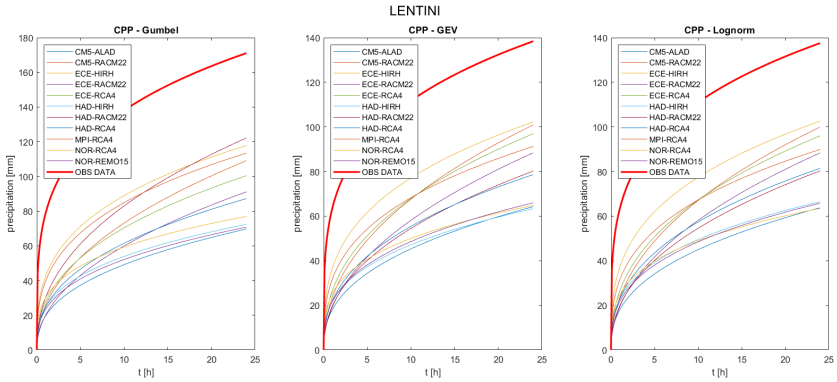

FIGURE A.32 IDF curves for Lentini station - TR = 10 years

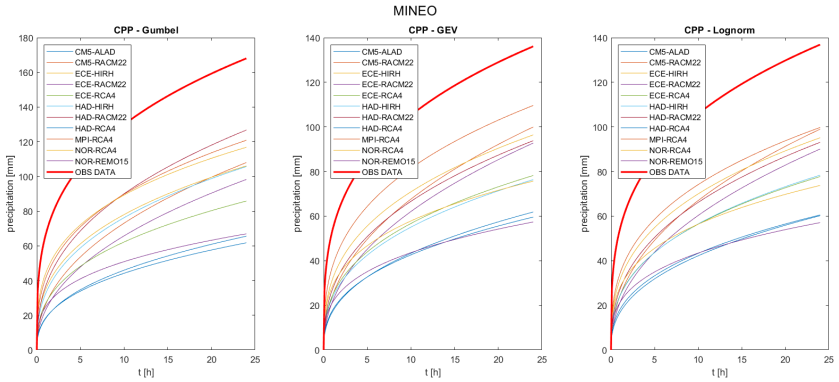

FIGURE A.33 IDF curves for Mineo station - TR = 10 years

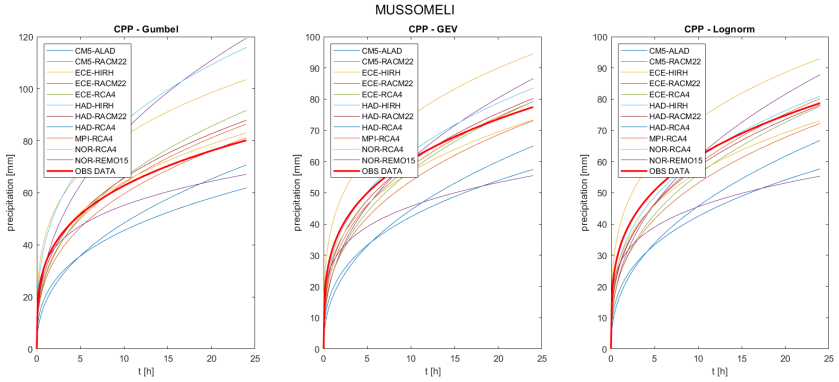

FIGURE A.34 IDF curves for Mussomeli station - TR = 10 years

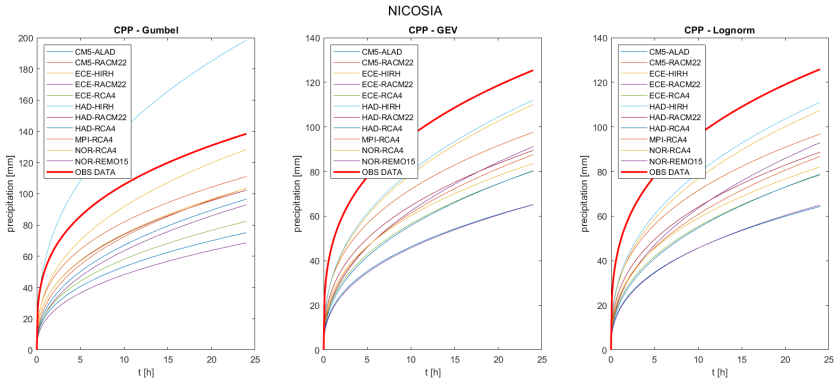

FIGURE A.35 IDF curves for Nicosia station - TR = 10 years

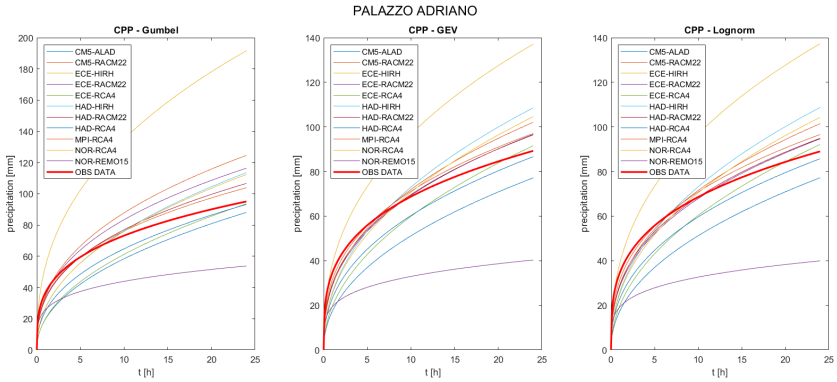

FIGURE A.36 IDF curves for Palazzo Adriano station - TR = 10 years

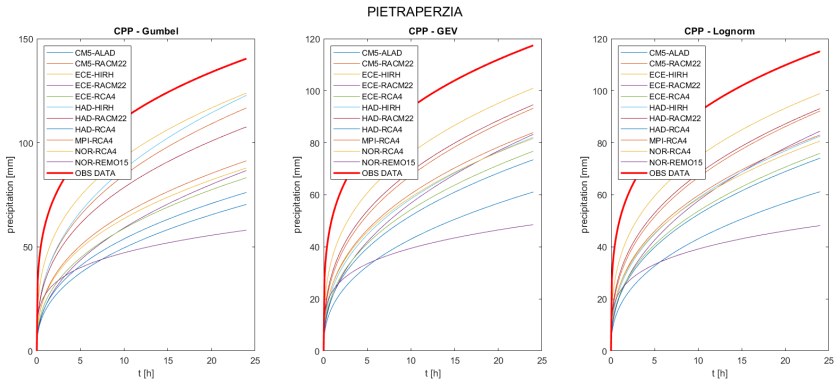

FIGURE A.37 IDF curves for Pietraperzia station - TR = 10 years

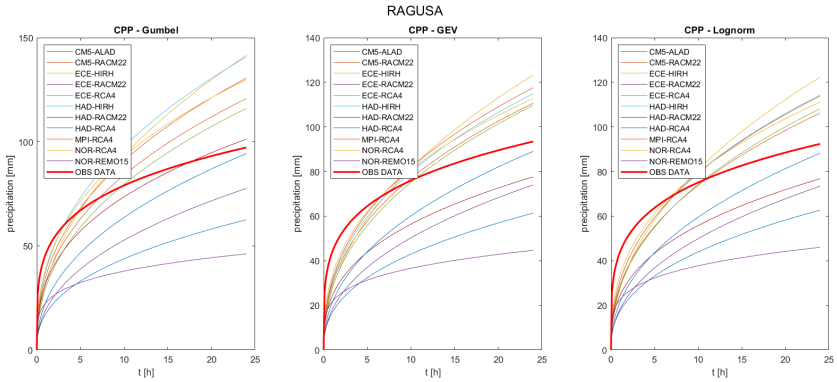

FIGURE A.38 IDF curves for Ragusa station - TR = 10 years

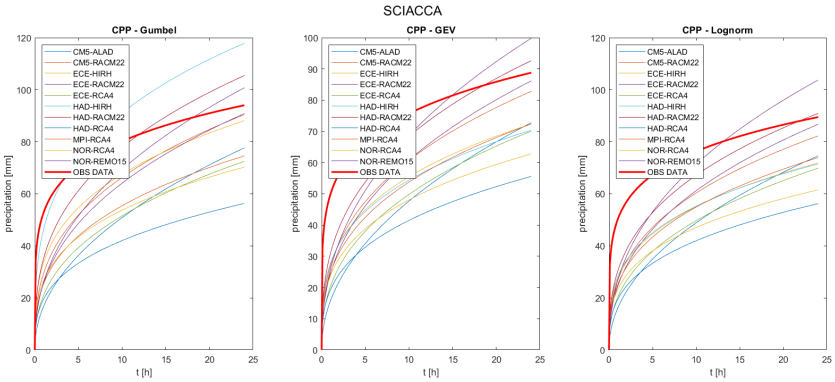

FIGURE A.39 IDF curves for Sciacca station - TR = 10 years

A.5 Bias correction for rainfall data

In the following figure is shown the graph for the 11 RCM models in the scenario RCP 4.5 2021-2050 with a comparison between annual and seasonal correction for rainfall data.

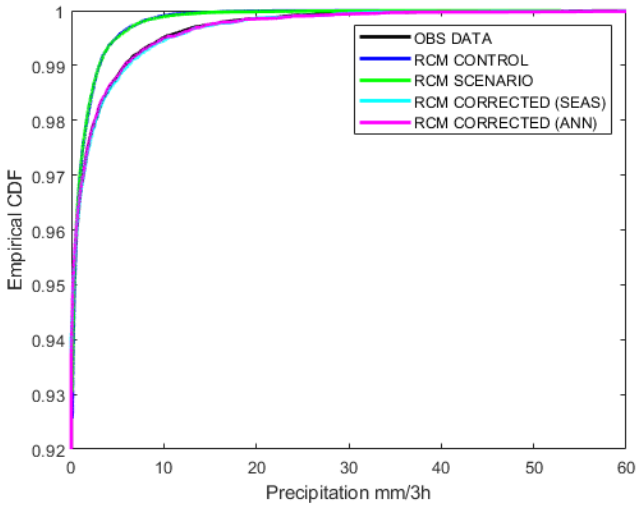

FIGURE A.40 Application of bias correction for the model CM5 ALAD with comparison between annual and seasonal window

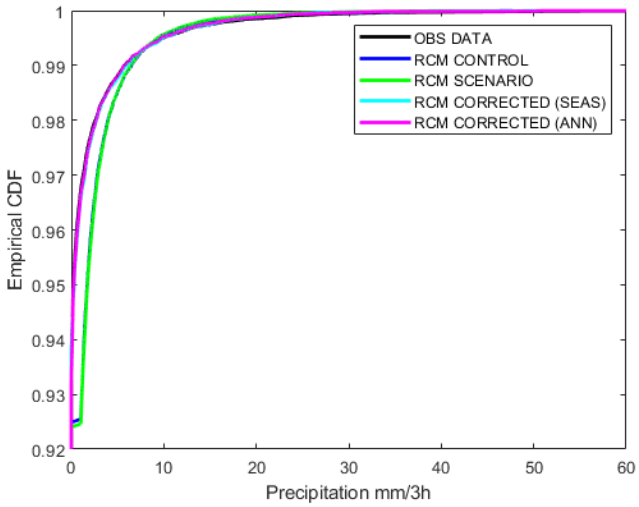

FIGURE A.41 Application of bias correction for the model CM5 RACM22 with comparison between annual and seasonal window

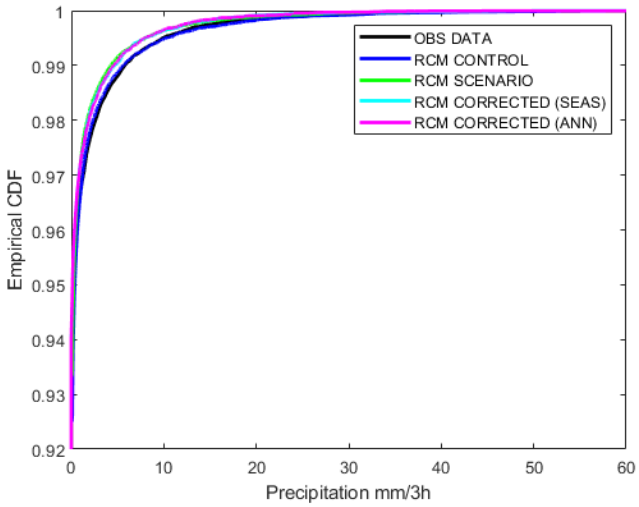

FIGURE A.42 Application of bias correction for the model ECE HIRH with comparison between annual and seasonal window

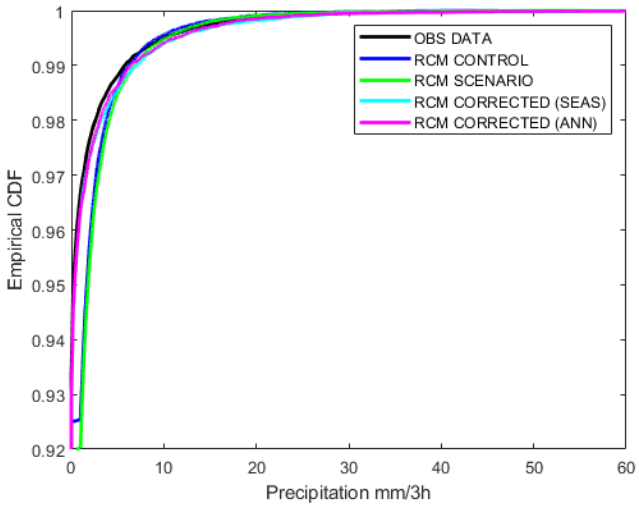

FIGURE A.43 Application of bias correction for the model ECE RACM22 with comparison between annual and seasonal window

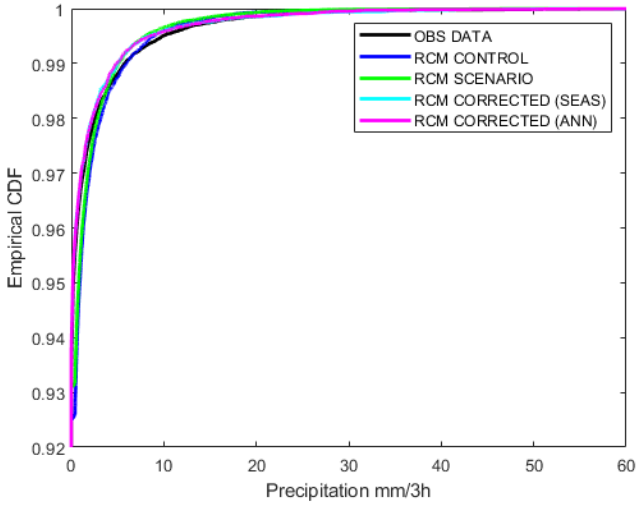

FIGURE A.44 Application of bias correction for the model ECE RCA4 with comparison between annual and seasonal window

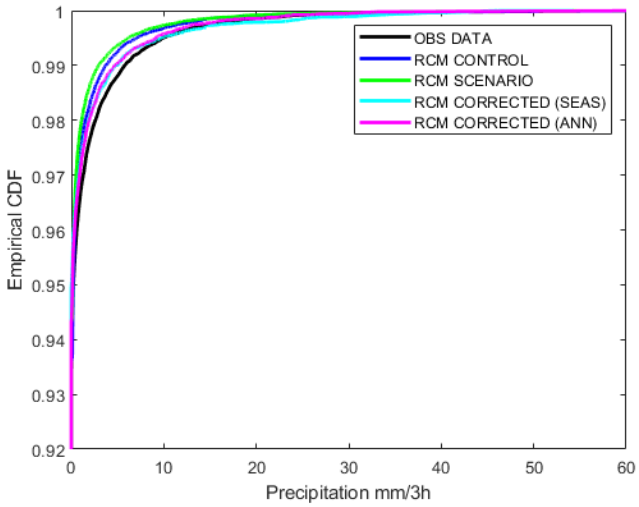

FIGURE A.45 Application of bias correction for the model HAD HIRH with comparison between annual and seasonal window

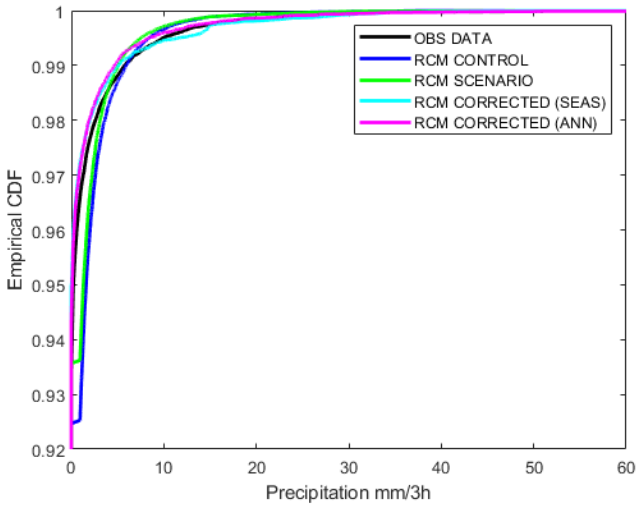

FIGURE A.46 Application of bias correction for the model HAD RACM22 with comparison between annual and seasonal window

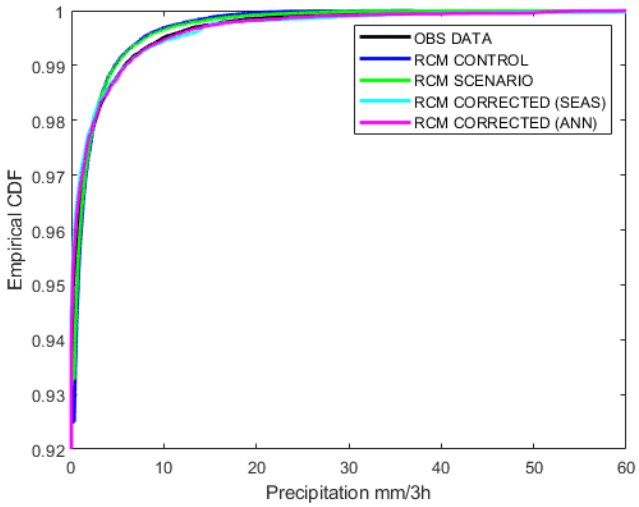

FIGURE A.47 Application of bias correction for the model HAD RCA4 with comparison between annual and seasonal window

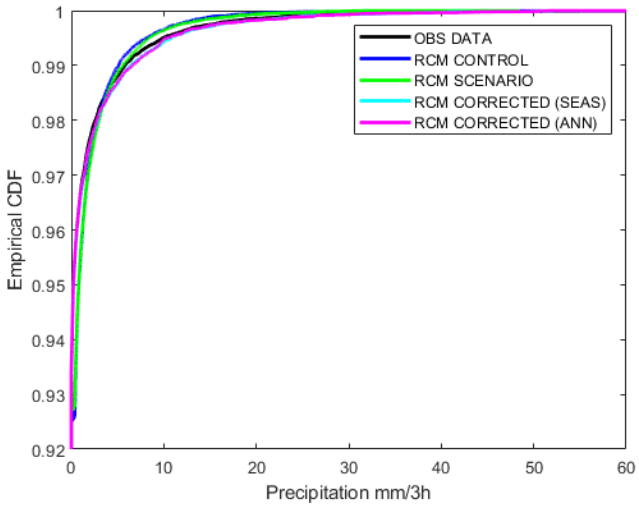

FIGURE A.48 Application of bias correction for the model MPI RCA4 with comparison between annual and seasonal window

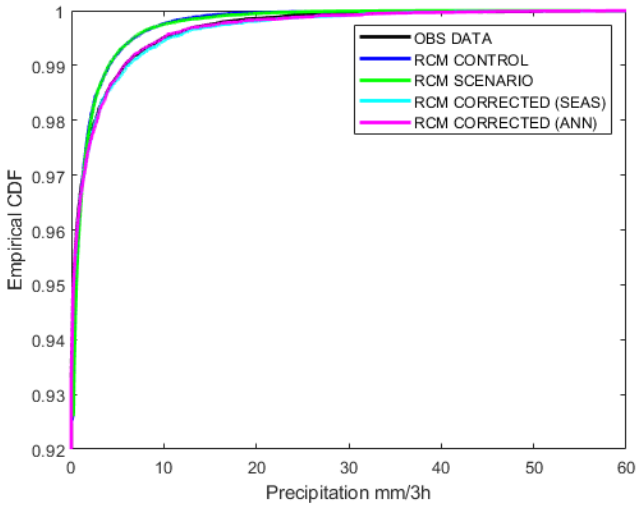

FIGURE A.49 Application of bias correction for the model NOR RCA4 with comparison between annual and seasonal window

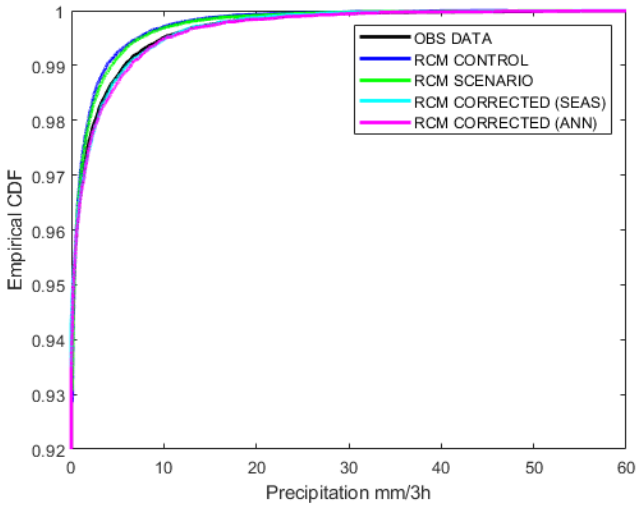

FIGURE A.50 Application of bias correction for the model NOR REMO15 with comparison between annual and seasonal window

A.6 Bias correction for temperature data

In the following figure is shown the graph for the 11 RCM models in the scenario RCP 4.5 2021-2050 with a comparison between annual and seasonal correction for temperature data.

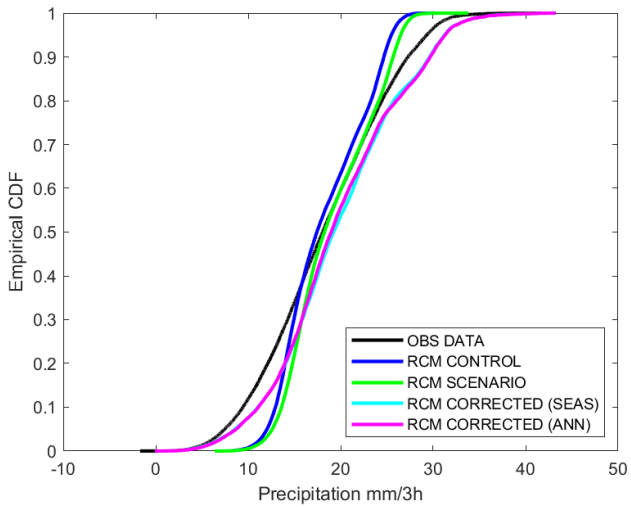

FIGURE A.51 Application of bias correction for the model CM5 ALAD with comparison between annual and seasonal window

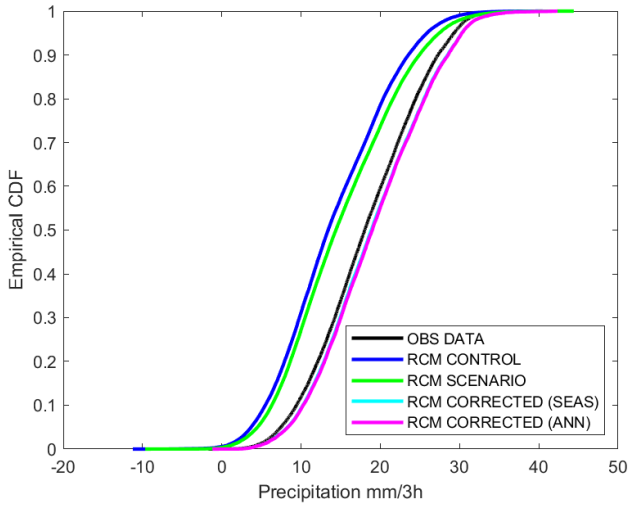

FIGURE A.52 Application of bias correction for the model CM5 RACM22 with comparison between annual and seasonal window

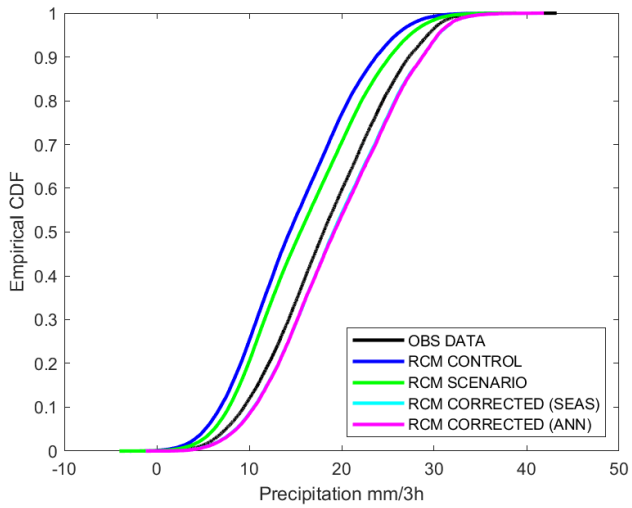

FIGURE A.53 Application of bias correction for the model ECE HIRH with comparison between annual and seasonal window

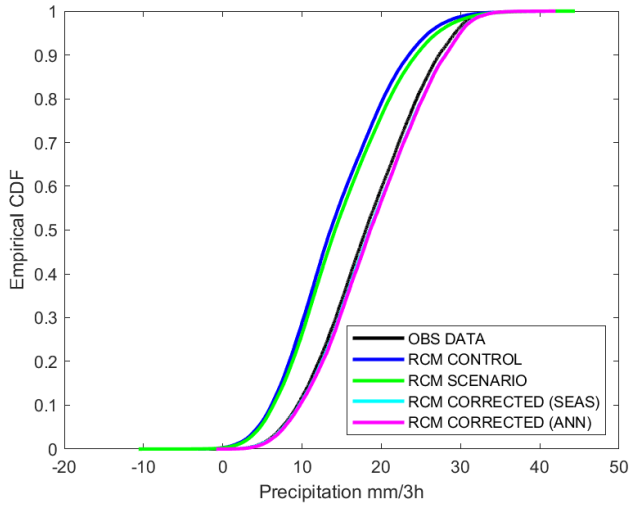

FIGURE A.54 Application of bias correction for the model ECE RACM22 with comparison between annual and seasonal window

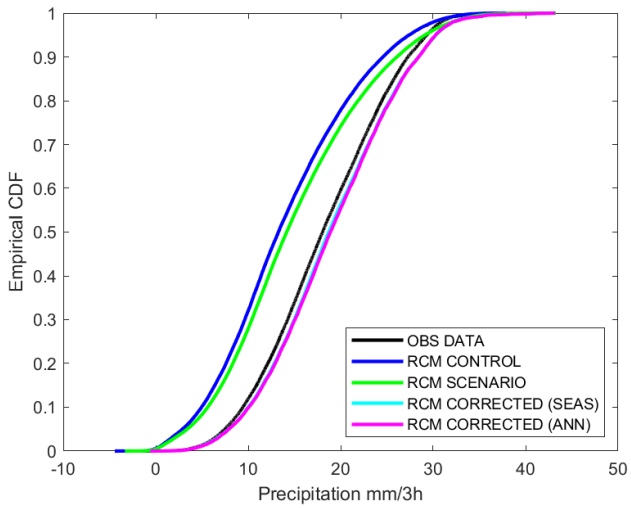

FIGURE A.55 Application of bias correction for the model ECE RCA4 with comparison between annual and seasonal window

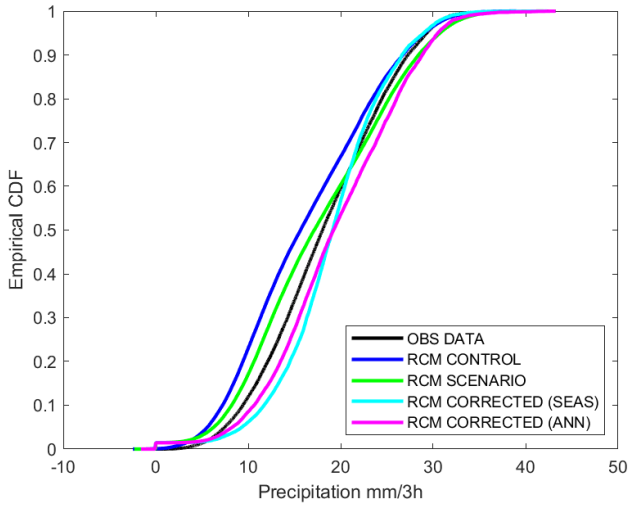

FIGURE A.56 Application of bias correction for the model HAD HIRH with comparison between annual and seasonal window

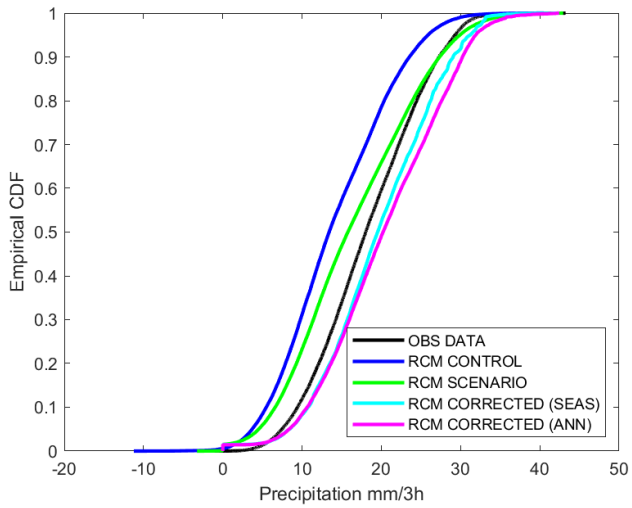

FIGURE A.57 Application of bias correction for the model HAD RACM22 with comparison between annual and seasonal window

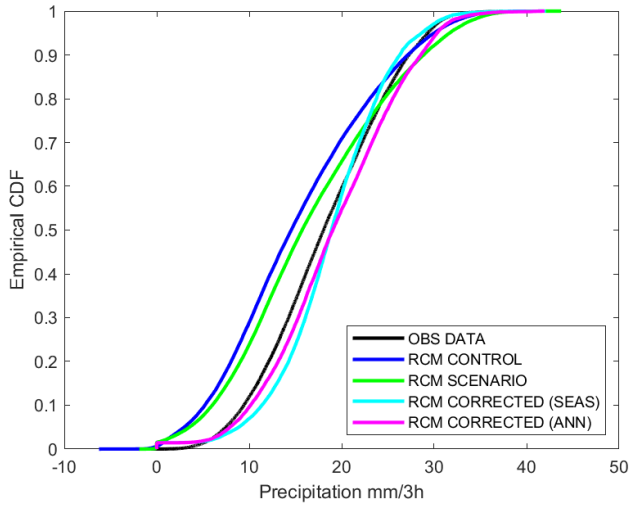

FIGURE A.58 Application of bias correction for the model HAD RCA4 with comparison between annual and seasonal window

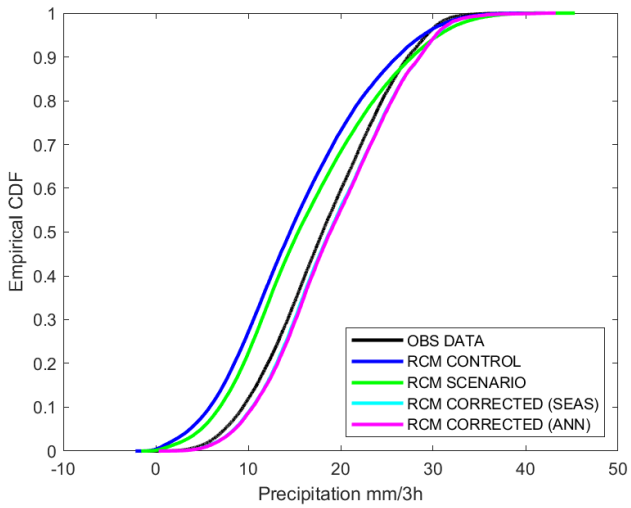

FIGURE A.59 Application of bias correction for the model MPI RCA4 with comparison between annual and seasonal window

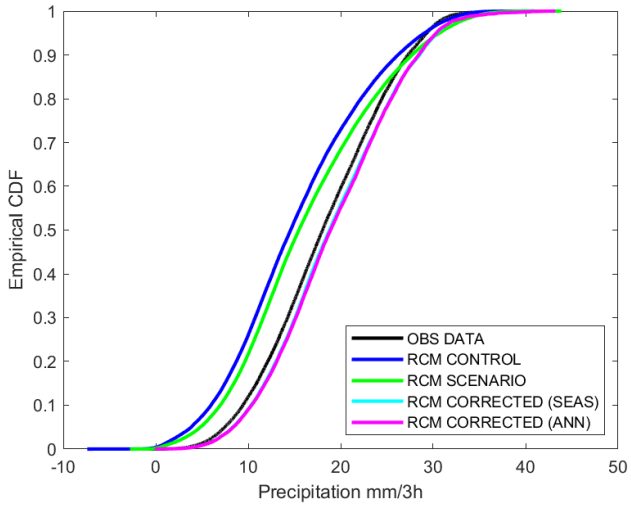

FIGURE A.60 Application of bias correction for the model NOR RCA4 with comparison between annual and seasonal window

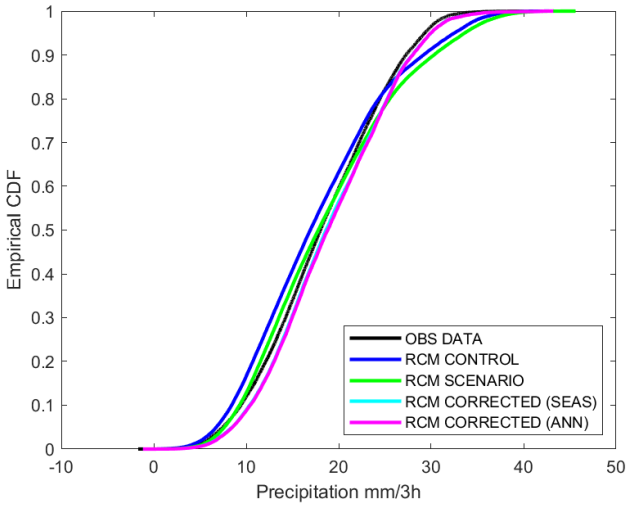

FIGURE A.61 Application of bias correction for the model NOR REMO15 with comparison between annual and seasonal window

Bibliography

Ahiablame, Laurent M., Bernard A. Engel, and Indrajeet Chaubey (2013). "Effectiveness of low impact development practices in two urbanized watersheds: Retrofitting with rain barrel/cistern and porous pavement". In: *Journal of Environmental Management* 119, pp. 151–161. DOI: 10.1016/j.jenvman.2013.01.019. URL: http://dx.doi.org/10.1016/j.jenvman.2013.01.019.

Akerlof, Karen et al. (2013). "Do people "personally experience" global warming, and if so how, and does it matter?" In: *Global Environmental Change* 23.1, pp. 81–91. DOI: 10.1016/j.gloenvcha.2012.07.006. URL: http://dx.doi.org/10.1016/j.gloenvcha.2012.07.006.

Arnbjerg-Nielsen, K. (Sept. 2006). "Significant climate change of extreme rainfall in Denmark". In: *Water Science and Technology* 54.6-7, pp. 1–8. ISSN: 0273-1223. DOI: 10.2166/wst.2006.572. eprint: https://iwaponline.com/wst/article-pdf/54/6-7/1/431297/1.pdf. URL: https://doi.org/10.2166/wst.2006.572.

Arnell, Nigel et al. (Jan. 2001). "Climate Change 2001: impacts, adaptation and vulnerability". In: *Chapter 4 Hydrology and Water Resources*, pp. 193–233.

Avvisati, Gala et al. (2019). "Perception of risk for natural hazards in Campania Region (Southern Italy)". In: *International Journal of Disaster Risk Reduction* 40.April, p. 101164. DOI: 10.1016/j.ijdrr.2019.101164. URL: https://doi.org/10.1016/j.ijdrr.2019.101164.

Ballew, Matthew T. et al. (2019). "Climate change in the american mind: Data, tools, and trends". In: *Environment* 61.3, pp. 4–18. DOI: 10.1080/00139157.2019.1589300.

Bartesaghi Koc, Carlos, Paul Osmond, and Alan Peters (2017). "Towards a comprehensive green infrastructure typology: a systematic review of approaches, methods and typologies". In: *Urban Ecosystems* 20.1,

pp. 15–35. DOI: 10.1007/s11252-016-0578-5. URL: http://dx.doi.org/10.1007/s11252-016-0578-5.

Bell, Colin D. et al. (2016). "Hydrologic response to stormwater control measures in urban watersheds". In: *Journal of Hydrology* 541, pp. 1488–1500. DOI: 10.1016/j.jhydrol.2016.08.049. URL: http://dx.doi.org/10.1016/j.jhydrol.2016.08.049.

Berndtsson, Justyna Czemiel, Tobias Emilsson, and Lars Bengtsson (2006). "The influence of extensive vegetated roofs on runoff water quality". In: *Science of the Total Environment* 355.1-3, pp. 48–63. DOI: 10.1016/j.scitotenv.2005.02.035.

Berndtsson, R. et al. (2019). "Drivers of changing urban flood risk: A framework for action". In: *Journal of Environmental Management* 240.October 2018, pp. 47–56. DOI: 10.1016/j.jenvman.2019.03.094. URL: https://doi.org/10.1016/j.jenvman.2019.03.094.

Besir, Ahmet B. and Erdem Cuce (2018). "Green roofs and facades: A comprehensive review". In: *Renewable and Sustainable Energy Reviews* 82.July 2017, pp. 915–939. DOI: 10.1016/j.rser.2017.09.106.

Bledsoe, Brian P. and Chester C. Watson (2001). "Effects of urbanization on channel instability". In: *Journal of the American Water Resources Association* 37.2, pp. 255–270. DOI: 10.1111/j.1752-1688.2001.tb00966.x.

Bonaccorso, B., A. Cancelliere, and G. Rossi (2012). "Methods for Drought Analysis and Forecasting". In: *Methods and Applications of Statistics in the Atmospheric and Earth Sciences. p., Hoboken, John and Sons, ISBN: 9780470503447*, pp. 150–184.

Bonaccorso, B. et al. (2003). "Spatial variability of drought: An analysis of the SPI in Sicily". In: *Water Resources Management* 17.4, pp. 273–296. ISSN: 09204741. DOI: 10.1023/A:1024716530289.

Bonaccorso, Brunella, Antonino Cancelliere, and Giuseppe Rossi (2015). "Probabilistic forecasting of drought class transitions in Sicily (Italy) using Standardized Precipitation Index and North Atlantic Oscillation Index". In: *Journal of Hydrology* 526. Drought processes, modeling, and mitigation, pp. 136–150. ISSN: 0022-1694. DOI: https://doi.org/10.1016/j.jhydrol.2015.01.070. URL: https://www.sciencedirect.com/science/article/pii/S0022169415000888.

Bonaccorso, Brunella et al. (2015). "SPI-Based Probabilistic Analysis of Drought Areal Extent in Sicily". In: *Water Resources Management* 29.2, pp. 459–470. ISSN: 15731650. DOI: 10.1007/s11269-014-0673-4.

Bordi, Isabella and Alfonso Sutera (Aug. 2001). "Fifty Years of Precipitation: Some Spatially Remote Teleconnections". In: *Water Resources Management* 15, pp. 247–280. DOI: 10.1023/A:1013353822381.

Bouman, Thijs et al. (2020). "When worry about climate change leads to climate action: How values, worry and personal responsibility relate to various climate actions". In: *Global Environmental Change* 62, p. 102061. DOI: 10.1016/j.gloenvcha.2020.102061.

Breznitz, S. (1984). "Cry Wolf". In: *New York: Psychology Press*. URL: https://doi.org/10.4324/9780203781203.

Brody, Samuel D et al. (2007). "Examining the Relationship Between Physical Vulnerability and Public Perceptions of Global Climate Change in the United States". In: *Environment and Behavior* 40.1, pp. 72–95. DOI: 10.1177/0013916506298800. URL: https://doi.org/10.1177/0013916506298800.

Bubeck, P., W. J.W. Botzen, and J. C.J.H. Aerts (2012). "A Review of Risk Perceptions and Other Factors that Influence Flood Mitigation Behavior". In: *Risk Analysis* 32.9, pp. 1481–1495. DOI: 10.1111/j.1539-6924.2011.01783.x.

Cancelliere, Antonino and Jose D. Salas (2004). "Drought length properties for periodic-stochastic hydrologic data". In: *Water Resources Research* 40.2. DOI: https://doi.org/10.1029/2002WR001750. eprint: https://agupubs.onlinelibrary.wiley.com/doi/pdf/10.1029/2002WR001750. URL: https://agupubs.onlinelibrary.wiley.com/doi/abs/10.1029/2002WR001750.

— (2010). "Drought probabilities and return period for annual streamflows series". In: *Journal of Hydrology* 391.1, pp. 77–89. ISSN: 0022-1694. DOI: https://doi.org/10.1016/j.jhydrol.2010.07.008. URL: https://www.sciencedirect.com/science/article/pii/S002216941000421X.

Capstick, Stuart B. et al. (2016). "Public understanding in Great Britain of ocean acidification". In: *Nature Climate Change* 6.8, pp. 763–767. DOI: 10.1038/nclimate3005.

Carson, T. B. et al. (2013). "Hydrological performance of extensive green roofs in New York City: Observations and multi-year modeling of three full-scale systems". In: *Environmental Research Letters* 8.2. DOI: 10.1088/1748-9326/8/2/024036.

Carter, Jeremy G. et al. (2017). "Adapting cities to climate change: exploring the role of green infrastructure". In: *Journal of Environmental Planning and Management*.

Chen, Jingqiu et al. (2017). "Urbanization impacts on surface runoff of the contiguous United States". In: *Journal of Environmental Management* 187, pp. 470–481. DOI: 10.1016/j.jenvman.2016.11.017. URL: http://dx.doi.org/10.1016/j.jenvman.2016.11.017.

Christensen, Jens H. et al. (2008). "On the need for bias correction of regional climate change projections of temperature and precipitation". In: *Geophysical Research Letters* 35.20. DOI: https://doi.org/10.1029/2008GL035694. eprint: https://agupubs.onlinelibrary.wiley.com/doi/pdf/10.1029/2008GL035694. URL: https://agupubs.onlinelibrary.wiley.com/doi/abs/10.1029/2008GL035694.

Christensen, Jens Hesselbjerg et al. (Jan. 2013). "Climate phenomena and their relevance for future regional climate change". English. In: *Climate Change 2013 the Physical Science Basis*. Vol. 9781107057999. Publisher Copyright: © Intergovernmental Panel on Climate Change 2014. United Kingdom: Cambridge University Press, pp. 1217–1308. ISBN: 9781107057999. DOI: 10.1017/CBO9781107415324.028.

Commissione Europea (2013). "COMUNICAZIONE DELLA COMMISSIONE AL PARLAMENTO EUROPEO, AL CONSIGLIO, AL COMITATO ECONOMICO E SOCIALE EUROPEO E AL COMITATO DELLE REGIONI Infrastrutture verdi – Rafforzare il capitale naturale in Europa". In:

Cook-Patton, Susan C. and Taryn L. Bauerle (2012). "Potential benefits of plant diversity on vegetated roofs: A literature review". In: *Journal of Environmental Management* 106, pp. 85–92. ISSN: 0301-4797. DOI: https://doi.org/10.1016/j.jenvman.2012.04.003. URL: https://www.sciencedirect.com/science/article/pii/S0301479712001843.

Coumou, Dim and Stefan Rahmstorf (2012). "A decade of weather extremes". In: *Nature Climate Change* 2.7, pp. 491–496. DOI: 10.1038/nclimate1452. URL: https://doi.org/10.1038/nclimate1452.

Czemiel Berndtsson, Justyna (2010). "Green roof performance towards management of runoff water quantity and quality: A review". In: *Ecological Engineering* 36.4, pp. 351–360. DOI: 10.1016/j.ecoleng.2009.12.014. URL: http://dx.doi.org/10.1016/j.ecoleng.2009.12.014.

Davis, Matthew S., Tullio Ricci, and Lara M. Mitchell (2005). "Perceptions of risk for volcanic hazards at Vesuvio and Etna, Italy". In: *Australasian Journal of Disaster and Trauma Studies* 2005.1.

Demski, Christina et al. (2017). "Experience of extreme weather affects climate change mitigation and adaptation responses". In: *Climatic Change* 140.2, pp. 149–164. DOI: 10.1007/s10584-016-1837-4. URL: http://dx.doi.org/10.1007/s10584-016-1837-4.

Dhakal, Krishna P. and Lizette R. Chevalier (2017). "Managing urban stormwater for urban sustainability: Barriers and policy solutions for green infrastructure application". In: *Journal of Environmental Management* 203, pp. 171–181. DOI: 10.1016/j.jenvman.2017.07.065. URL: http://dx.doi.org/10.1016/j.jenvman.2017.07.065.

Diakakis, Michalis, Georgios Priskos, and Michalis Skordoulis (2018). "Public perception of flood risk in flash flood prone areas of Eastern Mediterranean: The case of Attica Region in Greece". In: *International Journal of Disaster Risk Reduction* 28.December 2017, pp. 404–413. DOI: 10.1016/j.ijdrr.2018.03.018. URL: https://doi.org/10.1016/j.ijdrr.2018.03.018.

Du, Jinkang et al. (2012). "Assessing the effects of urbanization on annual runoff and flood events using an integrated hydrological modeling system for Qinhuai River basin, China". In: *Journal of Hydrology* 464-465, pp. 127–139. DOI: 10.1016/j.jhydrol.2012.06.057.

Eckart, Kyle, Zach McPhee, and Tirupati Bolisetti (2017). "Performance and implementation of low impact development – A review". In: *Science of the Total Environment* 607-608, pp. 413–432. DOI: 10.1016/j.scitotenv.2017.06.254. URL: http://dx.doi.org/10.1016/j.scitotenv.2017.06.254.

EPA (2015). "Green Infrastructure Opportunities That Arise During Municipal Operations". In: *Office of Wetlands, Ocean and Watersheds National Estuary Program.* January, p. 36. URL: https://www.epa.gov/sites/production/files/2015-09/documents/green_infrastructure_roadshow.pdf.

European Commission (2017). *Special Eurobarometer 459 Climate Change*. DOI: 10.2834/92702.

Feldman, Lauren and P. Sol Hart (2016). "Using Political Efficacy Messages to Increase Climate Activism". In: *Science Communication* 38.1, pp. 99–127. DOI: 10.1177/1075547015617941.

Getter, Kristin L. et al. (2011). "Seasonal heat flux properties of an extensive green roof in a Midwestern U.S. climate". In: *Energy and Buildings* 43.12, pp. 3548–3557. ISSN: 0378-7788. DOI: https://doi.org/10.1016/j.enbuild.2011.09.018. URL: https://www.sciencedirect.com/science/article/pii/S0378778811004063.

Giorgi, Filippo and Piero Lionello (2008). "Climate change projections for the Mediterranean region". In: *Global and Planetary Change* 63.2-3, pp. 90–104. ISSN: 09218181. DOI: 10.1016/j.gloplacha.2007.09.005.

Gravina, T. et al. (2017). "Landslide risk perception in Frosinone (Lazio, Central Italy)". In: *Landslides* 14.4, pp. 1419–1429. DOI: 10.1007/s10346-016-0787-2.

Gutowski Jr., W. J. et al. (2016). "WCRP COordinated Regional Downscaling EXperiment (CORDEX): a diagnostic MIP for CMIP6". In: *Geoscientific Model Development* 9.11, pp. 4087–4095. DOI: 10.5194/gmd-9-4087-2016. URL: https://gmd.copernicus.org/articles/9/4087/2016/.

Guzzetti, Fausto, Colin P. Stark, and Paola Salvati (2005). "Evaluation of flood and landslide risk to the population of Italy". In: *Environmental Management* 36.1, pp. 15–36. DOI: 10.1007/s00267-003-0257-1.

Haaland, Christine and Cecil Konijnendijk van den Bosch (2015). "Challenges and strategies for urban green-space planning in cities undergoing densification: A review". In: *Urban Forestry and Urban Greening* 14.4, pp. 760–771. DOI: 10.1016/j.ufug.2015.07.009. URL: http://dx.doi.org/10.1016/j.ufug.2015.07.009.

Haghighatafshar, Salar et al. (2020). "Paradigm shift in engineering of pluvial floods: From historical recurrence intervals to risk-based design for an uncertain future". In: *Sustainable Cities and Society* 61.June, p. 102317. DOI: 10.1016/j.scs.2020.102317. URL: https://doi.org/10.1016/j.scs.2020.102317.

Hammond, M. J. et al. (2015). "Urban flood impact assessment: A state-of-the-art review". In: *Urban Water Journal* 12.1, pp. 14–29. DOI: 10.1080/1573062X.2013.857421. URL: https://doi.org/10.1080/1573062X.2013.857421.

Hargreaves, G.H. and Zohrab Samani (1985). "Reference Crop Evapotranspiration from Temperature". In: *Applied Engineering in Agriculture* 1, pp. 96–99. DOI: http://dx.doi.org/10.13031/2013.26773. URL: http://dx.doi.org/10.13031/2013.26773.

Hart, Olga and Rolf Halden (July 2019). "On the need to integrate uncertainty into U.S. water resource planning". In: *Science of The Total Environment* 691. DOI: 10.1016/j.scitotenv.2019.07.164.

Helgeson, Jennifer, Sander van der Linden, and Ilan Chabay (2012). "The role of knowledge, learning and mental models in public perceptions of climate change related risks". In: *Learning for Sustainability in Times of Accelerating Change*, pp. 381–394. DOI: 10.3920/978-90-8686-757-8.

Hopmans, J.W. and J.N.M. Stricker (1989). "Stochastic analysis of soil water regime in a watershed". In: *Journal of Hydrology* 105.1, pp. 57–84. ISSN: 0022-1694. DOI: https://doi.org/10.1016/0022-1694(89)90096-6. URL: https://www.sciencedirect.com/science/article/pii/0022169489900966.

Huang, Chien Lin et al. (2015). "Optimal spatial design of capacity and quantity of rainwater harvesting systems for urban flood mitigation". In: *Water (Switzerland)* 7.9, pp. 5173–5202. DOI: 10.3390/w7095173.

Ipcc, An and Special Report (2018). *Report 15*. Vol. os8. 2, NP–NP. ISBN: 9789291691517. DOI: 10.1093/jicru/os8.2.report15.

ISTAT (2018). *Sistema statistico nazionale Istituto nazionale di statistica*. Vol. 1, pp. 978–88–458–1965–0.

Johannesson, Mikael Poul et al. (2017). "Citizens' preferences for tackling climate change. Quantitative and qualitative analyses of their

freely formulated solutions". In: *Global Environmental Change* 46.October 2016, pp. 34–41. DOI: 10.1016/j.gloenvcha.2017.06.005.

Jongman, Brenden, Philip J. Ward, and Jeroen C.J.H. Aerts (2012). "Global exposure to river and coastal flooding: Long term trends and changes". In: *Global Environmental Change* 22.4, pp. 823–835. DOI: 10.1016/j.gloenvcha.2012.07.004. URL: http://dx.doi.org/10.1016/j.gloenvcha.2012.07.004.

Kargas, George et al. (2017). "Simulation of green roof runoff under different substrate depths and vegetation covers by coupling a simple conceptual and a physically based hydrological model". In: *Journal of Environmental Management* 200, pp. 434–445. DOI: 10.1016/j.jenvman.2017.06.012. URL: http://dx.doi.org/10.1016/j.jenvman.2017.06.012.

Karteris, Marinos et al. (2016). "Towards a green sustainable strategy for Mediterranean cities: Assessing the benefits of large-scale green roofs implementation in Thessaloniki, Northern Greece, using environmental modelling, GIS and very high spatial resolution remote sensing data". In: *Renewable and Sustainable Energy Reviews* 58, pp. 510–525. DOI: 10.1016/j.rser.2015.11.098.

Kotlarski, S. et al. (2014). "Regional climate modeling on European scales: A joint standard evaluation of the EURO-CORDEX RCM ensemble". In: *Geoscientific Model Development* 7.4, pp. 1297–1333. DOI: 10.5194/gmd-7-1297-2014.

Krosnick, Jon A. et al. (2006). "The origins and consequences of democratic citizens' policy agendas: A study of popular concern about global warming". In: *Climatic Change* 77.1-2, pp. 7–43. DOI: 10.1007/s10584-006-9068-8.

Lechowska, Ewa (2018). "What determines flood risk perception? A review of factors of flood risk perception and relations between its basic elements". In: *Natural Hazards* 94.3, pp. 1341–1366. DOI: 10.1007/s11069-018-3480-z.

Li, Jingmin et al. (2019). "Bias adjustment for decadal predictions of precipitation in Europe from CCLM". In: *Climate Dynamics* 53.3-4, pp. 1323–1340. DOI: 10.1007/s00382-019-04646-y. URL: http://dx.doi.org/10.1007/s00382-019-04646-y.

Li, W. C. and K. K.A. Yeung (2014). "A comprehensive study of green roof performance from environmental perspective". In: *International Journal of Sustainable Built Environment* 3.1, pp. 127–134. ISSN: 22126104. DOI: 10.1016/j.ijsbe.2014.05.001.

Likert, R (1932). "A technique for the measurement of attitudes". In: *Archives of Psychology*.

Linden, Sander van der and Sander van der Linden (2017). *Determinants and Measurement of Climate Change Risk Perception, Worry, and Concern*. April, pp. 1–53. DOI: 10.1093/acrefore/9780190228620.013.318.

Liu, Wen, Weiping Chen, and Chi Peng (2014). "Assessing the effectiveness of green infrastructures on urban flooding reduction: A community scale study". In: *Ecological Modelling* 291, pp. 6–14. DOI: 10.1016/j.ecolmodel.2014.07.012. URL: http://dx.doi.org/10.1016/j.ecolmodel.2014.07.012.

Liu, Yaoze et al. (2015). "Enhancing a rainfall-runoff model to assess the impacts of BMPs and LID practices on storm runoff". In: *Journal of Environmental Management* 147, pp. 12–23. DOI: 10.1016/j.jenvman.2014.09.005. URL: http://dx.doi.org/10.1016/j.jenvman.2014.09.005.

M. Th. van Genuchten (1980). "A closed-form equation for predicting the hydraulic conductivity of unsaturated soils". In: *Soil Science Society of America Journal* 44, pp. 892–898. URL: https://hwbdocuments.env.nm.gov/LosAlamosNationalLabs/TA54/11569.pdf.

Maiolo, M. et al. (2017). "Synthetic sustainability index (SSI) based on life cycle assessment approach of low impact development in the Mediterranean area". In: *Cogent Engineering* 4.1, pp. 1–13. DOI: 10.1080/23311916.2017.1410272. URL: http://doi.org/10.1080/23311916.2017.1410272.

Mascaro, Giuseppe, Francesco Viola, and Roberto Deidda (2018). "Evaluation of Precipitation From EURO-CORDEX Regional Climate Simulations in a Small-Scale Mediterranean Site". In: *Journal of Geophysical Research: Atmospheres* 123.3, pp. 1604–1625. DOI: 10.1002/2017JD027463.

Mendicino, Giuseppe and Pasquale Versace (July 2007). "Integrated Drought Watch System: A Case Study in Southern Italy". In: *Water Resources Management* 21, pp. 1409–1428. DOI: 10.1007/s11269-006-9091-6.

Meyer, Volker, Sally Priest, and Christian Kuhlicke (2012). "Economic evaluation of structural and non-structural flood risk management measures: Examples from the Mulde River". In: *Natural Hazards* 62.2, pp. 301–324. DOI: 10.1007/s11069-011-9997-z.

Miceli, Renato, Igor Sotgiu, and Michele Settanni (2008). "Disaster preparedness and perception of flood risk: A study in an alpine valley in Italy". In: *Journal of Environmental Psychology* 28.2, pp. 164–173. DOI: 10.1016/j.jenvp.2007.10.006.

Mickovski, Slobodan B. et al. (2013). "Laboratory study on the potential use of recycled inert construction waste material in the substrate mix for extensive green roofs". In: *Ecological Engineering* 61.1 PARTC, pp. 706–714. DOI: 10.1016/j.ecoleng.2013.02.015. URL: http://dx.doi.org/10.1016/j.ecoleng.2013.02.015.

Morton, Thomas A. et al. (2011). "The future that may (or may not) come: How framing changes responses to uncertainty in climate change communications". In: *Global Environmental Change* 21.1, pp. 103–109. DOI: 10.1016/j.gloenvcha.2010.09.013. URL: http://dx.doi.org/10.1016/j.gloenvcha.2010.09.013.

Moser, Susanne C. and Lisa Dilling (2004). "Making climate hot". In: *Environment* 46.10, pp. 32–46. DOI: 10.1080/00139150409605820.

Nash, J.E. and J.V. Sutcliffe (1970). "River flow forecasting through conceptual models part I — A discussion of principles". In: *Journal of Hydrology* 10.3, pp. 282–290. ISSN: 0022-1694. DOI: https://doi.org/10.1016/0022-1694(70)90255-6. URL: https://www.sciencedirect.com/science/article/pii/0022169470902556.

Naumann, Sandra, Anzaldua Gerardo, and Pam Berry (2011). "Assessment of the potential of ecosystem-based approaches to climate change adaptation and mitigation in Europe". In: *Ecologic institute and Environmental Change Institute*, pp. 29–40.

Niu, Hao et al. (2010). "Scaling of Economic Benefits from Green Roof Implementation in Washington, DC". In: *Environmental Science & Technology* 44.11, pp. 4302–4308. DOI: 10.1021/es902456x.

Osaka, Shannon and Rob Bellamy (2020). "Natural variability or climate change? Stakeholder and citizen perceptions of extreme event attribution". In: *Global Environmental Change* 62.March, p. 102070. DOI: 10.1016/j.gloenvcha.2020.102070. URL: https://doi.org/10.1016/j.gloenvcha.2020.102070.

Palla, A. et al. (2011). "Storm water infiltration in a monitored green roof for hydrologic restoration". In: *Water Science and Technology* 64.3, pp. 766–773. DOI: 10.2166/wst.2011.171.

Palla, Anna, Ilaria Gnecco, and Luca G. Lanza (2010). "Hydrologic restoration in the urban environment using green roofs". In: *Water (Switzerland)* 2.2, pp. 140–154. DOI: 10.3390/w2020140.

Paton, Douglas and David Johnston (2001). "Disasters and communities: Vulnerability, resilience and preparedness". In: *Disaster Prevention and Management: An International Journal* 10.4, pp. 270–277. DOI: 10.1108/EUM0000000005930.

Peres, D J, M F Caruso, and A Cancelliere (2017). "Assessment of climate-change impacts on precipitation based on selected RCM projections". In: pp. 9–15.

Peterson, Thomas C. et al. (2008). "Changes in North American extremes derived from daily weather data". In: *Journal of Geophysical Research: Atmospheres* 113.D7. DOI: https://doi.org/10.1029/2007JD009453. eprint: https://agupubs.onlinelibrary.wiley.com/doi/pdf/10.1029/2007JD009453. URL: https://agupubs.onlinelibrary.wiley.com/doi/abs/10.1029/2007JD009453.

Petry, B (2002). "Keynote lecture: Coping with floods: complementarity of structural and non-structural measures". In: *Flood defence*, pp. 60–70. arXiv: 1-880132-54-0. URL: http://www.civil.ist.utl.pt/{~}joana/DFA-riscos-net/2007-08/keynotelecture-copingwithfloods.pdf.

Piro, Patrizia et al. (2018). "Energy and hydraulic performance of a vegetated roof in sub-mediterranean climate". In: *Sustainability (Switzerland)* 10.10, pp. 1–13. DOI: 10.3390/su10103473.

Prutsch, A. et al. (2014). *Methods and Tools for Adaptation to Climate Change. A Handbook for Provinces, Regions and Cities.*

Raaijmakers, Ruud, Jörg Krywkow, and Anne van der Veen (2008). "Flood risk perceptions and spatial multi-criteria analysis: An exploratory research for hazard mitigation". In: *Natural Hazards* 46.3, pp. 307–322. DOI: 10.1007/s11069-007-9189-z.

Raciti, Antonio and Laura Saija (2018). "From ecosystem services to Ecological Devices: The CoPED Summer School experience in the Simeto River Valley, Italy". In: *Journal of Urban Management* 7.3, pp. 161–171. DOI: 10.1016/j.jum.2018.04.005. URL: https://doi.org/10.1016/j.jum.2018.04.005.

Razzaghmanesh, M. and S. Beecham (2014). "The hydrological behaviour of extensive and intensive green roofs in a dry climate". In: *Science of the Total Environment* 499.1, pp. 284–296. DOI: 10.1016/j.scitotenv.2014.08.046. URL: http://dx.doi.org/10.1016/j.scitotenv.2014.08.046.

Ricci, Tullio, Rosa Nave, and Franco Barberi (2013). "Vesuvio civil protection exercise MESIMEX: Survey on volcanic risk perception". In: *Annals of Geophysics* 56.4. DOI: 10.4401/ag-6458.

Saidu, Idris and Merving Dharmasiri Lal (2015). "Flood risk inevitability and flood risk management in urban areas: A review". In: *Journal of Geography and Regional Planning* 8.8, pp. 205–209. DOI: 10.5897/jgrp2015.0510.

Saija, Laura et al. (2017). "Learning from practice: environmental and community mapping as participatory action research in planning". In: *Planning Theory & Practice* 18.1, pp. 127–153. DOI: 10.1080/14649357.2016.1262982. URL: https://doi.org/10.1080/14649357.2016.1262982.

Salvati, P. et al. (2014). "Perception of flood and landslide risk in Italy: A preliminary analysis". In: *Natural Hazards and Earth System Sciences* 14.9, pp. 2589–2603. DOI: 10.5194/nhess-14-2589-2014.

Schaap, Marcel G. (2002). "Rosetta v1.2: A computer program for estimating soil hydraulic parameters with hierarchical pedotransfer functions". In: 251, pp. 163–176. URL: www.cals.arizona.edu/research/rosetta/download/rosetta.pdf.

SEERISK (2013). *Joint Disaster Management Risk Assessment and Preparedness in the Danube Macro-region (SEERISK) project - Social awareness questionnaire*.

Senatore, A., L. Furnari, and G. Mendicino (2020). "Impact of high-resolution sea surface temperature representation on the forecast of small Mediterranean catchments' hydrological responses to heavy precipitation". In: *Hydrology and Earth System Sciences* 24.1, pp. 269–291. DOI: 10.5194/hess-24-269-2020. URL: https://hess.copernicus.org/articles/24/269/2020/.

Senatore, Alfonso et al. (2011). "Regional climate change projections and hydrological impact analysis for a Mediterranean basin in Southern Italy". In: *Journal of Hydrology* 399.1, pp. 70–92. ISSN: 0022-1694. DOI: https://doi.org/10.1016/j.jhydrol.2010.12.035. URL: https://www.sciencedirect.com/science/article/pii/S0022169410008139.

Shafique, Muhammad, Reeho Kim, and Muhammad Rafiq (2018). "Green roof benefits, opportunities and challenges – A review". In: *Renewable and Sustainable Energy Reviews* 90.April 2017, pp. 757–773. DOI: 10.1016/j.rser.2018.04.006.

Shen, Xiaomeng (2009). "FLOOD RISK PERCEPTION AND COMMUNICATION WITHIN RISK MANAGEMENT IN DIFFERENT CULTURAL CONTEXTS A COMPARATIVE CASE STUDY BETWEEN WUHAN , CHINA AND COLOGNE , GERMANY Xiaomeng Shen Beijing , VR China". In: *Comparative and General Pharmacology*.

Smiatek, Gerhard and Harald Kunstmann (Sept. 2019). "Simulating future runoff in a complex terrain Alpine catchment with EURO-CORDEX data". In: *Journal of Hydrometeorology* 20, pp. 1925–1940. DOI: 10.1175/JHM-D-18-0214.1.

Speak, A. F. et al. (2013). "Rainwater runoff retention on an aged intensive green roof". In: *Science of the Total Environment* 461-462, pp. 28–38. DOI: 10.1016/j.scitotenv.2013.04.085. URL: http://dx.doi.org/10.1016/j.scitotenv.2013.04.085.

Spence, A et al. (2011). "Perceptions of climate change and willingness to save energy related to flood experience". In: *Nature Climate Change*

1.1, pp. 46–49. DOI: 10.1038/nclimate1059. URL: https://doi.org/10.1038/nclimate1059.

Spence, Alexa, Wouter Poortinga, and Nick Pidgeon (2012). "The Psychological Distance of Climate Change". In: *Risk Analysis* 32.6, pp. 957–972. DOI: 10.1111/j.1539-6924.2011.01695.x.

Stovin, Virginia, Gianni Vesuviano, and Hartini Kasmin (2012). "The hydrological performance of a green roof test bed under UK climatic conditions". In: *Journal of Hydrology* 414-415, pp. 148–161. DOI: 10.1016/j.jhydrol.2011.10.022. URL: http://dx.doi.org/10.1016/j.jhydrol.2011.10.022.

Sun, Ting et al. (2013). "Hydrometeorological determinants of green roof performance via a vertically-resolved model for heat and water transport". In: *Building and Environment* 60, pp. 211–224. ISSN: 0360-1323. DOI: https://doi.org/10.1016/j.buildenv.2012.10.018. URL: https://www.sciencedirect.com/science/article/pii/S0360132312002831.

Sussams, L. W., W. R. Sheate, and R. P. Eales (2015). "Green infrastructure as a climate change adaptation policy intervention: Muddying the waters or clearing a path to a more secure future?" In: *Journal of Environmental Management* 147, pp. 184–193. DOI: 10.1016/j.jenvman.2014.09.003. URL: http://dx.doi.org/10.1016/j.jenvman.2014.09.003.

Tao, Wendong et al. (2014). "Constructed wetlands for treatment of combined sewer overflow in the US: A review of design challenges and application status". In: *Water (Switzerland)* 6.11, pp. 3362–3385. DOI: 10.3390/w6113362.

Taylor, K. E. (2001). "Summarizing multiple aspects of model performance in a single diagram". In: *J Geophys Res- Atmos* 106, pp. 7183–7192. URL: https://doi.org/10.1029/2000JD900719.

Terink, W. et al. (2009). "Bias correction of temperature and precipitation data for regional climate model application to the Rhine basin". In: *Hydrology and Earth System Sciences Discussions* 6, pp. 5377–5413. DOI: 10.5194/hessd-6-5377-2009. URL: https://hess.copernicus.org/preprints/6/5377/2009/.

Teutschbein, Claudia and Jan Seibert (2010). "Regional Climate Models for Hydrological Impact Studies at the Catchment Scale: A Review of Recent Modeling Strategies". In: *Geography Compass* 4.7, pp. 834–860. DOI: https://doi.org/10.1111/j.1749-8198.2010.00357.x. eprint: https://onlinelibrary.wiley.com/doi/pdf/10.1111/j.1749-8198.2010.00357.x. URL: https://onlinelibrary.wiley.com/doi/abs/10.1111/j.1749-8198.2010.00357.x.

— (2012). "Bias correction of regional climate model simulations for hydrological climate-change impact studies: Review and evaluation of different methods". In: *Journal of Hydrology* 456-457, pp. 12–29. DOI: 10.1016/j.jhydrol.2012.05.052. URL: http://dx.doi.org/10.1016/j.jhydrol.2012.05.052.

Theodosiou, Theodore (2009). "Green roofs in buildings: Thermal and environmental behaviour". In: *Advances in Building Energy Research* 3.1, pp. 271–288. DOI: 10.3763/aber.2009.0311.

UNFCCC. URL: https://unfccc.int/topics/adaptation-and-resilience/the-big-picture/what-do-adaptation-to-climate-change-and-climate-resilience-mean.

Valtanen, Marjo, Nora Sillanpää, and Heikki Setälä (2014). "Effects of land use intensity on stormwater runoff and its temporal occurrence in cold climates". In: *Hydrological Processes* 28.4, pp. 2639–2650. DOI: 10.1002/hyp.9819.

Van Der Linden, S. (2014). "On the relationship between personal experience, affect and risk perception: The case of climate change". In: *European Journal of Social Psychology* 44.5, pp. 430–440. DOI: 10.1002/ejsp.2008.

Vogel, Jason R. et al. (2015). "Critical Review of Technical Questions Facing Low Impact Development and Green Infrastructure: A Perspective from the Great Plains". In: *Water Environment Research* 87.9, pp. 849–862. DOI: 10.2175/106143015X14362865226392. URL: http://doi.wiley.com/10.2175/106143015X14362865226392.

Vuuren, Detlef P. van et al. (2011). "RCP2.6: Exploring the possibility to keep global mean temperature increase below 2°C". In: *Climatic Change* 109.1, pp. 95–116. ISSN: 01650009. DOI: 10.1007/s10584-011-0152-3.

Wachinger, Gisela and Ortwin Renn (2010). "Risk perception of natural hazards". In: *WP3-Report of the* 09, pp. 1–111. URL: http://caphaz-net.org/outcomes-results/CapHaz-Net{_}WP3{_}Risk-Perception2.pdf.

Weber, Elke U. (2016). "What shapes perceptions of climate change? New research since 2010". In: *Wiley Interdisciplinary Reviews: Climate Change* 7.1, pp. 125–134. DOI: 10.1002/wcc.377.

Westerhoff, Lisa (Università di Umeå SW) et al. (2010). *L'adattamento ai cambiamenti climatici esito delle indagini condotte nel Comune di Ferrara.pdf*.

Whitmarsh, Lorraine and Stuart Capstick (2018). *Perceptions of climate change*. Elsevier Inc., pp. 13–33. DOI: 10.1016/B978-0-12-813130-5.00002-3.

Wright, Timothy J. et al. (2016). "Retrofitting LID Practices into Existing Neighborhoods: Is It Worth It?" In: *Environmental Management* 57.4, pp. 856–867. DOI: 10.1007/s00267-015-0651-5.

Wu, Xiaodan et al. (2012). "An evaluation of the impacts of land surface modification, storm sewer development, and rainfall variation on waterlogging risk in Shanghai". In: *Natural Hazards* 63.2, pp. 305–323. DOI: 10.1007/s11069-012-0153-1.

Yan, Bing (Sept. 2011). "The Research of Ecological and Economic Benefits for Green Roof". In: Applied Mechanics and Materials 71, pp. 2763–2766. DOI: 10.4028/www.scientific.net/AMM.71-78.2763.

Yang, Guoxiang et al. (2011). "The impact of urban development on hydrologic regime from catchment to basin scales". In: *Landscape and Urban Planning* 103.2, pp. 237–247. DOI: 10.1016/j.landurbplan.2011.08.003. URL: http://dx.doi.org/10.1016/j.landurbplan.2011.08.003.

Yang, Jun, Qian Yu, and Peng Gong (2008). "Quantifying air pollution removal by green roofs in Chicago". In: *Atmospheric Environment* 42.31, pp. 7266–7273. ISSN: 1352-2310. DOI: https://doi.org/10.1016/j.atmosenv.2008.07.003. URL: https://www.sciencedirect.com/science/article/pii/S1352231008006262.

Yevjevich, Vujica (1969). "An objective approach to definitions and investigations of continental hydrologic droughts". In: *Journal of Hydrology* 7.3, p. 353. DOI: 10.1016/0022-1694(69)90110-3.

Zhang, Qianqian et al. (2015). "The capacity of greening roof to reduce stormwater runoff and pollution". In: *Landscape and Urban Planning* 144, pp. 142–150. DOI: 10.1016/j.landurbplan.2015.08.017. URL: http://dx.doi.org/10.1016/j.landurbplan.2015.08.017.